Modeling, Analysis and strategic study of Active dynamic control of complex mechanical system

Prabhat Kumar Sinha
(ID. No. : 11PHME201)
Ph.D Mechanical Engineering
Under Supervision of
Dr.A.S.Darbari (Associate Professor)
Department of Mechanical Engineering, SSET,
Sam Higginbottom Institute of Agriculture, Technology & Sciences
Allahabad ,U.P 211007

CONTENTS

ABSTRACT

In the past decade, lot of interest has been generated in area of intelligent system and structures because of their enormous possibility in vibration and acoustic control, shape control and health monitoring. A smart structure involved described actuator and sensors and one or more microprocessors. The responses from the sensors are analyzed by the microprocessors. Distributed parameter control theory is used to command the actuator to apply localized strains on the base structure with a view to minimize system response. Optimizing the effectiveness and reliability of integrated induced strain actuators requires an understanding of the mechanics of the mechanical interaction between the actuators and the host structures. Optimization in the vibration of automobile and structure with variable boundary condition is done by active vibration control through piezo electric patches. In this paper modelling, analysis and active vibration control of mechanical portal frame on which six piezoelectric patches are bonded in the beam as sensor/actuator. The piezoelectric patches are use to control such structures. The control may be P, PI and PID. However the paper addresses PID control because of its robustness. For computer experimentation a typical structure of portal frame is used to implement PID control. The structure is modelled using finite element method and solved for Eigen values. The piezo patches are fixed on different locations of the structure and PID controller is implemented to obtain the control response on the MATLAB platform of the Simulink toolbox. For modeling complex portal frame, numerical methods such as finite element method (FEM) are widely used. However commercially available FEM software such as ANSYS has the modelling capability to model a smart portal frame. The results are obtained and optimum location is found for the effective control of the structure. The control response obtained for the frame structure is optimized which be used for the controlling the vibration of mechanical equipment's. There is a need to develop a methodology so that commercially available frame elements may be used to analyze the deformation pattern and dynamic behavior of smart structure.

Keywords: Active Vibration Control, PID Controller, ANSYS, Simulink, MATLAB, Finite Element Analysis.

List of Tables

List of Figures

List of Symbols

Symbols No.	Details
J	Matrix
f^*	Correcting force
E	Error signal
R	Reference input
T_{em}	Mechanical terminal
T_{me}	Transduction coefficient
Z_e	Electrical impedance
Z_m	Mechanical impedance
V	Voltage
ε^T	Dielectric constant
D	Electric displacement
S	Strain
T	Stress
$d\omega$	displacement coefficient
E	Elastic modulus
G	Shear modulus
I	Second moment
k	Timoshenko shear coefficient
A	Cross sectional area
L	Length of beam
ω	Displacement
φ	Rotation
$M_{\chi\chi}$	Moment
Q_χ	Shear force(x-axis)
$\sigma_{\chi\chi}$	Axial stress
Z	Section modulus
$\varepsilon_{\chi\chi}$	Axial strain
P	Axial load
$\dot{Q}_i$	Non conservative forces or moment
q_i	Time derivative of coordinate system representing velocity
M	Bending moment
T	Kinetic energy of system
S	Shape function
γ	Mass per unit
U	Displacement function
Π	Total potential energy

δ	Deflection
F	Force
N	Number of element
l_a,l_b	Length
C_s	Sensor constant
D	Electric displacement
ξ^{σ}	Dielectric constant
E_z	Electric field
K^P,K^i,K^d	Proportional integral

Introduction

An active structure is an engineering structure containing sensors and actuators which actively modify the response of the structure to its environment. Research into active structural control is growing due to new challenges in extreme environments in the area such as space, undersea, polar, nuclear, chemical and biological applications. Development of seismic resistant buildings and structures had been another requirement in the era of high degree of urbanization.

Due to advances of rapid development in instrumentation technology, electronic, digital control system, the current research requirement is posing a lot of challenges to develop the above technologies at rapid pace. In the present research proposal a feasible application of active control of structures/ mechanical equipment's would be studied. Accordingly, algorithms will be developed to meet the challenges. The use of active control plays vital role in mechanical engineering such as improving machine-tool performances, vehicle dynamic characteristics, off-shore installations, aircraft structures and space shuttles, etc.

Advances in sensor, actuator and microprocessors technologies enabled us to control these equipment's actively and precisely. Long-term reliability of active-control systems has been a matter of controversy for civil structures which have service life of a century or more than century and loading with long return periods in an active control system, external power source supplies energy to control actuators which apply forces to the structure in a prescribed manner. The applied force can both add and dissipate energy from the structure.

A response function of the system measured with optical, mechanical, electrical or chemical sensors create signals which are sent to control actuators. Advances in theory and practice of active structural control technology have been modified the general perception of structures. Due to incorporated intelligence, structures become dynamic objects capable of interacting with complex environments.

The aim of an intelligent structure is a structure which maintains and improves structural performance by recognizing changes in behaviour and actions, adapting the structure to meet performance goals and using past events to improve future performance.

Intelligence is one of the desirable qualities of biological systems. Through mimicking living organisms, incorporation of intelligent control methodologies into

structural engineering has potential to enhance the concept of structures. Self-diagnosis, self-repair and learning is examples of behavioral bio mimicry.

Computing challenges which are important to the creation of the next generation of active structures are then identified. Active structural control is closely related to structural health monitoring (SHM). Distinction between active, adaptive, intelligent and bio mimetic structures. Adaptive structure improves its response to changing environments over time without reference to behaviour modelling and actions such as loading and temperature. Biomimetic structure is an intelligent structure that has the ability to carry out self-diagnosis and thus improve performance attributes such as damage tolerance through active control presents the categories of structural control.

The terms active control, adaptive control and intelligent control refer to sub domains of structural control. Active control systems and active control mechanisms involve shape control using active cables and active struts as well as control mechanisms which do not aim to control the shape of the structure.

After review the past research papers, it has been found that still the research is required in the particular area of control of vibration through piezo-patches.

1.1 Basic Concept of Structural Dynamics

Modern structures are increasingly slender and have reduced redundant strength due to improved analysis and design methods. Such structures are increasingly responsive to the manner in which loading is applied with respect to time and hence the dynamic behaviour of such structures must be allowed for in design; as well as the usual static considerations. Structural dynamics provides the basic equation necessary for structural dynamic analysis and develop both the lumped and the consistent-mass matrices involved in the analysis of a frame, bar, beam and truss. Structural dynamics also provides longhand solutions for the determination of the natural frequencies for bars and beams, and then illustrate the time-step integration process involved with the stress analysis of a bar subjected to a time dependent forcing function. Structural dynamics includes equation of motion of a discrete system, vibration modes, modal decomposition, collocated control system, Guyan reductionand Craig-Bampton reduction.

1.1.1 Active versus Passive

Consider a precision structure subjected to varying thermal conditions; unless carefully designed, it will distort as a result of the thermal gradients. One way to prevent this is to build the structure from a thermally stable composite material; this is the passive approach. An alternative way is to use a set of actuators and sensors connected by a feedback loop; such a structure is active. In this case, we exploit the main virtue of feedback, which is to reduce the sensitivity of the output to parameter variations and to attenuate the effect of disturbances within the bandwidth of the control system. Depending on the circumstances, active structures may be cheaper or lighter than passive structures of comparable performances; or they may offer performances which has no passive structure could offer, as in the following example. Until a few years ago, the general belief was that atmospheric turbulence would constitute an important limitation to the resolution of earth based telescopes; this was one of the main reasons for developing the Hubble Space Telescope. Nowadays, it is possible to correct in real time the disturbances produced by atmospheric turbulence on the optical wave front coming from celestial objects; this allows us to improve the ultimate resolution of the telescope by one order of magnitude, to the limit imposed by diffraction. The correction is achieved by a deformable mirror coupled to a set of actuators. A wave front sensor detects the phase difference in the turbulent wave front and the control computer supplies, the shape of the deformable mirror which is required to correct this error. Adaptive optics has become a standard feature in ground-based astronomy. The foregoing example is not the only one where active structures have proved beneficial to astronomy; another example is the primary mirror of large telescopes, which can have a diameter of 8 m or more. Large primary mirrors are very difficult to manufacture and assemble. A passive mirror must be thermally stable and very stiff, in order to keep the right shape in spite of the varying gravity loads during the tracking of a star, and the dynamic loads from the wind. There are two alternatives to that, both active and passive. The first one, adopted on the Very Large Telescope (VLT) at ESO in Paranal, Chile, consists of having a relatively flexible primary mirror connected at the back to a set of a hundred or so actuators. As in the previous example, the control system uses an image analyzer to evaluate the amplitude of the perturbation of the optical modes; next, the correction is computed to minimize the effect of the perturbation and is applied to the actuators. The influence matrix J between the actuator forces f and the optical mode

amplitudes w of the wave front errors can be determined experimentally with the image analyzer:

$$w = Jf \tag{1.1}$$

J is a rectangular matrix, because the number of actuators is larger than the number of optical modes of interest. Once the modal errors $w*$have been evaluated, the correcting forces can be calculated from

$$f* = J^T(JJ^T)^{-1}w* \tag{1.2}$$

where$J^T(JJ^T)^{-1}$is the pseudo-inverse of the rectangular matrix J. This is the minimum norm solution to Equ.(1). The second alternative, adopted on the Keck observatory at Mauna Kea, Hawaii, consists of using a segmented primary mirror. The potential advantages of such a design are lower weight, lower cost, ease of fabrication and assembly. Each segment has a hexagonal shape and is equipped with three computer controlled degrees of freedom (tilt and piston) and six edge sensors measuring the relative displacements with respect to the neighboring segments; the control system is used to achieve the optical quality of a monolithic mirror (by cophasingthe segments), to compensate for gravity and wind disturbances, and minimize the impact of the telescope dynamics on the optical performance. The aim is to use a number of smaller telescopes as an interferometer is to achieve a resolution which could only be achieved with a much larger monolithic telescope. One possible spacecraft architecture for such an interferometric mission is represented in Fig.1.2; it consists of a main truss supporting a set of independently pointing telescopes. The relative positions of the telescopes are monitored by a sophisticated metrology and the optical paths between the individual telescopes and the beam combiner are accurately controlled with optical delay lines, based on the information coming from a wave front sensor. Typically, the distance between the telescopes could be 50 m or more, and the order of magnitude of the error allowed on the optical path length is a few nanometers; the pointing error of the individual telescopes is as low as a few nano radians (i.e. one order of magnitude better than the Hubble Space Telescope). Clearly, such stringent geometrical requirements in the harsh space environment cannot be achieved with a precision monolithic structure, but rather by active means as suggested in Fig.1.2.The main requirement on the supporting truss is not precision but stability, the accuracy of the

optical path being taken care of by the wide-band vibration isolation/steering control system of individual telescopes and the optical delay lines (described below). Geometric stability includes thermal stability, vibration damping and pre-stressing the gaps in deployable structures (this is a critical issue for deployable trusses). In addition to these geometric requirements, this spacecraft would be sent in deep space rather than in low earth orbit, to ensure maximum sensitivity; this makes the weight issue particularly important.

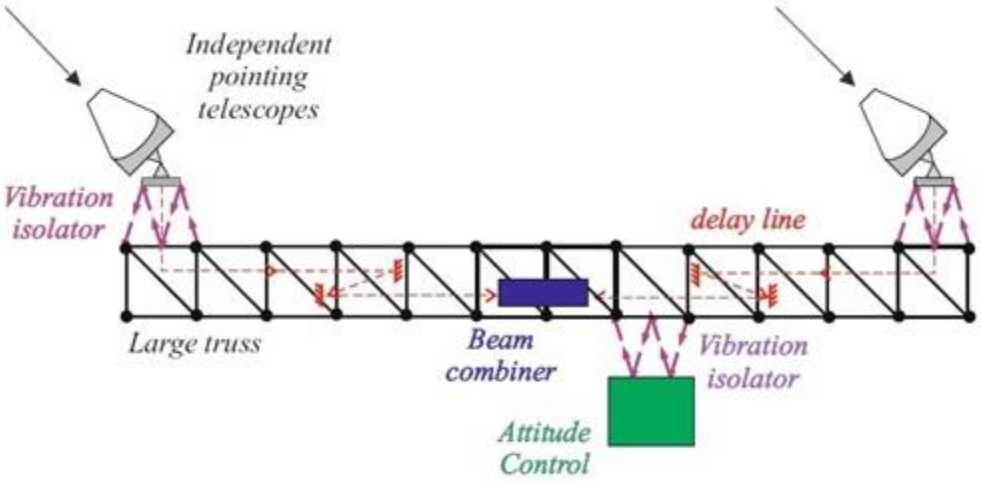

Fig. 1.1 Schematic view of a future interferometric mission.

Another interesting subsystem necessary to achieve the stringent specifications is the six degree of freedom vibration isolator at the interface between the attitude control module and the supporting truss; this isolator allows the low frequency attitude control torque to be transmitted, while filtering out the high frequency disturbances generated by the unbalanced centrifugal forces in the reaction wheels. Another vibration isolator may be used at the interface between the truss and the independent telescopes, possibly combined with the steering of the telescopes. The third component relevant to active control is the optical delay line; it consists of a high precision single degree of freedom translational mechanism supporting a mirror, whose function is to control the optical path length between every telescope and the beam combiner, so that these distances are kept identical to a fraction of the wavelength (e.g.$\lambda/20$). These examples were concerned mainly with performance. However, as technology developed and with the availability of low cost electronic components, it is likely that there will be a growing number of applications where active solutions will become cheaper than passive ones, for the same level of performance. In most cases, a bad design will remain bad, active or

not, and an active solution should normally be considered only after all other passive means have been exhausted. One should always bear in mind that feedback control can compensate for external disturbances only in a limited frequency band that is called the bandwidth of the control system. One should never forget that outside the bandwidth, the disturbance is actually amplified by the control system.

1.1.2 Vibration

Any motion which repeats itself after an interval of time is called vibration or oscillation. The swinging of a pendulum and the motion of a plucked string are typical examples of vibration. The theory of vibration deals with the study of oscillatory motions of bodies and the forces associated with them. In many engineering systems, a human being acts as an integral part of the system. The transmission of vibration to human beings results in discomfort and loss of efficiency. The vibration and noise generated by engines causes annoyance to people and sometimes damage to system. The vibration of a system involves the transfer of its potential energy to kinetic energy and of kinetic energy to potential energy, alternately. If the system is damped, some energy is dissipated in each cycle of vibration and must be replaced by an external source if a state of steady vibration is to be maintained.

Types of Vibrating System

1.1.2.1 Discrete and Continuous Systems

A large number of practical systems can be described using a finite number of degrees of freedom, especially those involving continuous elastic members, have an infinite number of degrees of freedom.The beam has an infinite number of mass points, we need an infinite number of coordinates to specify its deflected configuration. The infinite number of coordinates defines its elastic deflection curve. Thus the cantilever beam has an infinite number of degrees of freedom. Most structural and machine systems have deformable (elastic) members and therefore have an infinite number of degrees of freedom. Systems with a finite number of degrees of freedom are called discreteor lumped parameter systems, and those with an infinite number of degrees of freedom are called continuous or distributed systems.

1.1.2.2 Free and Forced Vibration

If a system, after an initial disturbance, is left to vibrate on its own, the ensuing vibration is known as free vibration. No external force acts on the system. The oscillation of a simple pendulum is an example of free vibration. If a system is subjected to an external force (often, a repeating type of force), the resulting vibration is known as forced vibration. The oscillation that arises in machines such as diesel engines is an example of forced vibration. If the frequency of the external force coincides with one of the natural frequencies of the system, a condition known as resonance occurs, and the system undergoes dangerously large oscillations. Failures of such structures as buildings, bridges, turbines, and airplane wings have been associated with the occurrence of resonance.

1.1.2.3 Undamped and Damped Vibration

If no energy is lost or dissipated in friction or other resistance during oscillation, the vibration is known as undamped vibration. If any energy is lost in this way, however, it is called damped vibration. In many physical systems, the amount of damping is so small that it can be disregarded for most engineering purposes. However, consideration of damping becomes extremely important in analyzing vibratory systems near resonance.

1.1.2.4 Linear and Nonlinear Vibration

If all the basic components of a vibratory system the spring, the mass, and the damper behave linearly, the resulting vibration is known as linear vibration. If, however, any of the basic components behave nonlinearly, the vibration is called nonlinear vibration. The differential equations which govern the behavior of linear and nonlinear vibratory systems are known as linear and nonlinear, respectively. If the vibration is linear, the principle of superposition holds, and the mathematical techniques of analysis are well developed. For nonlinear vibration, the superposition principle is not valid, and techniques of analysis are less well known.

1.1.2.5 Deterministic and Random Vibration

If the value or magnitude of the excitation (force or motion) acting on a vibratory system is known at any given time, the excitation is called deterministic. The resulting

vibration is known as deterministic vibration. In some cases, the excitation is nondeterministic or random, the value of the excitation at a given time cannot be predicted. In these cases, a large collection of records of the excitation may exhibit some statistical regularity. It is possible to estimate averages such as the mean and mean square values of the excitation.

1.2 Resonance

Resonance is a phenomenon that consists of a given system being driven by another vibrating system or by external forces to oscillate with greater amplitude at some preferential frequencies. Frequencies at which the response amplitude is a relative maximum are known as the system's resonant frequencies, or resonance frequencies. At resonant frequencies, small periodic driving forces have the ability to produce large amplitude oscillations. This is because the system stores vibrational energy. Resonance occurs when a system is able to store and easily transfer energy between two or more different storage modes (such as kinetic energy and potential energy in the case of a pendulum). However, there are some losses from cycle to cycle, called damping. When damping is small, the resonant frequency is approximately equal to the natural frequency of the system, which is a frequency of unforced vibrations. Some systems have multiple, distinct, resonant frequencies. Resonance phenomena occur with all types of vibrations or waves: there is mechanical resonance, acoustic resonance, electromagnetic resonance, nuclear magnetic resonance (NMR), electron spin resonance (ESR) and resonance of quantum wave functions. Resonant systems can be used to generate vibrations of a specific frequency (e.g., musical instruments), or pick out specific frequencies from a complex vibration containing many frequencies (e.g., filters). The term Resonance (from Latin resonantia ‘echo,’ from resonare ‘resound’) originates from the field of acoustics, particularly observed in musical instruments, e.g. when strings started to vibrate and to produce sound without direct excitation by the player.

1.3 Vibration Suppression

Mechanical vibrations span amplitudes from meters (civil engineering) to nanometers (precision engineering). Their detrimental effect on systems may be of various natures:

Failure: vibration-induced structural failure may occur by excessive strain during transient events (e.g. building response to earthquake), by instability due to particular operating conditions (flutter of bridges under wind excitation), or simply by fatigue (mechanical parts in machines).

Comfort: examples where vibrations are detrimental to comfort are numerous: noise and vibration in helicopters, car suspensions, wind-induced sway of buildings.

Operation of precision devices: There arenumerous systems in precision engineering, especially optical systems, put severe restrictions on mechanical vibrations. Precision machine tools, wafer steppers1 and telescopes are typical examples. The performances of large interferometers such as the VLTI are limited by micro-vibrations affecting the various parts of the optical path. Lightweight segmented telescopes (space as well as earth-based) will be impossible to build in their final shape with an accuracy of a fraction of the wavelength, because of the various disturbance sources such as deployment errors and thermal gradients (which dominate the space environment). Such systems will not exist without the capability to control actively the reflector shape. Vibration reduction can be achieved in many different ways, depending on the problem; the most common are stiffening, damping and isolation. Stiffening consists of shifting the resonance frequency of the structure beyond the frequency band of excitation. Damping consists of reducing the resonance peaks by dissipating the vibration energy. Isolation consists of preventing the propagation of disturbances to sensitive parts of the systems. Damping may be achieved passively, with fluid dampers, eddy currents, elastomers or hysteretic elements, or by transferring kinetic energy to Dynamic Vibration Absorbers (DVA). One can also use transducers as energy converters, to transform vibration energy into electrical energy which is dissipated in electrical networks, or stored (energy harvesting). Recently, semi-active devices (also called semi-passive) have become available; they consist of passive devices with controllable properties. The Magneto-Rheological (MR) fluid damper is a famous example; piezoelectric transducers with switched electrical networks is another one. Since they behave in a strongly nonlinear way, semi-active devices can transfer energy from one frequency to another, but they are inherently passive and, unlike active devices, cannot destabilize the system; they are also less vulnerable to power failure. When high performance is needed, active control can be used; this involves a set of sensors (strain, acceleration, velocity, force), a set of actuators (force, inertial, strain) and a control

algorithm (feedback or feedforward). Active damping is one of the main focuses of this book. The design of an active control system involves many issues such as how to configurate the sensors and actuators, how to secure stability and robustness (e.g. collocated actuator/sensor pairs); the power requirements will often determine the size of the actuators, and the cost of the project

1.4 Active Vibration Control

Active vibration control is the active application of force in an equal and opposite fashion to the forces imposed by external vibration. With this application, a precision industrial process can be maintained on a platform essentially vibration free. Many precision industrial processes cannot take place if the machinery is being affected by vibration. For example, the production of semiconductor wafers requires the machines used for the photolithography, steps may be used in an essentially vibration free environment or the sub-micrometer features will be blurred. Active vibration control is now also commercially available for reducing vibration in helicopters, offering better comfort with less weight than traditional passive technologies. The typical active vibration control system uses several components:

- A massive platform suspended by several active drivers (that may use voice coils, hydraulics, pneumatics, piezoelectric or other techniques).
- Three accelerometers that measure acceleration in the three degrees of freedom.
- An electronic amplifier system that amplifies and inverts the signals from the accelerometers. A PID controller can be used to get better performance than a simple inverting amplifier.
- For very large systems, pneumatic or hydraulic components that provide the high drive power required.

If the vibration is periodic, then the control system may adapt to the ongoing vibration, thereby providing better cancellation than would have been provided simply by reacting to each new acceleration without referring to past accelerations.

1.5 Control Strategies

There are two radically different approaches to disturbance rejection: feedback and feedforward. Although this text is entirely devoted to feedback control, it is important to

point out the salient features of both approaches, in order to enable the user to select the most appropriate one for a given application.

1.5.1 Feedback

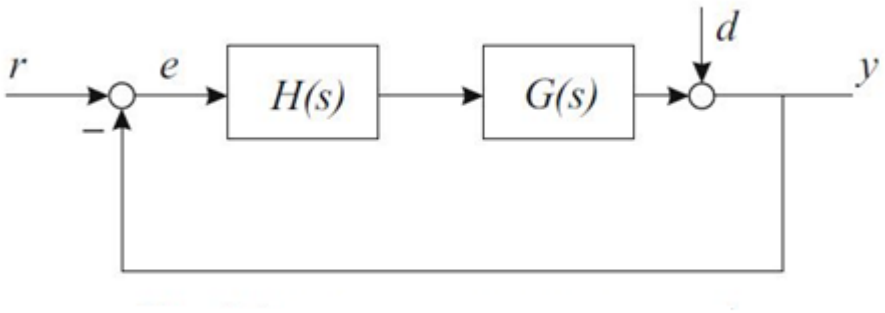

Fig. 1.2 Principle of feedback control

The principle of feedback is represented in Fig.1.4; the output y of the systemis compared to the reference input r, and the error signal, e = r−y, is passedinto a compensator H(s) and applied to the system G(s). The design problem consists of finding the appropriate compensator H(s) such that the closed loop system is stable and behaves in the desired manner. In the control of lightly damped structures, feedback control is used for two distinct and somewhat complementary purposes: active damping and model based feedback. The objective of active damping is to reduce the effect of the resonant peaks on the response of the structure. From

$$\frac{y(s)}{d(s)} = \frac{1}{1+GH} \tag{1.3}$$

Active damping can generally be achieved with moderate gains, another nice property is that it can be achieved without a model of the structure, and with guaranteed stability, provided that the actuator and sensor are collocated and have perfect dynamics. Of course actuators and sensors always have finite dynamics and any active damping system has a finite bandwidth.

The control objectives can be more ambitious, and we may wish to keep a control variable y (a position, or the pointing of an antenna) to a desired value r in spite of external disturbances d in some frequency range. From the previous formula and

$$F(s) = \frac{y(s)}{r(s)} = \frac{GH}{1+GH} \tag{1.4}$$

we readily see that this requires large values of GH in the frequency range where y ≅ ris sought. GH >>1 implies that the closed-loop transfer function F(s) is close to 1, which means that the output y tracks the input r accurately.

From Equ.(1.4), this also ensures disturbance rejection within the bandwidth of the control system.

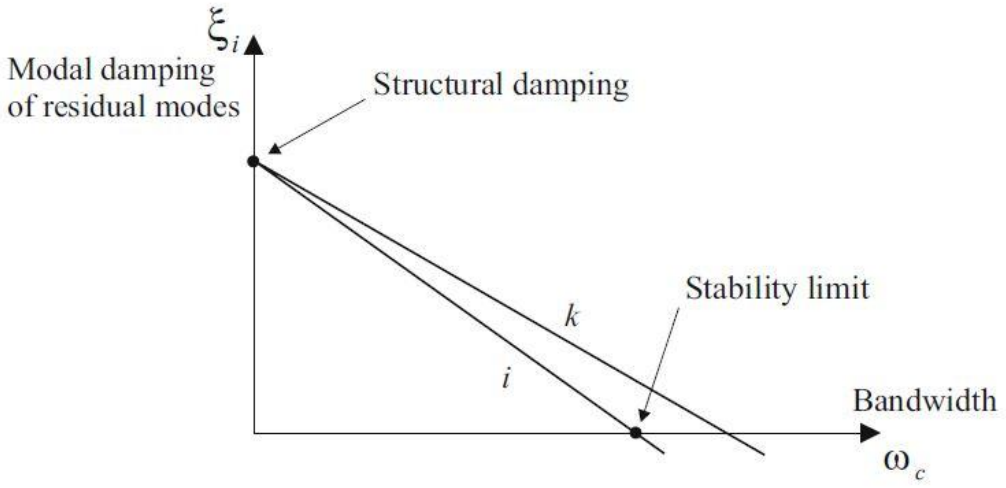

Fig 1.3 The Spillover

In general, to achieve this, we need a more elaborate strategy involving a mathematical model of the system which, at best, can only be a low-dimensional approximation of the actual system G(s). There are many techniques available to find the appropriate compensator, and only the simplest and the best established will be discussed in following lines. They all have a number of common features:

- The bandwidth ω_c of the control system is limited by the accuracy of the model; there is always some destabilization of the flexible modes outside ω_c(residual modes). The phenomenon whereby the net damping of the residual modes actually decreases when the bandwidth increases is known as spillover(Fig.1.3).
- The disturbance rejection within the bandwidth of the control system is always compensated by an amplification of the disturbances outside the bandwidth.

- When implemented digitally, the sampling frequency $\omega_s$must always be two orders of magnitude larger than $\omega_c$to preserve reasonably the behaviour of the continuous system. This puts some hardware restrictions on the bandwidth of the control system.

1.5.2 Feed-forward

When a signal correlated to the disturbance is available, feed-forward adaptive filtering constitutes an attractive alternative to feedback for disturbance rejection; it was originally developed for noise control (Nelson & Elliott), but it is very efficient for vibration control too. Its principle is explained in Fig.1.4. The method relies on the availability of a reference signal correlated to the primary disturbance; this signal is passed through an adaptive filter, the output of which is applied to the system by secondary sources. The filter coefficients are adapted in such a way that the error signal at one or several critical points is minimized.

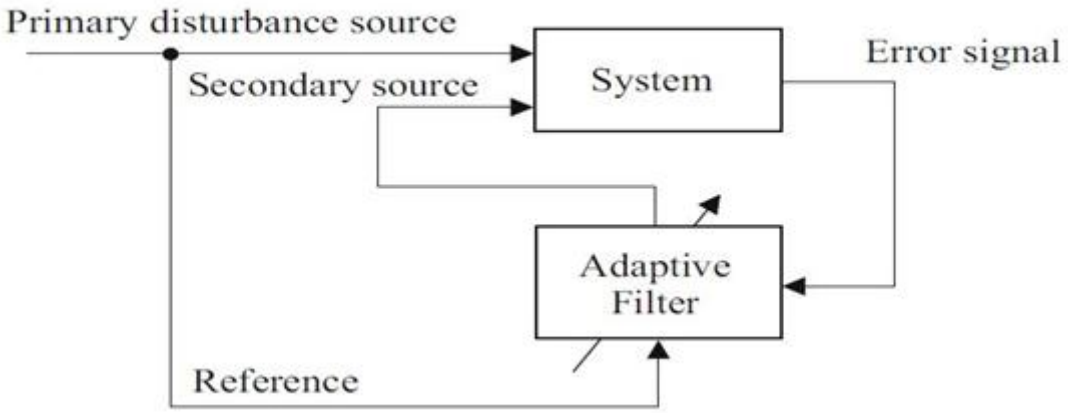

Fig. 1.4 Principle of feedforward control

The idea is to produce a secondary disturbance such that it cancels the effect of the primary disturbance at the location of the error sensor. Of course, there is no guarantee that the global response is also reduced at other locations and, unless the response is dominated by a single mode, there are places where the response can be amplified; the method can therefore be considered as a local one, in contrast to feedback which is global. Unlike active damping which can only attenuatethe disturbances near the resonances, feedforward works for any frequency and attempts to cancel the disturbance completely by generating a secondary signal of opposite phase. The method does not

need a model of the system, but the adaption procedure relies on the measured impulse response. The approach works better for narrow-band disturbances, but wide-band applications have also been reported. Because it is less sensitive to phase lag than feedback, feedforward control can be used at higher frequency (a good rule of thumb is $\omega_c \cong \omega_s/10$); this is why it has been so successful in acoustics. The main limitation of feedforward adaptive filtering is the availability ofa reference signal correlated to the disturbance. There are many applications where such a signal can be readily available from a sensor located on the propagation path of the perturbation. For disturbances induced by rotating machinery, an impulse train generated by the rotation of the main shaft can be used as reference.

1.5.3 Comparison of feedback and feed-forward control strategies

Type of control	Advantages	Disadvantages
Feedback Active damping	• no model needed guaranteed stability • when collocated • global method	• effective only near resonances • limited bandwidth ($\omega_c << \omega_s$)
Model based (LQG,H ∞...)	• attenuates all disturbances within ω_c	• disturbances outside ω_c are amplified • spillover
Feed forward Adaptive filtering of reference *(x-filtered LMS*)	• no model necessary • wider bandwidth ($\omega_c \approx \omega_s$ /10) • Works better for narrow-band disturb.	• reference needed • local method (response may be amplified in some part of the system) • large amount of real time computations

1.5.4 The Various Steps of the Design

The various steps of the design of a controlled structure are shown in Fig. 1.5. The starting point is a mechanical system, some performance objectives (e.g. position accuracy) and a specification of the disturbances applied to it; the controller cannot be designed without some knowledge of the disturbance applied to the system. If the frequency distribution of the energy of the disturbance (i.e. the power spectral density) is known, the open-loop performances can be evaluated and the need for an active

control system can be assessed. If an active system is required, its bandwidth can be roughly specified.

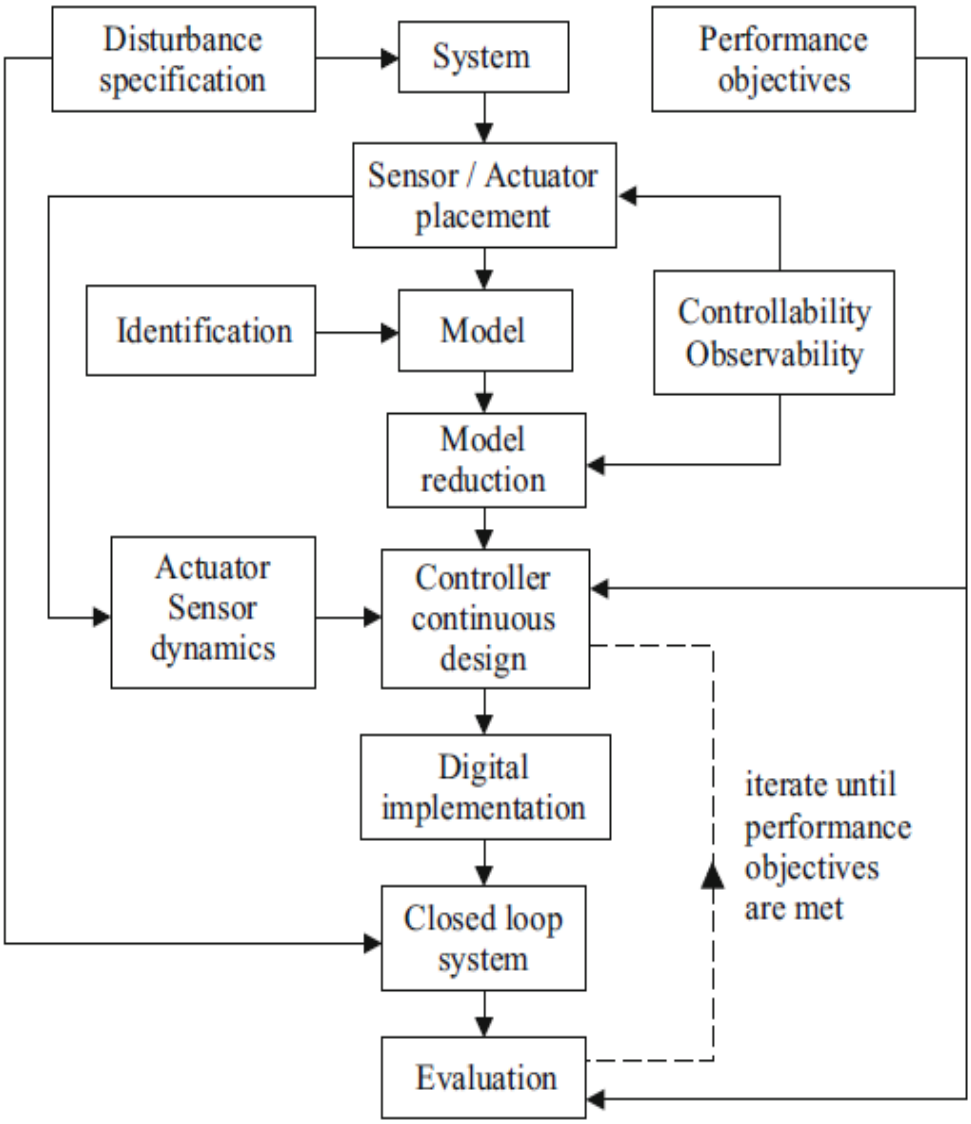

Fig. 1.5 The various steps of the design

The next step consists of selecting the proper type and location for a set of sensors to monitor the behavior of the system, and actuators to control it. The concept of controllability measures the capability of an actuator to interfere with the states of the system. Once the actuators and sensors have been selected, a model of the structure is developed, usually with finite elements; it can be improved by identification if experimental transfer functions are available. Such models generally involve too many degrees of freedom to be directly useful for design purposes; they must be reduced to produce a control design model involving only a few degrees of freedom, usually the

vibration modes of the system, which carry the most important information about the system behavior. At this point, if the actuators and sensors can be considered as perfect (in the frequency band of interest), they can be ignored in the model; their effect on the control system performance will be tested after the design has been completed. If, on the contrary, the dynamics of the actuators and sensors may significantly affect the behavior of the system, they must be included in the model before the controller design. Even though most controllers are implemented in a digital manner, nowadays, there are good reasons to carry out a continuous design and transform the continuous controller into a digital one with an appropriate technique. This approach works well when the sampling frequency is two orders of magnitude faster than the bandwidth of the control system, as is generally the case in structural control.

1.6 Transducer

A transducer is a device that converts one form of energy to another. Energy types Include (but are not limited to): electrical,mechanical, electromagnetic (including light), chemical, acoustic, and thermal energy. Usually a transducer converts a signal in one form of energy to a signal in another (for example, a loudspeaker driver converts an electric signal to sound), but any variable attenuation of energy may serve as input; for example, the light reflecting off the landscape, although it is not a signal, conveys information that image sensors, one form of transducer, can convert.

A sensor is a transducer whose purpose is to sense (i.e. detect) some characteristic of its environs; it is used to detect a parameter in one form and report it in another form of energy, often an electrical signal. For example, a pressure sensor might detect pressure (a mechanical form of energy) and convert it to electrical signal for display at a remote gauge. Transducers are widely used in measuring instruments.

An actuator is a transducer that accepts energy and produces the kinetic energy of movement (action). The energy supplied to an actuator might be electrical or mechanical (pneumatic, hydraulic, etc.). An electric motor and a hydraulic cylinder are both actuators, converting electrical energy and fluid power into motion for different purposes.

Combination transducers have both functions; they both detect and create action. The most common example is an antenna, a transducer of radio waves that can transmit, receive, or both (transceiver). Another example is the typical ultrasonic transducer, which switches back and forth many times a second between acting as an actuator to

produce ultrasonic waves, and acting as a sensor to detect ultrasonic waves. Rotating a DC electric motor's rotor will produce electricity, and voice-coil speakers can also act as microphones.

1.6.1 Electromechanical Transducer

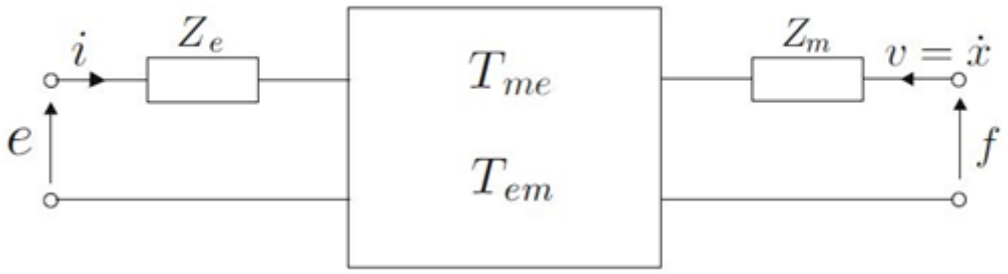

Fig. 1.6 Electrical analog representation of an electromechanical transducer

Constitutive Equations

The constitutive behavior of a wide class of electromechanical transducers can be modelled as in Fig.1.6, where the central box represents the conversion mechanism between electrical energy and mechanical energy, and vice versa. In Laplace form, the constitutive equations read

$e = Z_e i + T_{em} v$ (1.5)

$f = T_{me} i + Z_m v$ (1.6)

Where e is the Laplace transform of the input voltage across the electrical terminals, ithe input current, f the force applied to the mechanical terminals, and v the velocity of the mechanical part. $Z_e$is the blocked electrical impedance, measured for v = 0; Tem is the transduction coefficient representing the electromotive force (voltage) appearing in the electrical circuitper unit velocity in the mechanical part (in volt.sec/m). $T_{me}$is the transduction coefficient representing the force acting on the mechanical terminals to balance the electromagnetic force induced per unit current input on the electrical side (in N/Amp), and $Z_m$is the mechanical impedance, measured when the electrical side is open (i= 0).

In absence of external force (f = 0), v can be eliminated between the two foregoing equations, leading to

$$e = \left(Z_e - \frac{T_{em}T_{me}}{Z_m}\right) i \quad (1.7)$$

$-T_{em}T_{me}/Z_m$is called the motional impedance. The total driving point electricalimpedance is the sum of the blocked and the motional impedances.

Self-sensing

Equation (1) shows that the voltage drop across the electrical terminals of any electromechanical transducer is the sum of a contribution proportional to the current applied and a contribution proportional to the velocity of the mechanical terminals. Thus, if $Z_e$ican be measured and subtracted from e, a signal proportional to the velocity is obtained. This suggests the bridge structure of Fig.1.7. The bridge equations are as follows: for the branch containing the transducer,

$$e = Z_e I + T_{em} v + Z_b I \quad (1.8)$$

$$I = \frac{1}{Z_e + Z_b}(e - T_{em} v) \quad (1.9)$$

$$V_4 = Z_b I = \frac{Z_b}{Z_e + Z_b}(e - T_{em} v) \quad (1.10)$$

For the other branch,

$$e = kZ_e i + kZ_b i \quad (1.11)$$

$$V_2 = kZ_b i = \frac{Z_b}{Z_e + Z_b} e \quad (1.12)$$

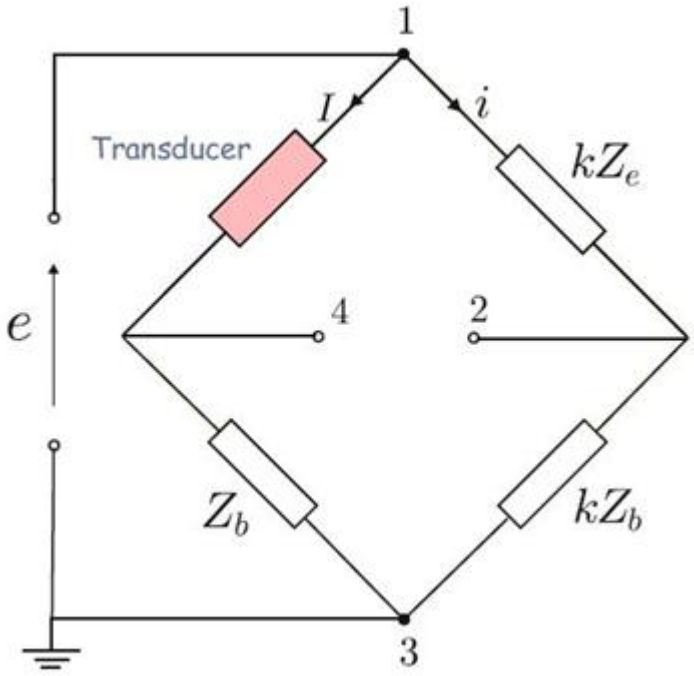

Fig. 1.7 Bridge circuit for self-sensing actuation

and the bridge outpu

$$V_4 - V_2 = \left(\frac{-Z_b T_{em}}{Z_e + Z_b}\right) v \tag{1.13}$$

is indeed a linear function of the velocity v of the mechanical terminals. Note,however, that $-Z_b T_{em}/(Z_e + Z_b)$ acts as a filter; the bridge impedance $Z_b$must be adapted to the transducer impedance $Z_e$to avoid amplitude distortionand phase shift between the output voltage V_4–$V_2$and the transducervelocity in the frequency band of interest.

1.6.2 Piezoelectric Transducer

The piezoelectric effect was discovered by Pierre and Jacques Curie in 1880. The direct piezoelectric effect consists in the ability of certain crystalline materials to generate an electrical charge in proportion to an externally applied force; the direct effect is used in force transducers. According to the inverse piezoelectric effect, an electric field parallel to the direction of polarization induces an expansion of the material. The piezoelectric effect is anisotropic; it can be exhibited only by materials whose crystal structure has no center of symmetry; this is the case for some ceramics below a certain temperature called the Curie temperature; in this phase, the crystal has built-in electric dipoles, but the dipoles are randomly orientated and the net electric dipole on a macroscopic scale is zero. During the poling process, when the crystal is cooled in the presence of a high electric field, the dipoles tend to align, leading to an electric dipole on a macroscopic scale. After cooling and removing of the poling field, the dipoles cannot return to their original position; they remain aligned along the poling direction and the material body becomes permanently piezoelectric, with the ability to convert mechanical energy to electrical energy and vice versa; this property will be lost if the temperature exceeds the Curie temperature or if the transducer is subjected to an excessive electric field in the direction opposed to the poling field. The most popular piezoelectric materials are Lead-Zirconate-Titanate (PZT) which is a ceramic, and Polyvinylidene fluoride (PVDF) which is a polymer. In addition to the piezoelectric effect, piezoelectric materials exhibit a pyro-electric effect, according to which electric charges are generated when the material is subjected to temperature; this effect is used to produce heat detectors. We

consider a transducer made of a one-dimensional piezoelectricmaterial of constitutive equation

$$D = \varepsilon^{T}E + d_{33}T \quad (1.14)$$

$$S = d_{33}E + s^{E}T \quad (1.15)$$

Where D is the electric displacement (charge per unit area, expressed in Coulomb/m^2), E the electric field (V/m), T the stress (N/m^2) and S the strain. $\varepsilon^{T}$is the dielectric constant (permittivity) under constant stress, $s^{E}$is the compliance when the electric field is constant (inverse of the Young's modulus) and d^{33} is the piezoelectric constant, expressed in m/V or Coulomb/Newton; the reason for the subscript 33 is that, by convention, index 3 is always aligned to the poling direction of the material, and we assume that the electric field is parallel to the poling direction. More complicated situations will be considered later. Note that the same constant d_{33}appears in (1) and (2). In the absence of an external force, a transducer subjected to a voltage with the same polarity as that during poling produces an elongation, and a voltage opposed to that during poling makes it shrink (inverse piezoelectric effect). In (2), this amounts to a positive d_{33}. Conversely (direct piezoelectric effect), if we consider a transducer with open electrodes (D = 0), according to (1), $E = -(d_{33}/\varepsilon^{T})T$, which means that a traction stress will produce a voltage with polarity opposed to that during poling, and a compressive stress will produce a voltage with the same polarity as that during poling.

1.7 Beam Theories

1.7.1 Timoshenko Beam Theory

The Timoshenko beam theory was developed by Russian scientist and engineer of Ukrainian ethnicity Stephen Timoshenko early in the 20th century.[47][48] The model takes into account shear deformation and rotational inertia effects, making it suitable for describing the behaviour of short beams, sandwich composite beams or beams subject to high-frequency excitation when the wavelength approaches the thickness of the beam. Physically, taking into account the added mechanisms of deformation effectively lowers the stiffness of the beam, while the result is a larger deflection under a static load and lower predicted eigen frequencies for a given set of boundary conditions. The latter

effect is more noticeable for higher frequencies as the wavelength becomes shorter, and thus the distance between opposing shear forces decreases.

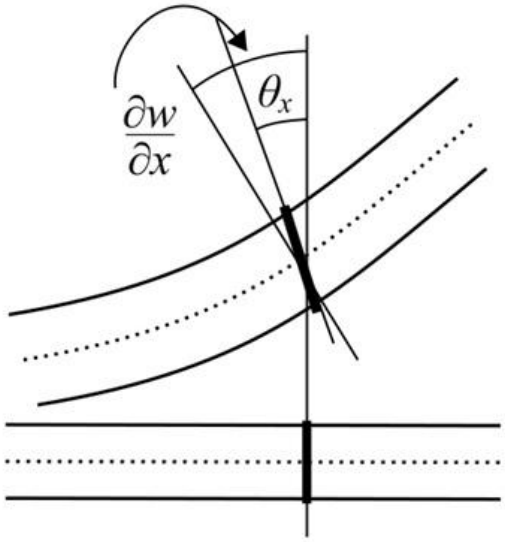

Fig: 1.8 Deformation of a Timoshenko beam. The normal rotates by an amount $\theta_x = \varphi(x)$ which is not equal to dw/dx.

In static Timoshenko beam theory without axial effects, the displacements of the beam are assumed to be given by

$$u_x(x,y,z) = -z\varphi(x) \tag{1.16}$$

$$u_y(x,y,z) = 0 \tag{1.17}$$

$$u_z(x,y) = \omega(x) \tag{1.18}$$

where (x,y,z) are the coordinates of a point in the beam, u_x,u_y,u_z are the components of the displacement vector in the three coordinate directions, φ is the angle of rotation of the normal to the mid-surface of the beam, and w is the displacement of the mid-surface in the z-direction. The governing equations are the following uncoupled system of ordinary differential equations:

$$\frac{d^2}{dx^2}\left(EI\frac{d\varphi}{dx}\right) = q(x,t) \tag{1.19}$$

$$\frac{d\omega}{dx} = \varphi - \frac{1}{kAG}\frac{d}{dx}\left(EI\frac{d\varphi}{dx}\right) \tag{1.20}$$

The Timoshenko beam theory for the static case is equivalent to the Euler-Bernoulli theory when the last term above is neglected, an approximation that is valid when

$$\frac{EI}{kL^2AG} \ll 1 \quad (1.21)$$

Where,

- L is the length of the beam.
- A is the cross section area.
- E is the elastic modulus.
- G is the shear modulus.
- I is the second moment of area.
- k, called the Timoshenko shear coefficient, depends on the geometry. Normally, k=5/6 for a rectangular section.

Combining the two equations gives, for a homogeneous beam of constant cross-section,

$$EI\frac{d^4\omega}{dx^4} = q(x) - \frac{EI}{kAG}\frac{d^2q}{dx^2} \quad (1.22)$$

The bending moment M_{xx} and the shear force Q_x in the beam are related to the displacement w and the rotation φ. These relations, for a linear elastic Timoshenko beam, are:

$$M_{xx} = -EI\frac{\partial\varphi}{\partial x} and Q_x = kAG\left(-\varphi + \frac{\partial\omega}{\partial x}\right) \quad (1.23)$$

Boundary conditions

The two equations that describe the deformation of a Timoshenko beam have to be augmentedwith boundary conditions if they are to be solved. Four boundary conditions are needed for the problem to be well-posed. Typical boundary conditions are:

- Simply supported beams: The displacement w is zero at the locations of the two supports. The bending moment M_{xx} applied to the beam also has to be specified. The rotation and the transverse shear force Q_x are not specified.
- Clamped beams: The displacement w and the rotation φ are specified to be zero at the clamped end. If one end is free, shear force Q_x and bending moment M_{xx} have to be specified at that end.

For a cantilever beam,one boundary is clamped while the other is free. Let us use a right handed coordinate system, where the x direction is positive towards right and the z direction is positive upward. Following normal convention, we assume that positive forces act in the positive directions of the x and z axes and positive moments act in the clockwise direction. We also assume that the sign convention of the stress resultants (M_{xx} and Q_x) is such that positive bending moments compress the material at the bottom of the beam (lower z coordinates) and positive shear forces rotate the beam in a counterclockwise direction.

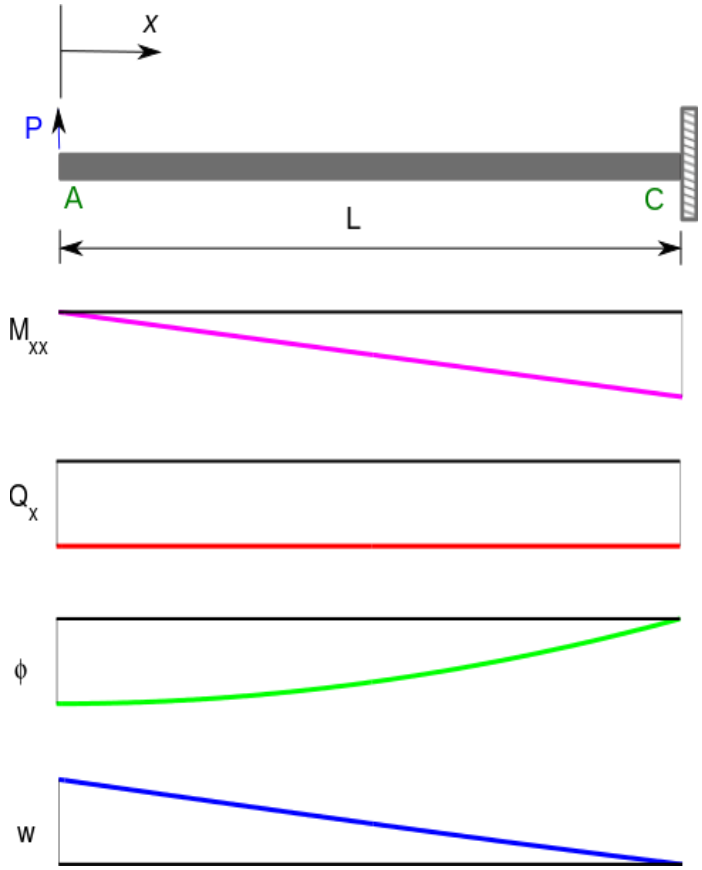

Fig: 1.9A cantilever Timoshenko beam under a point load at the free end.

Let us assume that the clamped end is at x = L and the free end is at x = 0. If a point load P is applied to the free end in the positive z direction, a free body diagram of the beam gives us

$$-Px - M_{xx} = 0 \; or M_{xx} = -Px \tag{1.24}$$

and

$$P + Q_x = 0 \; or Q_x = -P \tag{1.25}$$

Therefore, from the expressions for the bending moment and shear force, we have

$$Px = EI\frac{d\varphi}{dx} and \; -P = kAG\left(-\varphi + \frac{d\omega}{dx}\right) \tag{1.26}$$

Integration of the first equation, and application of the boundary condition φ = 0 at x = L, leads to

$$\varphi(x) = -\frac{P}{2EI}(L^2 - x^2) \tag{1.27}$$

The second equation can then be written as

$$\frac{d\omega}{dx} = -\frac{P}{kAG} - \frac{P}{2EI}(L^2 - x^2) \tag{1.28}$$

Integration and application of the boundary condition $w = 0$ at x = L gives

$$\omega(x) = \frac{P(L-x)}{kAG} - \frac{Px}{2EI}\left(L^2 - \frac{x^2}{3}\right) + \frac{PL^3}{3EI} \tag{1.29}$$

The axial stress is given by

$$\sigma_{xx}(x,z) = E\,\varepsilon_{xx} = -Ez\frac{d\varphi}{dx} = -\frac{Pxz}{I} = \frac{M_{xx}z}{I} \qquad (1.30)$$

1.7.2 Euler–Bernoulli Beam Theory

Euler–Bernoulli beam theory (also known as engineer's beam theory or classical beam theory)[49] is a simplification of the linear theory of elasticity which provides a means of calculating the load-carrying and deflection characteristics of beams. It covers the case for small deflections of a beam that is subjected to lateral loads only. It is thus a special case of Timoshenko beam theory. It was first enunciated circa 1750,[50] but was not applied on a large scale until the development of the Eiffel Tower and the Ferris wheel in the late 19th century. Following these successful demonstrations, it quickly became a cornerstone of engineering and an enabler of the Second Industrial Revolution.

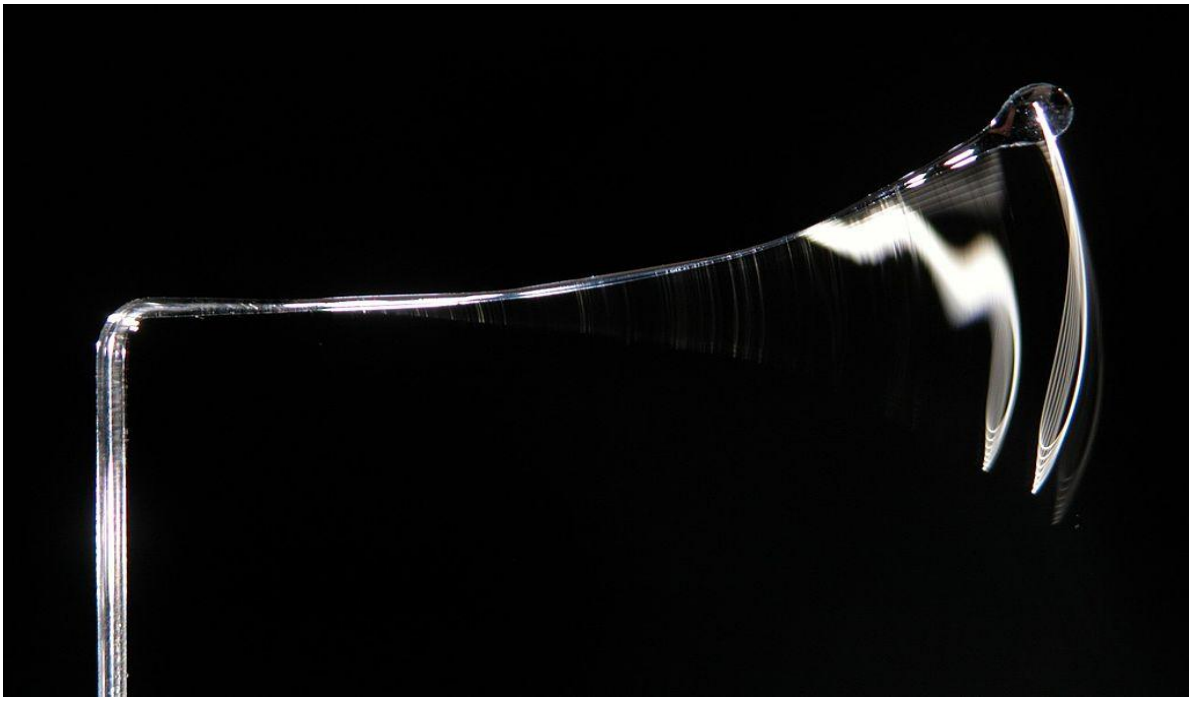

Fig: 1.10 This vibrating glass beam may be modeled as a cantilever beam with acceleration, variable linear density, variable section modulus, some kind of dissipation, springy end loading, and possibly a point mass at the free end.

This vibrating glass beam may be modeled as a cantilever beam with acceleration, variable linear density, variable section modulus, some kind of dissipation, springy end loading, and possibly a point mass at the free end.

The Euler-Bernoulli equation describes the relationship between the beam's deflection and the applied load:

$$\frac{d^2}{dx^2}\left(EI\frac{d^2\omega}{dx^2}\right) = q \tag{1.31}$$

The curve ω(x) describes the deflection of the beam in the z direction at some position x (the beam is modeled as a one-dimensional object). qis a distributed load, in other words a force per unit length (analogous to pressure being a force per area); it may be a function of x, ω, or other variables.

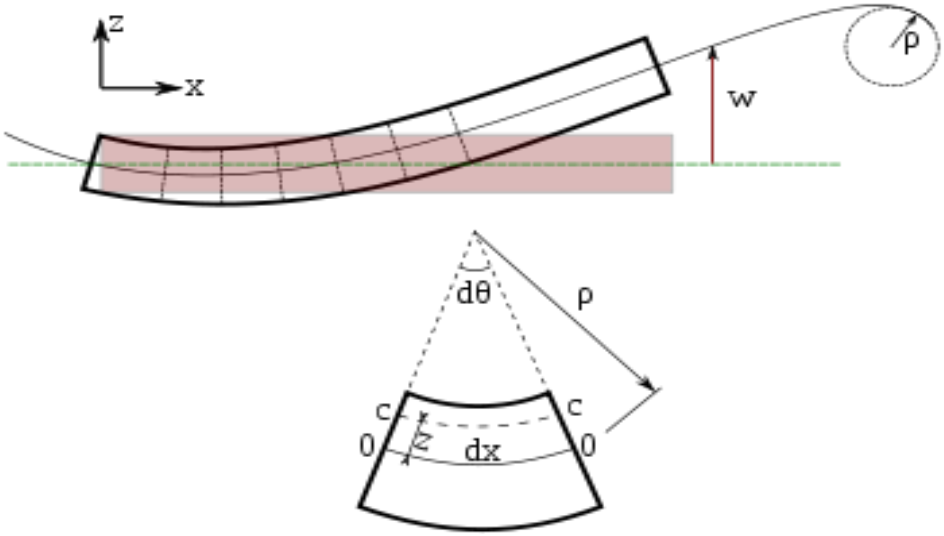

Fig: 1.11 Bending of an Euler–Bernoulli beam. Each cross-section of the beam is at 90 degrees to the neutral axis.

Note that E is the elastic modulus and that I is the second moment of area. I must be calculated with respect to the centroidal axis perpendicular to the applied loading. For an Euler-Bernoulli beam not under any axial loading this axis is called the Neutral axis. Often, EI is a constant, so that:

$$EI\frac{d^4\omega}{dx^4} = q(x) \tag{1.32}$$

This equation, describing the deflection of a uniform, static beam, is used widely in engineering practice. For more complicated situations the deflection can be determined by solving the Euler-Bernoulli equation using techniques such as the "slope deflection method", "moment distribution method", "moment area method, "conjugate beam method", "the principle of virtual work", "direct integration", "Castigliano's method", "Macaulay's method" or the "direct stiffness method".

Sign conventions are defined here since different conventions can be found in the literature. In this article, a right handed coordinate system is used as shown in the figure, bending of an Euler-Bernoulli beam. In this figure, the x and z direction of a right handed coordinate system are shown. Since $e_x * e_y = e_z$ where e_x, e_y and e_z are unit vectors in the direction of the x, y, and z axes respectively, the y axis direction is into the figure. Forces acting in the positive x and z directions are assumed positive. The sign of the bending moment is positive when the torque vector associated with the bending moment on the right hand side of the section is in the positive y direction (i.e. so that a positive value of M leads to a compressive stress at the bottom fibers).

With this choice of bending moment sign convention, in order to have dM=Qdx, it is necessary that Q the shear force acting on the right side of the section be positive in the z direction so as to achieve static equilibrium of moments. To have force equilibrium with dQ= qdx, the loading intensity must be positive in the minus z direction. In addition to these sign conventions for scalar quantities, we also sometimes use vectors in which the directions of the vectors are made clear through the use of the unit vectors, e_x, e_y, e_z.

Successive derivatives of w have important meanings where w is the deflection in the z direction:

$$M = -EI\frac{d^2\omega}{dx^2} \tag{1.33}$$

is the bending moment in the beam, and

$$Q = -\frac{d}{dx}\left(EI\frac{d^2\omega}{dx^2}\right) \tag{1.34}$$

is the shear force in the beam.

For cantilever beam, the boundary conditions is length L (fixed at x = 0) are

$$\hat{w}_n = 0\,, \quad \frac{d\hat{w}_n}{dx} = 0 \quad \text{at} \quad x = 0 \tag{1.35}$$

$$\frac{d^2\hat{w}_n}{dx^2} = 0\,, \quad \frac{d^3\hat{w}_n}{dx^3} = 0 \quad \text{at} \quad x = L\,. \tag{1.36}$$

If we apply these conditions, non-trivial solutions are found to exist only if $\cosh(\beta_n L)\,\cos(\beta_n L) + 1 = 0$. this nonlinear equation can be solved numerically. The first few roots are β_1 L = 1.875, β_2 L = 4.694, β_3 L = 7.855, β_4 L = 10.9955...

The corresponding natural frequencies of vibration are

$$\omega_1 = \beta_1^2\sqrt{\frac{EI}{\mu}} = \frac{3.515}{L^2}\sqrt{\frac{EI}{\mu}}\ , \quad \ldots \tag{1.37}$$

Boundary Conditions

The boundary conditions can also be used to determine the mode shapes from the solution for the displacement:

$$\hat{w}_n = A_1\left[\cosh\beta_n x - \cos\beta_n x + \frac{(\cos\beta_n L + \cosh\beta_n L)(\sin\beta_n x - \sinh\beta_n x)}{\sin\beta_n L + \sinh\beta_n L}\right] \tag{1.38}$$

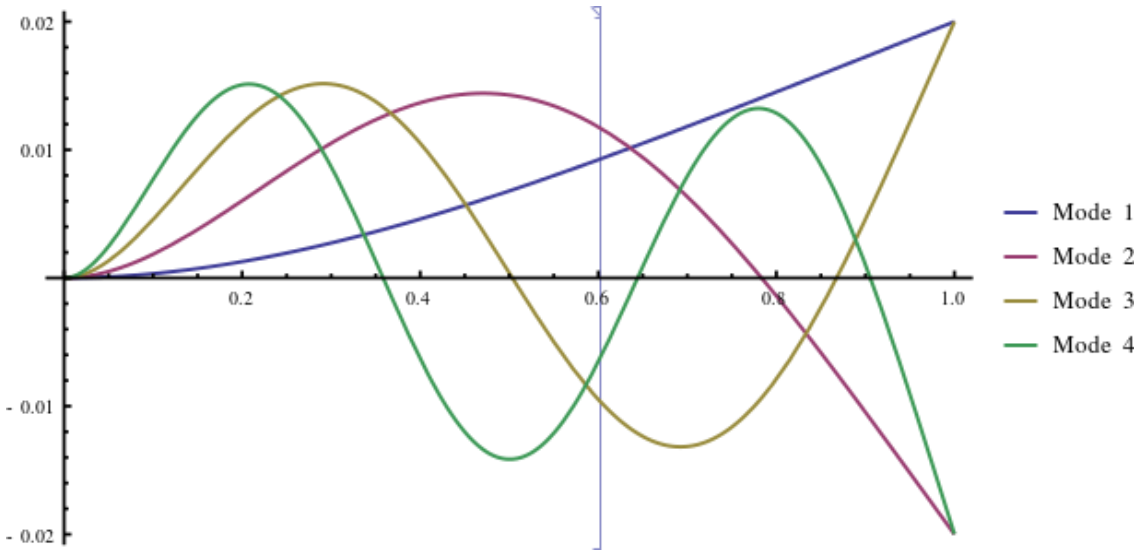

Fig: 1.12 Mode shapes for the first four modes of a vibrating cantilever beam.

The unknown constant (actually constants as there is one for each n), A_1, which in general is complex, is determined by the initial conditions at t = 0 on the velocity and displacements of the beam. Typically a value of A_1 = 1 is used when plotting mode shapes. Solutions to the undamped forced problem have unbounded displacements when the driving frequency matches a natural frequency ω_n, i.e., the beam can resonate. The natural frequencies of a beam therefore correspond to the frequencies at which resonance can occur.

Equation of Motion

Lagrange's equation to formulate equations of motion are given by

$$\frac{d}{dt}\left(\frac{dT}{d\dot{q}_i}\right) - \frac{\partial T}{\partial q_i} + \frac{\partial A}{\partial q_i} = Q_i(i = 1, 2, 3, \ldots\ldots\ldots\ldots n) \tag{1.39}$$

Where, t=time

T = Kinetic energy of system

q_i= Time derivative of coordinate system representing velocity

A = Potential energy of the system

Q_i = Non conservative forces or moment

Consider a single degree of freedom system that requires only one coordinate q to describe its behavior. To apply it in Eq.(1) to express the kinetic and potential energies of the system in terms of coordinate q and its derivative q'. Let q=x then, the kinetic and potential energy of the system are

$$T = \frac{1}{2}mx^{\cdot 2} \tag{1.40}$$

$$A = \frac{1}{2}kx^2 \tag{1.41}$$

Now, differentiating the kinetic energy term with respect to $q^{\cdot} = x^{\cdot}$

$$\frac{\partial T}{\partial q^{\cdot}} = \frac{\partial \dot{T}}{\partial x^{\cdot}} = \frac{\partial}{\partial x^{\cdot}}\left(\frac{1}{2}x^{\cdot 2}\right) = (2)\left(\frac{1}{2}\right)mx^{\cdot} = mx^{\cdot} \tag{1.42}$$

Then, taking the time derivative of $\frac{\partial T}{\partial x^{\cdot}}$ we get,

$$\frac{d}{dt}\left(\frac{\partial T}{\partial x^{\cdot}}\right) = \frac{d}{dt}(mx^{\cdot}) = mx^{\cdot\cdot} \tag{1.43}$$

Because T is the function of $x^{\cdot} and not x, \frac{\partial T}{\partial x} = 0$. Evaluating the potential term, $\partial A/\partial q$ in Eq.(1). We get,

$$\frac{\partial A}{\partial q} = \frac{\partial A}{\partial x} = \frac{\partial}{\partial x}\left(\frac{1}{2}kx^2\right) = kx \tag{1.44}$$

Substituting for each term in Eq.(1).We get,

$$\frac{d}{dt}\left(\frac{\partial T}{\partial q_i}\right) - \frac{\partial T}{\partial q_i} + \frac{\partial A}{\partial q_i} = Q_i \tag{1.45}$$

The governing differential equation of motion is given by

$$mx^{\cdot\cdot} + kx = 0 \tag{1.46}$$

Now, consider a system with two degree of freedom, consequently we need two coordinates x_1 and x_2 to formulate kinetic and potential energies,

$$T = \frac{1}{2}m_1\dot{x_1}^2 + m_2\dot{x_2}^2 \tag{1.47}$$

$$A = \frac{1}{2}k_1x_1^2 + \frac{1}{2}k_2(x_2 - x_1)^2 \tag{1.48}$$

Taking the derivative of each terms, as required by Eq.(1). We get,

$$\frac{\partial T}{\partial \dot{x_1}} = m_1\dot{x_1} and \frac{d}{dt}\left(\frac{\partial T}{\partial \dot{x_1}}\right) = m_1\ddot{x_1} \tag{1.49}$$

$$\frac{\partial T}{\partial \dot{x_2}} = m_2\dot{x_2} and \frac{d}{dt}\left(\frac{\partial T}{\partial \dot{x_2}}\right) = m_2\ddot{x_2} \tag{1.50}$$

$$\frac{\partial T}{\partial x_1} = \frac{\partial T}{\partial x_2} = 0 \tag{1.51}$$

$$\frac{\partial A}{\partial x_1} = k_1x_1 + k_2(x_1 - x_2) \tag{1.52}$$

$$\frac{\partial A}{\partial x_2} = k_2(x_2 - x_1) \tag{1.53}$$

Substituting each term in Lagrange's equation in Eq.(1). We get,

$$m_1\ddot{x_1} + (k_1 + k_2)x_1 - k_2x_2 = 0 \tag{1.54}$$

$$m_2\ddot{x_2} - k_2x_1 + k_2x_2 = 0 \tag{1.55}$$

We can express equation of motion in a matrix form by

$$\begin{bmatrix} m_1 & 0 \\ 0 & m_2 \end{bmatrix}\begin{Bmatrix} \ddot{x_1} \\ \ddot{x_2} \end{Bmatrix} + \begin{bmatrix} k_1 + k_2 & -k_2 \\ -k_2 & k_2 \end{bmatrix}\begin{Bmatrix} x_1 \\ x_2 \end{Bmatrix} = \begin{Bmatrix} 0 \\ 0 \end{Bmatrix} \tag{1.56}$$

Now, finite element formulation of axial members by using Lagrange's equations, formulating the mass matrix for an axial member and then using it for calculating the natural frequencies of an axial member.

Formulating Mass Matrix

The displacement of an axial member is expressed by using one-dimensional shape function S_i and S_j,

$$u = S_i U_i + S_j U_j \tag{1.57}$$

Now, the shape function in terms of the local coordinate x, as shown in figure are given by

$$S_i = 1 - \frac{x}{L} \tag{1.58}$$

$$S_j = \frac{x}{L} \tag{1.59}$$

For a dynamic problem the displacement function is a function of x and time t, i.e. u=u(x,t). The total kinetic energy of the member is the sum of the kinetic energies of its constituent particles

$$T = \int_0^L \frac{\gamma}{2} \dot{u}^2 dx \tag{1.60}$$

The velocity of the member is expressed in terms of $U_i and U_j$ is given by

$$\dot{u} = S_i \dot{U_i} + S_j \dot{U_j} \tag{1.61}$$

Where

u· = Velocity of the particles along the member.

γ = mass per unit length

Substituting Eq. (6) into Eq. (5), we get

$$T = \frac{\gamma}{2} \int_0^L (S_i U_i + S_j U_j)^2 \, dx \tag{1.62}$$

After taking derivatives as required by Lagrange's Equation (1). We get,

$$\frac{\partial T}{\partial U_i} = \frac{\gamma}{2} \int_0^L 2 \, S_i \left(S_i U_i + S_j U_j\right)^2 dx \tag{1.63}$$

$$\frac{\partial T}{\partial U_j} = \frac{\gamma}{2} \int_0^L 2 S_j \left(S_i U_i + S_j U_j\right)^2 dx \tag{1.64}$$

$$\frac{d}{dt}\left(\frac{\partial T}{\partial \dot{u}_j}\right) = \gamma \left[\int_0^L S_j^2 \ddot{U_i} dx + \int_0^L S_i S_j \ddot{U_j} \, dx\right] \tag{1.65}$$

$$\frac{d}{dt}\left(\frac{\partial T}{\partial \dot{U_j}}\right) = \gamma \left[\int_0^L S_i S_j \ddot{U_i} dx + \int_0^L S_j^2 \ddot{U_j} dx\right] \tag{1.66}$$

Here S_i and S_j are the functions of x alone, whereas $U_i^{\cdot\cdot} and U_j^{\cdot\cdot}$ represent accelerations at node i and j respectively, which are function of time.

Evaluating the integrals of Eq.(8) & Eq.(9). We get,

$$\gamma \int_0^L S_i^2 dx = \gamma \int_0^L \left(1 - \frac{x}{L}\right)^2 dx = \frac{\gamma L}{3} \quad (1.67)$$

$$\gamma \int_0^L S_j^2 \, dx = \gamma \int_0^L \left(\frac{x}{L}\right)^2 dx = \frac{\gamma L}{3} \quad (1.68)$$

Solving Eq. (8) through Eq.(9) into Eq.(6) and Eq.(7) gives the mass matrix,

$$[M] = \frac{\gamma L}{6}\begin{bmatrix} 2 & 1 \\ 1 & 2 \end{bmatrix} \quad (1.69)$$

Formulating Stiffness Matrix

During the deformation the member under axial loading, the strain energy stored is given by

$$A^{(e)} = \int_v \frac{\sigma\varepsilon}{2} dV = \int_v \frac{E\varepsilon^2}{2} dV \quad (1.70)$$

Now, the total potential energy Π for the body contains n elements and m modes is given by

$$\Pi = \sum_{e=1}^{n} A^{(e)} - \sum_{i=1}^{m} F_i u_i \quad (1.71)$$

The deflection for an element with nodes I & j in terms of local shape function is given by,

$$u^{(e)} = S_i u_i + S_j u_j \quad (1.72)$$

The strain in each member is calculated by

$$\varepsilon = \frac{-u_i + u_j}{\varrho} \quad (1.73)$$

Substituting Eq.(13) into Eq.(10) yields the strain energy for an arbitrary element (e) and minimizing w.r.t. u_i and u_j leads in matrix form

$$\begin{Bmatrix} \frac{\partial A^{(e)}}{\partial u_i} \\ \frac{\partial A^{(e)}}{\partial \mathrm{u}_j} \end{Bmatrix} = \frac{AE}{L}\begin{bmatrix} 1 & -1 \\ -1 & 1 \end{bmatrix}\begin{Bmatrix} u_i \\ u_j \end{Bmatrix} \quad (1.74)$$

Eq. (14) is Stiffness matrix

$$[K] = \frac{AE}{L}\begin{bmatrix} 1 & -1 \\ -1 & 1 \end{bmatrix} \quad (1.75)$$

Solving mass and stiffness matrix for eigen values by using the form

$$[M]^{-1}[K]\{U\}=\omega^2\{U\} \quad (1.76)$$

1.8 Need of the Work

The present thesis addresses the control of dynamic performance of mechanical equipments such as in this work a portal frame structure. This has been the need of most of the machine tool structure under high precision machining and Nano range surface finish requirement at present. In previous research's active vibration control is applied on simple structures like cantilever beam but today due to the advancement of technology, complex structures are for different applications with different boundary conditions. So, it is required to control the vibration of these structures. For preventing the vibration strategic modelling and analysis would be used in controlling vibration and equally used for other applications such as chassis design of a vehicle, a space launch bed, railway coach design for high comfort requirement etc. Advances in theory and practice of active structural control technology have modified the general perception of structures. Due to incorporated intelligence, structures become dynamic object capable of interacting with complex structure in complex environments. The aim of an intelligent structure is to enhance the structural performance by sensing the changes in behavior of loading, adapting the structure to meet goals and retrieving past events to improve the future performance. The intelligent control methodology into structural engineering has potential to enhance the concept of control. This research would be a tool to improve the dynamic behavior of all these stated structures.

1.9 Objective of the Thesis

- To conduct the parametric study on the dynamic behaviour of the existing complex structure.
- To develop the mathematical model of free vibrations of existing beam structure of metallic isotropic Material embedded with piezoelectric patches.
- To carry out modifications options for parameter to have optimal control strategy.
- To apply the above modification to develop a model and control the vibration of an existing complex structure under given dynamic condition.

CHAPTER - 2

REVIEW OF LITERATURE

After the study of different research papers, we have categorized all the paper into three sections those are as

1. Experimental work
2. Analytical work
3. Experimental and analytical work

2.1 EXPERIMANTAL WORK

Clarkson et al. (1981) carried out a study on experimental determination of modal densities and loss factors of flat plates and cylinders. In their experiments several accelerometers were required to determine the spatial average. The testswas repeated several times with different driving positions to obtain the average force position.

Reza Ahmadian et al. (1996), investigated, analyzed and compared the dynamic behavior of framed structures made of orthotropic materials. They demonstrated the vibration measurements of the framed structures and successfully achieved the modal analysis techniques and control.

L. Wu et al. (1997) studied the initial decay rate of vibrating plates in relation to estimates of loss factor. They worked experimentally on the initial decay rate of the energy decay curves on single, coupled, undamped, and damped rectangular plates. They confirmed that the loss factors obtained using the decay rate and the power input methods agree with each other for undamped, lightly damped, highly damped (up to a specific frequency) and coupled plates.

YavuzYaman et al. (2002), presented smart rectangular plate of a aluminum modeled in cantilever configuration with surface bonded piezoelectric sensor and electric patches which were bonded on the top and bottom surface. They investigated the actuator response increased with the increased size the response which behave in critical and concluded that the von-mises stresses used in the actuator were determined the maximum possible piezoelectric actuation valve prior to the operation and the piezoelectric is not expected to fail.

Shad Roundy et al. (2003), suggested that the conversion of vibrations was the best or most versatile method to scavenge ambient power. They investigated and evaluated Different conversion mechanisms to specific optimized designs for both capacitive Micro-Electro-Mechancial Systems (MEMS) and piezoelectric converters. Simulations show that the potential power density from piezoelectric conversion is significantly higher. Experimentally verify the accuracy of the models for piezoelectric converters.

M. Ericka et al.(2005), investigated the capability of harvesting electric energy from mechanical vibrations in a dynamic environment through a unimorph piezoelectric membrane transducer. They performed the experiments with a vibrating machine moving a macroscopic 25mm diameter piezoelectric membrane. The maximum power of 1.8mW was generated at the resonance frequency (2.58KHz) under an acceleration of 2g and a load resistance of 56 k. Analytical modeling of the generator was carried out and an equivalent electromechanical circuit.

S.P.Beeby et al.(2006)), carried out a study on experimental determination vibration energy harvesting of Vibration-powered generators. They presented the characteristic equations for inertial-based generators along with the specific damping equations that related to the three main transduction mechanisms which employed to extract energy from the system when mechanically stressed. Electrostatic generators utilize the relative movement between electrically isolated charged capacitor plates to generate energy. After which it was concluded that the work done against the electrostatic force between the plates provides the harvested energy from ambient vibrations generating output power with energy harvesting solution.

JaquesLottin et al. (2006), model of the flexible structure with efficient location of sensors and actuators encountered in the domain of active vibration optimum control scheme. The solution obtained by a finite element of the system and ANSYS software were used to build a general FEM description with the structure dynamic tool box to derive a state space with specific control scheme.

Aldo Giordano et al.(2007), carried out the studied to derived a formula for predicting the horizontal capacity of masonry portals in which four collapse mechanisms have been selected on account of mechanical and engineering considerations, and closed form expressions for the multipliers for each of them. The expressions have allowed to

perform extensive parametric analyses, varying the geometrical ratios that determine the portal configuration.

Sheng Wang et al.(2007), presented the capability of harvesting electrical energy from mechanical vibrations in a dynamic environment through a piezoelectric drum Under a pre-stress and a cyclic stress of a power of was generated at the resonance frequency of the transducer across an resistor. The transducer increases while the resonance frequency of the transducer decreases when the pre-stress increases. They experimentally concluded that the energy from the drum transducer could be increased along with the pre-stress, and the resonance frequency would be lowered with increasing pre-stress.

Jing-QuanLiu et al.(2008), carried out the designed and investigated to improve frequency flexibility of power generator array and cantilevers array which could be tuned to the frequency and expanded the excited frequency bandwidth in ambient low frequency vibration. Theyinvestigated the serial connection among cantilevers of the array and micro-power generator array has utilized PZT film as the transducer to harvest ambient low-level vibration. Theyconcluded that the arrayed device used to improving operation bandwidth and power output of power generator with the applications in wireless/embedded sensor networks.

John Kymissis et al.(2009), examined three different devices that can be built into a shoe, (where excess energy is readily harvested) and used for generating electrical power "parasitically" while walking. Two of these are piezoelectric in nature: a unimorph strip made from piezo-ceramic composite material and a stave made from a multilayer laminate of PVDF foil. The third is a shoe-mounted rotary magnetic generator. The PVDF stave produced peaks of roughly ±60 Volts, while the Thunder Unimorph gave significantly larger response, with peaks approaching 150 Volts.

Israel Lopez et al.(2010), reported the flight vehicle structural damage monitoring, diagnosis, prognosis and control developed to the uncertainty in the area of damage sensing, diagnosis, prognosis and control in flight vehicles. They presented mathematical and statistical methods in analyzing uncertainty were presented and compared. They identified and promising new ideas to control the under uncertainty.

.**E. Minazara et al.(2010),** designed a piezoelectric generator and installed it on a bicycle handlebar and utilized the mechanical vibrations energy of piezoelectric

generator that available on a bicycle toproduce electricity. They investigated that the static converter transforms the electrical energy in a suitable form to the targeted portable application. A value of generated electrical power wassufficient to recharge a battery or to power low consumption devices.

Mauro Manetti et al.(2010), Carried out the control scheme that provided precise active shape control of deformable mirror shells using a very large number of control points into account position measurement and control force noises and saturations, quantization errors, acquisition and computational delays. They suggested the controller combines a low frequency centralized feed forward and a high frequency fully decentralized feedback, with each single actuator mated to a single sensor. They obtained the Numerical results that confirm the validity of the control.

AchimBleicher et al.(2011), investigated a model of active vibration control for a stress ribbon bridge with an extremely light pneumatic actuator nonlinear bridge. A linearized model which represents the nonlinear behavior of the stress ribbon for multi-modal motions by using sensors to measure the nodal displacement were presented. To improve the control performance faster proportional pressure valves with faster pressure control to control higher modes and control strategy easily extended to multi-variable control system. The efficiency of the controller in reducing forced and random vibrations were reported.

J.K.Dutt et al.(2011), presented the coupled transverse-tensional vibration of Rotor–shaft systems. They presented the numerical simulation the effectiveness and influence of actively controlling the transverse rotor motion on its tensional frequencies. Theycontrolled the non- contact electromagnetic force from an actuator and Transverse vibration and that was also control the tensional oscillations. The Stability Limit Speed (SLS) of the system is also increased of the active control action and the system protect against tensional instability, and the system stabilize by control action of transverse vibration.

Zhanfeng Song et al.(2012), carried out the studied an adaptive disturbance rejection controller for wind turbines combined effects of internal dynamics, grid disturbances, cross-coupling. They demonstrated through frequency analysis as well as simulation validation that control scheme constrains the rotor currents during grid disturbances. They obtained the results, that the frequency-domain responses, stability and the strong

robustness of the control system against parameter uncertainties and external disturbances.

Bin Zi et al.(2012), modeling, analysis, and control of the cable-supporting system including actuator dynamics for the next generation large spherical radio telescope. They established the dynamic formulations of the electromechanical coupling system including servomechanism dynamics and parabolic curve of the long-span cable sag effects. The parabolic equation, and the dynamic modeling for control into account of the characteristics of nonlinearity, slow time-variant and multivariable coupling, a fuzzy control plus proportional-integral control method was utilized to control the wind-induced vibration of the cable-supporting system.

Jiˇrı´ Tuma et al.(2013), carried out a study on experimental determination for the active vibration control of journal bearings with the use of piezo actuators which actively controlled and the vibration was measured by a pair of proximity probes. The force produced by piezo actuators and acting at the bushing controlled according to the error signals which derived from the proximity probe output signals. It was experimentally proved that the active vibration control extends the range of the operational speed.

ZengkangGan et al. (2015), reported that unwanted vibration from vehicle seats were increasing the damage. They presented a model to reduce the vibration level transmitted to the seat pan and the occupants body under low frequency periodic excitation seat using electromagnetic linear actuators and effective performance was found for cancelling periodic vibration containing single and multiple frequencies the control system. After which they verified that the effectiveness of the active seat and adaptive control approach to reduce occupants vibration level under low frequency periodic excitation.

Marcelo A. Trindade et al. (2015) carried out the study to implementation of spatial modal filters based on arrays of piezoelectric sensors for a free rectangular plate. The modal sensors and actuators working in closed loop enable to observe and control independently specific vibration modes which reduce the apparent dynamical complexity of the system and the necessary energy to control them.

Arun P. Parameswaran et al. (2015) Reported the vibration of piezoelectric laminate cantilever beam which was considered as a smart system for the dominant first two

flexural modes of vibrations. The experimentally studied for individual as well as multiple dominant modes of flexural vibrations was carried out and the accuracy of the developed analytical model with frequency response. Simulation studies were conducted in the first resonance, second resonance well as for the first two flexural modes of vibrations to verify the operational efficiency of the developed robust control strategy.

.**Yik R. Teo et al. (2015),** presented a model for improvement to Integral Force Feedback for vibration control of structures and mechanical systems. They achieved the improved method, arbitrary damping for any mechanical system. It has been experimentally demonstrated that the actively damping for a high high-performance mechanical systems to critically damped with a first-order control law. The closed-loop frequency responses dominant first resonance mode has been attenuated improved. The experimental results of lens positioner increased in the maximum damping.

2.2 ANALYTICAL WORK

D.J.Meadet al. (1969) carried out a study to forced transverse vibration of a three-layer sandwich beam with a viscoelastic core. They derived differential equations of motion for the system for different boundary conditions. The orthogonality of the corresponding complex modes and control were obtained.

C.D.Johnson et al.(1980) offered an efficient method to predict damping in a structure with constrained viscoelastic layers. They estimated the modal damping ratio from undamped normal modes via the modal strain energy method (MSE).

Said I.Hilmy et al.(1984)) carried out the study of realistic element model and element for- simulation which accurately reflects structural and material behavior of central importance. The control of nonlinear dynamic behavior of steel frames and structural nonlinear response in an interactive computer graphics environment.

.

Abdel et al.(1987), compared three active control mechanisms, active tendon mechanism, active tuned-mass damper mechanism, and the aerodynamic appendage mechanism, in terms of feasibility of active control of tall buildings against wind. They concluded that a combination of active tendons and active tuned-mass damper

mechanisms was an attractive solution. The applications involving vibration control or seismic risk mitigation. Applications involve mix of structural elements and complete structures.

M.R.Maheriet al.(1995) used finite elements method based on laminated plate theories to predict modal properties of a free-free Fibre Reinforced Polymer (FRP) plate and validated their work with experimental results.

M.J.Lam et al.(1997) compare theactive and passive control by CLD treatment and piezoelectric actuation. They introduced two new hybrid configurations to model the damping of viscoelastic material and investigated the treatment of a beam with separate active and passive CLD elements. After whichthey concluded that the hybrid treatment was a better approach to suppress vibration than active treatment.

Wilkie et al.(1998) reported the effectiveness of embedded piezoelectric active fiber composite laminate for alleviating adverse vibratory loads on helicopter rotor blades at high-speed, high thrust forward flight conditions. Maximum stall limited rotor thrust using active blade twisting was approximately 5–10% greater than that achievable with a conventional passive blade structure. By using the active fiber composite blades 10–15% increase in dynamic stall limited forward flight speed was obtained.

S.S.Joshi et al.(2000) introduced a methodology that included optical-structural modeling, damper modeling to find the damper location for space-borne interferometers with cost functional formulation and combinatorial optimization. It was defined a cost criterion of a system that allows consideration of multiple dissimilar disturbance sources and multiple dissimilar performance metrics. They considered a discrete combinatorial optimization problem of a finite number of dampers and finite number of possible damper locations. They investigated both Genetic Algorithm and Simulated Annealing methods, and observed more efficiency from Simulated Annealing.

A.K.Agrawalet al.(2000) worked on combinatorial optimization of the location of passive dampers on seismic and wind-excited buildings. They usedthree intelligent search algorithms, namely, sequential, Worst-Out-Best-In (WOBI) and Exhaustive Single Point Substitution (ESPS), to determine the best locations of dampers. The WOBI and ESPS could be implemented to effectively improve the optimal locations of the dampers which was determined by a sequential search method.

S.W.Park et al.(2001) addressed different approaches related to the mathematical modeling of viscoelastic dampers and compared their theoretical basis. The standard mechanical model (SMM) comprises of linear springs and dampers, accurately. They described the broadband rheological behaviour of common viscoelastic dampers. SMM was shown to be more advantageous than other models such as the fractional derivative model and the modified power law.

J.Roet al.(2002) used the MSE method to optimize the location of the active constrained layer damping (ACLD) patches on flexible structures. A finite element approach to determine the modal strain energies of plates treated with ACLD. They minimize the total weight of ACLD treatments subjected to achieving a certain level of modal damping ratio.

H.Zhenget al.(2004) applied a Genetic Algorithm-based penalty function method to optimize partial CLD treated beams. To minimize the vibrational energy of vibrating beams with passive CLD treatment. They performed a parameter sensitivity analysis to determine the dominant parameters on the vibration response of the damped beam. It was shown that the vibration response of the CLD treated beam showed more sensitivity to the location/length of the covered passive CLD patches and the shear modulus of the viscoelastic layer than other parameters such as the thickness of the viscoelastic layer, and the constraining layer (CL) with its elastic modulus fixed.

C.A. Morales et al.(2005) carried out the experimentally investigated generic expressions of substructure-synthesis mass and stiffness matrices of the one-portal frame by low-order eigen value problems and highly accurate eigen solutions. After which they presented easy and accurate computation of its natural frequencies and mode shapes through the solution of low-order eigen problems.

F.Aminiet al.(2006) compare that the effects of the locations of the controllers on the control force and control performance, the number of controllers reduced optimization. They concluded that optimum system with lesser numbers of controllers will work more effectively than a non-optimum system with more semi-active dampers.

Townly et al.(2006) presented various device sizes and structure have been tested for power measurements as device. The effort to standardize comparisons in spite of these changing parameters, the dependence of generator power output on device dimensions has been investigated. It is difficult to produce sufficient displacement at small scales to generate a considerable voltage. Therefore a very attractive power devices indefinitely. Due to the difficulty in reaching low frequencies with MEMS scale devices, these types of energy harvesters would be the apply with very high frequency vibrations.

Chih-Liang Chu et al.(2006) reported the Active vibration control of a flexible beam mounted on an elastic base. system is analyzed using a finite element approach. The study utilized the independent modal space control (IMSC) method for active control of a flexible beam supported on elastic base. To improve analysis accuracy the study considers Timoshenko beam theory for system analyzed. Numerical results compared with those obtained using ANSYS.

John E. Mottershead et al.(2006) reported that the abiding problem of vibration absorption has occupied engineering scientists for over a century and there remain abundant examples of the need for vibration suppression in many industries. They developed the techniques for the dynamic of the system (possibly a car or a helicopter) could be adjusted after it has been built. They presented two main approaches, structural modification by passive elements and active control. They presented the mathematical theory of vibration absorption.

Heung SooKim et al.(2006) reviews key ideas and performances piezoelectric energy harvesting from vibration, types of vibration devices, piezoelectric materials and mathematical modeling of vibrational energy harvestings. They investigated three issues that limit the broad technological impact of the vibration-based piezoelectric energy harvesters. Firstly, development of high coupling coefficient piezoelectric materials is essential to improve the performance of piezoelectric energy harvesters. Secondly, the energy harvesters should be able to sustain under harsh vibrations and shocks. Thirdly, development of efficient electronic circuitry for energy harvesters .Finally they utilized the optimum level of energy of vibration and their control.

Y.C.Shuet al.(2006) used an analysis of AC–DC power output for a rectified piezoelectric harvester and conversion of energy from the oscillating mass to electricity have adopted a simple model which was based on the assumption that the electrical

damping. The electronic load required a stabilized DC voltage while a vibrating piezoelectric element generates an AC voltage with the desired output needs to be rectified, filtered and regulated to ensure electrical compatibility. They investigated the optimal AC–DC power output to reflect the real electrical performance in many practical applications.

Ziegler et al.(2005) presented an objective of shape control is elimination of the structural deformations caused by external disturbances. Other objectives include control of reception and transmission orientation as well as aerodynamic vibration control. Shape control is usually carried out through active cables and struts.

Nudehi et al.(2006) investigated that experimentally the use of end forces for vibration control on a beam structure fitted with a cable mechanism and motor for applying the end force, and a piezoelectric patch for taking vibration measurements. Result shows that the modes of the beam were effectively controlled andthe natural frequencies are less than the bandwidth of the motor.

P.J.Torviket al.(2007) modified the method of modal strain energy to improve loss factor estimations for damped structures. It was found that the traditional application of MSE method would be appropriate for the damping element with a very low stiffness. However, they observed that the error, resulting from the use of MSE, would increase significantly for systems with higher damping element stiffness, unless the material loss factor of the damping element is small (i.e., << 1).

Antonello De Luca et al.(2007) Suggested a simple formula for predicting the horizontal capacity of masonry portals. The principle of virtual works for holonomic systems was applied to derive expressions for the collapse multiplier of a chosen load distribution. They were selected four collapse mechanisms of mechanical and engineering considerations, and closed form expressions for the multipliers for each of them has been derived. Those expressions have allowed toperform extensive parametric analyses, varying the geometrical ratios that determine the portal configuration. As a result, the ranges of the main geometrical ratios, in which one or another mechanism prevail, have been derived. An abacus provided to evaluate the collapse multiplier of any portal. Finally, a simplified expression is proposed, whose results show scatters from the exact solution almost always below 6%. Such an expression may turn out valuable for designers from the point of view of seismic vulnerability assessment.

Mats Jonasson et al.(2008) investigated the complex design task involving the control of the electric damper and its machine parameters was optimized the power dissipation of the electric damper as low as possible during the process. They concluded the results and demonstrated that the proposed suspension could easily adopt with control parameters and the performance was better than passive suspensions.

Ibrahim. R.A et al.(2008) studied the nonlinear vibration isolation significant developments due to pressing demands for the protection of structural installations, nuclear reactors, mechanical components, and sensitive instruments from earthquake ground motion, shocks, and impact loads. They evaluated that the developments of nonlinear isolators in the absence of active control and inherent nonlinear phenomena for Specific types of nonlinear isolators including ultra-low-frequency isolators. For vertical vibration isolation, they described the different techniques of reducing the resonant frequency of the isolator and controlled the transmissibility on excitation amplitude.

Preumont et al.(2008) carried out the study of the classical problem of active and passive damping of a piezoelectric truss. They investigated that the Voltage control and charge (current) control implementations. The performance was controlled by the modal fraction of strain energy in the active strut and the electromechanical coupling factor.

Josep M. Mirats et al. (2009) presented a special class of structures whose elements simultaneously perform the purposes of structural force, actuation, sense and feedback control and a very high resistance/weight coefficient to easily deformable. They obtained stable configurations, shape changing algorithms which deal with the problem of finding stable trajectories between them and, also control algorithms which take into account the dynamic model of the tensegrity structure and possible external perturbations to achieve the desired goal and performance.

Malekzadeh et al.(2009) has presented a three dimensional elasticity approach based on a layer wise theory. They investigated the dynamic response of cross-ply laminated thick plates subjected to the moving loads.

C. Mei et al.(2009) reported a hybrid approach consisting of complementary wave and mode-based control is described on Timoshenko theory. In modal Active Vibration Control, to control the characteristics of modes of vibration i.e their damping factors, natural frequency or mode shapes. Active wave control aims to control the distribution of energy in structure by either reducing the transmission of waves from one part of the structure to another or by absorbing the energy carried by other waves. In proposed hybrid approach, wave control is first designed and is targeted at higher frequencies. Two control strategies there, one optimally absorbs the vibrational energy and the other adds optimal damping to structure. Modal control is then designed for the lower modes of structure based on modified equation of motion of structure-plus-wave-controller. Hybrid approach exhibits better broadband active vibration control performance than the cases with either modal or wave control alone. While control design based on the classical Euler-Bernoulli model theory was applicable to slim beams, the present design based on the advanced Timoshenko model was suitable for deep as well as slim beam elements.

Fabio Minghini et al.(2009) presented the elastic instability of PultrudedFibre Reinforced Polymer (PFRP) portal frames with a second order displacement field, accounting for the shear strain influence on both non-uniform bending and torsion. They analyzed kinematical model of two-node locking -free finite element with seven degrees of freedom per node stiffness. Computational formulation adopted can easily be implemented for an imperfection sensitivity analysis behavior on membrane, shear, bending and torsion deformations.

ArpitaMukherjee et al.(2009) carried out the study the relation between the parameters characterizing piezoelectric material‘s properties relevant for energy harvesting from cantilever-based energy-harvesting devices (EHD), harvesting energy from vibrational motion. They presented the study which would help in selection of piezoelectric materials for EHDs for different applications the dependence of the output power on load resistance and frequency of vibration has been studied. The performance of some popular piezoelectric materials having same size with respect to their output power has been compared. They concluded that the study will be useful to overcome any space constraint of the EHD by selecting proper piezoelectric material depending on the requirement and the frequency of vibration.

H.R.Hamidzadeh et al.(2009) investigated the effect of viscoelastic core thickness on the modal loss factors of a thick three-layer cylinder. They accomplished the constrained-layer damping by sandwiching a linear viscoelastic material between two isotropic elastic cylinders having the same properties. The governing equations were derived using Newton's second law of motion, and employing the complex elastic moduli for the sandwiched layer. Then the natural frequencies and modal loss factors for different circumferential wave numbers were determined. It was concluded that most frequency factors changed linearly when the middle-layer thickness varied, i.e. frequency factors were linear functions of the middle-layer thickness, and for circumferential wave number n = 0, all six modes of the modal loss factors increased linearly when the core thickness increased.

Qinglei Hu et al.(2009), presented a dual-stage control system design method for the three-axis-rotational maneuver and vibration stabilization of a spacecraft with flexible appendages embedded with piezo-ceramics as sensors/actuators. They presented attitude control system and vibration suppression and design of attitude controller. They presented asymptotic attitude maneuvering in the closed-loop system and insensitive to the interaction of elastic modes in the presence of unknown disturbances and inside the region the variable-structure control (VSC) law with a linear sliding surface was activated..

U.K.Singhet al.(2009) targeted the transformation of mechanical vibration into electrical energy using piezoelectric material. A source vibration model was first designed and simulated to match the supplied spectrum from CRC mining. Then various loads were tested to achieve input and output impedance matching for the maximum power transfer. Input and output impedance matching were studied with having different loads. Finally an ideal simulation with the RL load was considered to be included to be informative and relevant parts for this project. Thus this device can be used as power source for such low power electronics working in a suitable condition. Use of this device is scalable and viable in many other applications where vibration can be found and improved the regulation of maximum power to the load

N.Challamel et al.(2010), worked on theoretical and numerical modeling of out-of-plane vibrations of composite beams with interlayer slip or three-layer sandwich beams. They presented Hamilton's principle to derive the governing differential equations for the out-of-plane vibrations problems. After which they presented a phenomenon of cut-on frequency associated with a change of the shape of the natural modes with respect to a critical frequency.

Justin D. Marshall et al.(2010) compare design, analyze and test a prototype hybrid device. The prototype device was tested successfully both cyclically and statically. They demonstrated experimental tests that the device had the properties and behavior expected. After which they developed, analyzed, experiments test of potential and create a hybrid device with existing passive control technology and standard steel sections.

Stella S. Dearin et al.(2010) designed, fabricated and tested a prototype dimple actuators used as electrostatic devices represents an alternative to current design which use external forces or mechanical asymmetries to control the direction of out-of-plane deflections. The performance of these devices was promising in terms of robustness, power consumption and out-of-plane deflections. They concluded the evaluation suggest that robustness and frequency response will improve with miniaturization.

AlirezaKhaligh et al.(2010) presented the progress in kinetic energy harvesting for wide applications ranging which implanted devices and wearable electronic devices to mobile electronics and self-powered wireless network nodes. The advances in energy harvesters adopting piezoelectric and electromagnetic transduction mechanisms were presented. Piezoelectric generators convert mechanical strain on the active material to electric charge while electromagnetic generators make use of the relative motion between a conductor and a magnetic flux to induce charge in the conductor.The output voltage is very high and the current flowing out from piezoelectric generators used for very high impedance of such materials. The kinetic harvesting techniques have been shown to capability of delivering power to the load from microwatts to milli-watts. With the development the harvested power was possible to drive the microcontroller units, sensors, or other devices directly. The most promising applications were included ambient intelligence, condition monitoring devices, implantable and wearable electronics, and wireless sensor networks.

AndrezaTangerinoMineto et al.(2010) reported the simple transverse mode type piezoelectric generator model. In which the Euler–Bernoulli beam theory were used the effect of backward piezoelectric coupling in the beam equation. They capture the influence of the natural frequency (uncoupled with the resistance) in power generation for some values of the resistance where the peak value does not vary with the resistance. Results obtained from the electrical power calculations indicated that optimal resistance values which could be achieved for a particular PZT length and location that will give maximum output electrical power.

R. Setola et al.(2010) employed a spline shaped function to interpolate the available measurements and taken into account the boundary condition. They introduced a spline functions for sort of spatial filtering on the high frequency mode and thus increase the robustness of the control scheme against spillover. Reconstructor joined to a suitable controller which was able to reduce vibration of beam subjected to persistent multi-frequency disturbance acting at unknown beam abscissa and reduced the noise of the flexible structure when they excited by some external pseudo-periodic cause.

Paul D. Mitcheson et al.(2010) proposed a wide range of motion powered energy harvesters. Energy harvesting of substantial and increasing research attention, and motion-driven devices representd a large fraction of the activity. Motion energy harvesting devices are now offered commercially by several companies, mainly for applications where machine vibration is the motion source, although body-powered applications (particularly body sensor networks) are actively pursued. Fundamental analysis indicates that for body motion in particular, achievable power levels for miniature harvesters could be powered. Wireless sensor nodes are the most promising application area for vibration harvesting, with a wide range of application areas and corresponding motion sources. Reported and investigated implementations of energy harvester's progress on miniaturization.

J.G.Rocha et al.(2010) describes the use of piezoelectric polymers to harvest energy from people walking and the fabrication of a shoe capable of generating and accumulating the energy. In this scope, electro-active β-polyvinylidene fluoride used as energy harvesting element was introduced into a bicolor sole prepared by injection, together with the electronics needed to increase energy transfer and storage efficiency.

An electrostatic generator was also included to increase energy harvesting. The integrated energy generating elements harvesting human energy, piezoelectric materials associated with electrostatic generators was the most promising elements to optimize the energy transfer, and the precise determination of the geometry and number of the piezoelectric generators could be performed.

Peng Lina et al.(2010) investigated collective rotating motions of second-order multi-agent systems of rotating consensus problems using local relative information. They presented a protocol and given a necessary and sufficient condition for rotating consensus of the complex system and obtained the simulation results to demonstrate the effectiveness of theoretical results.

Chi-Chang Lin et al.(2010) carried out the study of semi-active friction-type multiple tuned mass dampers (SAF-MTMDs) for the response control of seismic structures more adaptive to their excitations formulating its dynamic equation. The Different from of passive friction-type systems and the friction force of each mass unit in the SAF-MTMD varies on-line using a variable friction mechanism that produces a controllable clamping force on the friction interface. They presented numerical simulation and compared the control performance of the control system using passive friction-typetuned mass dampers system and obtained the result that SAF-MTMD system alleviates the detuning effect shift in structural frequency.

Martin Proetzsch et al.(2010) developed the methodology for complex robotic systems using the behavior-based control architecture iB2C (integrated Behavior-Based Control). They presented that how architectural principles support several behavior-based mechanisms, e.g. coordination mechanisms, behavior interaction, and hierarchical abstraction. They provided analysis tools and visualization techniques which help to manage the complexity of large behavior-based networks and a step by step description of constructing a behavior-based control structure for the outdoor robot.

V.Sudhakar et al.(2010) developed a super convergent finite element for analysis of sandwich beams with soft core. Their element was a two-nodded, six degrees of freedom per node. They assumed that all the axial and flexural loads were taken by face sheets, while the core takes only the shear loads, however they considered exact representation of beam stiffness in the formulation. They investigated the element under

static loadings for free vibration of the sandwich beams with metallic as well as composite face sheets

Lin et al.(2010), analysed soil–structure interaction effect on vibration control effectiveness of active tendon systems for an irregular building which modeled as a torsionally coupled structure subjected to base excitations such as those induced by earthquakes. A direct output feedback control algorithm was successfully applied to a two-way eccentric building with active tendon systems in outer frames.

A.V.Lopatin et al.(2010) modeled and analyzed symmetrical vibrations of composite sandwich panels. They solved the vibration problem for a sandwich plate with identical composite facings and orthotropic core. They used Hamilton's variational principle to derive differential equation of symmetric vibrations. They presented that the tangential displacements of the core material were negligible and the normal displacements of the core material were nonlinearly varying from the value of the facing deflection to zero. With these assumptions, they also defined the effective modulus of elasticity of the core material in transverse direction. They finally compared the computational results which obtained from the finite element analysis

Shea et al.(2011) presented advances in theory and practice of active structural control technology which modified the general perception of structures. Due to incorporated intelligence, structures become dynamic objects capable of interacting with complex environments.

N.R. Fisco et al.(2011) presented active and-semi active control of structures using a variety of systems include active tuned mass dampers, distributed actuators, active tendon systems and active coupled building systems. Semi-active control systems include magneto rheological (MR) fluid dampers, semi-active stiffness dampers, semi-active tuned liquid column dampers and piezoelectric dampers. They concluded the hybrid control systems and control strategies of conclusions.

IoanDoré Landau et al.(2011) investigated both experimentally and analytically adaptive feed forward compensation in active vibration control systems and existence of an inherent internal positive feedback coupling. Theoretical analysis has pointed out the presence of a sufficient condition for stability involving a positive real condition on a certain transfer function. This condition can be relaxed by taking into account the nature of the disturbance (broadband) or by an appropriate filtering of the regresses

vector. They obtained the Real time results on an active vibration control system. The algorithms have been compared theoretically and experimentally with two other algorithms for which an analyzed in the context of the internal positive feedback controller.

F. Braghin et al.(2011) presented the magnetostrictive actuators deliver high-output forces and can be driven at high frequencies, were a promising technology in active vibration control. They presented the numerical transfer functions of two different actuators between the supplied current and the force useful for vibration control has been compared to the experimental ones showing that the model correctly predicts the actuators dynamic behavior in a range of frequencies. Finally the model is validated through experimental tests carried out on two different magnetostrictive actuator and control.

H.D.Chalak et al.(2011) investigated that the vibration of laminated sandwich beams with soft core. They developed a finite element beam model to obtain the free vibration response of the laminated sandwich beams having a soft core. In their developed model the in-plane displacement variation was considered to be cubic for both the face sheets and the core. Their proposed model would satisfy the condition of transverse shear stress continuity at the layer interfaces and the zero transverse shear stress condition at the top and bottom of the beam.

Sinan et al.(2011) has presented many review articles and application based research papers. They has also given a comprehensive study of the past research in the area including all possible methodologies available from passive to active control of equipments/ structures.

Samuel da Silva et al.(2011) investigated the common metrics for linear finite element (FE) model using vibration test data. They also presented distances involving natural frequencies, frequency response or impulse response functions, modal shapes, etc. They obtained the results which allow characterizing the practical applicability method for further use in industrial structures.

F.X.Xinet al.(2011) theoretically formulated the wave propagation in an infinite sandwich panel reinforced by orthogonal rib-stiffeners during harmonic point force excitation. They determined the response of the sandwich using the Fourier transform and the periodical nature of the structure.

Mohebpour et al.(2011) presented a comprehensive study of the dynamic analysis of laminated composite beams traversed by a moving oscillator. They developed an algorithm based on ‘first order shear deformation theory (FSDT) to investigate the interaction effects of dynamic properties of both the sub-systems such as velocity of motion, suspension stiffness, mass ratio and damping ratio of both the sub-systems, on the system responses. They investigated the dynamic behavior of the system components and problem of laminated composite plates traversed by a moving oscillator. The governing equations of motion of the plate, based on the first order shear deformation theory (FSDT). Two sets of equation of motion are coupled using the concept of contact force in terms of the contact displacements and its derivatives. After which they conducted the parametric analysis and the effects of suspension stiffness, mass ratio, travelling velocity, damping ratio of each the sub-system and the oscillator eccentricity.

Liang Wanget al.(2011), investigated experimentally a method for the vibration control of an iron cantilever beam with axial velocity using the noncontact force by permanent magnets and magnetic control system. They presented control method for the beam with constant length or varying length. Numerical simulation and actual experiments are implemented and the results show that the control method effective and the simulations fit well with the experiments.

ArmenBagdasaryan et al.(2011) presented a method for dynamic model synthesis and discrete simulation of complex hierarchical control systems. They evaluated that the proposed simulation models and technique used for design of applied weakly-formalized control systems and computer environments for simulation and analysis of state dynamics in complex dynamical hierarchical systems. After which they proposed models and technique were sufficiently universal and at the same time they could be equally used for various kinds of systems such as technical, engineering, discrete event systems, organizational, socio-economic, strategic planning, long-term forecasting systems, and decision support systems.

M. Domaneschi et al.(2012) presented a method of controlling in real time the hysteresis component in simulated semi-active control systems through the Bouc-Wen model. compare theoretical formulation of the original tuning the parameters which could be managed for hysteresis regulation embedded into the analytical formulation of

the model selected for implementing the semi-active characteristic and control the structural effects.

A.Arikogluet al.(2012) analyzed vibration and damping of a three-layered sandwich plate with composite face layers and a viscoelastic core. The principle of virtual work to derive the governing equations and related boundary conditions The eigenvalue problem was solved using the generalized differential quadrature method to determine both the natural frequencies and loss factors. A comparison was made between their results and those reported in the literature. The core material providing the highest damping would depend on the geometrical properties of the plate.

N.H.Diyana et al.(2012) chosen a unimorph piezoelectric energy harvester to harvest wideband mechanical energy. The derivation of the mathematical modelling is based on the Euler-Bernoulli beam theory. MATLAB and COMSOL Multiphysics software are used to study the influence of the structure in generating output voltage due to base excitations. Finally, the results of the frequency response are displayed in the form of voltage within frequency range of 0 to 3500 Hz, at which the comb-shaped piezoelectric beam structure shows better performance as there exist more natural frequencies in the specified range of frequency.

Hui-Min Yen et al.(2012) presented problem of designing robust tracking controls for a class of uncertain nonholonomic systems actuated by brushed direct current (DC) motors. The class of electrically driven nonholonomic mechanical systems perturbed by plant uncertainties, unmodeled time-varying perturbations, and external disturbances. They developed adaptive neural network-based dynamic feedback tracking controller for intelligent robust tracking control such that all the states and signals of the closed-loop system were control.

Hyun-Su Kim et al.(2012) investigated a multi-objective optimal fuzzy control system for the response reduction of a wind-excited tall building. A semi-active tuned mass damper (STMD) of a 100kN magneto-rheological (MR) used for vibration control subjected to wind load and its natural period was tuned to the first-mode natural period of vibration of the building structure. They concluded that the damping force of the MR damper was controlled by a fuzzy logic controller based on numerical results.

Patrick S. Keogh et al.(2012) Perform the rotor dynamic behavior and ensure robust performance with Cases of weak and strong rotor dynamic coupling and contact events.

They demonstrated how rotor dynamic design tools could be adapted to assess stability and rotor dynamic response. An analytical tool which based on matrix transfer function singular values to provide stability boundaries.

Morales.AL. et al.(2012) studied a fuzzy design method using the finite element procedure to simulate and analyze active vibration control of structures subjected to uncertain parameters. They presented computationally expensive probabilistic methods or complex robust control techniques of uncertainty propagation on both stability and performance of a vibration control system of structure.

X.Q.Peng et al.(2012) studied a finite element model with third order theory used for active vibration control and active position control of composite beam with distributed piezoelectric sensor and actuators.The Piezoelectric materials such as Lead ZirconateTitanate (PZT), exhibit mechanical deformation when subjected to an applied electric field to converse piezoelectric effect and also generate voltage or charge when subjected to a force or deformation. Third order laminated theory was developed for the active vibration control of composite beam with distributed piezoelectric sensor and actuators. In the case of shape control all the piezoelectric on the upper and lower surface of the beam are used as actuator. They concluded the conversion of piezoelectric effect, the distributed piezoelectric actuator contract or expand depending on negative or opposite active voltage and for upward displacement, the upper actuators needed a negative voltage and lower actuators needed a positive one.

Dan J. Gordon et al.(2012) studied and investigated the use of the pole-placement technique to achieve active vibration damping, bandwidth disturbance rejection and positioning control of ball screw drives. They presented a simple and physically intuitive model for two oscillatory poles were placed to speed up the damping of axial vibrations. They compared and concluded the P-PI position-velocity cascade controller and PPC design the prefilter which were combined together.

Iván M. Díaz et al.(2012) designed the stability and actuator saturations to improve the efficiency of a given inertial actuator when the Active vibration Control system was based upon velocity feedback. A closed loop within the actuator and designed to artificially modification of actuator frequency response of maximum stroke and force. They concluded that the strategy of modifications and adaptability were improved the performance of the smart structure.

Mohammad Saranik et al.(2012) presented the mathematical model and shaking-table test for inelastic behaviour of frame structures subjected to dynamic loads. They presented in this test. For changes in modal parameters due to the development of Low-Cycle Fatigue damage in frame connections and a nonlinear numerical simulation was performed using a Fatigue Damage-Based Hysteretic model. They concludes that the response of the damaged frame of a two-story steel portal frame with bolted connections can be predicted.

J.S.Grewal et al.(2013) worked on the vibration analysis and design optimization of sandwich beams with constrained viscoelastic core layer. A finite element method to analyze the dynamic properties of sandwich beam-type structures. A comparison was made between their results for linear and nonlinear models with those available in the literature. The natural frequency and loss factor at the first mode of clamped-free sandwich beam did not show considerable difference in linear and nonlinear models. The difference was more significant for the clamp-clamp boundary condition. Eventually, they performed systematic parametric studies to verify the effects of the location and length of both treated and untreated patches on both natural frequency and the modal loss factor of the sandwich structure.

K.Misiureket al.(2013) worked on the dynamic response of a finite, simply supported sandwich beam subjected to a moving force with a constant velocity. Their system included a classic sandwich beam with a rectangular cross-section consisting of two thin, stiff, elastic sheets and a thick core layer. They showed that from the two infinite series, whose sum reveals the classical solution for transverse displacement and the rotation of the cross-section, the one representing aperiodic vibrations of the beam could be presented in a closed form.

JuntaoFei et al.(2013) reported Considerable attention has been devoted to active vibration control using intelligent materials as actuators. The results on active control schemes for vibration suppression of flexible steel cantilever beam with bonded piezoelectric actuators. The PZT patches are surface bonded near the fixed end of flexible steel cantilever beam. The dynamic model of the flexible steel cantilever beam was derived. Active vibration control methods, such as optimized parameter PID compensator, strain rate feedback control are investigated and implemented using xPC

Target real time system. Experimental results demonstrate that the proposed methods achieve effective vibration suppression results of steel cantilever beam.

Duoc T. Phan et al.(2013) design and developed the hot-rolled steel portal frames sensitive to serviceability deflection limits. To reduce frame deflections, practitioners increase the size of the eaves haunch and the sizes of the steel sections which used for the column and rafter members of the frame. They investigated that the effect of such deflection limits using a real-coded niching genetic algorithm (RC-NGA) that optimizes frame weight deflection.

F.Alijaniet al.(2013) investigated the geometrically nonlinear vibrations of completely free laminated and sandwich rectangular plates. The governing equations using multi-modal energy approach based on Lagrange equations. Their numerical analysis was based on the nonlinear classical and higher-order shear deformation theories. They found the solution based on highly accurate natural modes calculated by linear analysis.

Wei Zhan et al.(2013) forward an optimization approach for Multiple Active Tuned Mass Dampers (MATMDs) system under seismic and wind-induced building vibration. A model of an n-storey building with MATMD system was established and a joint optimization method was used to obtain an optimal state- feedback controller gain and the parameters of the MATMD system. A mixed H2/H1/GH2 control is employed to attenuate the seismic and wind-induced vibration of the building with the constraints of the actuating forces and strokes of the masses. Genetic algorithm (GA) was used to search for the optimal parameters and obtain the corresponding controller gain. comparison, the GA-based approach obtained a better set of parameters and achieve better control performance. When comparing with an Active Tuned Mass Damper (ATMD), an MATMD system could achieved similar control effects with much smaller acting forces.

Y.F. Wang et al.(2013) investigated both experimentally and analytically to eliminate or inhibit the friction-induced self-excited vibration. They developed a framework of modeling friction force and control compensation using neuro-fuzzy system and data mining techniques. They presented the typical motion dynamics with friction were used in simulation. They demonstrated that approaches for friction modeling and adaptive

compensation control technique were effective for controlling friction self-excited vibration.

S.G.Won et al.(2013) used the virtual work principle to derive a 2-node damped beam element for three-layered symmetric straight damped sandwich structures. In the forced vibration, they add three pairs of boundary conditions to the three-constrained-layer damped beam, so the rotation of the mid-surface was added for the damped beam element to have three degrees of freedom per node. They also considered the frequency dependence of the viscoelastic material properties.Their proposed damped beam element showed more rapid convergences in resonance frequencies.

R. Subasri, S. Suresh et al.(2014) presented a discrete direct adaptive ELM controller for the active control of a base isolated benchmark structure with the hysteretic isolation system. They presented ELM controller was single hidden layer neural controller with random selection of input weights compensates the nonlinearity and provides desired vibration suppression. They analyzed the controller was effective and decreases the super structure accelerations and drifts. It also signifies a decrease in base displacements by a marginal increase in the control force.

Giovanni Ferrari et al.(2015) experimentally investigated the active vibration control of a free rectangular sandwich plate by using the Positive Position Feedback (PPF) algorithm and four normal modes were controlled by four nearly collocated couples of piezoelectric sensors and actuators. They experimental investigated the results that the structure has controlled to the specific type of sensors and their conditioning, as well as to the phase shifts vibration at different points.

Yunlong Li et al.(2015) presented an Active control simulation of the acoustic and vibration response of a vibro-acoustic cavity of an airplane based on a PID controller. They developed numerical vibro-acoustic model by using an Eulerian model, which was a coupled model based on the finite element formulation. They optimize the actuator placement to get an effective closed-loop control system. An iterative method to determine the optimal parameters of the PID controller for the controller design. The numerical and experimental results show that a PID-based active control system can effectively suppress the noise inside the cavity using a sound pressure signal as the controller input.

YingWuet al.(2015) investigated that the dynamics modeling and control strategy investigation of a class of parallel manipulators for active vibration isolation. They presented the dynamic analysis and robust nonlinear control of a six-DOF active micro-vibration isolation manipulator with parameter, including stiffness, damping and the mass center location. They presented that the controller was the combination of linear control component, nonlinear component and uncertain component. The robust nonlinear controllers have good adjustability to the control algorithm.

K. Khorshidi et al.(2015) investigated the vibro-control behavior of circular plates coupled with piezoelectric layers subjected to sound pressure plane wave load. They obtained the exact closed-form solution for the system with clamped boundary conditions. The frequencies and mode shapes of the system are presented in different ratio of thickness. And the system equations have been moved in state space and LQR method and FLC (Fuzzy Logic Controller). They provided the active vibration control of circular plates coupled with piezoelectric layers excited by plane sound wave.

M.C. Ray et al.(2015) analyzed of active damping of geometrically non-linear vibrations of functionally graded magneto-electro-elastic (FGMEE) plates integrated with the patches of the active constrained layer damping(ACLD) treatment. They developed the constrained visco elastic layer of the ACLD treatment and modeled by using a Golla–Hughes–McTavish (GHM) method in time domain and material properties of the FGMEE plate are assumed to be functionally graded along the thickness direction according to a simple power-law distribution based on the layer-wise shear deformation theory. The Influence of the variation of the power law index, material gradation, edge boundary conditions and the piezo electric fiber orientation angle in the1–3 PZC constraining layer of the ACLD treatment and control.

Shun-Qi Zhang et al.(2015) presented simulations of the static and dynamic response including shape and vibration control of piezoelectric bonded smart structures using various geometrically nonlinear shell theories based on the first-order shear deformation (FOSD) hypothesis. Large rotation of structures under deformations beyond the range of moderate rotations and applying an appropriate voltage for desired shape achieved the significantly suppressed the vibration.

Antonio Zippo et al.(2015) experimentally investigated active vibration control of a free-edge rectangular sandwich plate of carbon-fiber reinforced polymer (CFRP)

subjected to an orthogonal disturbance and electrodynamics exciter. They controlled the plate by Macro Fibre Composite (MFC) actuators and sensors and it appears to robust and efficient in reducing vibration in linear (small amplitude) and nonlinear (large amplitude) vibrations regimes. The control strategy which allows to effectively controlling each resonance both individually or simultaneously.

L.L. Sun et al.(2015) carried out the study of the behavior of a feedforward active isolation system d to actuator output constraints. They developed the models to analyze the system response and to produce a transfer matrix for the design of an integrated passive– active isolation system with the combination of the vibration transmission energy of the squared control forces. The control strategies rely nun constrained actuator outputs given substantial power transmission reductions over a wide frequency range and expected power transmission reductions for modified control strategies that constrained actuator outputs were considerably less than typical reductions with uncon-strained actuator outputs shown to be more effective at the resonance frequencies of the supporting plate.

SyDzung Nguyen et al.(2015) carried out the study a novel neuro-fuzzy controller (NFC) for car-driver's seat-suspension system featuring magnetorheological (MR) dampers. The NFC is built based on the algorithm for building adaptive neuro-fuzzy inference systems (ANFISs) named B-ANFIS, which has been developed in Part 1, and fuzzy logic inference systems (FISs). a control strategy based on a ride-comfort-oriented tendency (RCOT) is established. Subsequently, optimal FISs are built based on a genetic algorithm (GA) to estimate the desired damping force that satisfies the RCOT corresponding to the road status at each time. The desired force values are calculated according to the status of road at each time. The corresponding exciting current value to be applied to the MR damper is then determined by the I-ANFIS. In order to validate the effectiveness of the developed neuro-fuzzy controller, control performances of the seat-suspension systems featuring MR dampers are evaluated under different road conditions.

Wei Sha et al.(2015) investigated that the bodywork vertical vibration acceleration of a quarter car modelis selected as a control objective and Fuzzy-PID control strategy based on improved cultural algorithms for vibration reduce. They presented the design

Fuzzy-PID controller and optimize control rules and accelerate optimization speed for global optimal performance. They concluded numerical results to show the active suspension, with Fuzzy-PID control strategy in which control rules were optimized by improved cultural algorithm and significantly suppress the bodywork vertical vibration acceleration to improved comfort.

HarijonoDjojodihardjo et al.(2015) developed a space structure which treating flexible beam attached to central-body. The efficient analytical method for vibration analysis of a Euler–Bernoulli beam with Spring Loading at the Tip has been developed on MATLAB. They presented the Extension of generic problem of Active Vibration Suppression of a cantilevered Euler–Bernoulli beam with piezoelectric sensor and actuator attached. They presented three generic configurations of the combined beam and piezoelectric elements and the equation of motion of the beam was expressed using Hamilton's principle, and Galerkin's method. The robustness of the approach was assessed.

SelimPul et al.(2015) performed comparative studies experimental and theoretical both on apex connection of an industrial portal frame constructed with cold-formed back-to-back double sigma profile rafters . By those experiments performed, local buckling behavior of the apex plate and load–displacement behavior of the system were investigated under monotonic vertical loading. This investigation was conducted for conditions that the gap between rafters ends at the apex plate are 90, 180, 360, and 450 mm and apex plate is unstiffened/stiffened. Experimental results for the model with 360 mm gap were compared to those of nonlinear quasi-static finite element analysis performed using a finite elements and a good agreement between those results was observed. The connection's behavior is controlled by the apex plate. No significant damage occurred on the profiles after the tests.

Kendra L. Van Buren et al.(2015) carried out Numerical simulations, irrespective of the discipline or application, by arbitrary numerical and modeling choices. The application of the simulation of the first four resonant frequencies of a one-story aluminum portal frame structure under free–free boundary conditions. The main challenge of the portal frame structure resides in modeling the joint connections, for which different modeling assumptions were available. Test-analysis correlation was

performed to compare the lower and upper bounds of numerical predictions obtained from parametric studies of the joint modeling strategies to the range of experimentally obtained natural frequencies to convert what is learned from these experimental studies to models that "envelope" the range of observed bolt behavior that combines small-scale experiments, sensitivity analysis studies, and bounding-case models, and produced lower and upper bounds of resonant frequency predictions that match those measured experimentally on the frame structure.

CzesławI.Bajer et al.(2015) Reported the semi-active control of vibrations of structural elements of Elastomer composites with ferromagnetic particles that act as magnet or theological fluids are used. The damping coefficient and the shear modulus of the elastomer increases when it is exposed to an electro-magnetic field. The control of the process in time allows us to reduce vibrations more effectively than if the elastomer is permanently exposed to a magnetic field. They given the analytical solution for the vibrations of a sandwich beam filled with an elastomer and applied to the analytical formula. The numerical solution of the minimization problem results in a periodic, perfectly rectangular control function if free vibrations are considered. Such a temporarily acting magnetic field is more efficient than a constantly acting one. The surplus reaches 20–50% or more, depending on the filling ratio of the elastomer. The resulting control was verified experimentally in the vibrations of a cantilever sandwich beam. The proposed semi-active control could be directly applied to engineering vibrating structural elements, for example helicopter rotors, air craft wings, pads under machines, and vehicles.

Moon K. Kwak et al.(2015) investigated the active vibration control of a rectangular plate either partially or fully submerged in a fluid. They derived a dynamic model for a cantilever plate in air and submerged in water with piezoceramic sensors and actuators. After which they measured the natural frequencies by observing the transfer function between the piezoceramic sensor and the piezoceramic actuator. The theoretical results on the changes in the natural frequencies were consistent with the measured results. The active vibration controller was designed by using a multi-input multi-output positive position feedback controller combined with a block-inverse technique by using a digital controller.

2.3 EXPERIMENTAL AND ANALYTICAL WORK

D.Ross-Kerwin-Ungar et al.(1959) they used the finite element model of CLD-treated beams in their proposed inference method. They also performed experimental studies on beams with CLD treatments. After choosing the amount of CLD to be used to control unwanted vibrations, one of the most important aspects to be aware of is the locations of the damping patches. A great deal of research has been done on the optimal location of damping elements on a structure.

I.Takewaki et al.(1997-2000) studied the location optimization of a passive damper location via minimum transfer function. The sum of amplitudes of the transfer functions for the undamped fundamental natural frequency of a structural system is minimized, subject to a constraint on the sum of damping coefficients of the added dampers. The advantage of this method is that the results are not affected by the characteristics of input motions because of the application of a general dynamical property (amplitude of a transfer function), independent of system inputs.

P.K.Sinha et al.(2000) carried out the study of the shear actuator induce distributed force/moments in the sandwich beam in contrast to the extension-bending actuators, which developed to concentrated force/moment and was found more efficient in actively controlling vibration. Actuator thickness & position play an important role in deciding the performance. The extension-bending actuator produces more transverse deflection than the shear actuator. It has been observed that moderately thin shear actuators was found to be more efficient and also the face laminated thickness has a significant effect on the efficiency of the shear actuator.

YavuzYaman et al.(2001) presented the active vibration control technique applied to a smart beam which consists of an aluminum beam modeled in cantilevered configuration with surface bonded piezoelectric (PZT) patches. The study used ANSYS (v5.6) package program. They first investigates the effects of element selection in finite element modeling. The effects of the piezoelectric patches on the resonance frequencies of the smart structure was presented. The developed finite element model was reduced to a state-space form suitable for a controller design. The effectiveness of the technique in the modeling of the uncertainties was also presented.

Te‟oLenquist da Rocha et al.(2004) Active Vibration control by smart material technology is increasing day by day. To obtain optimized control performance, actuator

and sensor must be placed at locations to excite the desired mode more effectively. It may be modeled by finite element method using MATLAB, ANSYS etc. H norm each sensor and actuator position is determined for selected modes of plate and computed using linear matrix inequalities technique. PZT elements are positioned at the optimal position using two first mode of structure.

N. E. duToit et al.(2005) reported that the Active Vibration control by smart material technology to obtain optimized control performance, actuator and sensor must be placed at locations to excite the desired mode more effectively. It modeled by finite element method using MATLAB, ANSYS etc.The sensor and actuator position was determined for selected modes of plate and computed using linear matrix inequalities technique. PZT elements are positioned at the optimal position using two first mode of structure. It is likely that the power density will be increased by as much as an order of magnitude.

Qinglei Hu et al.(2006) reported that Vibration reduction vibration control has been used as a solution for flexible space crafts to achieve the degree of vibration or suspension for required precision painting accuracy and negative feedback control was an effective method for active damping which was the greatest immunity against the destabilizing effects of spillover the availability of the variable structure output feedback control (VSOFC) approach to flexible spacecraft for large angle rotational moments with active vibration control using piezo-ceramics. They design to achieve good robustness and distribution rejection during sliding phase.

Adam et al.(2007) have presented intelligence is one of the desirable qualities of biological systems. Through mimicking living organisms, incorporation of intelligent control methodologies into structural engineering has potential to enhance the concept of structures. Self-diagnosis, self-repair and learning is an example of behavioral biomimicry.

Guillaume Barrault et al.(2008) developed a new procedure has been developed for designing a global vibration attenuation feedback controller based on a truncated experimental model that excludes both lower order and higher order modes outside the bandwidth of interest. They presented the an experiment which carried out on an irregularly shaped shell demonstrated the effectiveness of the controlling high frequency vibration modes of a complex structure.

ZekiKiral et al.(2008) calculated the dynamic response of the beam by using the finite element method to design a suitable control technique. The numerical results were verified by vibration measurements. Two laser displacement sensors were used to measure the dynamic response of the beam and moving load was obtained by pressured air directed to the beam vi nozzle. Active vibration control of a cantilever smart beam was considered and simulation of closed loop vibration control with displacement feedback was achieved by using a commercial finite element package.

Morten Bisgaard et al. (2010) design and control system for a helicopter slung load system. They presented the position and velocity estimates of the slung load and was designed to existing navigation in autonomous helicopters. The Sensor input was provided by a vision system on the helicopter that measures the position of the slung load. The controller was a combined feedforward and feedback scheme for simultaneous avoidance of swing excitation and active swing damping. The flight tests show the effectiveness of the combined control system, yielding load swing reduction compared to the baseline controller.

John H et al.(2011) demonstrated a method for determining the optimality of control algorithms based on multiple performance objectives on the control of semi-active vehicle suspensions of dynamic systems. They presented that the two performance objectives considered were ride quality and thermal performance. They develop a multi-objective genetic algorithm to compare the performance of candidate control algorithms. They concluded that optimal control inputs for systems actuated by smart materials (piezoelectric actuators, shape memory alloys, etc.) that were utilized in noise and vibration control

Fakhzan and Muthalif et al.(2011) modeled an energy harvester system of unimorphpiezoelectic cantilever beam with a tip mass generates electric current or voltage from the piezoelectric strain effect due to base excitation. The step by step analytical solution and the simulation were shown in the form of voltage around the natural frequencies. small damping factor an alternative way was implemented to designing the energy harvester with more number of beams with same or different natural frequency. They concluded that more beams will simultaneously generating voltage which will increase the power storage.

Xingjian Jing et al.(2011) investigated and developed the frequency response functions and nonlinear output spectrum of block-oriented nonlinear systems, which demonstrated. They presented that the relationship between frequency response functions on the linear part of the model and model parameters. The nonlinear parts of these models were multivariate polynomial function and results provided a significant insight into the analysis and design of block-oriented nonlinear systems.

G. Boschetti et al.(2011) experimentally studied that the effectiveness and ease of implementation of a non-time based control strategy for the simultaneous active vibration control and path tracking of multi-degree-of-freedom linear systems. They presented that reducing elastic vibrations while guaranteeing coordinated motion among the system rigid-body degrees of freedom and the accurate tracking of desired paths through space. Experimental validation of the innovative non-time based control scheme, Delayed Reference Control (DRC), proposed for simultaneous path tracking and active vibration damping of mechanical systems.

Jing Na et al.(2011) evaluated an adaptive neural controller is proposed for nonlinear systems with a nonlinear dead-zone and multiple time-delays. They developed a novel high-order neural network (HONN) with only a scalar weight parameter to account for unknown nonlinearities. The Simulations and experiments for a turntable servo system with permanent-magnet synchronous motor (PMSM) were provided to verify the reliability and effectiveness with superior performance.

Yuan Yun et al.(2011) developed the vibration isolation system for highly sensitive equipment applications, which attenuates the vibration transmission above some corner frequencies so as to protect the instrument from the jitters induced by various disturbance sources. They established the general Kane's dynamics model for a class of parallel mechanisms, they designed a set of controllers which explicitly trade between nominal performance and robust stability and obtained controller by using LMI control toolbox of MATLAB. The results of the time history responses and selected frequency responses of the moving platform along each axis and isolation effect due to the good performance of designed controller.

Saadon et al.(2011) propose a comparative study on the obtained results of the energy delivered from the ambient vibration based MEMS energy harvester using the ANSYS and COVENTORWARE approaches. The improvement reflected in the experimental

results for vibration based MEMS piezoelectric energy harvesters indicates excellent application scope in power MEMS and green energy. After around 12.5 ms, a stable oscillation with respect to time is observed, and the oscillating voltage amplitude is around ± 2l V. The difference is that the envelope of the lumped-mass model continues to increase after 15 ms possibly because the damping ratio does not match the system, thereby causing continued increase in voltage.

Joono Cheong et al.(2012) developed mathematical model to obtain the closed-form invariant slow manifold, along with required admissible boundary conditions for the exact dynamic inversion of singularly perturbed second-order linear systems through asymptotic expansion in a singular parameter. They presented a converging infinite series under desired output constraints support functions in the complex domain.

MirosławGalickiet al.(2012) presented the solution of complex mobile manipulator at the feedback level of control stage the desired trajectory, tracked (end goal task) with zero platform velocity and tracking trajectory by the end-effectors. They concluded by the numerical simulation results which consisting that the non-holonomic differentially steered wheeled mobile robot and a holonomic manipulator of two revolute kinematic pairs and their controls.

Xianfu Zhang et al.(2012) presented a lower triangular model with time-varying gain finite-time stabilization for a nonlinear system. They presented the finite-time Lyapunov stability theorem and dynamic gain control design to state feedback finite-time stabilization controllers with dynamical gains for a class of time-varying nonlinear systems. The controller of finite time stabilized the state transformation and dynamic gain.

JuhaOrivuori et al.(2012) presented active vibration isolation of frequency varying tonal disturbances in an engine mounted on a raft and adaptive nonlinear control algorithm with frequency tracking was introduced to tackle this problem. They evaluated the method was robust to measurement noise and additional output disturbances and yielding a high level of vibration suppression with fast convergence rate and provided good control performance.

MurelitharanMuniandy et al.(2012) presented a novel drive train mechanism that minimizes systematic odometry errors for indoor non-holonomic differential drive wheeled mobile robot. The innovative and robust drive train mechanical design the

dual planetary drive (DPD) that were both drive a non-holonomic wheeled robot in straight lines effectively and minimize systematic odometry error without the need for complex electronic feedback control systems.

Ahmad 'Athifet al.(2012) design for simulation and control of an the Intelligent Pneumatic Actuators (IPA) system for application that requires better control and accuracy using Proportional-Integrative (PI) controller and pole-placement feedback controller. The flow for the controller design starts with the mathematical calculation, procedures and the implementation of the simulation control by using MATLAB software. The results of simulation were compared and analyzed to the performance of the controllers.

KhairulAnam et al.(2012) presented that the exoskeleton control system categorized according to the model system, the physical parameters, the hierarchy and the usage control systems in the existing and these considerations given different control schemes and how to achieve the best control performances. The variation control system implementation and utilized today need improvement to meet the need of the next exoskeleton control system such as the assist as needed, the user's intention detection, the modularity, the safety and the stability.

Lili Dong et al. (2012) carried out the study a novel design of a robust decentralized load frequency control (LFC) for the regulating area control error (ACE) in the system uncertainties and external disturbances which based on active disturbance for systems like turbines of various types, such as non-reheat, reheat, and hydraulic They presented the simulation results to verified the effectiveness and comparison with an existing PI-type controller tuned via genetic algorithm linear matrix inequalities (GALMIs). The comparison results show the superiority of the solution for stability and robustness of the closed-loop system using frequency-domain analysis.

HanifRamli et al. (2012) presented Active Force Control (AFC) based architecture in characterizing the twin rotor multi-input multi-output (MIMO) system (TRMS). They presented architecture was expected to produce an optimum control gains in both pitch and yaw responses by introducing decoupling function between pitch and yaw responses The optimized performance by the realization of hybrid strategy in which an artificial intelligence Fuzzy Logic was integrated into the control architecture.

CHAPTER - 2

Materials and Methods

It is identified from these review papers that there is a need to study for active control strategies for self-diagnosis and self-repair enabled structures where information technology may be incorporated within the structures for active control of mechanical system as well. This would help itself to provide efficient safe and robust active system. Keeping in view of this requirement, the present research work is outlined as follows.

3.1 Material

Material	Alloy Steel	Carbon Fiber Reinforced Plastic
Modulus of Elasticity	$2x10^5$ N/mm^2	$22x10^4$ N/mm^2
Density	$7803x10^{-9}$ kg/mm^3	$1720x10^{-9}$ kg/mm^3
Poisson's Ratio	0.33	0.3

3.2 Smart Materials

Piezoelectric materials belong to the so-called smart materials, or multifunctional materials, which have the ability to respond significantly to stimuli of different physical natures. The coupling between the physical fields of different types is expressed by the non-diagonal cells in the figure; if its magnitude is sufficient, the coupling can be used to build discrete or distributed transducers of various types, which can be used as sensors, actuators, or even integrated in structures with various degrees of tailoring and complexity (e.g. as fibers), to make them controllable or responsive to their environment (e.g. for shape morphing, precision shape control, damage detection, dynamic response alleviation,...).

3.3 Smart Structures

An active structure consists of a structure provided with a set of actuators and sensors coupled by a controller; if the bandwidth of the controller includes some vibration

modes of the structure, its dynamic response must be considered. If the set of actuators and sensors are located at discrete points of the structure, they can be treated separately.

The distinctive feature of smart structures is that the actuators and sensors are often distributed, and have a high degree of integration inside the structure, which makes a separate modelling impossible.Moreover, in some applications like vibroacoustics, the behavior of the structure itself is highly coupled with the surrounding medium; this also requires a coupled modelling. From a mechanical point of view, classical structural materials are entirely described by their elastic constants relating stress and strain, and their thermal expansion coefficient relating the strain to the temperature. Smart materials are materials where strain can also be generated by different mechanisms involving temperature, electric field or magnetic field, etc... as a result of some coupling in their constitutive equations. The most celebrated smart materials are briefly described below:

• Shape Memory Alloys (SMA) allow one to recover up to 5 % strain from the phase change induced by temperature. Although two-way applications are possible after education, SMA are best suited to one-way tasks such as deployment. In any case, they can be used only at low frequency and for low precision applications, mainly because of the difficulty of cooling. Fatigue under thermal cycling is also a problem. The best known SMA is called NITINOL; SMA are little used in active vibration control. The super elastic behavior of SMA may be exploited to achieve damping, for low frequency and low cycle applications, such as earthquake protection.

• Piezoelectric materials have a recoverable strain of 0.1 % under electric field; they can be used as actuators as well as sensors. There are two broad classes of piezoelectric materials used in vibration control: ceramic sand polymers. The piezo polymers are used mostly as sensors, because they require extremely high voltages and they have a limited control authority; the best known is the polyvinylidene fluoride (PVDF or PV F2). Piezo ceramics are used extensively as actuators and sensors, for a wide range of frequency including ultrasonic applications; they are well suited for high precision in the nanometer range (1nm = 10-9m). The best known piezo ceramic is the Lead ZirconateTitanate (PZT); PZT patches can be glued or co-fired on the supporting structure.

• Magnetostrictive materials have a recoverable strain of 0.15 % under magnetic field; the maximum response is obtained when the material is subjected to compressive loads. Magnetostrictive actuators can be used as load carrying elements (in compression alone) and they have a long lifetime. They can also be used in high precision applications. The best known is the TERFENOL-D; it can be an alternative to PZT in some applications (sonar).

• Magneto-rheological (MR) fluids consist of viscous fluids containing micron sized particles of magnetic material. When the fluid is subjected to a magnetic field, the particles create columnar structures requiring a minimum shear stress to initiate the flow. This effect is reversible and very fast (response time of the order of millisecond). Some fluids exhibit the same behavior under electrical field; they are called electro-rheological (ER) fluids; however, their performances (limited by the electric field breakdown) are currently inferior to MR fluids. MR and ER fluids are used in semi-active devices.

3.4 Finite Element Method

The finite element method (FEM) is a numerical technique for solving a wide range of engineering problems by finding approximate solution. Finite element method works on the principle of "DIVIDE" and "ANALYZE" that feature makes finite element method unique from others. In finite element method, a complex region is defining a continuum is discretized into simple geometric shapes called finite element. These elements are considered to be interconnected at specific joints called nodes or nodal point. The nodes are usually lie on the element boundaries where adjacent elements are considered to be connected. Since the actual variation of the field variable (temperature, pressure, stress) inside the continuum is unknown. The variation of the field variable inside a finite element can be approximated and define in terms of the values of the field variable at the node. By solving the equation, which are generally in the form of matrix equation, the nodal values of the field variable will be known. FEM is now become an integral part of CAE. Many powerful commercial software are available and enabling its widespread use in several industries. The approximate solution becomes exact when the geometry is divided into numerous or infinite elements and each element of geometry must define with a complete set of polynomials (infinite terms).

3.4.1 Applications of the Finite Element Method

The finite element method is an effective tool to analyze both structural and nonstructural problems. Even in some biomechanical engineering problems, includes analyses of human spine, hip joints, skull, hip joints, heart and eye etc.

Structural areas:

1. Stress analysis, including truss and frame analysis.
2. Heat Transfer Problem
3. Machine Design
4. Fluid Mechanics
5. Stress concentration problems commonly associated with holes, fillets, or other changes in geometry in a body.
6. Vibration analysis

3.4.2 Software packages for FEM

1. ANSYS
2. NASTRAN
3. ABAQUS
4. COSMOS Works
5. ALGOR
6. LS-DYNA

3.5 Finite Element Modelling

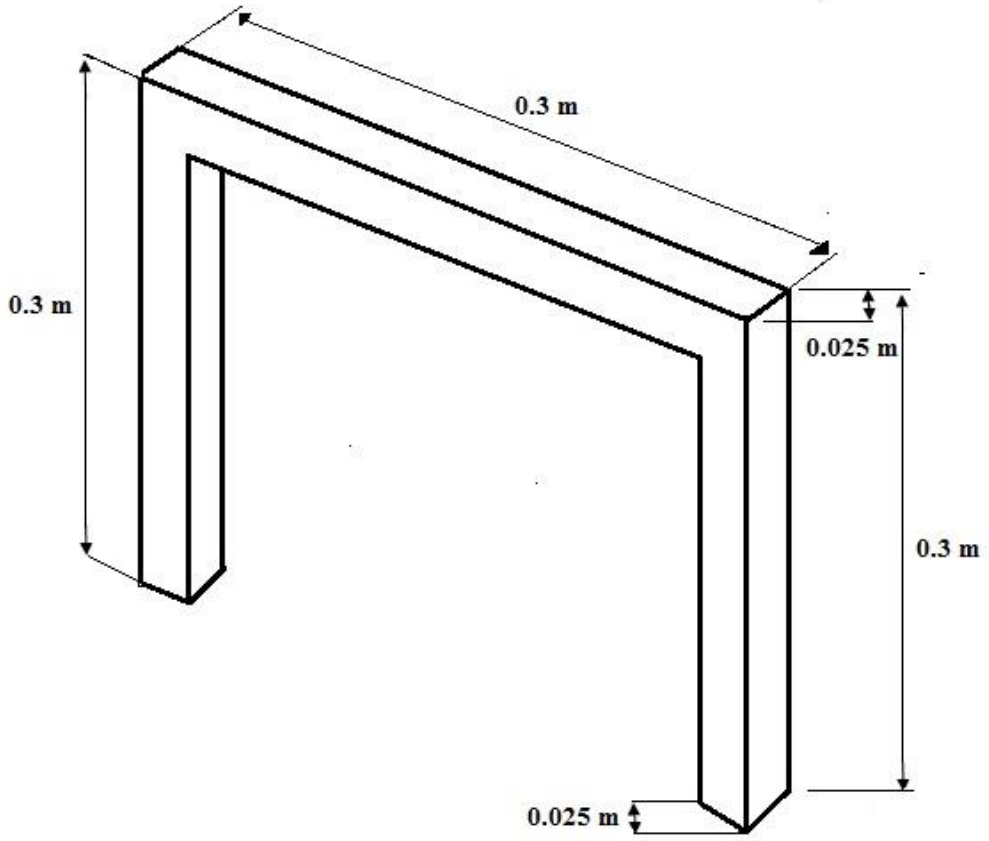

3.1 Geometric Dimensions of Portal Frame Structure

Modelling includes idealization of a practical problem into physical model and further governing equation would be written after putting realistic boundary conditions and application of real-world mechanical forces and surrounding conditions. A mechanical portal frame structure is widely used for mounting of machines. Therefore, dynamic performance of this structure has important role in controlling the performance of the machine tool. The use of a portal frame has does not limit the applications of the concept. This can be equally applied to a chassis of vehicle to have comfort ride to the passengers in the vehicle and other similar system.

This work includes following steps:

- FE modelling of portal frame structure and obtaining dynamic system parameters in terms of stiffness, mass and damping matrices.
- Eigen solution to obtain the dynamic parameters such as naturals frequencies, mode shapes and damping characteristics.

- Response analysis of the structure in terms of frequency response functions and co-relating the design aspects.
- Develop strategic option to actively control the response of the structure using smart materials or other damping features such as turned absorber or using viscos-layers in between metalling elements.
- Perform sensitivity analysis to obtain the most effective parameters of the system which control its dynamic behavior.

Based on the sensitivity analysis optimizing the strategy to have economically viable solutions of the machine tool behavior in dynamic domain.

Output / Input	Strain	Electric charge	Magnetic flux	Temperature	Light
Stress	Elasticity	Piezoelectricity	Magneto-striction		Photoelasticity
Electric field	Piezoelectricity	Permittivity			Electro-optic effect
Magnetic field	Magneto-striction	Magneto-electric effect	permeability		Magneto-optic
Heat	Thermal expansion	Pyro-electricity		Specific heat	
Light	Photo striction				Refractive index

Fig. 3.2 Stimulus-response relations indicating various effects in materials. The smart material corresponding to the non-diagonal cells.

3.6 Finite Element Formulation

In this section, FEM formulationfor portal frame structure is carried out by taking the whole frame piecewise (element) for active vibration control. A mathematical model has been developed such that an equivalence of parameters is obtained between the excitation and the piezoelectric actuator effect and eigen values, eigen vector are obtained.

3.6.1 Equation of Motion

Lagrange's equation to formulate equations of motion are given by

$$\frac{d}{dt}\left(\frac{dT}{d\dot{q}_i}\right) - \frac{\partial T}{\partial q_i} + \frac{\partial A}{\partial q_i} = Q_i (i = 1, 2, 3, \ldots\ldots\ldots\ldots n) \tag{3.1}$$

Where, t=time

T = Kinetic energy of system

q_i= Time derivative of coordinate system representing velocity

A = Potential energy of the system

Q_i = Non conservative forces or moment

Consider a single degree of freedom system that requires only one coordinate q to describe its behavior. To apply it in Eq.(1) to express the kinetic and potential energies of the system in terms of coordinate q and its derivative q'. Let q=x then, the kinetic and potential energy of the system are

$$T = \frac{1}{2} m x^{\cdot 2} \tag{3.2}$$

$$A = \frac{1}{2} k x^2 \tag{3.3}$$

Now, differentiating the kinetic energy term with respect to $q^{\cdot} = x^{\cdot}$

$$\frac{\partial T}{\partial q^{\cdot}} = \frac{\partial \dot{T}}{\partial x^{\cdot}} = \frac{\partial}{\partial x^{\cdot}}\left(\frac{1}{2} x^{\cdot 2}\right) = (2)\left(\frac{1}{2}\right) m x^{\cdot} = m x^{\cdot} \tag{3.4}$$

Then, taking the time derivative of $\frac{\partial T}{\partial x^{\cdot}}$ we get,

$$\frac{d}{dt}\left(\frac{\partial T}{\partial x^{\cdot}}\right) = \frac{d}{dt}(m x^{\cdot}) = m x^{\cdot\cdot} \tag{3.5}$$

Because T is the function of $x^{\cdot} and not x, \frac{\partial T}{\partial x} = 0$. Evaluating the potential term, $\partial A / \partial q$ in Eq.(1). We get,

$$\frac{\partial A}{\partial q} = \frac{\partial A}{\partial x} = \frac{\partial}{\partial x}\left(\frac{1}{2} k x^2\right) = kx \tag{3.6}$$

Substituting for each term in Eq.(1).We get,

$$\frac{d}{dt}\left(\frac{\partial T}{\partial \dot{q_i}}\right) - \frac{\partial T}{\partial q_i} + \frac{\partial A}{\partial q_i} = Q_i \tag{3.7}$$

The governing differential equation of motion is given by

$$m\ddot{x} + kx = 0 \tag{3.8}$$

Now, consider a system with two degree of freedom, consequently we need two coordinates x_1 and x_2 to formulate kinetic and potential energies,

$$T = \frac{1}{2}m_1\dot{x_1}^2 + m_2\dot{x_2}^2 \tag{3.9}$$

$$A = \frac{1}{2}k_1x_1^2 + \frac{1}{2}k_2(x_2 - x_1)^2 \tag{3.10}$$

Taking the derivative of each terms, as required by Eq.(1). We get,

$$\frac{\partial T}{\partial \dot{x_1}} = m_1\dot{x_1} and \frac{d}{dt}\left(\frac{\partial T}{\partial \dot{x_1}}\right) = m_1\ddot{x_1} \tag{3.11}$$

$$\frac{\partial T}{\partial \dot{x_2}} = m_2\dot{x_2} and \frac{d}{dt}\left(\frac{\partial T}{\partial \dot{x_2}}\right) = m_2\ddot{x_2} \tag{3.12}$$

$$\frac{\partial T}{\partial x_1} = \frac{\partial T}{\partial x_2} = 0 \tag{3.13}$$

$$\frac{\partial A}{\partial x_1} = k_1x_1 + k_2(x_1 - x_2) \tag{3.14}$$

$$\frac{\partial A}{\partial x_2} = k_2(x_2 - x_1) \tag{3.15}$$

Substituting each term in Lagrange's equation in Eq.(1). We get,

$$m_1\ddot{x_1} + (k_1 + k_2)x_1 - k_2x_2 = 0 \tag{3.16}$$

$$m_2\ddot{x_2} - k_2x_1 + k_2x_2 = 0 \tag{3.17}$$

We can express equation of motion in a matrix form by

$$\begin{bmatrix} m_1 & 0 \\ 0 & m_2 \end{bmatrix}\begin{Bmatrix} \ddot{x_1} \\ \ddot{x_2} \end{Bmatrix} + \begin{bmatrix} k_1 + k_2 & -k_2 \\ -k_2 & k_2 \end{bmatrix}\begin{Bmatrix} x_1 \\ x_2 \end{Bmatrix} = \begin{Bmatrix} 0 \\ 0 \end{Bmatrix} \tag{3.18}$$

Now, finite element formulation of axial members by using Lagrange's equations, formulating the mass matrix for an axial member and then using it for calculating the natural frequencies of an axial member.

Formulating Mass Matrix

The displacement of an axial member is expressed by using one-dimensional shape function S_i and S_j,

$$u = S_i U_i + S_j U_j \tag{3.19}$$

Now, the shape function in terms of the local coordinate x, as shown in figure are given by

$$S_i = 1 - \frac{x}{L} \tag{3.20}$$

$$S_j = \frac{x}{L} \tag{3.21}$$

For a dynamic problem the displacement function is a function of x and time t, i.e. u=u(x,t). The total kinetic energy of the member is the sum of the kinetic energies of its constituent particles

$$T = \int_0^L \frac{\gamma}{2} \dot{u}^2 dx \tag{3.22}$$

The velocity of the member is expressed in terms of $U_i and U_j$ is given by

$$\dot{u} = S_i U_i + S_j U_j \tag{3.23}$$

Where

$\dot{u}$ = Velocity of the particles along the member.

γ = mass per unit length

Substituting Eq. (6) into Eq. (5), we get

$$T = \frac{\gamma}{2} \int_0^L (S_i U_i + S_j U_j)^2 \, dx \tag{3.24}$$

After taking derivatives as required by Lagrange's Equation (1). We get,

$$\frac{\partial T}{\partial U_i} = \frac{\gamma}{2} \int_0^L 2 \, S_i \left(S_i U_i + S_j U_j\right)^2 dx \tag{3.25}$$

$$\frac{\partial T}{\partial U_j} = \frac{\gamma}{2}\int_0^L 2S_j\left(S_i\dot{U_i} + S_j\dot{U_j}\right)^2 dx \quad (2.26)$$

$$\frac{d}{dt}\left(\frac{\partial T}{\partial \dot{u}_j}\right) = \gamma\left[\int_0^L S_j^2\ddot{U_i}dx + \int_0^L S_iS_j\ddot{U_j}\,dx\right] \quad (3.27)$$

$$\frac{d}{dt}\left(\frac{\partial T}{\partial U_j}\right) = \gamma\left[\int_0^L S_iS_j\ddot{U_i}dx + \int_0^L S_j^2\ddot{U_j}dx\right] \quad (3.28)$$

Here S_i and S_j are the functions of x alone, whereas $\ddot{U_i} and \ddot{U_j}$ represent accelerations at node i and j respectively, which are function of time.

Evaluating the integrals of Eq.(8) & Eq.(9). We get,

$$\gamma\int_0^L S_i^2 dx = \gamma\int_0^L\left(1-\frac{x}{L}\right)^2 dx = \frac{\gamma L}{3} \quad (3.29)$$

$$\gamma\int_0^L S_j^2\,dx = \gamma\int_0^L\left(\frac{x}{L}\right)^2 dx = \frac{\gamma L}{3} \quad (3.30)$$

Solving Eq. (8) through Eq.(9) into Eq.(6) and Eq.(7) gives the mass matrix,

$$[M] = \frac{\gamma L}{6}\begin{bmatrix}2 & 1\\ 1 & 2\end{bmatrix} \quad (3.31)$$

Formulating Stiffness Matrix

During the deformation the member under axial loading, the strain energy stored is given by

$$A^{(e)} = \int_v \frac{\sigma\varepsilon}{2}dV = \int_v \frac{E\varepsilon^2}{2}dV \quad (3.32)$$

Now, the total potential energy Π for the body contains n elements and m modes is given by

$$\Pi = \sum_{e=1}^{n} A^{(e)} - \sum_{i=1}^{m} F_i u_i \quad (3.33)$$

The deflection for an element with nodes I & j in terms of local shape function is given by,

$$u^{(e)} = S_i u_i + S_j u_j \quad (3.34)$$

The strain in each member is calculated by

$$\varepsilon = \frac{-u_i + u_j}{\varrho} \tag{3.35}$$

Substituting Eq.(13) into Eq.(10) yields the strain energy for an arbitrary element (e) and minimizing w.r.t. u_i and u_j leads in matrix form

$$\begin{Bmatrix} \frac{\partial A^{(e)}}{\partial u_i} \\ \frac{\partial A^{(e)}}{\partial u_j} \end{Bmatrix} = \frac{AE}{L}\begin{bmatrix} 1 & -1 \\ -1 & 1 \end{bmatrix}\begin{Bmatrix} u_i \\ u_j \end{Bmatrix} \tag{3.36}$$

Eq. (14) is Stiffness matrix

$$[K] = \frac{AE}{L}\begin{bmatrix} 1 & -1 \\ -1 & 1 \end{bmatrix}$$

Solving mass and stiffness matrix for eigen values by using the formula

$$[M]^{-1}[K]\{U\}=\omega^2\{U\} \tag{3.37}$$

3.6.2 Guyan Reduction

The size of a discretized model obtained by finite elements is essentially governed by the representation of the stiffness of the structure. For complicated geometries, it may become very large, especially with automated mesh generators. Before solving the eigenvalue problem, it may be advisable to reduce the size of the model by condensing the degrees of freedom with little or no inertia and which are not excited by external forces, nor involved in the control. The degrees of freedom to be condensed, denoted x_2 in what follows, are often referred to as slaves; those kept in the reduced model are called masters and are denotedx_1.

To begin with, consider the undamped forced vibration of a structure where the slaves x_2 are not excited and have no inertia; the governing equation is

$$\begin{pmatrix} M_{11} & 0 \\ 0 & 0 \end{pmatrix}\begin{pmatrix} \ddot{x_1} \\ \ddot{x_2} \end{pmatrix} + \begin{pmatrix} K_{11} & K_{12} \\ K_{21} & K_{22} \end{pmatrix}\begin{pmatrix} x_1 \\ x_2 \end{pmatrix} = \begin{pmatrix} f_1 \\ 0 \end{pmatrix} \tag{3.38}$$

$$M_{11}\ddot{x_1} + K_{11}x_1 + K_{12}x_2 = f_1 \tag{3.39}$$

$$K_{21}x_1 + K_{22}x_2 = 0 \tag{3.40}$$

According to the second equation, the slaves x_2 are completely determined by the masters x_1:

$$x_2 = -K_{22}^{-1}K_{21}x_1 \quad (3.41)$$

Substituting into Equ.(21), we find the reduced equation

$$M_{11}\ddot{x}_1 + (K_{11} - K_{12}K_{22}^{-1}K_{21})x_1 = f_1 \quad (3.42)$$

which involves only x1. Note that in this case, the reduced equation has been obtained without approximation.

The idea in the so-called Guyan reduction is to assume that the master slave relationship (4) applies even if the degrees of freedomx_2 have some inertia (i.e. when the sub-matrix$M_{22} \neq 0$) or applied forces. Thus, one assumes the following transformation

$$x = \begin{pmatrix} x_1 \\ x_2 \end{pmatrix} = \begin{pmatrix} I \\ -K_{22}^{-1}K_{21} \end{pmatrix} \mathrm{x}_1 = Lx_1 \quad (3.43)$$

The reduced mass and stiffness matrices are obtained by substituting the above transformation into the kinetic and strain energy:

$$T = \frac{1}{2}\dot{x}^T M\dot{x} = \frac{1}{2}\dot{x}_1^T L^T ML\dot{x}_1 = \frac{1}{2}\dot{x}_1^T \widehat{M}\dot{x}_1 \quad (3.44)$$

$$u = \frac{1}{2}x^T Kx = \frac{1}{2}x_1^T L^T KLx_1 = \frac{1}{2}x_1^T \widehat{K}x_1 \quad (3.45)$$

With $\widehat{M} = L^T ML\widehat{K} = L^T KL$

The second equation produces $\widehat{K} = K_{11} - K_{12}K_{22}^{-1}K_{21}$ as in Equ.(24). Ifexternal loads are applied to x_2, the reduced loads are obtained by equating the virtual work

$$\delta x^T f = \delta x_1^T L^T f = \delta x_1^T \hat{f}_1$$

or

$$\hat{f}_1 = L^T f = f_1 - K_{12}K_{22}^{-1}f_2 \quad (3.46)$$

Finally, the reduced equation of motion reads

$$\widehat{M}\ddot{x}_1 + \widehat{K}x_1 = \hat{f}_1(3.47) \quad (3.47)$$

Usually, it is not necessary to consider the damping matrix in the reduction, because it is rarely known explicitly at this stage. The Guyan reduction can be performed automatically in commercial finite element packages, the selection of masters and slaves being made by the user. In the selection process the following should be kept in mind:

- The degrees of freedom without inertia or applied load can be condensed without affecting the accuracy.
- Translational degrees of freedom carry more information than rotational ones. In selecting the masters, preference should be given to translations, especially if large modal amplitudes are expected.
- It can be demonstrated that the error in the mode shape φ_i associated with the Guyan reduction is an increasing function of the ratio

$$\frac{\omega_i^2}{v_1^2} \tag{3.48}$$

Where $\omega_i$is the natural frequency of the mode and v_1 is the first natural frequency of the constrained system, where all the degrees of freedom x_1 (masters) have been blocked [v_1 is the smallest solution of $det\ (K_{22} - v^2 M_{22})$]. Therefore, the quality of a Guyan reduction is strongly related to the natural frequencies of the constrained system and v_1 should be kept far above the frequency band $\omega_b$where the model is expected to be accurate.

3.7 ANSYS

ANSYS, Inc. is an engineering modelling and simulation software that offers engineering simulation solution sets in engineering simulation that a design process requires. Here, we are using ANSYS WORKBENCH 14.0 in which modelling of beam is done in geometry component system, material is selected from engineering data library and simulation & analysis is performed in modal analysis. ANSYS takes the various parameters like thickness t, cross-sectional area A, modulus of elasticity E, shear modulus G, density ρ and passions ratio υ. In this research natural frequencies and mode shapes are considered for dynamic analysis.

3.8 Modal Analysis

Steps Involved in a Modal Analysis

3.8.1 Preprocessing

The preprocessor stage in a general FEA package involves the following:

- Defining the element type as planned before the analysis. This may be one-, two-, or three-dimensional.

- **Creating the geometry**. The geometry is drawn in one-, two-, or three-dimensional space according to what kind of elements are going to be used. The model may be created in the preprocessor, or it can be imported from other CAD or CAE systems via a neutral file format (IGES, STEP, ACIS, Parasolid, DXF, etc.). The same units should be applied in all models, otherwise the results will be difficult to interpret or, in extreme cases, the results will not show up mistakes made during the loading and restraining of the model.
- **Applying a mesh**. Mesh generation is the process of dividing the continuum into a number of discrete parts or finite elements. The finer the mesh, the more accurate the result, but the longer the processing time. Therefore, a compromise between accuracy and solution speed is usually made. The mesh may be created manually or generated automatically, or, as in most cases, in a combined manner.

  Manual meshing is a long and tedious process for models with a fair degree of geometric complication, but with useful tools emerging in preprocessors, the task is becoming easier. Automatic mesh generators are very useful and popular. The mesh is created automatically by a mesh engine; the only requirement is to define the mesh density along the model's edges. Automatic meshing has limitations as regards mesh quality and solution accuracy. Automatic brick element mesher are limited in function, but are steadily improving. Any mesh is usually applied to the model by simply selecting the mesh command on the preprocessor list of the user interface.

  Usually a complex geometry needs to be decomposed into many smaller components in order to use the automatic meshing tool.
- **Assigning properties**. Material properties (Young's modulus; Poisson's ratio; the density; and if applicable, the coefficients of expansion, friction, thermal conductivity, damping effect, specific heat, etc.) will have to be defined. In addition element properties may need to be set. If two-dimensional elements are being used, the thickness property is required. One-dimensional beam elements require area, Ixx ;Iyy ; Izz ; J; and the direction of the beam axis in three-dimensional space. Shell elements, which are two-dimensional elements in three-dimensional space, require orientation and neutral surface offset parameters to be defined. Special elements such as mass, contact, spring, gap,

coupling, damper, and so on require properties (specific to the element type) to be defined for their use.

- **Applying loads**. In the case of transient response analysis, some type of load is usually applied to the analysis model. The loading may be in the form of a point force, a pressure or a displacement, or a temperature or heat flux in a thermal analysis. The loads may be applied to a point, an edge, a surface, or even a complete body. The loads should be in the same unit system as the model geometry and material properties specified. In the case of modal analyses, a load does not have to be specified for the analysis to run.
- **Applying boundary conditions**. Structural boundary conditions are usually in the form of zero displacements; thermal boundary conditions are usually specified temperatures. A boundary condition may be specified to act in all directions or in certain directions only. Boundary conditions can be placed on nodes, key points, lines, or areas. The boundary conditions applied on lines or areas can be of a symmetric or antisymmetric type, one allowing in plane rotations and out of plane translations, the other allowing in plane translations and out of plane rotations for a given line or area. The application of correct boundary conditions is critical to the accurate solution of the design problem.

3.8.2 Solution

The FEA solver can be logically divided into three main parts: the presolver, the mathematical-engine, and the postsolver. The presolver reads in the model created by the preprocessor and formulates the mathematical representation of the model. All the parameters defined during the preprocessing stage are used to do this, so if something has been omitted the presolver is very likely to stop the call to the mathematical-engine. If the model is correct, the solver proceeds to form the element stiffness matrix and the element mass matrix for the problem and calls the mathematical-engine, which calculates the result. The results are returned to the solver and the postsolver is used to calculate strains, stresses, velocities, response, and so on for each node within the component or continuum. All these results are sent to a result file that may be read by the postprocessor.

Now, for modelling of beam the key structure is designed, then this area is extruded and a three-dimensional model was obtained. After meshing, the beam was discretized into elements and nodes. Cantilever boundary conditions can also be

modelled by constraining all degree of freedom except the required. After this the result is obtained.

3.8.3 Postprocessing

Here the results of the analysis are read and interpreted. They can be presented in the form of a table, a contour plot, a deformed shape of the component, or the mode shapes and natural frequencies if frequency analysis is involved. Most postprocessors provide animation tools. Contour plots are usually the most effective way of viewing results for structural type problems. Slices can be made through three-dimensional models to facilitate the viewing of internal stress and deformation patterns. All postprocessors now include the calculation of stresses and strains in any of the x; y; or z directions; or indeed in a direction at an angle to the coordinate axes. The principal stresses and strains may also be plotted, or if required, the yield stresses and strains according to the main theories of failure (Von Mises, St Venant, Tresca, etc.).

3.9 Active Control of Portal Frame Structure

Active vibration control is the active application of force in an equal and opposite fashion to the forces imposed by external vibration. With this application, a precision industrial process can be maintained on a platform essentially vibration-free.

Many precision industrial processes cannot take place if the machinery is being affected by vibration. For example, the production of semiconductor wafers requires that the machines used for the photolithography steps be used in an essentially vibration-free environment or the sub-micrometre features will be blurred. Active vibration control is now also commercially available for reducing vibration in helicopters, offering better comfort with less weight than traditional passive technologies.In the past, passive techniques were used. These include traditional vibration dampers, shock absorbers, and base isolation.

The typical active vibration control system uses several components:

- A massive platform suspended by several active drivers (that may use voice coils, hydraulics, pneumatics, piezo-electric or other techniques)
- Three accelerometers that measure acceleration in the three degrees of freedom

- An electronic amplifier system that amplifies and inverts the signalsfrom the accelerometers. A PID controller can be used to get better performance than a simple inverting amplifier.
- For very large systems, pneumatic or hydraulic components that provide the high drive power required.

If the vibration is periodic, then the control system may adapt to the ongoing vibration, thereby providing better cancellation than would have been provided simply by reacting to each new acceleration without referring to past accelerations.

3.9.1 MATLAB

MATLAB (MATrixLABoratory) is a high-performance interacting data-intensive software environment for high-efficiency engineering and scientific numerical calculations. MATLAB enable the users to solve a wide spectrum of analytical and numerical problems using matrix-based methods, attain excellent interfacing and interactive capabilities, compile with high-level programming languages, ensure robustness in data-intensive analysis and heterogeneoussimulations, and provide easy access to straight forward implementation of state-of-the-art numerical algorithms, guarantee powerful graphical features.

MATLAB allows matrix manipulations, plotting of functions and data, implementation of algorithms, creation of user interfaces, and interfacing with programs written in other languages, including C, C++, Java, Fortran and Python.

Although MATLAB is intended primarily for numerical computing, an optional toolbox uses the MuPAD symbolic engine, allowing access to symbolic computing capabilities. An additional package, Simulink, adds graphical multi-domain simulation and model-based design for dynamic and embedded systems.

Here, we are using MATLAB and Simulink 2014a in which simulation, analysis and active vibration control is done through Simulink.

3.9.2 Simulink

Simulink, developed by Math Works, is a graphical programming environment for modeling, simulating and analyzing multi-domain dynamic systems. Its primary interface is a graphical block diagramming tool and a customizable set of block libraries. It offers tight integration with the rest of the MATLAB environment and

can either drive MATLAB or be scripted from it. Simulink is widely used in automatic control and digital signal processing for multi-domain simulation andModel-Based Design. Simulink can automatically generate C source code for real-time implementation of systems. As the efficiency and flexibility of the code improves, this is becoming more widely adopted for production systems, in addition to being a tool for embedded system design work because of its flexibility and capacity for quick iteration. Embedded Coder creates code efficient enough for use in embedded systems.

Simulink Real-Time (formerly known as xPC Target), together with x86-based real-time systems, is an environment for simulating and testing Simulink and Stateflow models in real-time on the physical system. Another MathWorks product also supports specific embedded targets. When used with other generic products. Simulink and State flow can automatically generate synthesizable VHDL and Verilog. Simulink Verification and Validation enables systematic verification and validation of models through modeling style checking, requirements traceability and model coverage analysis. Simulink Design Verifier uses formal methods to identify design errors like integer overflow, division by zero and dead logic, and generates test case scenarios for model checking within the Simulink environment.

The systematic testing tool TPT is marketed as a way to perform a formal verification and validation process to stimulate Simulink models but also for use during the development phase where the developer generates inputs to test the system. By the substitution of the Constant and signal generator blocks of Simulink, Math Works claim that the stimulation becomes reproducible.

Sim Events is used to add a library of graphical building blocks for modeling queuing systems to the Simulink environment, and to add an event-based simulation engine to the time-based simulation engine in Simulink.

3.10 Controllers

Active vibration control is done through PID controllers which are running on different types of loop and configuration. Mainly there are two types of loop, open loop and closed loop with SISO controller and five types of controller configuration P, I, PI, PD, PID. The basic control loop can be simplified for a single-input-single-output (SISO) system as in Fig.1. Here we are neglecting any disturbance present in the system.

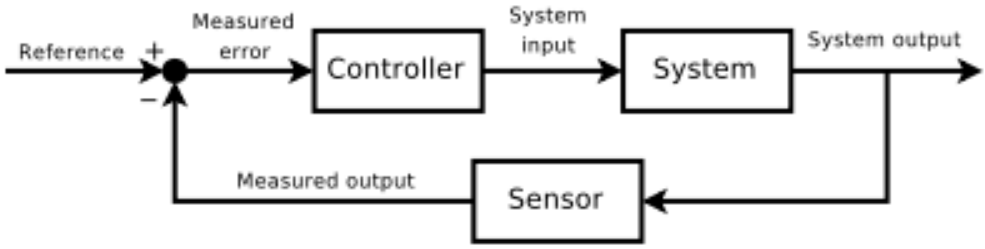

Fig. 3.3 A Closed Loop SISO System

The controller may have different structures. Different design methodologies are there for designing the controller in order to achieve desired performance level. But the most popular among them is Proportional-Integral-derivative (PID) type controller. In fact more than 95% of the industrial controllers are of PID type. As is evident from its name, the output of the PID controll0er u(t) can be expressed in terms of the input e(t), as:

$$u(t) = K_p\left[e(t) + \tau_d \frac{de(t)}{dt} + \frac{1}{\tau_i}\int_0^t e(\tau)d\tau\right] \tag{3.49}$$

and the transfer function of the controller is given by:

$$C(s) = K_p\left(1 + \tau_d s + \frac{1}{\tau_i s}\right) \tag{3.50}$$

The terms of the controller are defined as:

K_d = Proportional gain

T_d= Derivative time, and

τ_i= Integral time

In the following sections we shall try to understand the effects of the individual components- proportional, derivative and integral on the closed loop response of this

system. For the sake of simplicity, we consider the transfer function of the plant as a simple first order system without time delay as:

$$P(s) = \frac{K}{1+\tau s} \tag{3.51}$$

3.10.1 Proportional Control

Proportional control is sufficient for some systems, and examples of proportional control can be found in Robotics with the Boe-Bot. As circuit schematics are used to describe circuits, block diagrams are used to describe control systems. A block diagram for proportional control is shown in Fig.3.4. The circle on the left is called a summing junction, and it shows how the measured sensor value is subtracted from the desired sensor value (the set point) to calculate the error. This is the error that needs to be corrected by the control system. Proportional control attempts to correct this error by multiplying it by some constant value (Kp). The resulting actuator output exerts a correcting influence on the system. By definition, this influence is proportional to the measured error. With the proportional control action only, the closed loop system looks like:

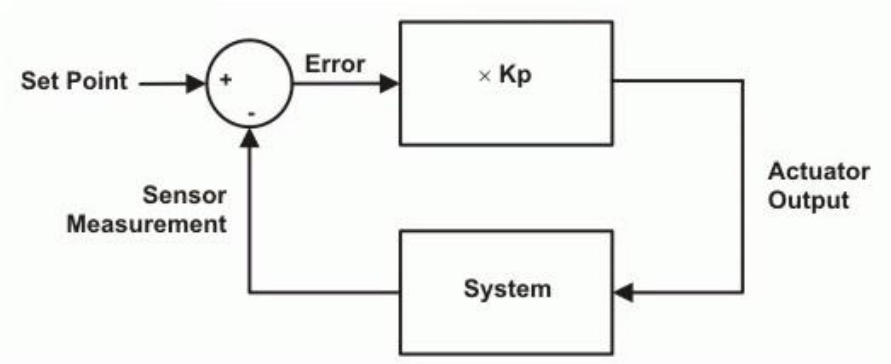

Fig. 3.4 Proportional Control Block Diagram

Now the closed loop transfer function can be expressed as:

$$\frac{c(s)}{r(s)} = \frac{\frac{KK_p}{1+\tau s}}{1+\frac{KK_p}{1+\tau s}} = \frac{KK_p}{1+KK_p+\tau s} = \frac{KK_p}{1+KK_p}\frac{1}{1+\tau' s} \tag{3.52}$$

where $\tau' = \frac{\tau}{1+KK_p}$

For a step input $r(s)=\frac{A}{s}$,

$$c(s)=\frac{KK_p}{1+KK_p}\frac{A}{s\left(1+\tau' s\right)}$$

or, $$c(t)=\frac{AKK_p}{1+KK_p}\left(1-e^{-st/\tau'}\right) \tag{3.53}$$

The system response is shown below

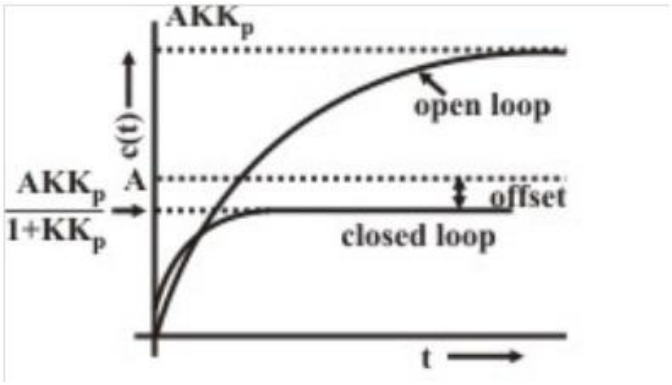

Fig. 3.5 Response with a proportional controller

From eqn. (5) and Fig. 3.4, it is apparent that:

1. The time response improves by a factor (i.e. the time constant decreases).

2.There is a steady state offset between the desired response and the output response

$$A\left(1-\frac{KK_p}{1+KK_p}\right)=\frac{A}{1+KK_p} \tag{3.54}$$

This offset can be reduced by increasing the proportional gain; but that may also cause increase oscillations for higher order systems.

The offset, often termed as "steady state error" can also be obtained from the error transfer function and the error function e(t) can be expressed in terms of the Laplace transformation form:

$$e(s)=\frac{1}{1+\frac{KK_p}{1+\tau s}}\frac{A}{s}=\frac{1+\tau s}{1+KK_p+\tau s}\frac{A}{s} \tag{3.55}$$

Using the final value theorem, the steady state error is given by:

$$e_{ss} = \underset{t\to\infty}{Lt}\ e(t) = \underset{s\to 0}{Lt}\ s\,e(s) = \underset{s\to 0}{Lt}\frac{1+\tau s}{1+KK_p+\tau s}\frac{A}{s} = \frac{A}{1+KK_p} \tag{3.56}$$

Often, the proportional gain term, Kp is expressed in terms of "Proportional Band". It is inversely proportional to the gain and expressed in percentage. For example, if the gain is 2, the proportional band is 50%. Strictly speaking, proportional band is defined as the %error to move the control valve from fully closed to fully opened condition. However, the meaning of this statement would be clear to the reader afterwards.

3.10.2 Integral Control

An integral controller is not particularly difficult to implement. In an analog system, an integral control system integrates the error signal to generate the control signal. If the error signal is a voltage, and the control signal is also a voltage, then a proportional controller is just an analog integrator. In a digital control system, an integral control system computes the error from measured output and user input to a program, and integrates the error using some standard integration algorithm, then generates an output/control signal from that integration.

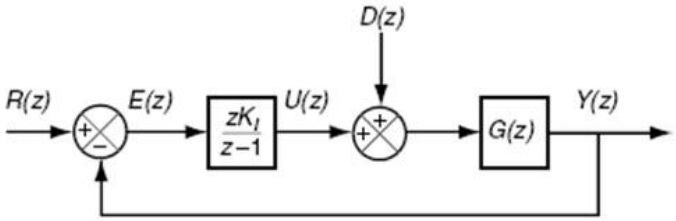

Fig. 3.6 Integral Control

Proceeding in the same way as in eqn. (4), in this case, we obtain,

$$\frac{c(s)}{r(s)} = \frac{\dfrac{K}{\tau_i s(1+\tau s)}}{1+\dfrac{K}{\tau_i s(1+\tau s)}} = \frac{K}{K+\tau_i s+\tau\tau_i s^2} \tag{3.57}$$

From the first observation, it can be seen that with integral controller, the order of the closed loop system increases by one. This increase in order may cause instability of the closed loop system, if the process is of higher order dynamics.

For a step input $r(s) = \frac{A}{s}$,

$$e(s) = \frac{1}{1 + \frac{K}{\tau_i(1+\tau s)}} \frac{A}{s} = \frac{\tau_i s(1+\tau s)}{\tau_i s(1+\tau s) + K} \frac{A}{s} \tag{3.58}$$

$$e_{ss} = \underset{s \to 0}{Lt}\, s\, e(s) = 0$$

So the major advantage of this integral control action is that the steady state error due to step input reduces to zero. But simultaneously, the system response is generally slow, oscillatory and unless properly designed, sometimes even unstable. The step response of this closed loop system with integral action is shown in Figure below.

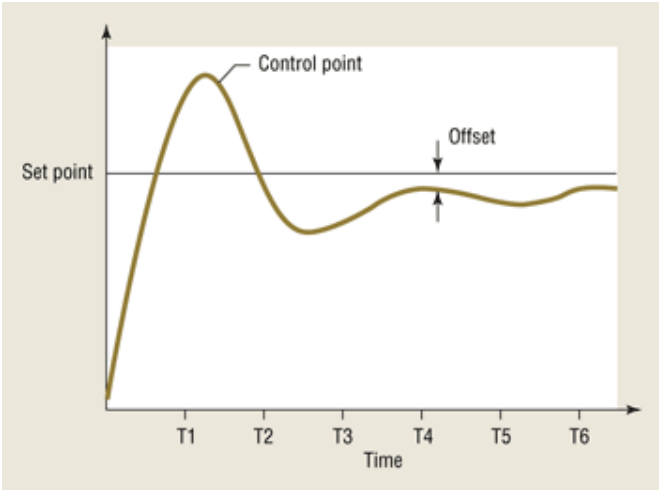

Fig. 3.7 Step Response with Integral Control Action

3.10.3 Proportional Plus Integral (P-I) Control

With P-I controller the block diagram of the closed loop system with the same process is given in Figure 3.8.

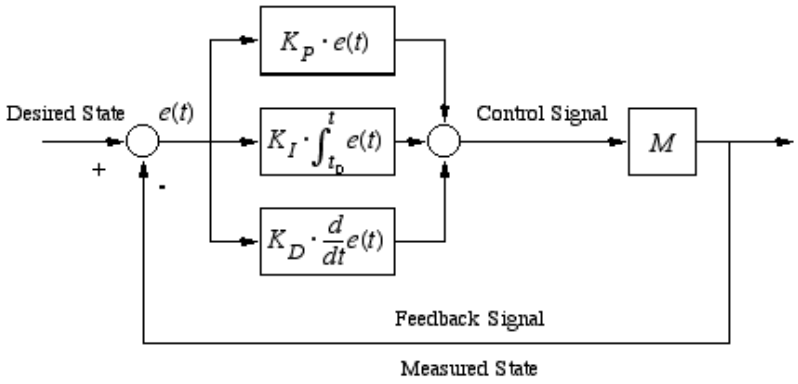

It is evident from the above discussions that the P-I action provides the dual advantages of fast response due to P-action and the zero steady state error due to I-action. The error transfer function of the above system can be expressed as:

$$\frac{e(s)}{r(s)} = \frac{1}{1+\dfrac{KK_p(1+\tau_i s)}{\tau_i s(1+\tau s)}} = \frac{\tau_i s(1+\tau s)}{s^2\tau\tau_i + (1+KK_p)\tau_i s + KK_p} \tag{3.59}$$

In the same way as in integral control, we can conclude that the steady state error would be zero for P-I action. Besides, the closed loop characteristics equation for P-I action is:

$$s^2\tau\tau_i + (1+KK_p)\tau_i s + KK_p = 0\,; \tag{3.60}$$

From which we can obtain, the damping constant as:

$$\xi = \left(\frac{1+KK_p}{2}\right)\sqrt{\frac{\tau_i}{KK_p\tau}} \tag{3.61}$$

Whereas, for simple integral control the damping constant is:

$$\xi = \left(\frac{1}{2}\right)\sqrt{\frac{\tau_i}{K\tau}} \tag{3.62}$$

Comparing these two, one can easily observe that, by varying the term Kp, the damping constant can be increased. So we can conclude that by using P-I control, the steady state error can be brought down to zero, and simultaneously, the transient response can be improved. The output responses due to (i) P, (ii) I and (iii) P-I control for the same plant can be compared from the sketch shown in Fig. 6.

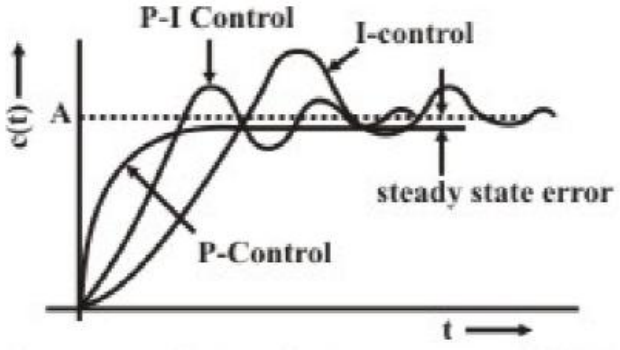

Fig. 3.9 Transient Responses with P, PI and PID

3.10.4 Proportional plus Derivative (P-D) Control

The transfer function of a P-D controller is given by:

$$C(s) = K_p(1 + \tau_d s) \tag{3.63}$$

P-D control for the process transfer function apparently is not very useful, since it cannot reduce the steady state error to zero. But for higher order processes, it can be shown that the stability of the closed loop system can be improved using P-D controller. For this, let us take up the process transfer function. Looking at Fig.7, we can easily conclude that with proportional control, the closed loop transfer function is

$$\frac{c(s)}{r(s)} = \frac{\frac{K_p}{Js^2}}{1 + \frac{K_p}{Js^2}} = \frac{K_p}{Js^2 + K_p} \tag{3.64}$$

and the characteristics equation is Js2 + Kp = 0; giving oscillatory response. But with P-D controller, the closed loop transfer function is:

$$\frac{c(s)}{r(s)} = \frac{\frac{K_p(1 + \tau_d s)}{Js^2}}{1 + \frac{K_p(1 + \tau_d s)}{Js^2}} = \frac{K_p(1 + \tau_d s)}{Js^2 + K_p(1 + \tau_d s)} \tag{3.65}$$

Whose characteristics equation is Js2 + Kpτds + Kp = 0; that will give a stable closed loop response. The step responses of this process with P and P-D controllers are compared

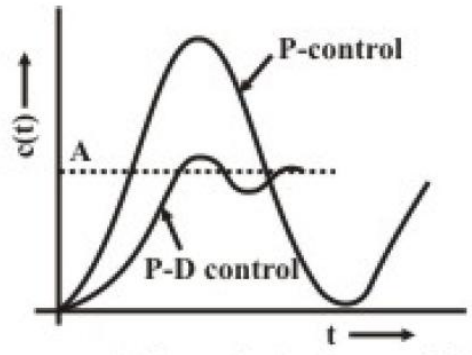

Fig. 3.10 Improvement of transient response with P-D control

3.10.5 Proportional-Integral-Derivative (PID) control

It is clear from above discussions that a suitable combination of proportional, integral and derivative actions can provide all the desired performances of a closed loop system. The transfer function of a P-I-D controller is given by:

$$C(s) = K_p\left(1 + \tau_d s + \frac{1}{\tau_i s}\right) \tag{3.66}$$

The order of the controller is low, but this controller has universal ap
be used in any type of SISO system, e.g. linear, nonlinear, time delay etc. Many of the MIMO systems are first decoupled into several SISO loops and PID controllers are designed for each loop. PID controllers have also been found to be robust, and that is the reason, it finds wide acceptability for industrial processes. However, for proper use, a controller has to be tuned for a particular process; i.e. selection of P,I,D parameters are very important and process dependent. Unless the parameters are properly chosen, a controller may cause instability to the closed loop system.

3.10.6 Guideline for selection of controller mode

1. Proportional Controller: It is simple regulating type; tuning is easy. But it normally introduces steady state error. It is recommended for process transfer functions having a pole at origin, or for transfer functions having a single dominating pole.

2. Integral Control: It does not exhibit steady state error, but is relatively slow responding. It is particularly effective for:

(i) Very fast process, with high noise level

(ii) Process dominated by dead time

(iii) High order system with all-time constants of the same magnitude.

3. Proportional plus Integral (P-I) Control: It does not cause offset associated with proportional control. It also yields much faster response than integral action alone. It is widely used for process industries for controlling variables like level, flow, pressure, etc., those do not have large time constants.

4. Proportional plus Derivative (P-D) Control: It is effective for systems having large number of time constants. It results in a more rapid response and less offset than is

possible by pure proportional control. But one must be careful while using derivative action in control of very fast processes, or if the measurement is noisy (e.g. flow measurement).

5. Proportional plus Integral plus Derivative (P-I-D) Control: It finds universal application. But proper tuning of the controller is difficult. It is particularly useful for controlling slow variables, like pH, temperature, etc. in process industries.

3.11Control Formulation

3.11.1 Finite Element formulation of regular frame element

A two nodes finite element of a rectangular beam element is shown in fig. below

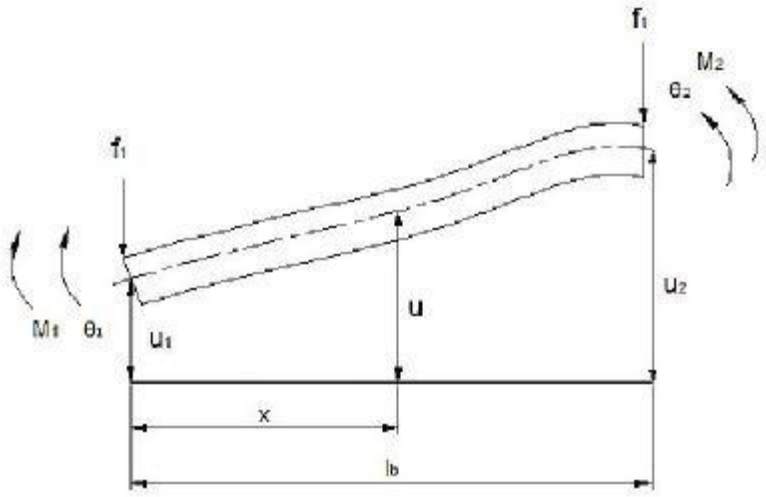

The node undergoes both translational and rotational displacement and they are u_1, θ_1, u_2 and θ_2. The linear forces are F_1 and F_2 corresponding to displacements u_1 and u_2 and rotational forces (Bending moment) are M_1 and M_2 corresponding to the rotational displacements θ_1 and θ_2. The transverse displacement with in the element is assumed to be a cubic polynomial as

$$u(x,t) = a_1 + a_2x + a_3x^2 + a_4x^3 \tag{3.67}$$

Substituting the boundary conditions the shape function of frame elements can be obtained as

$$\{N(x)\}^T = [N_1(x)N_2(x)N_3(x)N_4(x)] =$$

$$\left[1-\frac{3x^2}{l_b^2}+\frac{2x^3}{l_b^3}x-\frac{2x^2}{l_b}+\frac{x^3}{l_b^2}\frac{3x^2}{l_b^2}-\frac{2x^3}{l_b^3}\frac{-x^2}{l_b}+\frac{x^3}{l_b^2}\right] \tag{3.68}$$

The nodal displacement function can be written as

$$\{q\}^T=[u_1\theta_1u_2\theta_2] \tag{3.69}$$

The Lagrange's Equation gives the Kinetic energy and Potential energy of the system respectively as:

$T=\frac{1}{2}\{\dot{q}\}^T[m]\{\dot{q}\}$.

$$U=\frac{1}{2}\{q\}^T[k]\{q\} \tag{3.70}$$

Using Lagrange's Equation the element stiffness matrix and mass matrix of a element are computed given by[14][15]

$$[k_b]=\frac{E_bI_b}{l_b^3}\begin{bmatrix}12 & 6l_b & -12 & 6l_b\\ 6l_b & 4l_b^2 & -6l_b & 2l_b^2\\ -12 & -6l_b & 12 & -6l_b\\ 6l_b & 2l_b^2 & -6l_b & 4l_b^2\end{bmatrix} \tag{3.71}$$

$$[m_b]=\frac{\rho_bA_bl_b}{420}\begin{bmatrix}156 & 22l_b & 54 & -13l_b\\ 22l_b & 4l_b^2 & 13l_b & -3l_b^2\\ 54 & 13l_b & 156 & -22l_b\\ -13l_b & -3l_b^2 & -22l_b & 4l_b^2\end{bmatrix} \tag{3.72}$$

For deriving the sensor equation results, first and second spatial derivatives of the shape function are used.

$$\{n_1(x)\}=\left\{\frac{dN(x)}{dx}\right\}=\{N'(x)\}and\{n_2(x)\}=\left\{\frac{d^2N(x)}{dx^2}\right\}=\{N'(x)\} \tag{3.74}$$

3.11.2 Finite Element formulation of smart frame element

When PZT patches are assumed as Euler-Bernoulli frame elements the elemental mass and stiffness matrices of PZT frame element can be computed as:

$$\left[k_p\right]=\frac{E_pI_p}{l_p^3}\begin{bmatrix}12 & 6l_p & -12 & 6l_p\\ 6l_p & 4l_p^2 & -6l_p & 2l_p^2\\ -12 & -6l_p & 12 & -6l_p\\ 6l_p & 2l_p^2 & -6l_p & 4l_p^2\end{bmatrix} \tag{3.75}$$

$$[m_p] = \frac{\rho_p A_p l_p}{420}\begin{bmatrix} 156 & 22l_p & 54 & -13l_p \\ 22l_p & 4l_p^2 & 13l_p & -3l_p^2 \\ 54 & 13l_p & 156 & -22l_p \\ -13l_p & -3l_p^2 & -22l_p & 4l_p^2 \end{bmatrix} \quad (3.76)$$

The smart frame element is obtained by sandwiching the regular beam element in between the two PZT patches. In which $EI = E_b I_b + 2E_p I_p$ is the flexural rigidity and $\rho A = b_b(\rho_b t_b + 2\rho_p t_p)$ is the mass per unit length of smart frame element, t_p is the thickness of PZT patches i.e. thickness of Actuator and Sensor. So the elemental mass and stiffness matrices of smart frame element are

$$[k] = \frac{EI}{l_p^3}\begin{bmatrix} 12 & 6l_p & -12 & 6l_p \\ 6l_p & 4l_p^2 & -6l_p & 2l_p^2 \\ -12 & -6l_p & 12 & -6l_p \\ 6l_p & 2l_p^2 & -6l_p & 4l_p^2 \end{bmatrix} \quad (3.77)$$

$$[m] = \frac{\rho A l_p}{420}\begin{bmatrix} 156 & 22l_p & 54 & -13l_p \\ 22l_p & 4l_p^2 & 13l_p & -3l_p^2 \\ 54 & 13l_p & 156 & -22l_p \\ -13l_p & -3l_p^2 & -22l_p & 4l_p^2 \end{bmatrix} \quad (3.78)$$

3.11.3 Sensor Equation

Following linear PZT Constitutive equations [6], [13] will be used for driving the Sensor and Actuator equations.

$$\varepsilon_x = S_{11}^E \sigma_x + d_{31} E_z \quad .$$

$$D_z = d_{31}\sigma_x + \xi_{33}^\sigma E_z \quad (3.79)$$

Where ε is strain, σ is stress, S^E is compliance when electric field is constant, d_{31} is PZT constant, E is electric field, D is electric displacement, ξ^σ is dielectric constant under constant stress. The direct PZT effect is used to calculate the output charge on the sensor layer created by the strains in the beam. Since no electric field is applied to the sensor layer, we get

$$D_z = C_{11} d_{31} \varepsilon_x \quad (3.80)$$

Where C_{11} is the young's modulus of elasticity.

The charge measured through the electrode of the sensor is given by

$$q(t) = \int_S D_z ds \tag{3.81}$$

The current on the surface of the sensor is given by

$$i(t) = \frac{dq(t)}{dt} \tag{3.82}$$

We know that strain at a point in a beam is given as $\varepsilon_x = zd^2u/dx^2$, where z is a coordinate on the beam w.r.t. neutral axis. Width $b_b=b_s=b_a$. As such current generated can be written as [10]

$$i(t) = zC_{11}d_{31}b_b \int_0^{l_p} \{n_2(x)\}^T \{\dot{q}\} dx \tag{3.83}$$

Where $z=t_b/2+t_s$ for maximum strain.

Voltage generated by the sensor is

$$V^s(t) = G_s i(t) \tag{3.84}$$

Where G_s is the gain of the signal conditioning device

$$V^s(t) = G_s C_{11} d_{31} z b_b [0 \quad -1 \quad 0 \quad 1][\dot{u}_1 \dot{\theta}_1 \dot{u}_2 \dot{\theta}_2]^T \tag{3.85}$$

This can be written as

$$V^s(t) = C_s [0 \quad -1 \quad 0 \quad 1]\{\dot{q}\} \tag{3.86}$$

Where $C_s = G_s C_{11} d_{31} z b_b$ is sensor constant. The above equation can be written as

$$V^s(t) = \{g\}^T \{\dot{q}\} \tag{3.87}$$

Where {g} is a Constant Vector of size (4x1)

3.11.4 Actuator Equation

From equation [12] the stress developed in the actuator is

$$\sigma_x = C_{11} d_{31} E_z \tag{3.88}$$

Where E_z is the Electric Field.

The resultant bending moment produced by the actuator is given by [10]

$$M_a = C_{11} d_{31} \left(\frac{t_a + t_b}{2}\right) V^a(\text{t}) \tag{3.89}$$

Where $V^a(t)$ is the voltage applied on the actuator which is given by

$$V^a(t) = Controllergain x V^s(t) \tag{3.90}$$

The force produced by the actuator is given by

$$\{F_{Actu}\} = C_{11} d_{31} b_b \left(\frac{t_a + t_b}{2}\right) \int_{l_a} V^a(t) \{n_1(x)\} dx \tag{3.91}$$

This can also be expressed as

$$\{F_{Actu}\} = \{H\} V^a(t) \tag{3.92}$$

Where {H} is a constant vector of size (4X1) and is given as

$$\{H\}^T = C_{11} d_{31} b_b \left(\frac{t_a + t_b}{2}\right) [-1 \quad 0 \quad 1 \quad 0]$$

Or

$$\{H\}^T = C_a [-1 \quad 0 \quad 1 \quad 0] \tag{3.93}$$

Where C_a is the Actuator Constant and is given by

$$C_a = C_{11} d_{31} b_b \left(\frac{t_a + t_b}{2}\right) \tag{3.94}$$

3.11.5 Control Law Using PID Controller

Now, calculating an appropriate controlled voltage that can be fed to the Actuator, for that a PID controller is used in this research. A typical PID control law that can be used for Active Vibration Control is:

$$y(t) = K_p + K_i \int e(t) dt + K_d \dot{e}(t) \tag{3.95}$$

Where y(t) is control signal, K_p, K_i and K_d are proportional, integral and derivative respectively. These three gains can be tuned in order to provide fine control for the application.

A typical PID controller shown below:

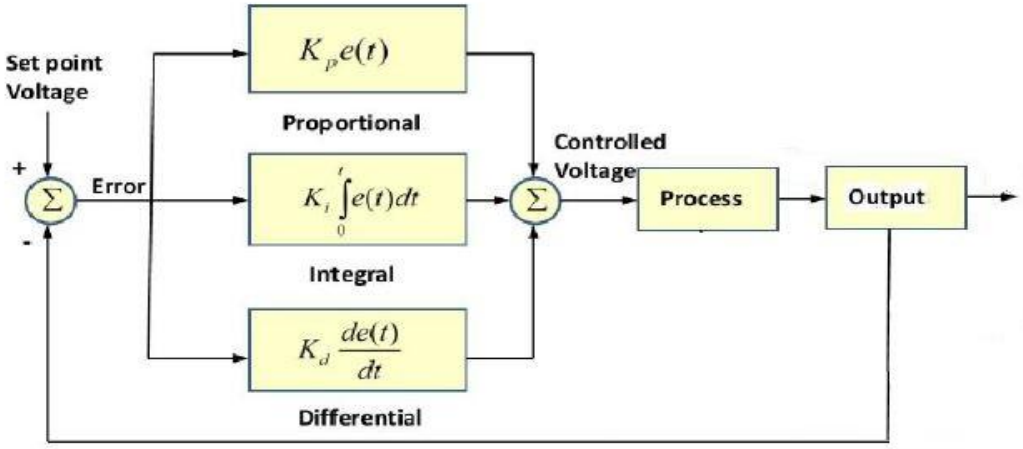

3.11.6 Dynamic Equation of Smart Structure

Now formulating and solving the equation of motion of entire structure that is give by

$$[M]\{\ddot{q}\} + [K]\{\dot{q}\} = \{F_{Dist}\} + \{F_{Actu}\} \tag{3.96}$$

Consider a generalized coordinate using a transformation $\{q\} = [\psi]\{x\}$ for the first two dominant vibratory modes then the equation of motion becomes

$$[M^r]\{\ddot{x}\} + [K^r]\{x\} = \{F^r_{Dist}\} + \{F^r_{Actu}\} \tag{3.97}$$

If damping of the structure is also considered then assuming proportional damping as

$$[C] = \alpha[M] + \beta[K] \tag{3.98}$$

The generalized dynamic equation of motion is given as

$$[M^r]\{\ddot{x}\} + [C^r]\{\dot{x}\} + [K^r]\{x\} = \{F^r_{Dist}\} + \{F^r_{Actu}\} \tag{3.99}$$

3.11.7 State Space Formulation forthe First Two Dominant Vibration Modes

Let the {x}={y} as

$$\{x\} = \begin{bmatrix} x_1 \\ x_2 \end{bmatrix} = \{y\} = \begin{bmatrix} y_1 \\ y_2 \end{bmatrix} \tag{3.100}$$

And

$$\{\dot{x}\} = \{\dot{y}\} = \begin{bmatrix} \dot{y}_1 \\ \dot{y}_2 \end{bmatrix} = \begin{bmatrix} y_3 \\ y_4 \end{bmatrix} and \{\ddot{x}\} = \{\ddot{y}\} = \begin{bmatrix} \dot{y}_3 \\ \dot{y}_4 \end{bmatrix} \tag{3.101}$$

Equation of motion now can be written as

$$[M^r]\begin{bmatrix} \dot{y}_3 \\ \dot{y}_4 \end{bmatrix} + [C^r]\begin{bmatrix} y_3 \\ y_4 \end{bmatrix} + [K^r]\begin{bmatrix} y_1 \\ y_2 \end{bmatrix} = \{F^r_{\mathrm{Dist}}\} + \{F^r_{Actu}\} \tag{3.102}$$

This can be simplified as

$$\begin{bmatrix}\dot{y}_3\\ \dot{y}_4\end{bmatrix} = -[M^r]^{-1}[K^r]\begin{bmatrix}y_1\\ y_2\end{bmatrix} - [M^r]^{-1}[C^r]\begin{bmatrix}y_3\\ y_4\end{bmatrix} + [M^r]^{-1}\{F^r_{Dist}\} + [M^r]^{-1}\{F^r_{Actu}\} \quad (3.103)$$

The above equation can be written in state form as

$$\begin{bmatrix}\dot{y}_1\\ \dot{y}_2\\ \dot{y}_3\\ \dot{y}_4\end{bmatrix} = \begin{bmatrix}[0] & [I]\\ -[M^r]^{-1}[K^r] & -[M^r]^{-1}[C^r]\end{bmatrix}\begin{bmatrix}y_1\\ y_2\\ y_3\\ y_4\end{bmatrix} + \begin{bmatrix}\{0\}\\ \overline{[M^r]^{-1}\psi^T\{H\}}\end{bmatrix}V^a(t) + \begin{bmatrix}\{0\}\\ \overline{[M^r]^{-1}\psi^T\{f\}}\end{bmatrix}u(t) \quad (3.104)$$

Now, the sensor voltage is taken as output of the structure which can be written as

$$V^s(t) = [\{0\}\{g\}^T[\psi]][y_1 y_2 \;\; y_3 \;\; y_4]^T \quad (3.105)$$

So, the state space model of smart structure for the first two dominant vibratory modes is given by

$$\{\dot{y}\} = [A]\{y(t)\} + [B]V^a(t) + [D]u(t)$$

And

$$V^s(t) = [E]^T\{y(t)\} + [F]V^a(t) \quad (3.106)$$

Where,

$$[A] = \begin{bmatrix}[0] & [I]\\ -[M^r]^{-1}[K^r] & -[M^r]^{-1}[C^r]\end{bmatrix}, [B] = \begin{bmatrix}\{0\}\\ \overline{[M^r]^{-1}\psi^T\{H\}}\end{bmatrix},$$

$$[D] = \begin{bmatrix}\{0\}\\ \overline{[M^r]^{-1}\psi^T\{f\}}\end{bmatrix}, [E] = \begin{bmatrix}\{0\}\\ \overline{\{g\}^T[\psi]}\end{bmatrix}, \text{and } [F] = \text{Null Matrix}$$

CHAPTER - 4

RESULTS AND DISCUSSION

A portal frame structure with six elements of equal length is considered here. The frame consists of three parts and each part is divided into two elements. Here, two materials are considered for the structural analysis of portal frame, which are alloy steel and carbon fiber reinforced plastic and having different boundary conditions. The two portal frames of two different materials are modelled and analyzed for the deformations at six basic natural frequencies which are obtained by ANSYS.

After the modal analysis, active vibration control is performed. For this piezoelectric sensor and actuator are placed at six different positions (one at a time). The sensor used is PZT-5H sensor and actuators patches. For analysis, only collocated positions are considered. The physical properties of sensor and actuator have been given in table 1. The PZT patches are operated with typical PID controller. The displacement amplitude graph is generated by PID controller which shows the uncontrolled and controlled vibration for each element.

4.1 MODE SHAPE

4.1.1There are six types of basic mode Shapes of Alloy Steel as shown in figure 4.1 to 4.6.

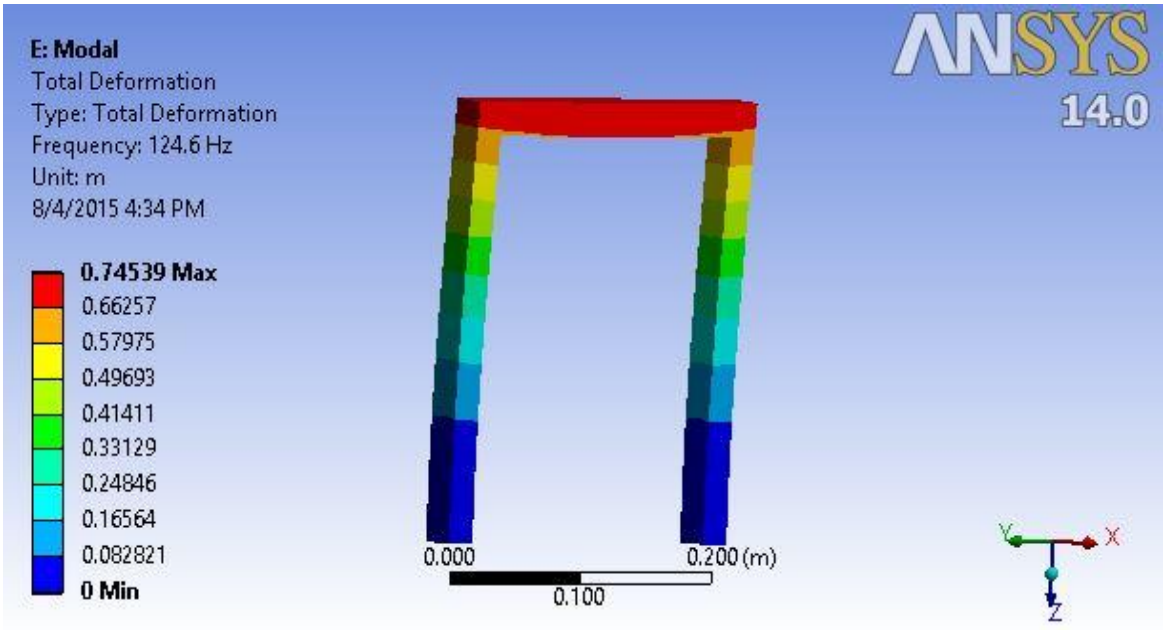

Fig.4.1 First Mode Shape at natural frequency 124.6 Hz

The first basic mode shape is shown in fig 4.1 for alloy steel. The shape is rectangular open at the bottom and both ends are fixed. The magnitude of deformation is represented by red, blue, violet, yellow and green. These colors represent the magnitude of deformation at 124.6 Hz.

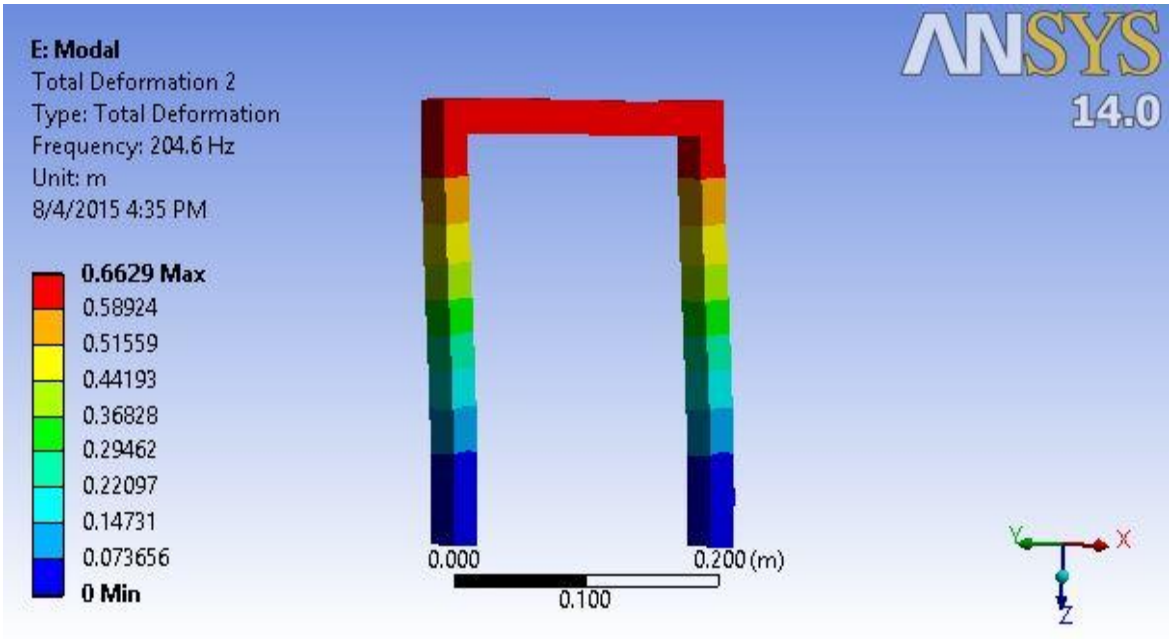

Fig. 4.2 Second Mode Shape at natural frequency 204.6 Hz

The second basic mode shape is shown in fig. 4.2 for alloy steel. The shape is rectangular open at the bottom and both ends are fixed. The magnitude of deformation is represented by red, blue, violet, yellow, green. These colors represent the magnitude of deformation at 204.6 Hz.

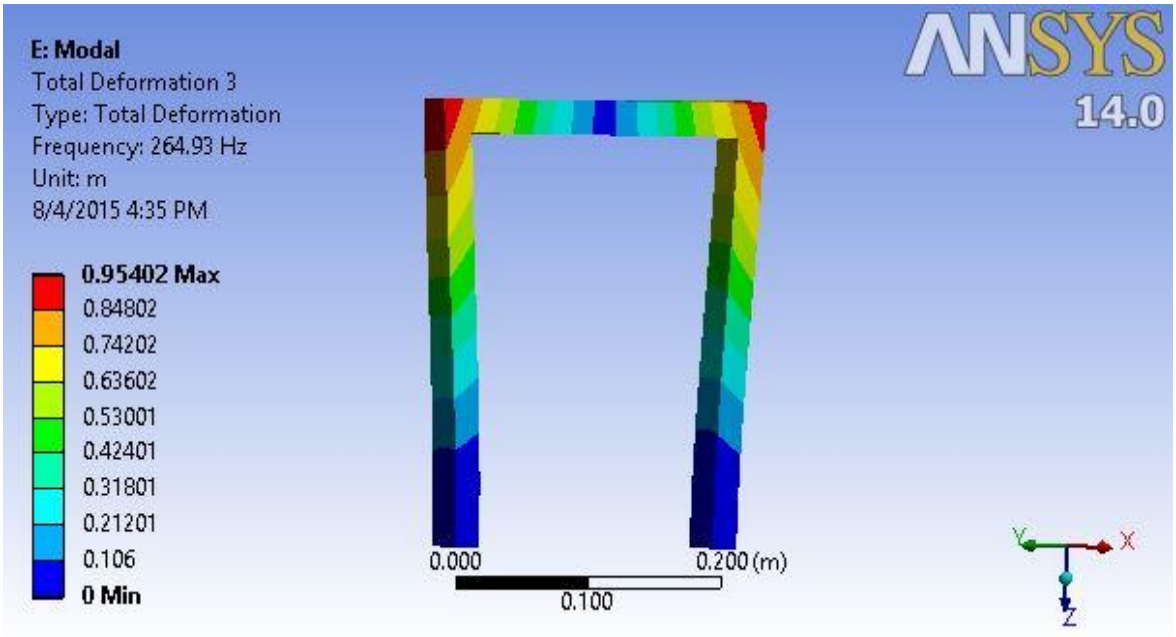

Fig.4.3 Third Mode Shape at natural frequency 264.93 Hz

The third basic mode shape is shown in fig.4.3 for alloy steel. The shape is rectangular open at the bottom and both ends are fixed. The magnitude of deformation is represented by red, blue, violet, yellow, green. These colors represent the magnitude of deformation at 264.93 Hz.

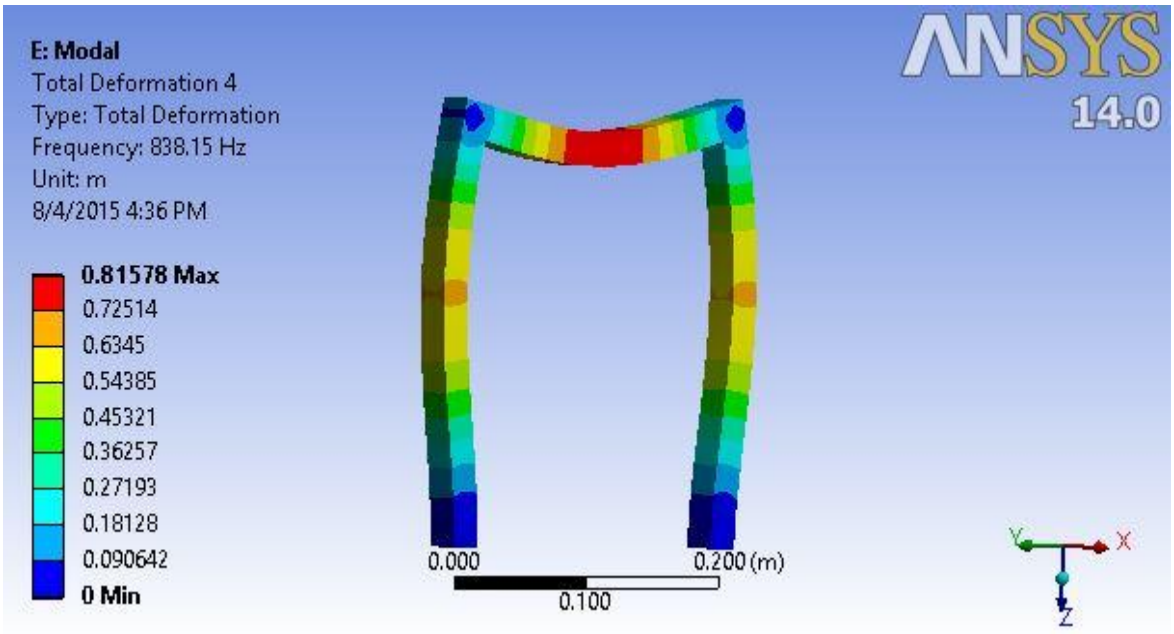

Fig. 4.4 Fourth Mode Shape at natural frequency 838.15 Hz

The fourth basic mode shape is shown in fig.4.4 for alloy steel. The shape is rectangular open at the bottom and both ends are fixed. The magnitude of deformation is represented by red, blue, violet, yellow, green. These colors represent the magnitude of deformation at 838.15 Hz.

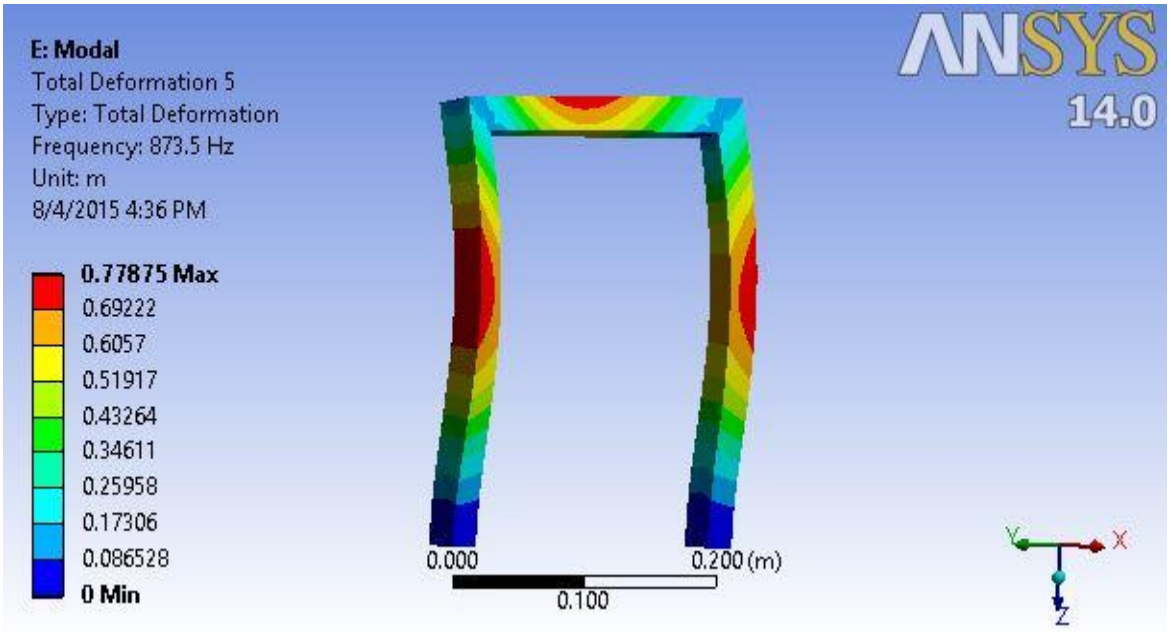

Fig. 4.5 Fifth Mode Shape at natural frequency 873.5 Hz

The fifth basic mode shape is shown in fig.4.5 for alloy steel. The shape is rectangular open at the bottom and both ends are fixed. The magnitude of deformation is represented by red, blue, violet, yellow, green. These colors represent the magnitude of deformation at 873.5 Hz.

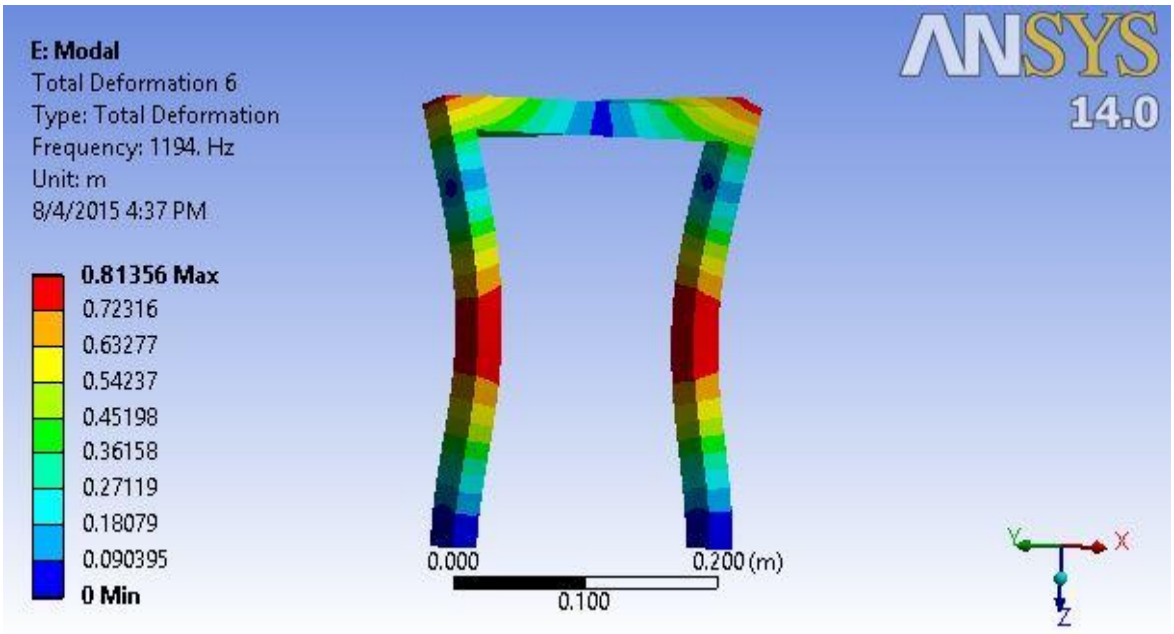

Fig. 1.6 Sixth Mode Shape at natural frequency 1194 Hz

The sixth basic mode shape is shown in fig.1.6 for alloy steel. The shape is rectangular open at the bottom and both ends are fixed. The magnitude of deformation is represented by red, blue, violet, yellow, green. These colors represent the magnitude of deformation at 1194 Hz.

4.1.2 There are six types of basic mode Shapes of Carbon Fiber Reinforced Plastic as shown in figure 4.7 to 4.12.

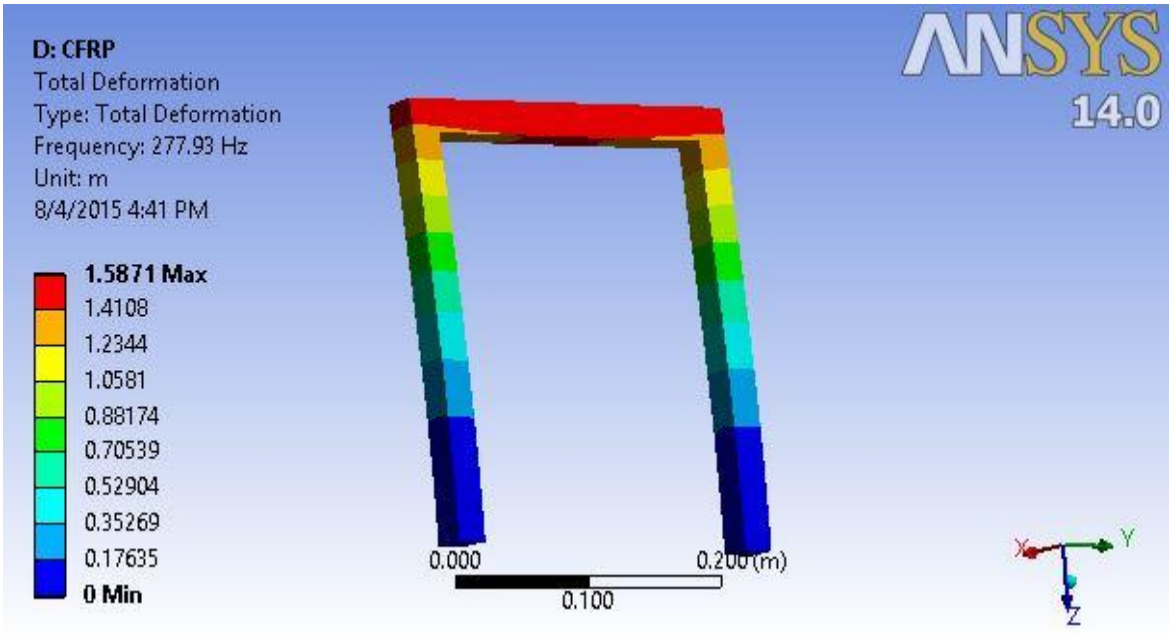

Fig.4.7 First Mode Shape at natural frequency 277.93 Hz

The first basic mode shape is shown in fig. 4.7 for alloy steel. The shape is rectangular open at the bottom and both ends are fixed. The magnitude of deformation is represented by red, blue, violet, yellow, green. These colors represent the magnitude of deformation at 277.93 Hz.

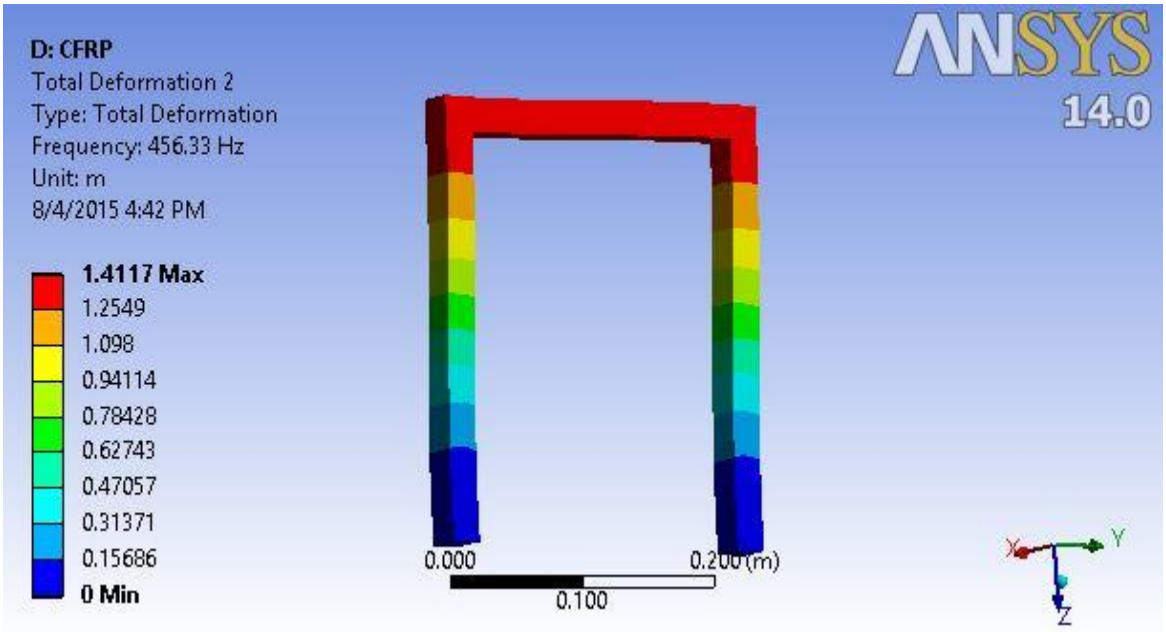

Fig.4.8 Second Mode Shape at natural frequency 456.33 Hz

The second basic mode shape is shown in fig. 4.8 for alloy steel. The shape is rectangular open at the bottom and both ends are fixed. The magnitude of deformation is represented by red, blue, violet, yellow, green. These colors represent the magnitude of deformation at 456.33 Hz.

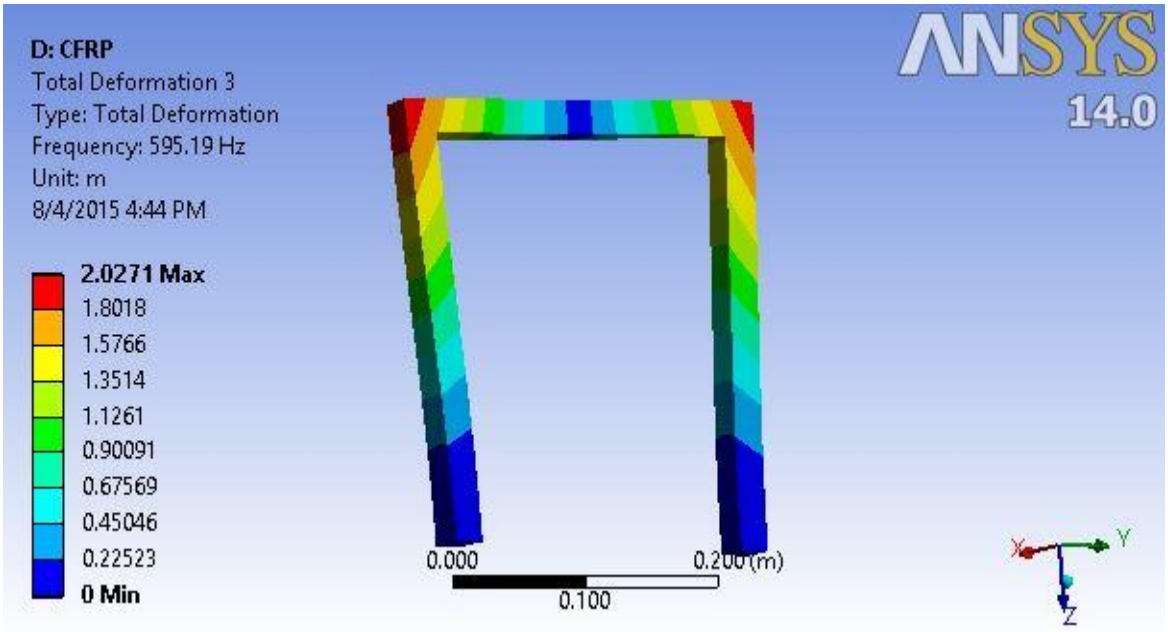

Fig. 4.9 Third Mode Shape at natural frequency 595.19 Hz

The third basic mode shape is shown in fig.4.9 for alloy steel. The shape is rectangular open at the bottom and both ends are fixed. The magnitude of deformation is represented by red, blue, violet, yellow, green. These colors represent the magnitude of deformation at 595.19 Hz.

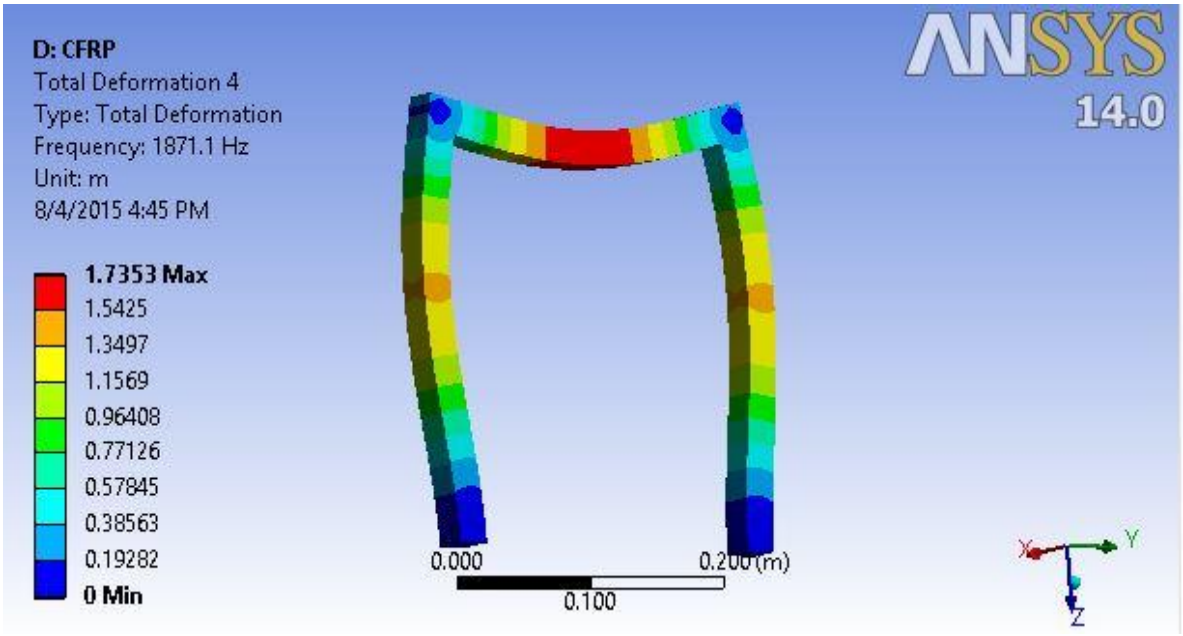

Fig.4.10 Fourth Mode Shape at natural frequency 1871.1 Hz

The fourth basic mode shape is shown in fig.4.10 for alloy steel. The shape is rectangular open at the bottom and both ends are fixed. The magnitude of deformation is represented by red, blue, violet, yellow, green. These colors represent the magnitude of deformation at 1871.1 Hz.

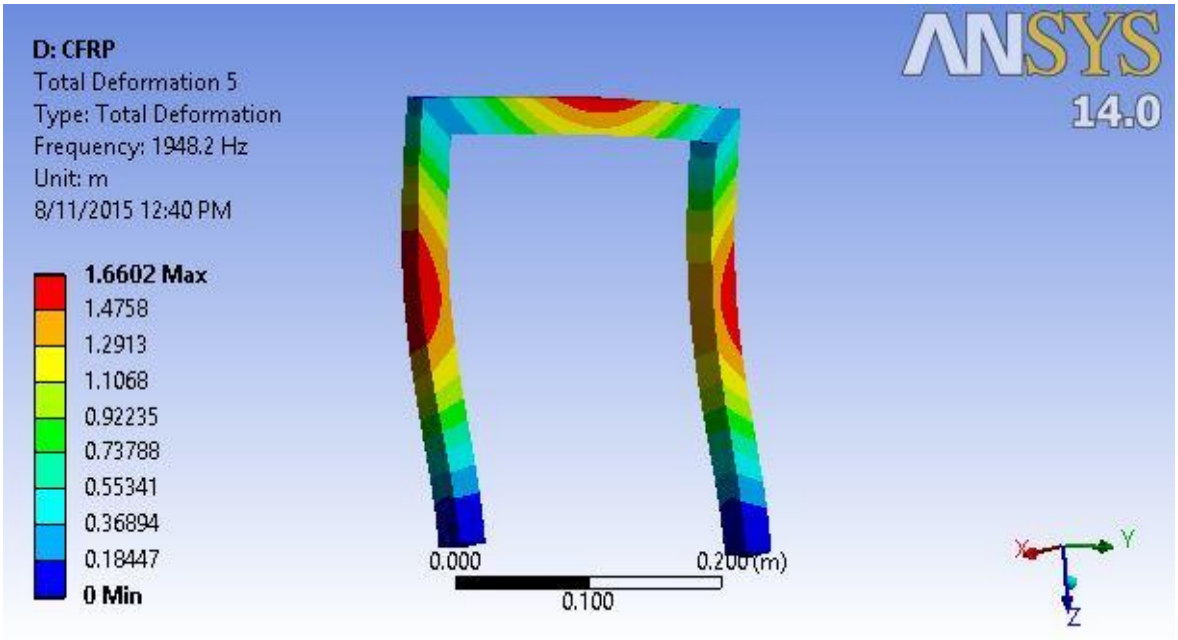

Fig.4.11 Fifth Mode Shape at natural frequency 1948.2 Hz

The fifth basic mode shape is shown in fig.4.11 for alloy steel. The shape is rectangular open at the bottom and both ends are fixed. The magnitude of deformation is represented by red, blue, violet, yellow, green. These colors represent the magnitude of deformation at 1948.2 Hz.

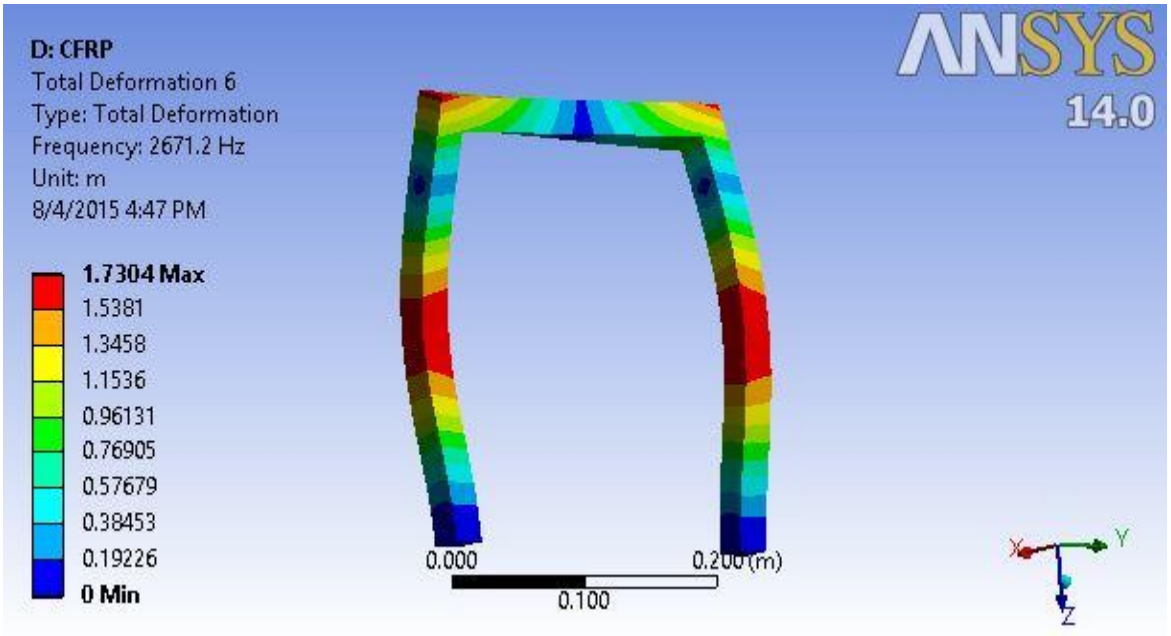

Fig.4.12 Sixth Mode Shape at natural frequency 2671.2 Hz

The sixth basic mode shape is shown in fig.4.12 for alloy steel. The shape is rectangular open at the bottom and both ends are fixed. The magnitude of deformation is represented by red, blue, violet, yellow, green. These colors represent the magnitude of deformation at 2671.2 Hz.

- From the input of the data of the software the results varies with respect to magnitude of frequency for different mode shape
- For different mode shape the results obtained from the software on the basis of data shows variation of the frequency and deformation.
- Carbon Reinforced plastic is a composite material in sandwich, therefore its frequency for the first mode shape higher than alloy steel.
- In case of reinforced composite, the maximum deformation reduces from frequency from 595.19Hz to1871.1Hz and increases at 2671.2Hz due to its occurring at mid span where buckling is also taking place.

4.2 Displacement Graph of Portal Frame of Alloy Steel with eccentric Load

In this case collocated patches are serially placed on each element of the portal frame of alloy steel. The response are taken by giving excitation on the eccentric point of the horizontal element of portal frame structure and the output is plotted by using sensors, at this stage actuators are not activated i.e. without control. The graph shows that the displacement amplitude at that frequency which is generated due to excitation.

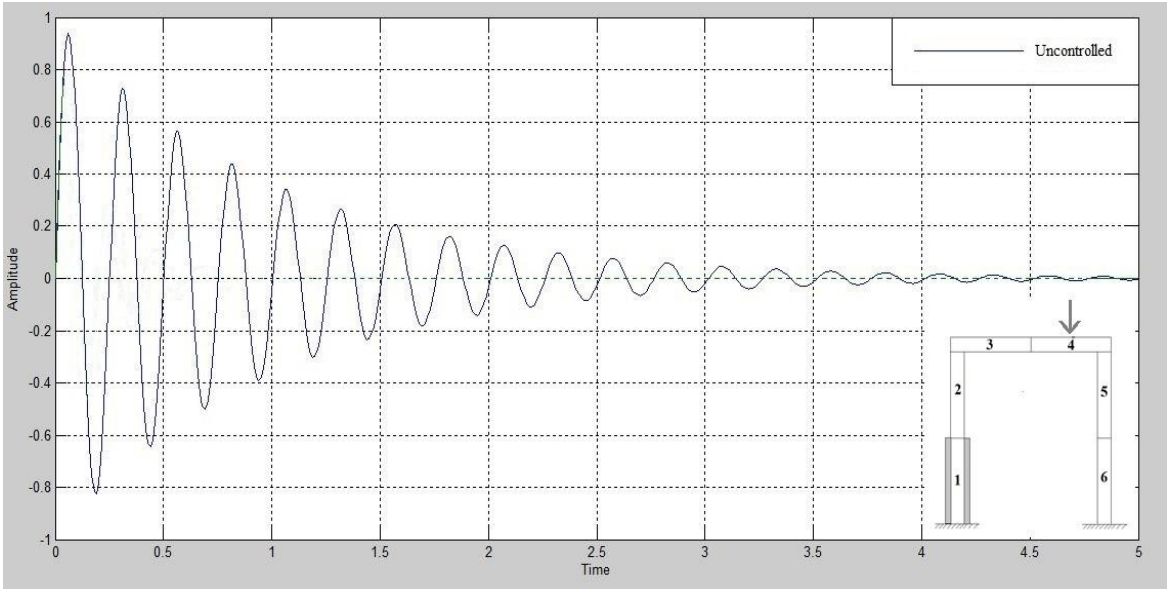

Fig. 4.13 Displacement of Element-1 of Portal Frame (Alloy Steel) having eccentric load

The displacement graph of portal frame of alloy steel is shown in fig.4.13.This graph is generated by the Simulink for the first element and the excitation is applied on the eccentric point of the horizontal element of portal frame structure without PID control. The graph shows that the amplitude is maximum at 0.1 sec time but as the time increases the amplitude is decreased due to damping effect.

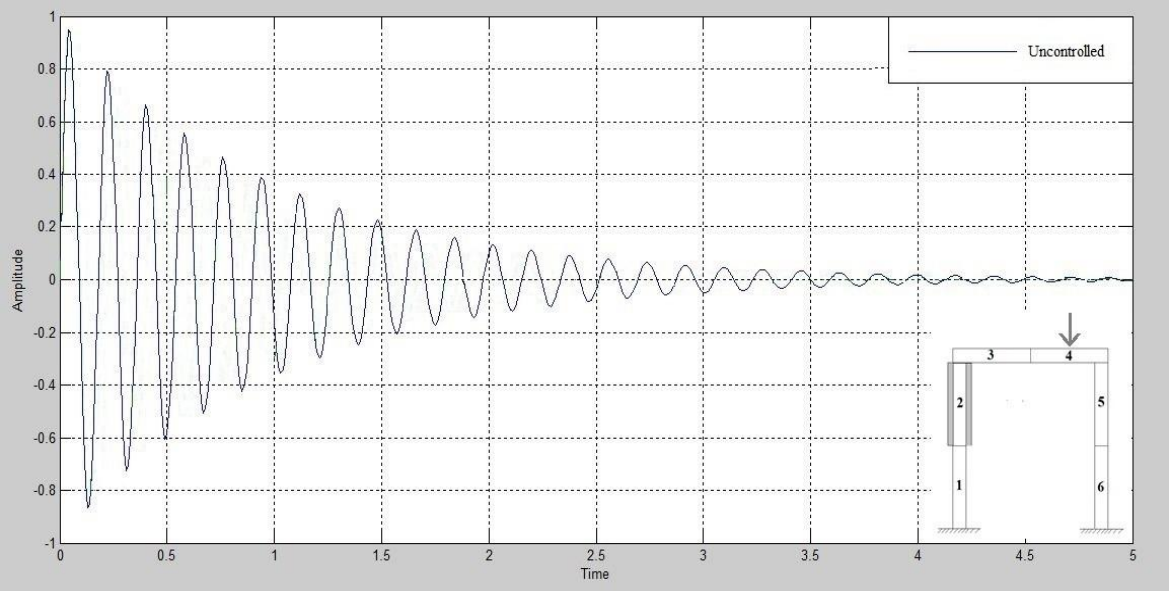

Fig.4.14 Displacement of Element-2 of Portal Frame (Alloy Steel) having eccentric load

The displacement graph of portal frame of alloy steel is shown in fig.4.14. This graph is generated by the Simulink for the second element and the excitation is applied on the eccentric point of the horizontal element of portal frame structure without PID control. The graph shows that the amplitude is maximum at 0.1 sec time but as the time increases the amplitude is decreased due to damping effect.

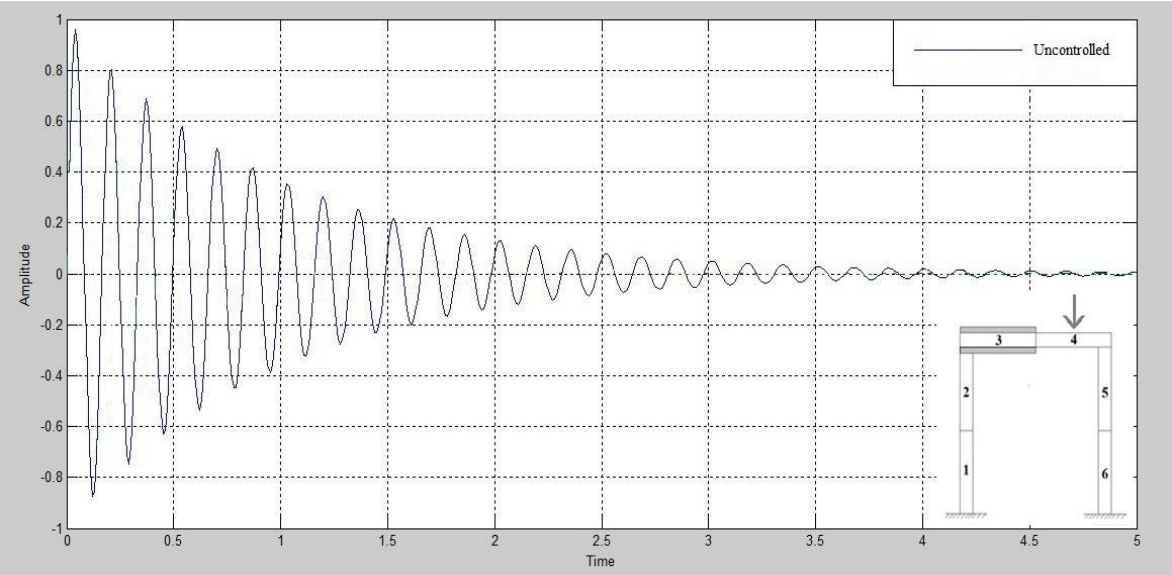

Fig.4.15 Displacement of Element-3 of Portal Frame (Alloy Steel) having eccentric load

The displacement graph of portal frame of alloy steel is shown in fig.4.15 This graph is generated by the Simulink for the third element and the excitation is applied on the eccentric point of the horizontal element of portal frame structure without PID control. The graph shows that the amplitude is maximum at 0.1 sec time but as the time increases the amplitude is decreased due to damping effect.

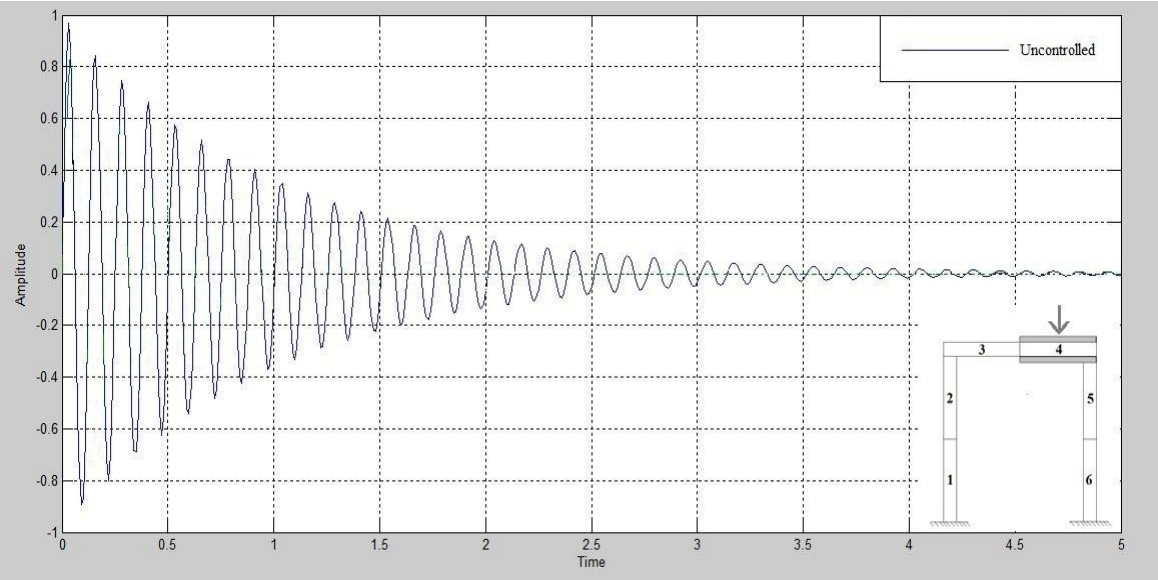

Fig.4.16 Displacement of Element-4 of Portal Frame (Alloy Steel) having eccentric load

The displacement graph of portal frame of alloy steel is shown in fig.4.16 .This graph is generated by the Simulink for the fourth element and the excitation is applied on the eccentric point of the horizontal element of portal frame structure without PID control. The graph shows that the amplitude is maximum at 0.1 sec time but as the time increases the amplitude is decreased due to damping effect.

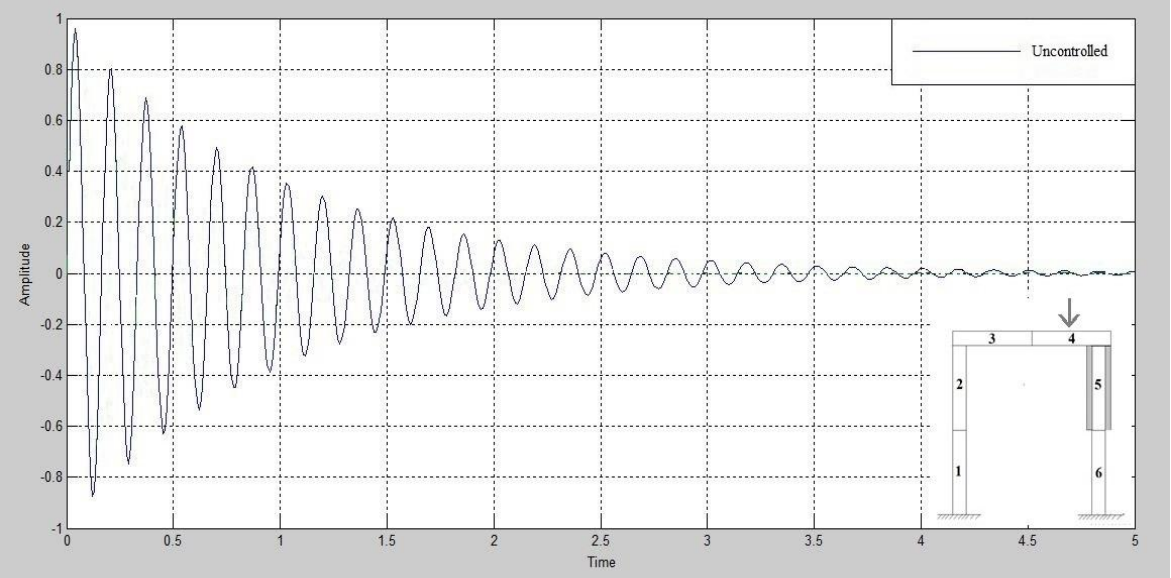

Fig.4.17 Displacement of Element-5 of Portal Frame (Alloy Steel) having eccentric load

The displacement graph of portal frame of alloy steel is shown in fig.4.17. This graph is generated by the Simulink for the fifth element and the excitation is applied on the eccentric point of the horizontal element of portal frame structure without PID control. The graph shows that the amplitude is maximum at 0.1 sec time but as the time increases the amplitude is decreased due to damping effect.

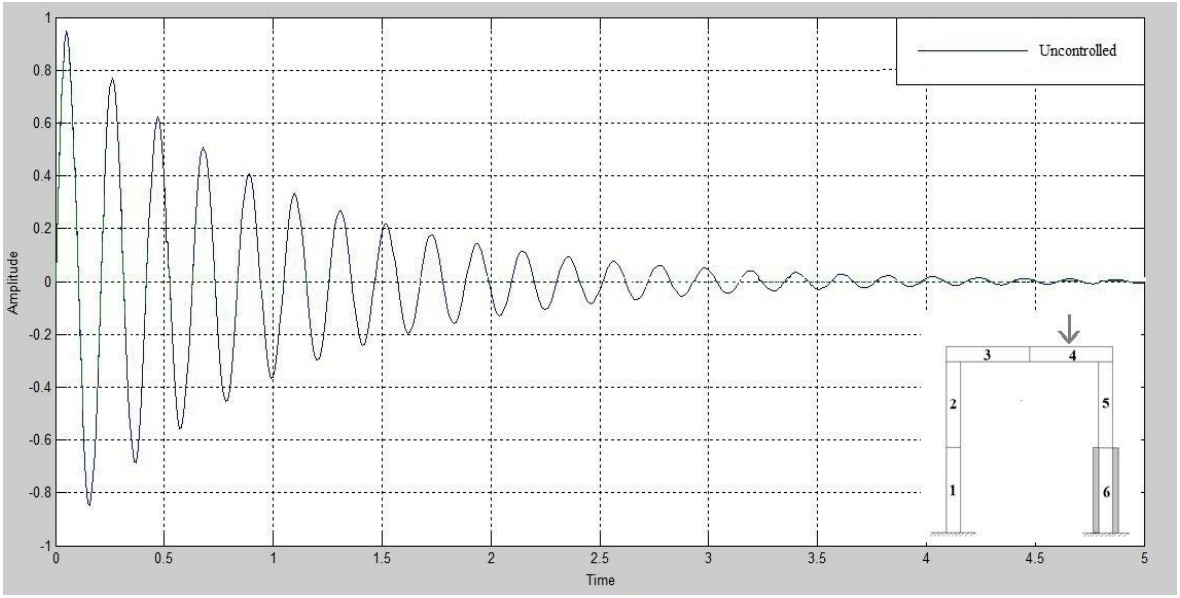

Fig.4.18 Displacement of Element-6 of Portal Frame (Alloy Steel) having eccentric load

The displacement graph of portal frame of alloy steel is shown in fig.4.18. This graph is generated by the Simulink for the sixth element and the excitation is applied on the eccentric point of the horizontal element of portal frame structure without PID control. The graph shows that the amplitude is maximum at 0.1 sec time but as the time increases the amplitude is decreased due to damping effect.

4.3Displacement Graph of Portal Frame of Alloy Steel with eccentric Load and having PZT Patch and PID Controller

In this case collocated patches are serially placed on each element of the portal frame of alloy steel. The response are taken by giving excitation on the eccentric point of the portal frame and the output is plotted by using sensors, at this stage actuators are active i.e. actuator is controlling vibration generated due to excitation. The graph shows that the displacement amplitude at that frequency which is generated due to excitation and displacement amplitude of their control.

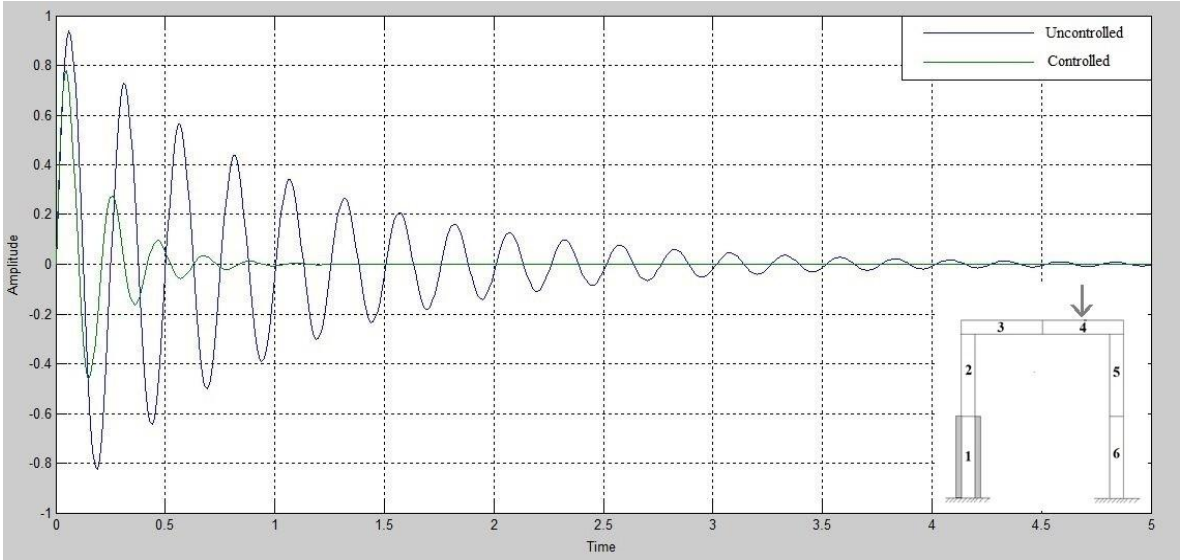

Fig.4.19 Displacement of Element-1 of Portal Frame (Alloy Steel) having side load

The displacement graph of portal frame of alloy steel is shown in fig.4.19. This graph is generated by the Simulink for the first element and the excitation is applied on the eccentric point of the horizontal element of portal frame structure with PID control. The graph shows that the amplitude is maximum at 0.1 sec time but as the time increases the amplitude is decreased due to damping effect. The vibration generated in portal frame due to force of 1 KN applied on fourth element is controlled in 1 sec.

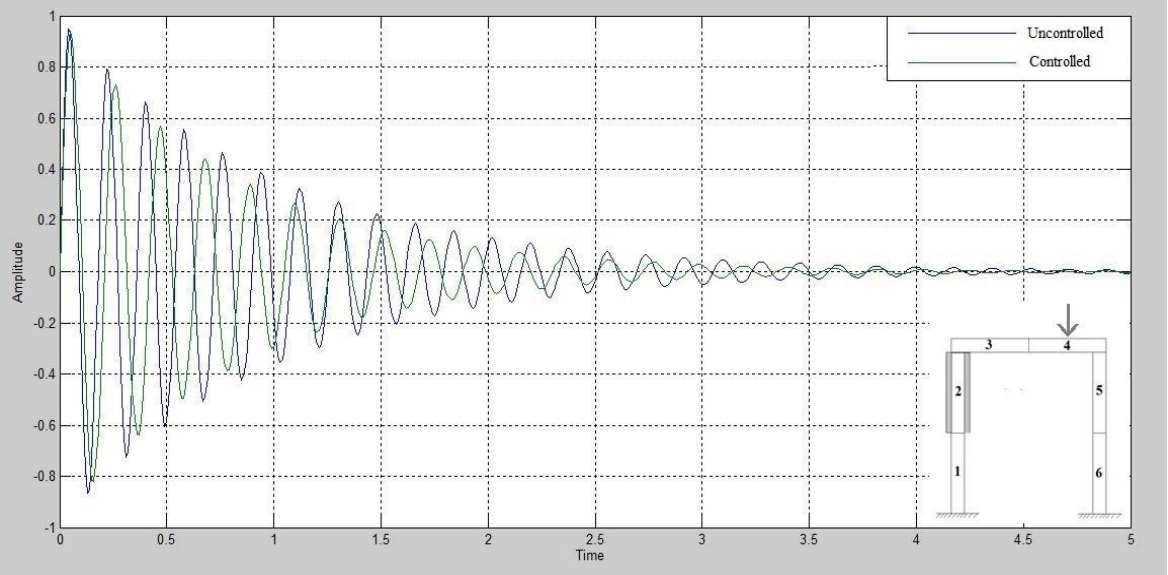

Fig.4.20 Displacement of Element-2 of Portal Frame (Alloy Steel) having side load

The displacement graph of portal frame of alloy steel is shown in fig.4.20. This graph is generated by the Simulink for the second element and the excitation is applied on the eccentric point of the horizontal element of portal frame structure with PID control. The graph shows that the amplitude is maximum at 0.1 sec time but as the time increases the amplitude is decreased due to damping effect. The vibration generated in portal frame due to force of 1 KN applied on fourth element is controlled in 5 sec.

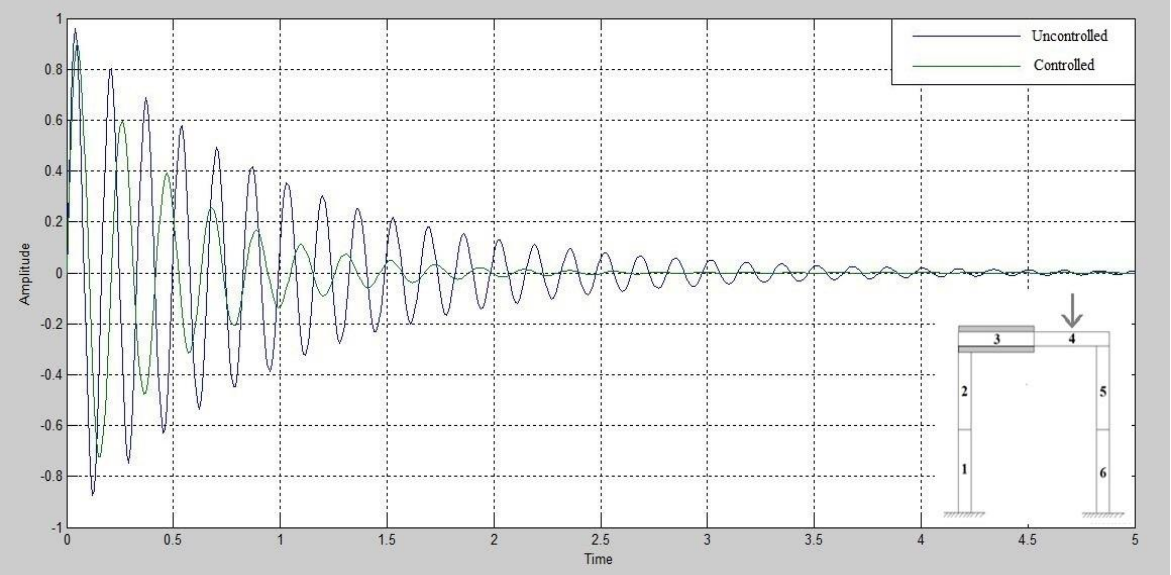

Fig.4.21 Displacement of Element-3 of Portal Frame (Alloy Steel) having side load

The displacement graph of portal frame of alloy steel is shown in fig.4.21.This graph is generated by the Simulink for the third element and the excitation is applied on the eccentric point of the horizontal element of portal frame structure with PID control. The graph shows that the amplitude is maximum at 0.1 sec time but as the time increases the amplitude is decreased due to damping effect. The vibration generated in portal frame due to force of 1 KN applied on fourth element is controlled in 3 sec.

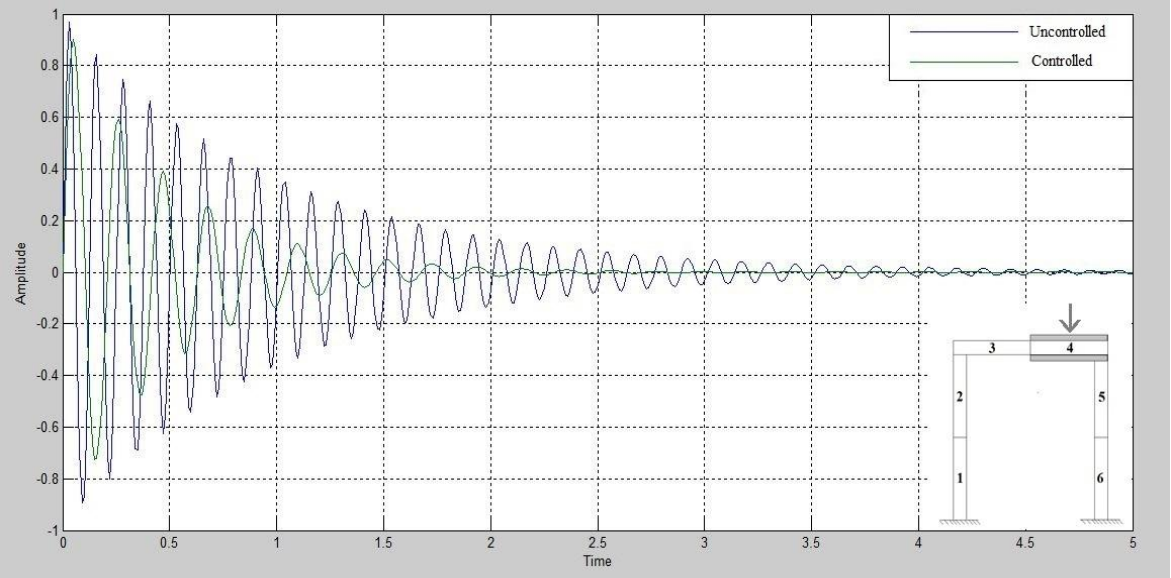

Fig.4.22 Displacement of Element-4 of Portal Frame (Alloy Steel) having side load

The displacement graph of portal frame of alloy steel is shown in fig.4.22. This graph is generated by the Simulink for the fourth element and the excitation is applied on the eccentric point of the horizontal element of portal frame structure with PID control. The graph shows that the amplitude is maximum at 0.1 sec time but as the time increases the amplitude is decreased due to damping effect. The vibration generated in portal frame due to force of 1 KN applied on fourth element is controlled in 2.5 sec.

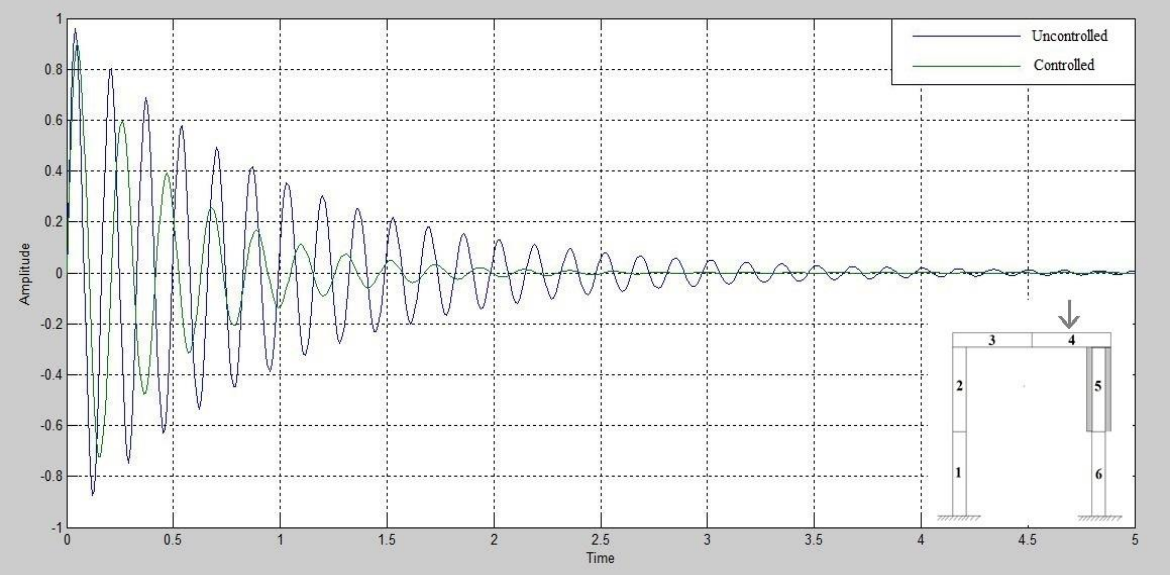

Fig.4.23 Displacement of Element-5 of Portal Frame (Alloy Steel) having side load

The displacement graph of portal frame of alloy steel is shown in fig.4.23. This graph is generated by the Simulink for the fifth element and the excitation is applied on the eccentric point of the horizontal element of portal frame structure with PID control. The graph shows that the amplitude is maximum at 0.1 sec time but as the time increases the amplitude is decreased due to damping effect. The vibration generated in portal frame due to force of 1 KN applied on fourth element is controlled in 2.5 sec.

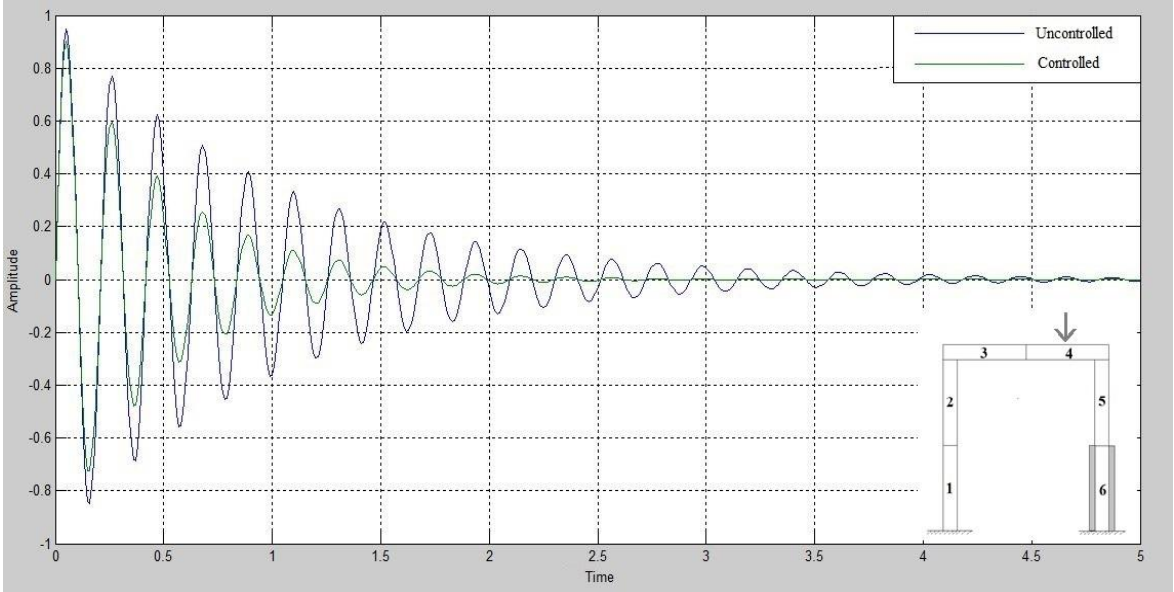

Fig.4.24 Displacement of Element-6 of Portal Frame (Alloy Steel) having side load

The displacement graph of portal frame of alloy steel is shown in fig.4.24. This graph is generated by the Simulink for the sixth element and the excitation is applied on the eccentric point of the horizontal element of portal frame structure with PID control. The graph shows that the amplitude is maximum at 0.1 sec time but as the time increases the amplitude is decreased due to damping effect. The vibration generated in portal frame due to force of 1 KN applied on fourth element is controlled in 2.5 sec.

4.4 Displacement Graph of Portal Frame of Alloy Steel with Mid Load

In this case collocated patches are serially placed on each element of the portal frame of alloy steel. The response are taken by giving excitation on the mid of the portal frame and

the output is plotted by using sensors, at this stage actuators are not activated i.e. without control. The graph shows that the displacement amplitude at that frequency which is generated due to excitation.

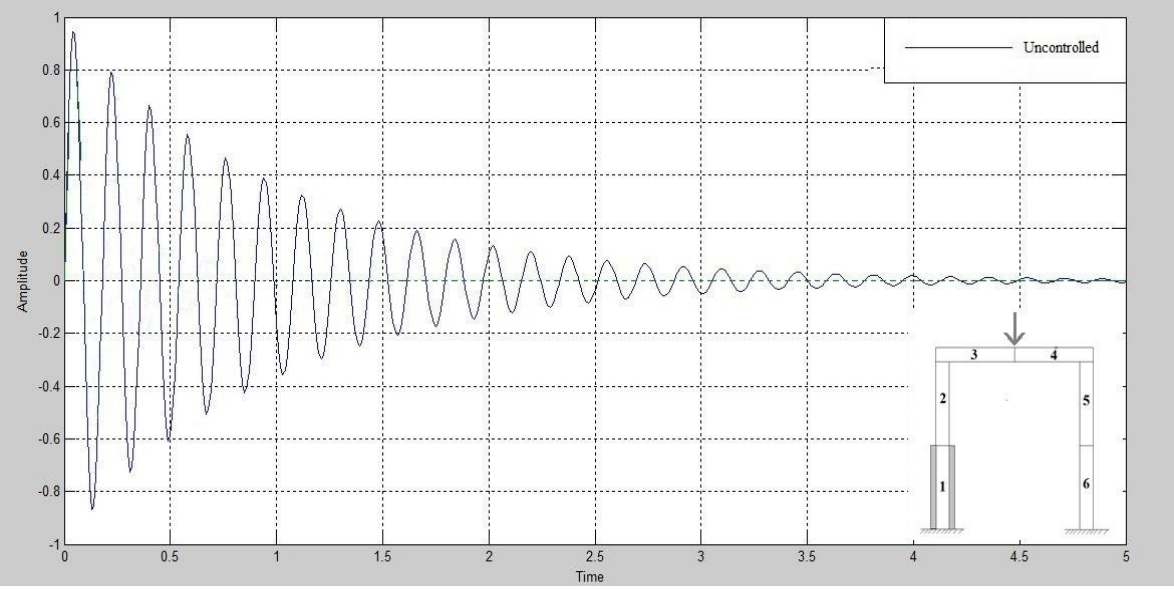

Fig.4.25. Displacement of Element-1 of Portal Frame (Alloy Steel) having midpoint load

The displacement graph of portal frame of alloy steel is shown in fig.4.25. This graph is generated by the Simulink for the first element and the excitation is applied on the midpoint of the horizontal element of portal frame structure without PID control. The graph shows that the amplitude is maximum at 0.1 sec time but as the time increases the amplitude is decreased due to damping effect.

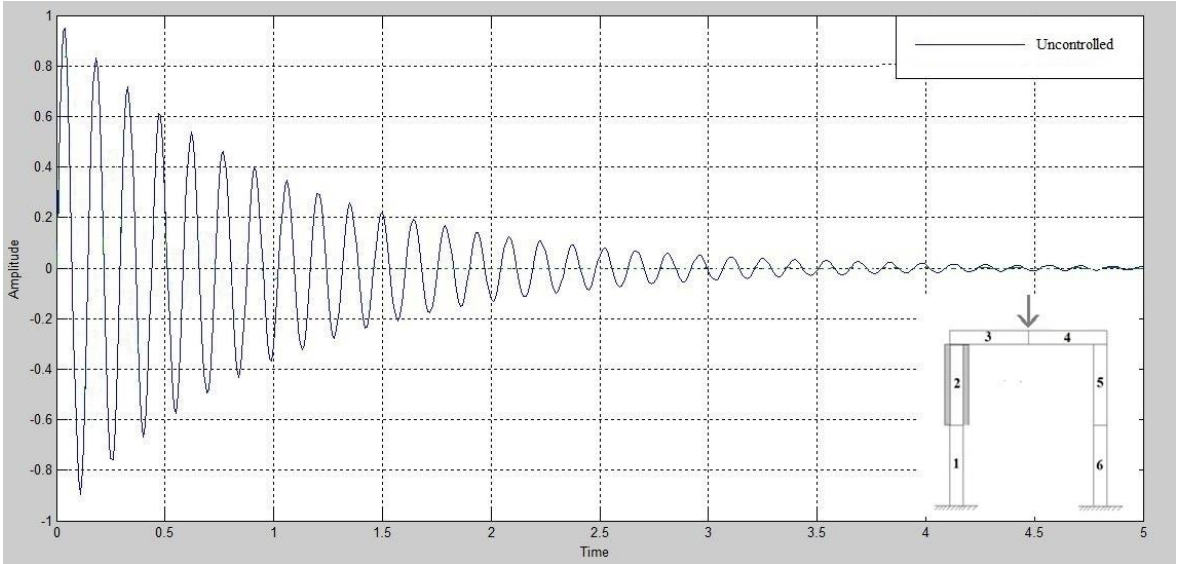

Fig.4.26 Displacement of Element-2 of Portal Frame (Alloy Steel) having midpoint load

The displacement graph of portal frame of alloy steel is shown in fig.4.26. This graph is generated by the Simulink for the second element and the excitation is applied on the midpoint of the horizontal element of portal frame structure without PID control. The graph shows that the amplitude is maximum at 0.1 sec time but as the time increases the amplitude is decreased due to damping effect.

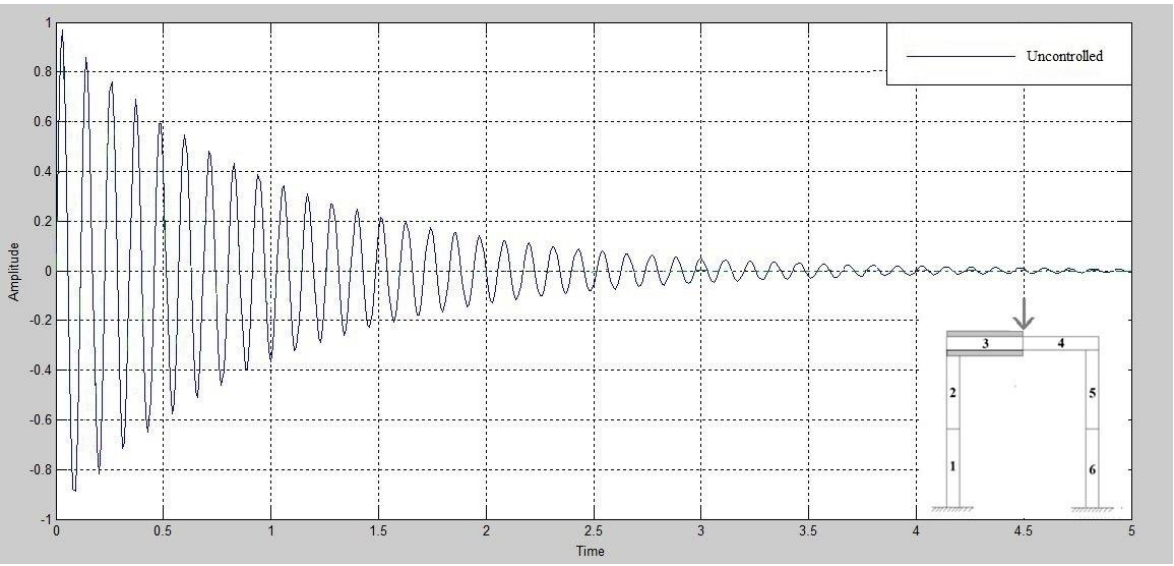

Fig.4.27. Displacement of Element-3 of Portal Frame (Alloy Steel) having midpoint load

The displacement graph of portal frame of alloy steel is shown in fig.4.27. This graph is generated by the Simulink for the third element and the excitation is applied on the midpoint of the horizontal element of portal frame structure without PID control. The graph shows that the amplitude is maximum at 0.1 sec time but as the time increases the amplitude is decreased due to damping effect.

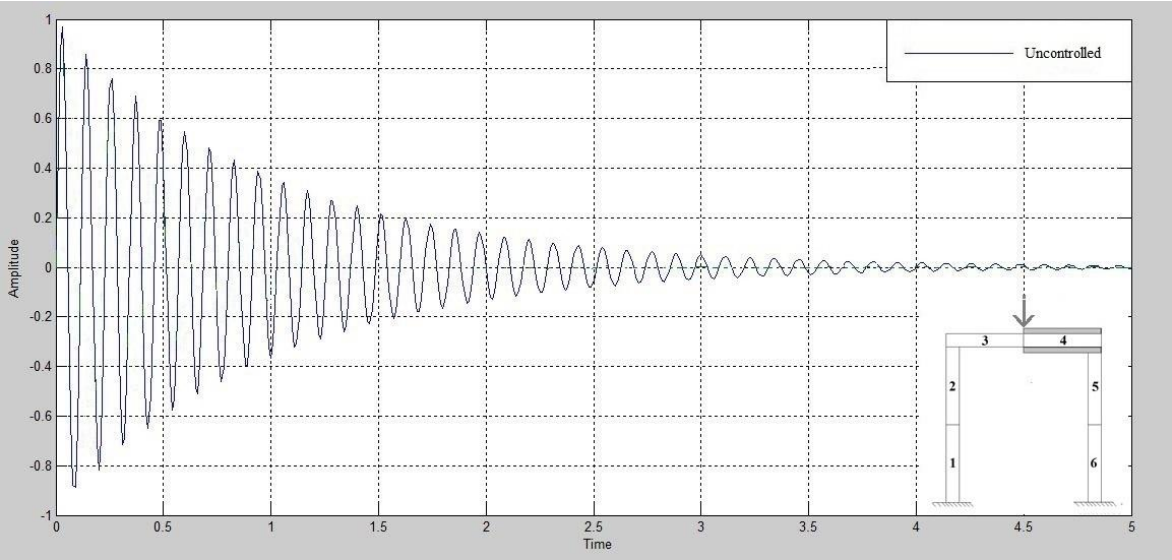

Fig.4.28 Displacement of Element-4 of Portal Frame (Alloy Steel) having midpoint load

The displacement graph of portal frame of alloy steel is shown in fig.4.28. This graph is generated by the Simulink for the fourth element and the excitation is applied on the midpoint of the horizontal element of portal frame structure without PID control. The graph shows that the amplitude is maximum at 0.1 sec time but as the time increases the amplitude is decreased due to damping effect.

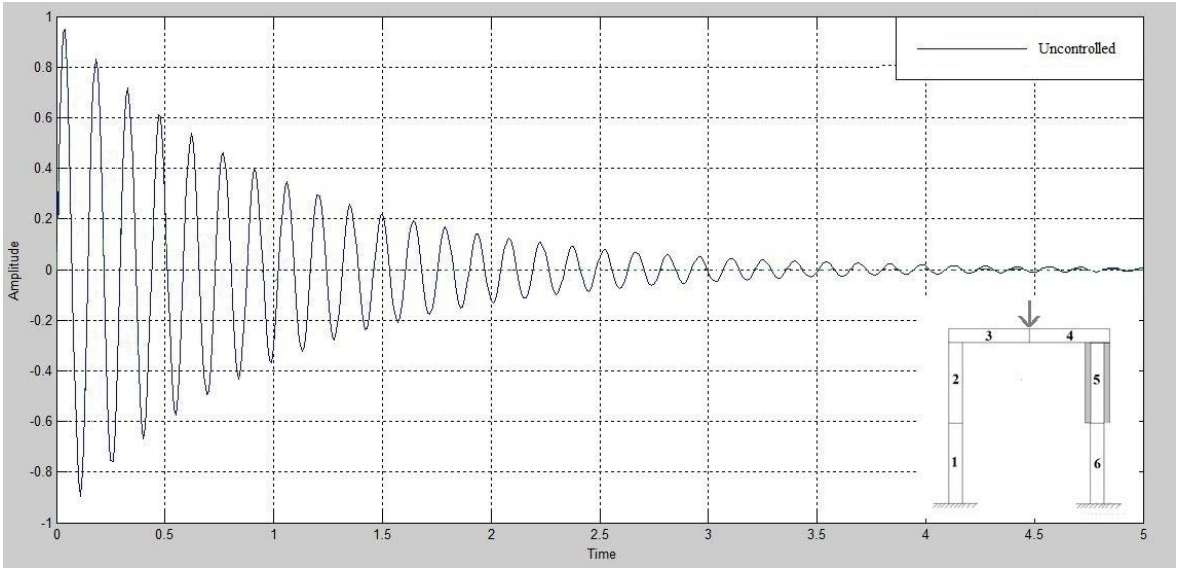

Fig.4.29 Displacement of Element-5 of Portal Frame (Alloy Steel) having midpoint load

The displacement graph of portal frame of alloy steel is shown in fig.4.29.This graph is generated by the Simulink for the fifth element and the excitation is applied on the midpoint of the horizontal element of portal frame structure without PID control. The graph shows that the amplitude is maximum at 0.1 sec time but as the time increases the amplitude is decreased due to damping effect.

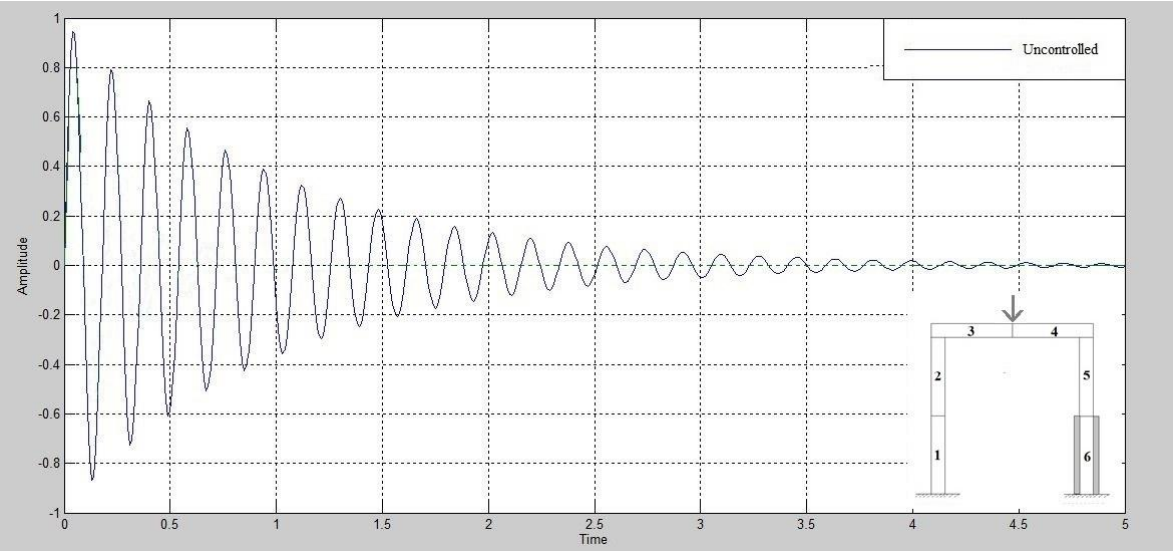

Fig.4.30 Displacement of Element-6 of Portal Frame (Alloy Steel) having midpoint load

The displacement graph of portal frame of alloy steel is shown in fig.4.30. This graph is generated by the Simulink for the sixth element and the excitation is applied on the midpoint of the horizontal element of portal frame structure without PID control. The graph shows that the amplitude is maximum at 0.1 sec time but as the time increases the amplitude is decreased due to damping effect.

4.5Displacement Graph of Portal Frame of Alloy Steel with Mid-Load and having PZT Patch and PID Controller

In this case collocated patches are serially placed on each element of the portal frame of alloy steel. The response are taken by giving excitation on the mid of the portal frame and the output is plotted by using sensors, at this stage actuators are active i.e. actuator is controlling vibration generated due to excitation. The graph shows that the displacement amplitude at that frequency which is generated due to excitation and displacement amplitude of their control.

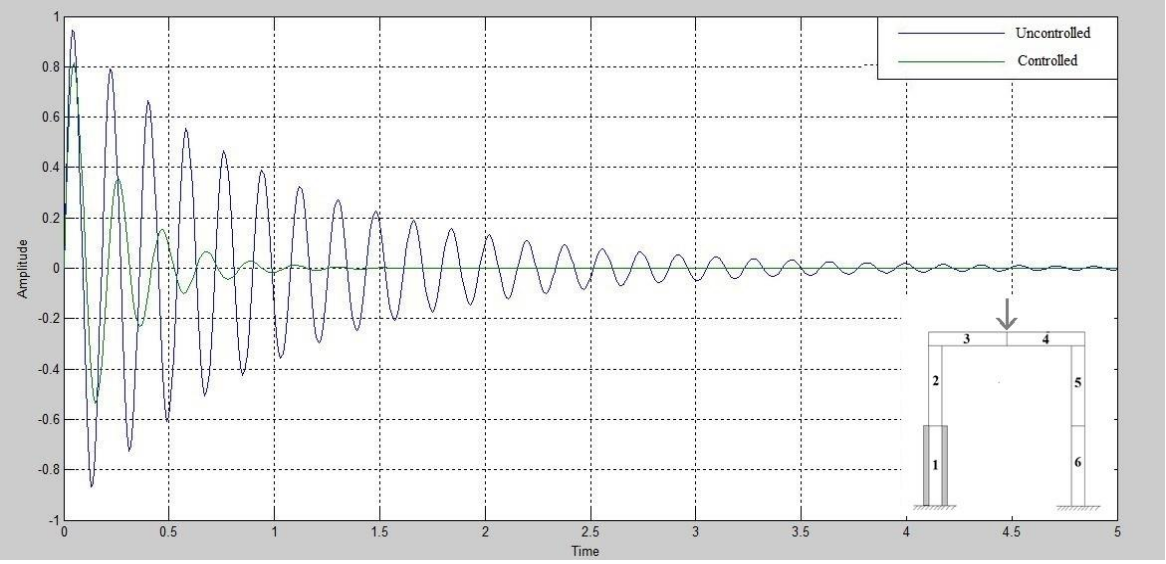

Fig.4.31 Displacement of Element-1 of Portal Frame (Alloy Steel) having midpoint load

The displacement graph of portal frame of alloy steel is shown in fig.4.31. This graph is generated by the Simulink for the first element and the excitation is applied on the midpoint of the horizontal element of portal frame structure with PID control. The graph shows that the amplitude is maximum at 0.1 sec time but as the time increases the amplitude is decreased due to damping effect. The vibration generated in portal frame due to force of 1 KN applied on fourth element is controlled in 1.5 sec.

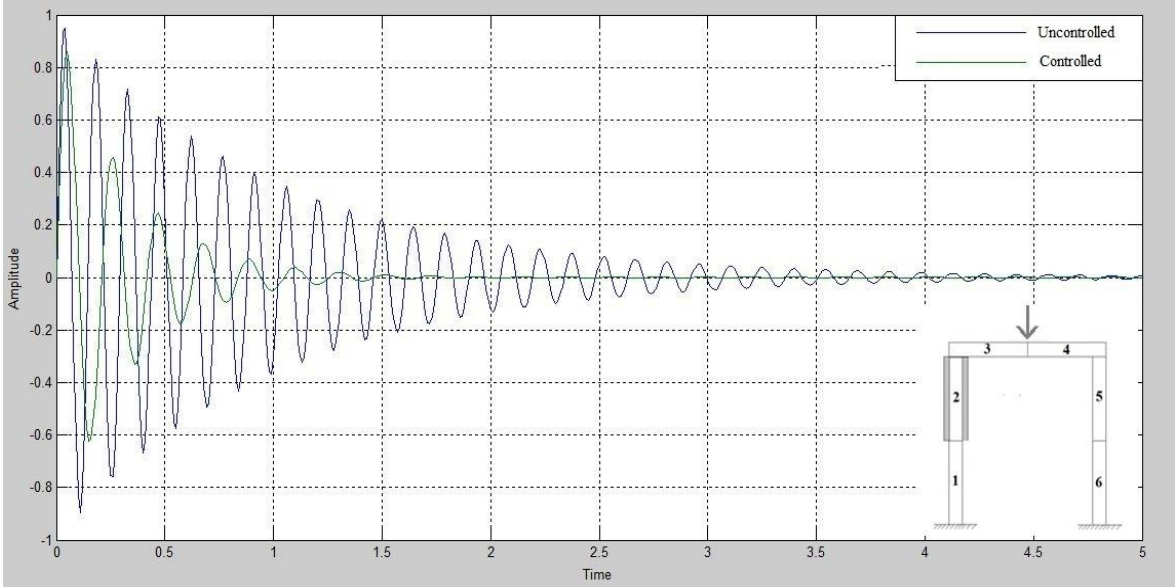

Fig.4.32. Displacement of Element-2 of Portal Frame (Alloy Steel) having midpoint load

The displacement graph of portal frame of alloy steel is shown in fig.4.32.This graph is generated by the Simulink for the second element and the excitation is applied on the midpoint of the horizontal element of portal frame structure with PID control. The graph shows that the amplitude is maximum at 0.1 sec time but as the time increases the amplitude is decreased due to damping effect. The vibration generated in portal frame due to force of 1 KN applied on fourth element is controlled in 2 sec.

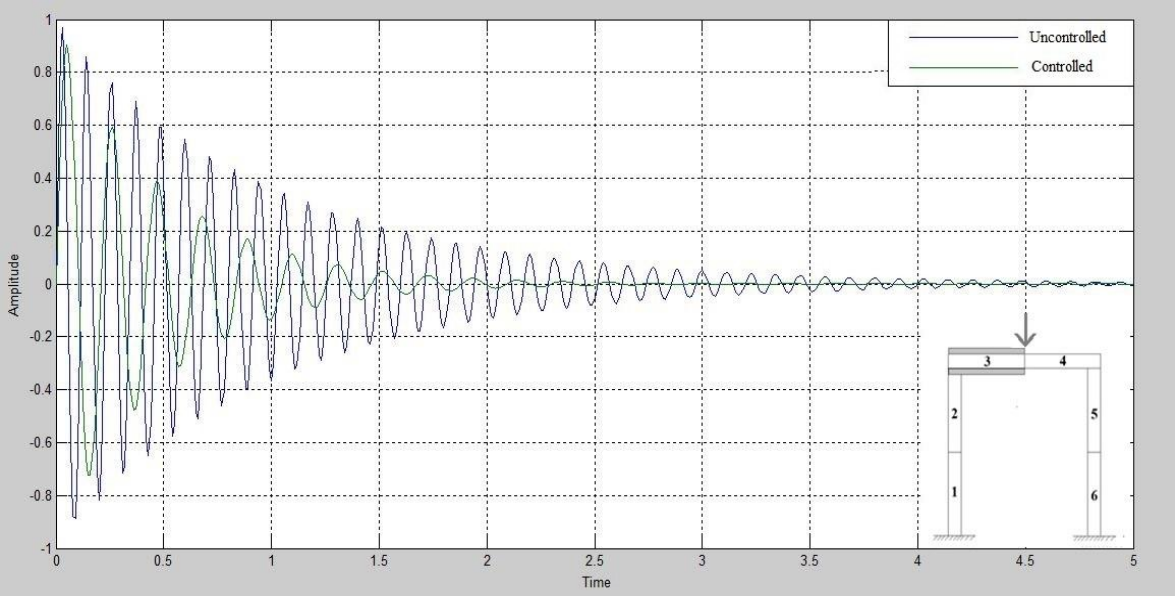

Fig.4.33 Displacement of Element-3 of Portal Frame (Alloy Steel) having midpoint load

The displacement graph of portal frame of alloy steel is shown in fig.4.33. This graph is generated by the Simulink for the third element and the excitation is applied on the midpoint of the horizontal element of portal frame structure with PID control. The graph shows that the amplitude is maximum at 0.1 sec time but as the time increases the amplitude is decreased due to damping effect. The vibration generated in portal frame due to force of 1 KN applied on fourth element is controlled in 2.5 sec.

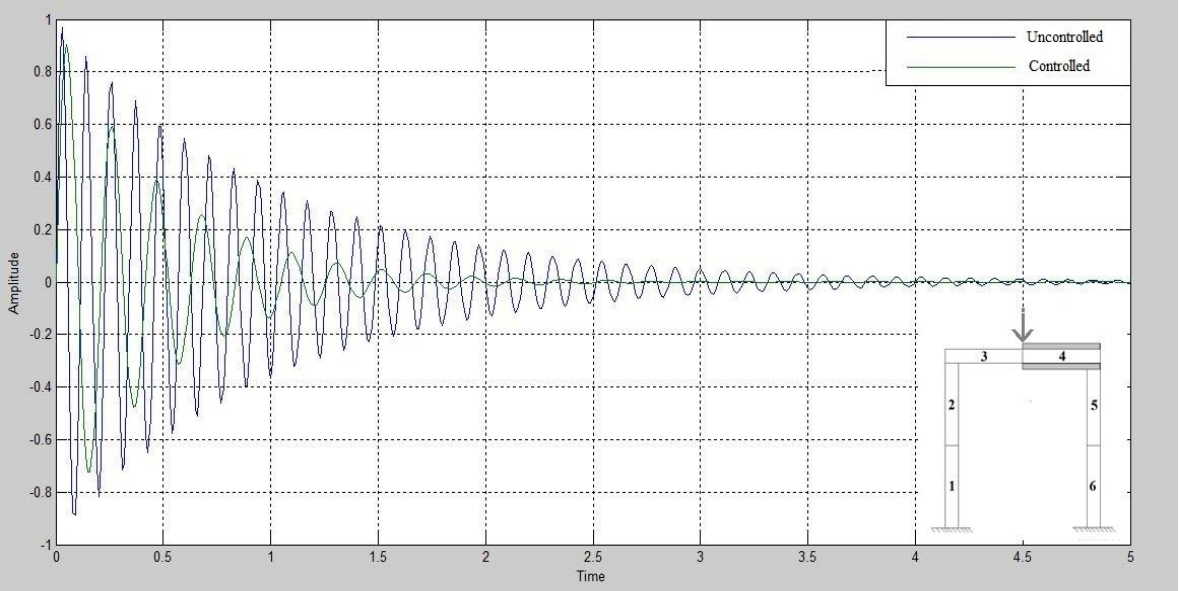

Fig.4.34 Displacement of Element-4 of Portal Frame (Alloy Steel) having midpoint load

The displacement graph of portal frame of alloy steel is shown in fig.4.34.This graph is generated by the Simulink for the fourth element and the excitation is applied on the midpoint of the horizontal element of portal frame structure with PID control. The graph shows that the amplitude is maximum at 0.1 sec time but as the time increases the amplitude is decreased due to damping effect. The vibration generated in portal frame due to force of 1 KN applied on fourth element is controlled in 3 sec.

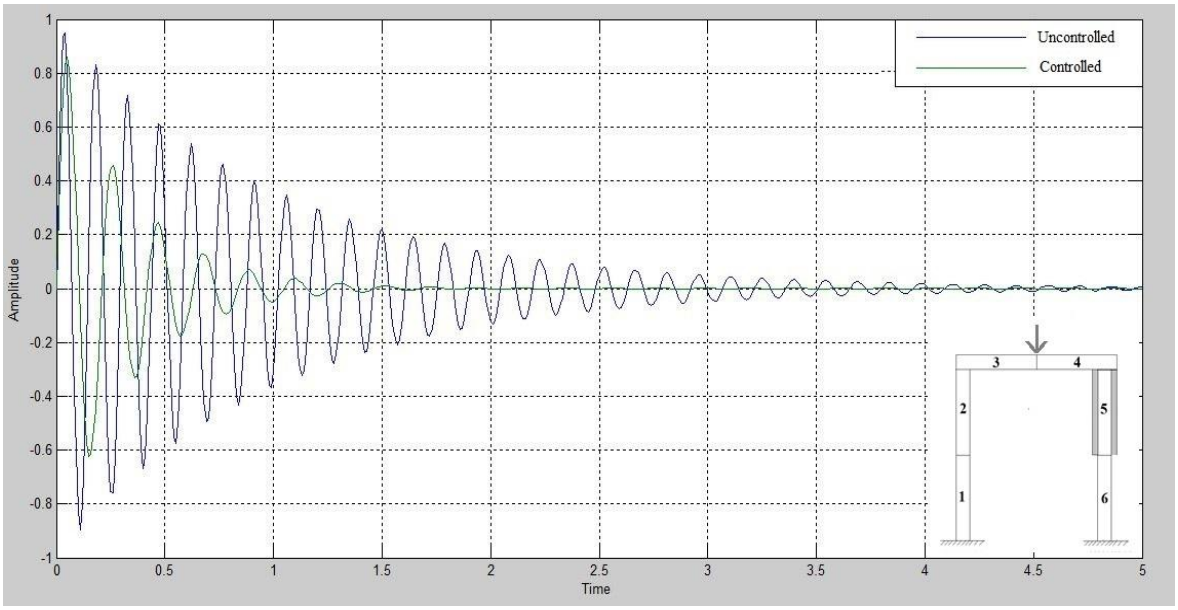

Fig.4.35 Displacement of Element-5 of Portal Frame (Alloy Steel) having midpoint load

The displacement graph of portal frame of alloy steel is shown in fig.4.35. This graph is generated by the Simulink for the fifth element and the excitation is applied on the midpoint of the horizontal element of portal frame structure with PID control. The graph shows that the amplitude is maximum at 0.1 sec time but as the time increases the amplitude is decreased due to damping effect. The vibration generated in portal frame due to force of 1 KN applied on fourth element is controlled in 2 sec.

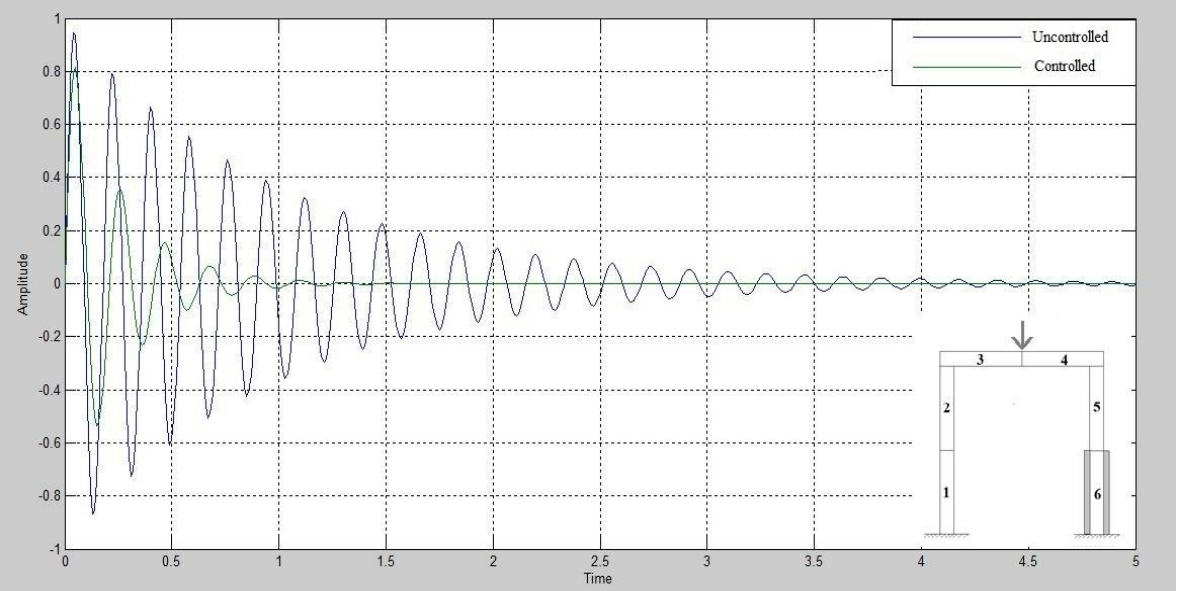

Fig.4.36 Displacement of Element-6 of Portal Frame (Alloy Steel) having midpoint load

The displacement graph of portal frame of alloy steel is shown in fig.4.36.This graph is generated by the Simulink for the sixth element and the excitation is applied on the midpoint of the horizontal element of portal frame structure with PID control. The graph shows that the amplitude is maximum at 0.1 sec time but as the time increases the amplitude is decreased due to damping effect. The vibration generated in portal frame due to force of 1 KN applied on fourth element is controlled in 1.5 sec.

4.6 Displacement Graph of Portal Frame of Carbon Fiber Reinforced Plastic with eccentric Load

In this case collocated patches are serially placed on each element of the portal frame of carbon fiber reinforced plastic. The response are taken by giving excitation on the eccentric point of the portal frame and the output is plotted by using sensors, at this stage actuators are not activated i.e. without control. The graph shows that the displacement amplitude at that frequency which is generated due to excitation.

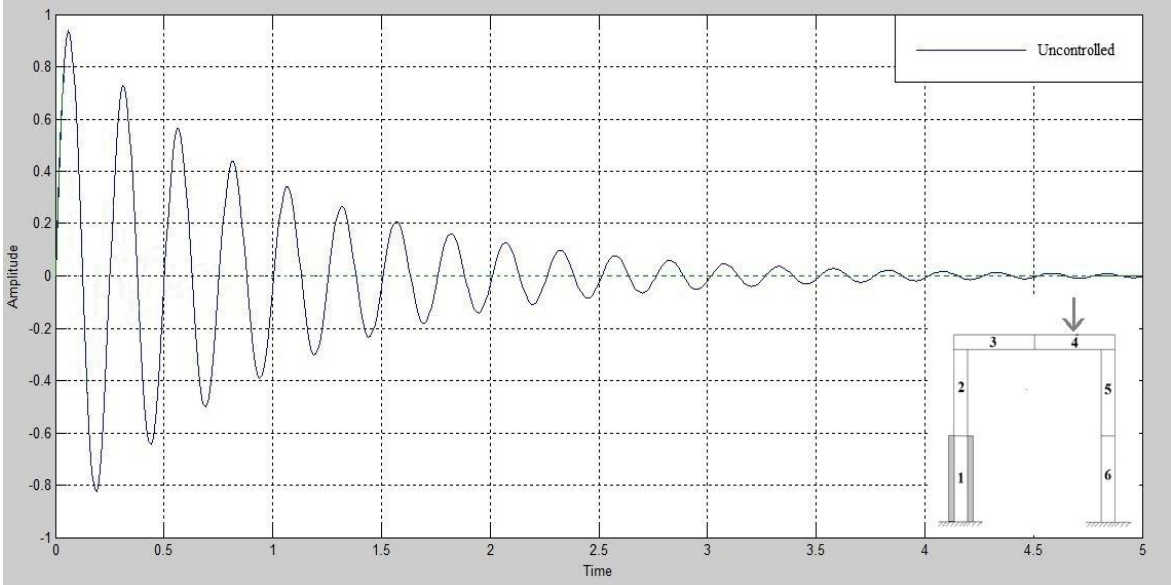

Fig.4.37. Displacement of Element-1 of Portal Frame (CFRP) having eccentric load

The displacement graph of portal frame of carbon fiber reinforced plastic is shown in fig.4.37. This graph is generated by the Simulink for the first element and the excitation is applied on the midpoint of the horizontal element of portal frame structure without PID control. The graph shows that the amplitude is maximum at 0.1 sec time but as the time increases the amplitude is decreased due to damping effect.

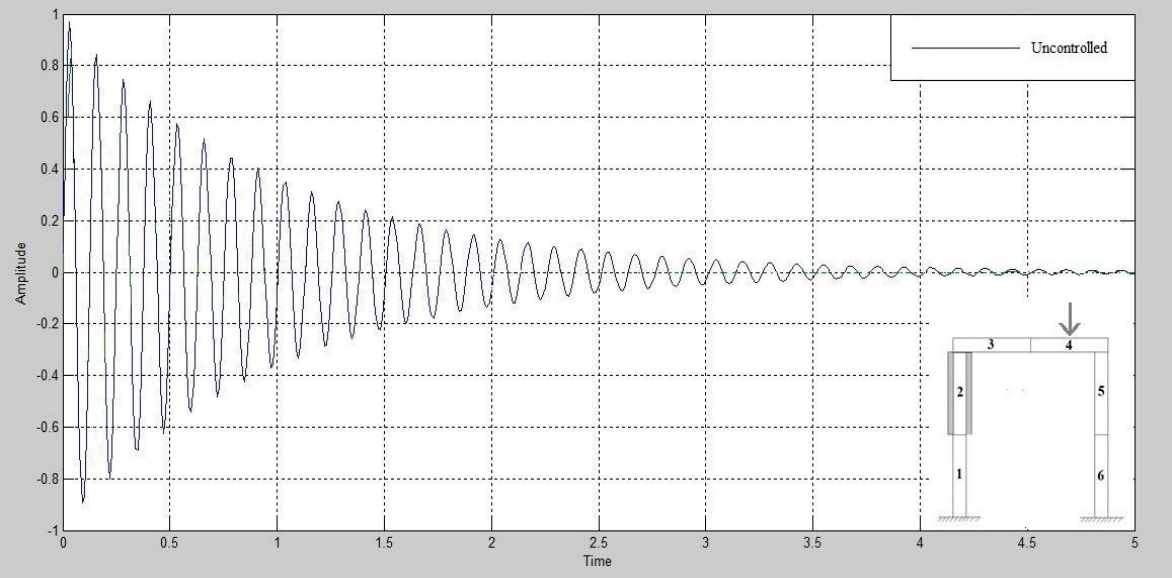

Fig.4.38Displacement of Element-2 of Portal Frame (CFRP) having eccentric load

The displacement graph of portal frame of carbon fiber reinforced plastic is shown in fig.4.38. This graph is generated by the Simulink for the second element and the excitation is applied on the midpoint of the horizontal element of portal frame structure without PID control. The graph shows that the amplitude is maximum at 0.1 sec time but as the time increases the amplitude is decreased due to damping effect.

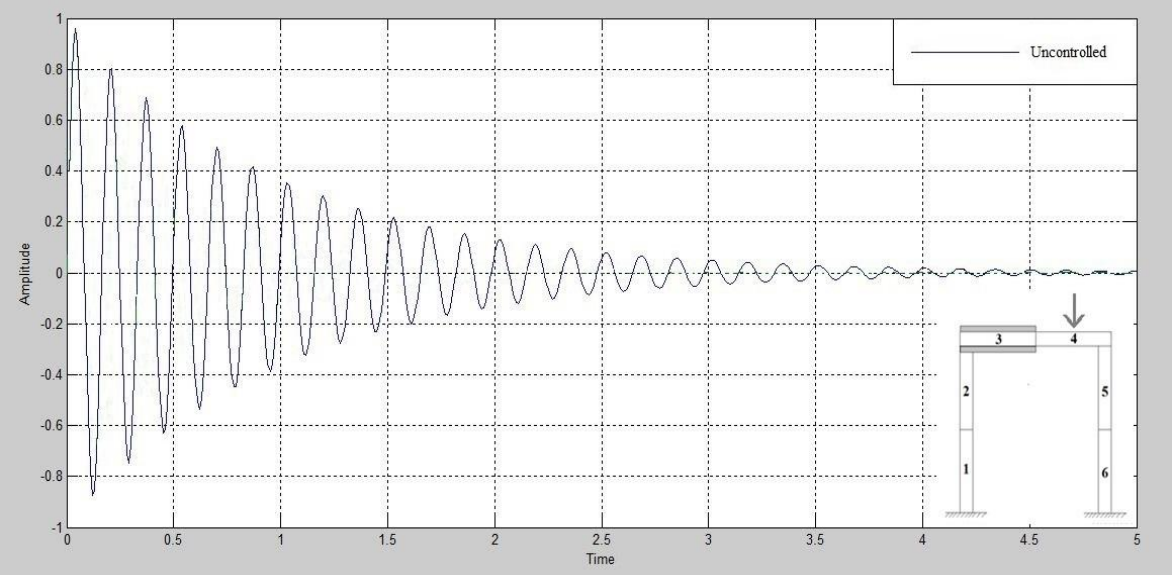

Fig.4.39 Displacement of Element-3 of Portal Frame (CFRP) having eccentric load

The displacement graph of portal frame of carbon fiber reinforced plastic is shown in fig.4.39. This graph is generated by the Simulink for the third element and the excitation is applied on the midpoint of the horizontal element of portal frame structure without PID control. The graph shows that the amplitude is maximum at 0.1 sec time but as the time increases the amplitude is decreased due to damping effect.

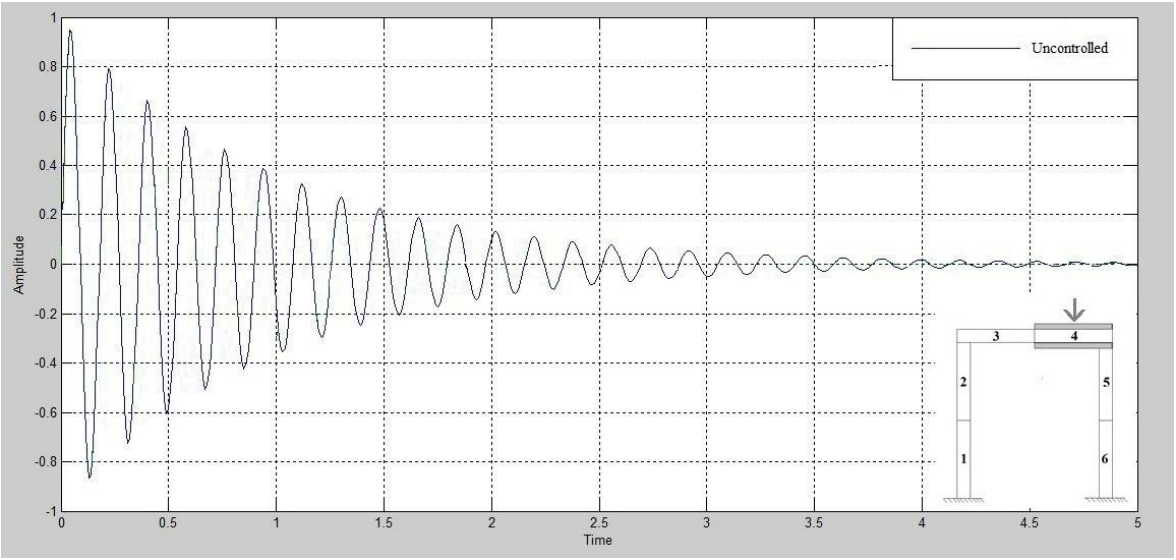

Fig.4.40 Displacement of Element-4 of Portal Frame (CFRP) having eccentric load

The displacement graph of portal frame of carbon fiber reinforced plastic is shown in fig.4.40. This graph is generated by the Simulink for the fourth element and the excitation is applied on the midpoint of the horizontal element of portal frame structure without PID control. The graph shows that the amplitude is maximum at 0.1 sec time but as the time increases the amplitude is decreased due to damping effect.

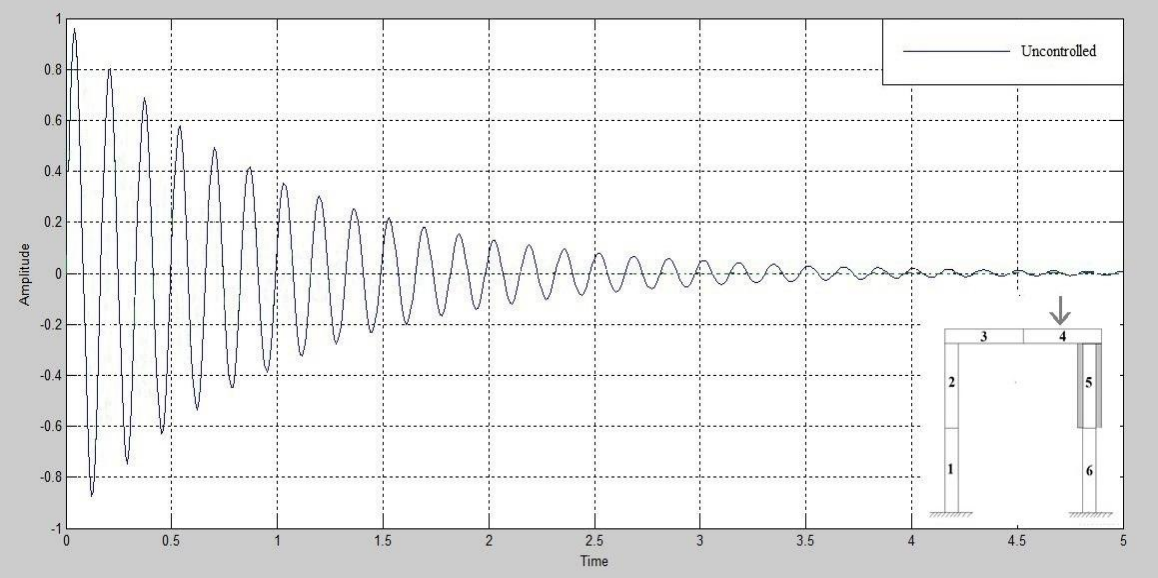

Fig.4.41 Displacement of Element-5 of Portal Frame (CFRP) having eccentric load

The displacement graph of portal frame of carbon fiber reinforced plastic is shown in fig.4.41. This graph is generated by the Simulink for the fifth element and the excitation is applied on the midpoint of the horizontal element of portal frame structure without PID control. The graph shows that the amplitude is maximum at 0.1 sec time but as the time increases the amplitude is decreased due to damping effect.

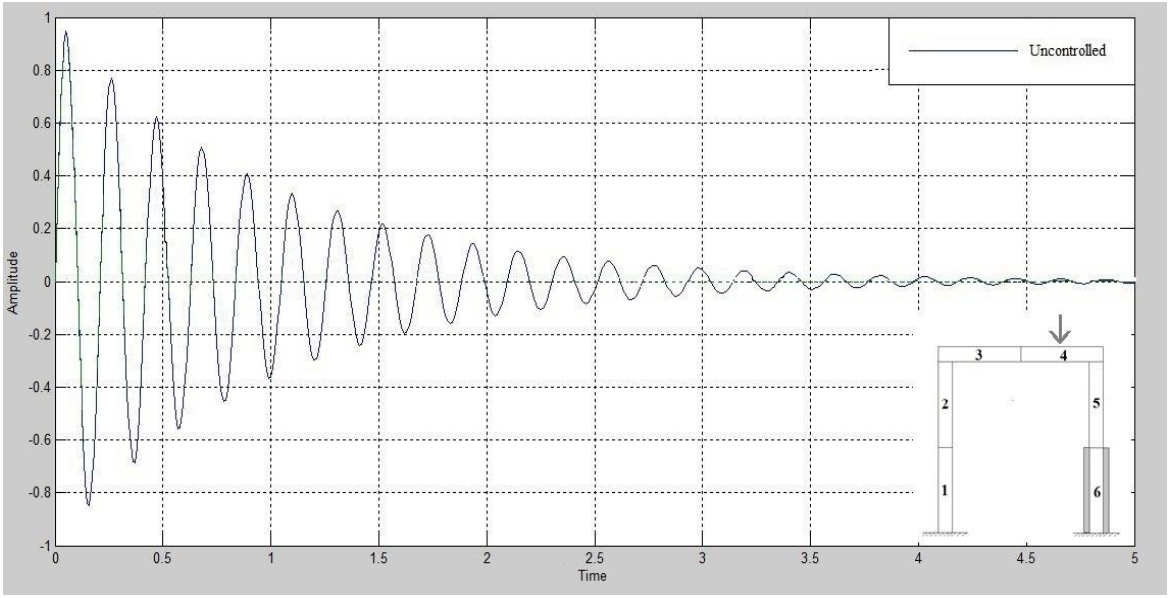

Fig.4.42. Displacement of Element-6 of Portal Frame (CFRP) having eccentric load

The displacement graph of portal frame of carbon fiber reinforced plastic is shown in fig.4.42. This graph is generated by the Simulink for the sixth element and the excitation is applied on the midpoint of the horizontal element of portal frame structure without PID control. The graph shows that the amplitude is maximum at 0.1 sec time but as the time increases the amplitude is decreased due to damping effect.

4.7Displacement Graph of Portal Frame of Carbon Fiber Reinforced Plastic with eccentric Load and having PZT Patch and PID Controller

In this case collocated patches are serially placed on each element of the portal frame of carbon fiber reinforced plastic. The response are taken by giving excitation on the eccentric point of the portal frame and the output is plotted by using sensors, at this stage actuators are active i.e. actuator is controlling vibration generated due to excitation. The graph shows that the displacement amplitude at that frequency which is generated due to excitation and displacement amplitude of their control.

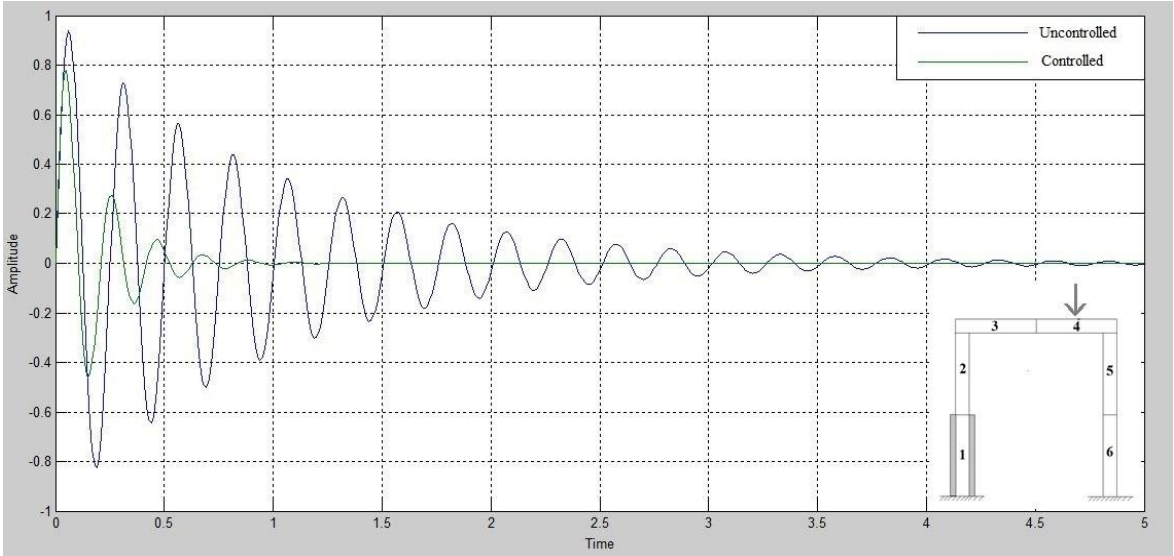

Fig.4.43 Displacement of Element-1 of Portal Frame (CFRP) having eccentric load

The displacement graph of portal frame of carbon fiber reinforced plastic is shown in fig.4.43. This graph is generated by the Simulink for the first element and the excitation is applied on the eccentric point of the horizontal element of portal frame structure with PID control. The graph shows that the amplitude is maximum at 0.1 sec time but as the time increases the amplitude is decreased due to damping effect. The vibration generated in portal frame due to force of 1 KN applied on fourth element is controlled in 1.5 sec.

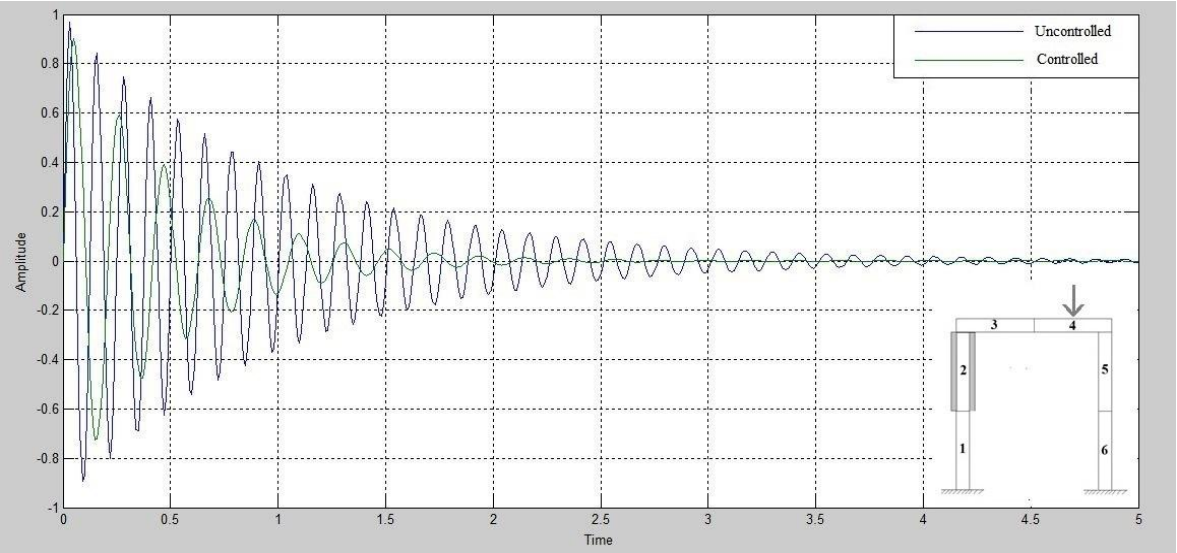

Fig.4.44 Displacement of Element-2 of Portal Frame (CFRP) having eccentric load

The displacement graph of portal frame of carbon fiber reinforced plastic is shown in fig4.44. This graph is generated by the Simulink for the second element and the excitation is applied on the eccentric point of the horizontal element of portal frame structure with PID control. The graph shows that the amplitude is maximum at 0.1 sec time but as the time increases the amplitude is decreased due to damping effect. The vibration generated in portal frame due to force of 1 KN applied on fourth element is controlled in 3 sec.

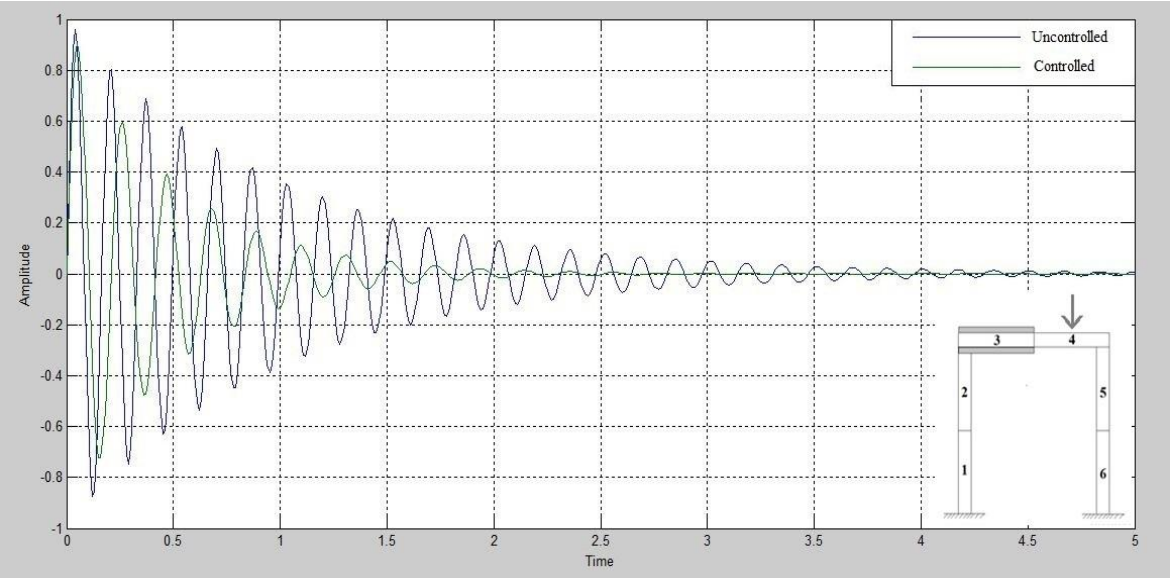

Fig.4.45Displacement of Element-3 of Portal Frame (CFRP) having eccentric load

The displacement graph of portal frame of carbon fiber reinforced plastic is shown in fig4.45. This graph is generated by the Simulink for the third element and the excitation is applied on the eccentric point of the horizontal element of portal frame structure with PID control. The graph shows that the amplitude is maximum at 0.1 sec time but as the time increases the amplitude is decreased due to damping effect. The vibration generated in portal frame due to force of 1 KN applied on fourth element is controlled in 3 sec.

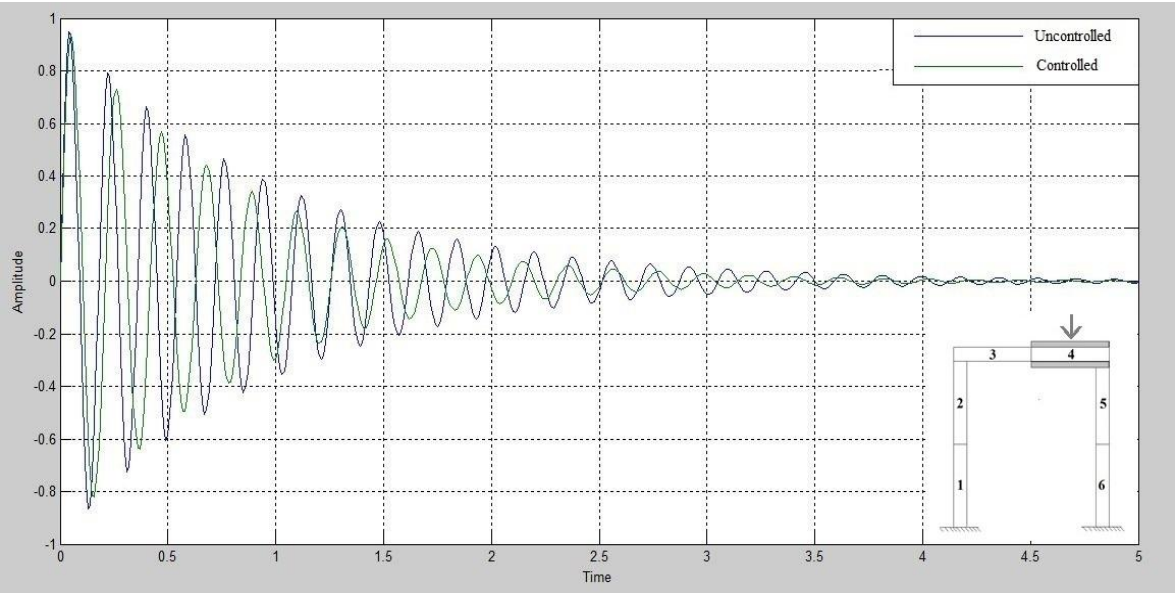

Fig.4.46 Displacement of Element-4 of Portal Frame (CFRP) having eccentric load

The displacement graph of portal frame of carbon fiber reinforced plastic is shown in fig.4.46. This graph is generated by the Simulink for the fourth element and the excitation is applied on the eccentric point of the horizontal element of portal frame structure with PID control. The graph shows that the amplitude is maximum at 0.1 sec time but as the time increases the amplitude is decreased due to damping effect. The vibration generated in portal frame due to force of 1 KN applied on fourth element is controlled in 5 sec.

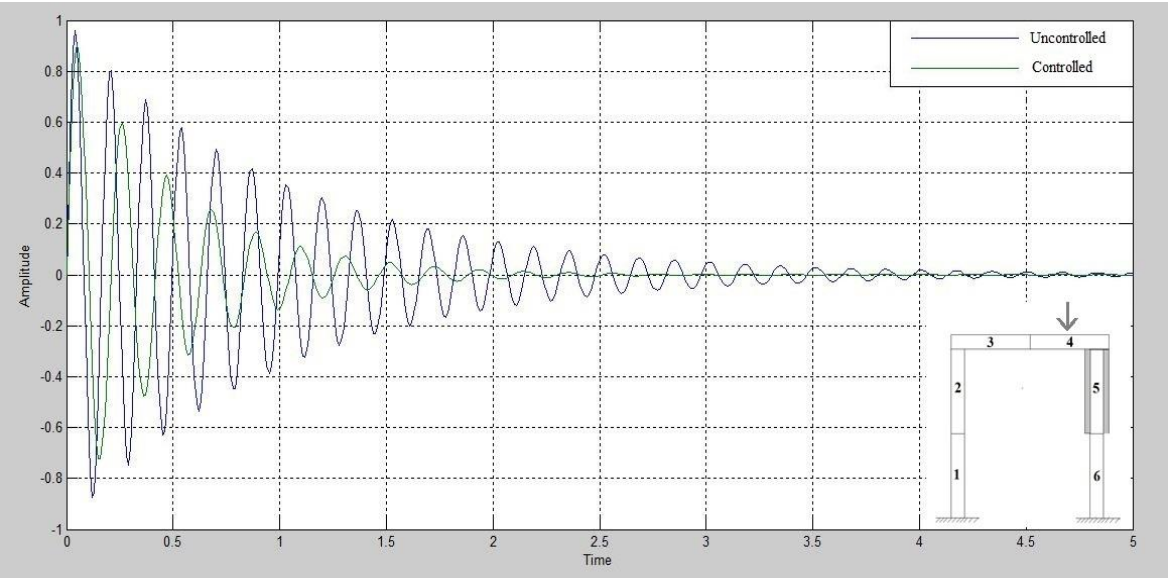

Fig.4.47. Displacement of Element-5 of Portal Frame (CFRP) having eccentric load

The displacement graph of portal frame of carbon fiber reinforced plastic is shown in fig.4.47. This graph is generated by the Simulink for the fifth element and the excitation is applied on the eccentric point of the horizontal element of portal frame structure with PID control. The graph shows that the amplitude is maximum at 0.1 sec time but as the time increases the amplitude is decreased due to damping effect. The vibration generated in portal frame due to force of 1 KN applied on fourth element is controlled in 2.5 sec.

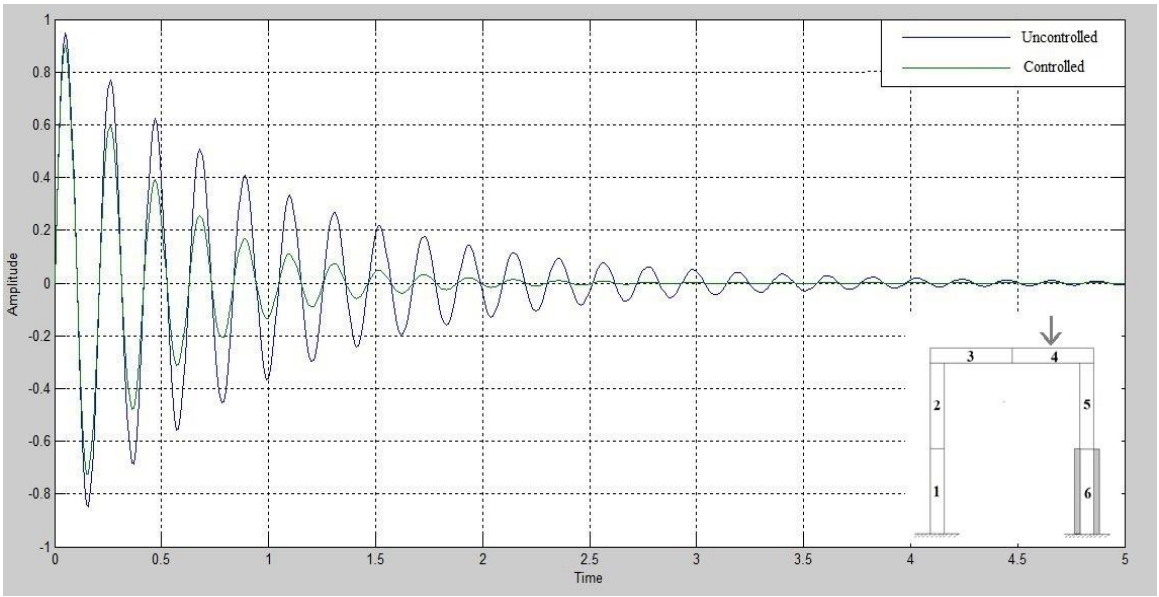

Fig.4.48 Displacement of Element-6 of Portal Frame (CFRP) having eccentric load

The displacement graph of portal frame of carbon fiber reinforced plastic is shown in fig.4.48. This graph is generated by the Simulink for the sixth element and the excitation is applied on the eccentric point of the horizontal element of portal frame structure with PID control. The graph shows that the amplitude is maximum at 0.1 sec time but as the time increases the amplitude is decreased due to damping effect. The vibration generated in portal frame due to force of 1 KN applied on fourth element is controlled in 2.5 sec.

4.8 Displacement Graph of Portal Frame of Carbon Fiber Reinforced Plastic with Mid-Load

In this case collocated patches are serially placed on each element of the portal frame of carbon fiber reinforced plastic. The response are taken by giving excitation on the mid of the portal frame and the output is plotted by using sensors, at this stage actuators are not activated i.e. without control. The graph shows that the displacement amplitude at that frequency which is generated due to excitation.

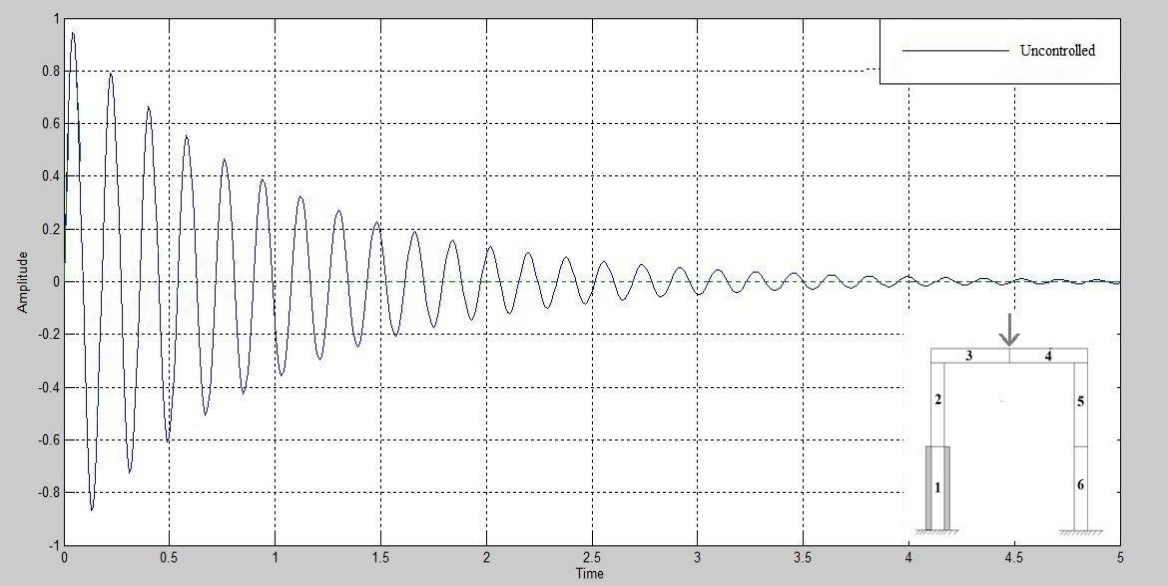

Fig.4.49 Displacement of Element-1 of Portal Frame (CFRP) having midpoint load

The displacement graph of portal frame of carbon fiber reinforced plastic is shown in fig.4.49. This graph is generated by the Simulink for the first element and the excitation is applied on the midpoint of the horizontal element of portal frame structure without PID control. The graph shows that the amplitude is maximum at 0.1 sec time but as the time increases the amplitude is decreased due to damping effect.

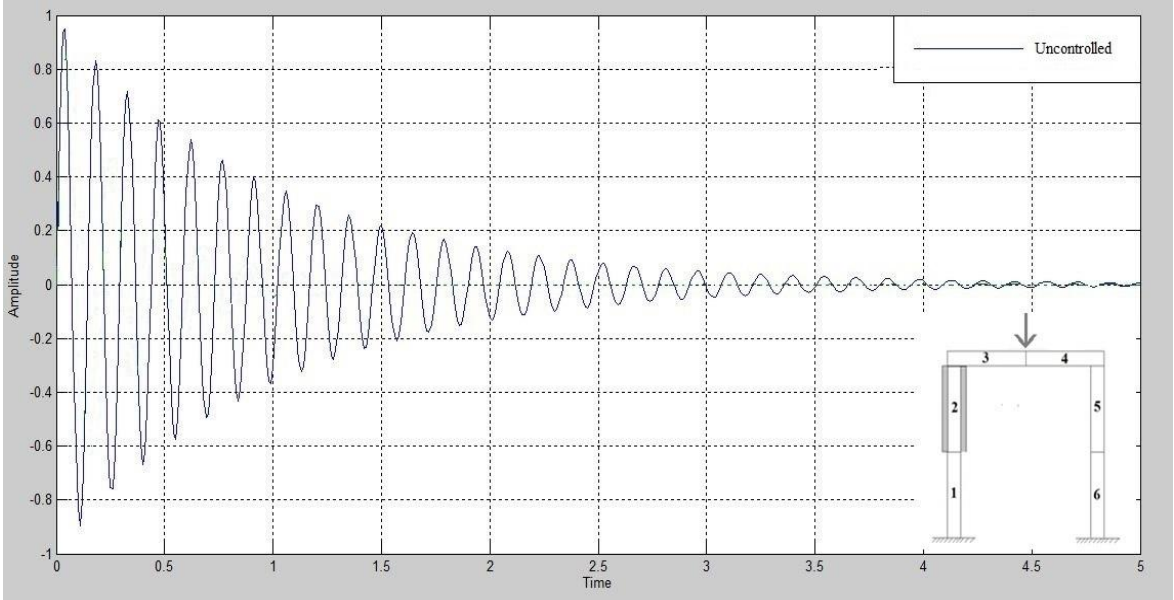

Fig.4.50 Displacement of Element-2 of Portal Frame (CFRP) having midpoint load

The displacement graph of portal frame of carbon fiber reinforced plastic is shown in fig.4.50 This graph is generated by the Simulink for the second element and the excitation is applied on the midpoint of the horizontal element of portal frame structure without PID control. The graph shows that the amplitude is maximum at 0.1 sec time but as the time increases the amplitude is decreased due to damping effect.

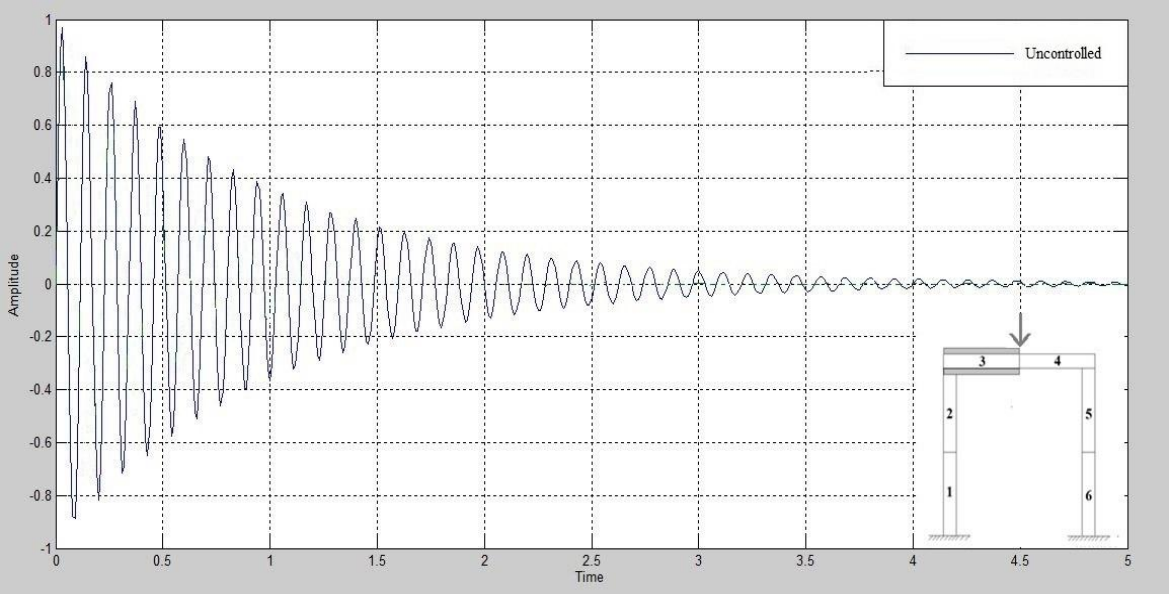

Fig.4.51 Displacement of Element-3 of Portal Frame (CFRP) having midpoint load

The displacement graph of portal frame of carbon fiber reinforced plastic is shown in fig.4.51. This graph is generated by the Simulink for the third element and the excitation is applied on the midpoint of the horizontal element of portal frame structure without PID control. The graph shows that the amplitude is maximum at 0.1 sec time but as the time increases the amplitude is decreased due to damping effect.

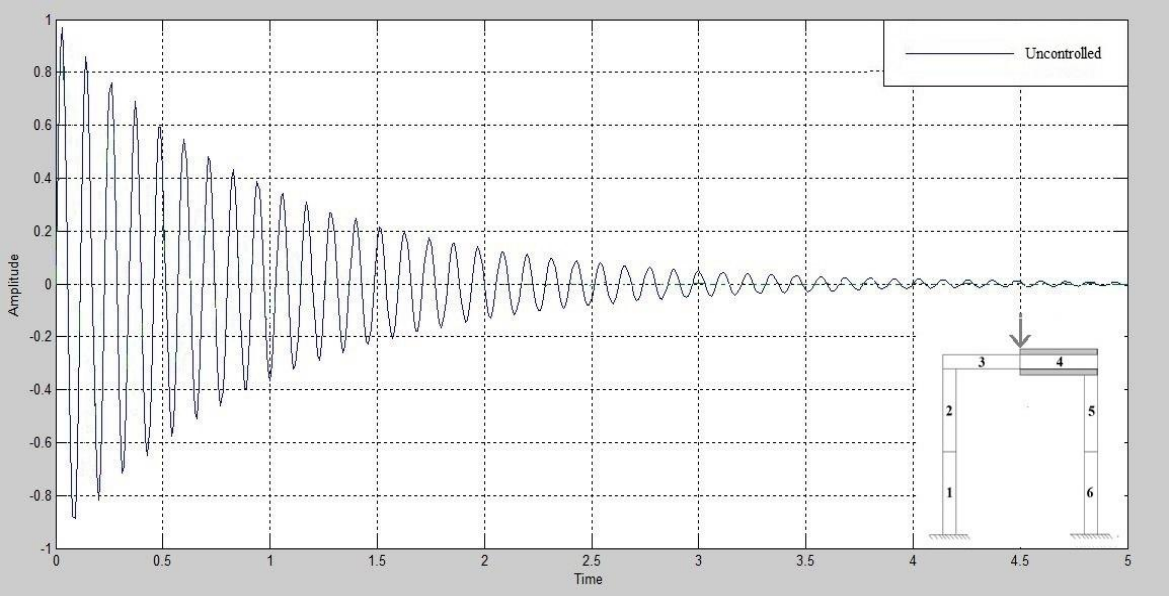

Fig.4.52 Displacement of Element-4 of Portal Frame (CFRP) having midpoint load

The displacement graph of portal frame of carbon fiber reinforced plastic is shown in fig.4.52. This graph is generated by the Simulink for the fourth element and the excitation is applied on the midpoint of the horizontal element of portal frame structure without PID control. The graph shows that the amplitude is maximum at 0.1 sec time but as the time increases the amplitude is decreased due to damping effect.

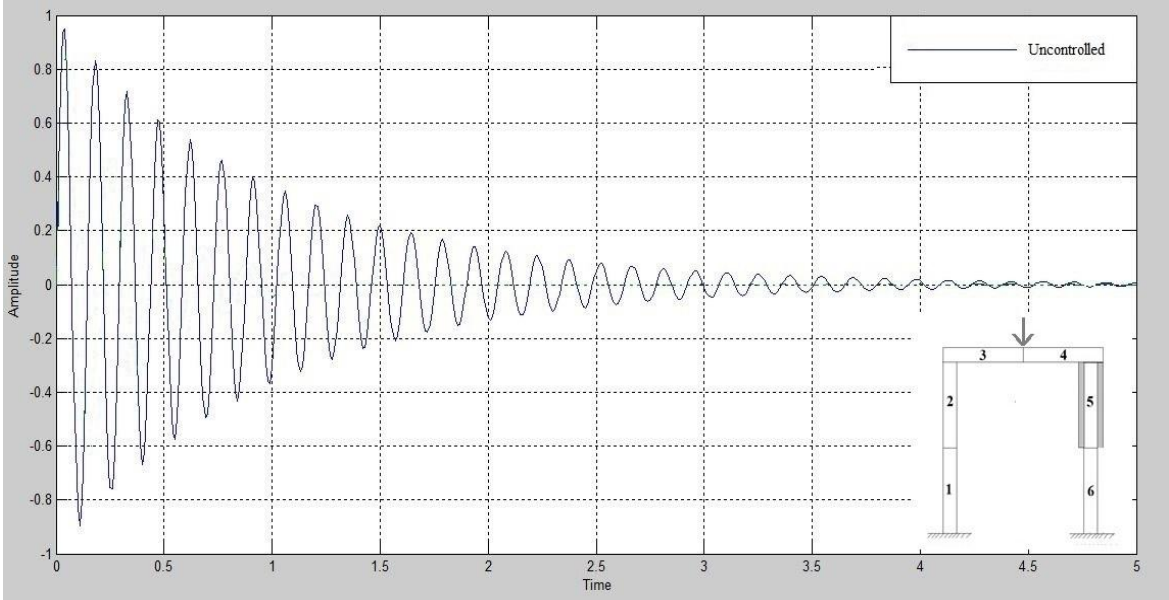

Fig.4.53 Displacement of Element-5 of Portal Frame (CFRP) having midpoint load

The displacement graph of portal frame of carbon fiber reinforced plastic is shown in fig.4.53.This graph is generated by the Simulink for the fifth element and the excitation is applied on the midpoint of the horizontal element of portal frame structure without PID control. The graph shows that the amplitude is maximum at 0.1 sec time but as the time increases the amplitude is decreased due to damping effect.

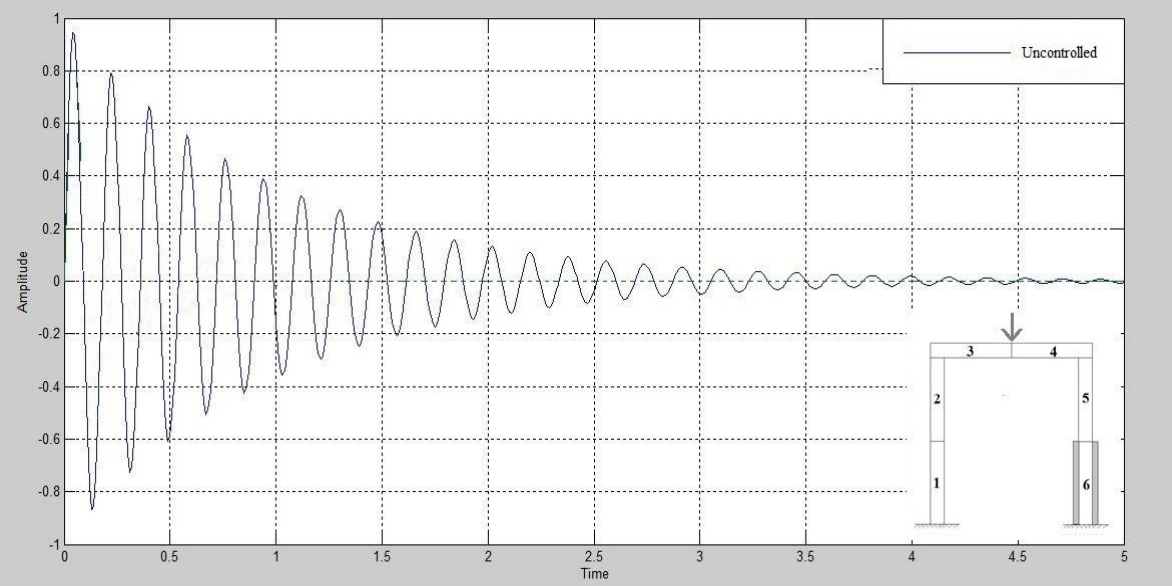

Fig.4.54 Displacement of Element-6 of Portal Frame (CFRP) having midpoint load

The displacement graph of portal frame of carbon fiber reinforced plastic is shown in fig4.54.This graph is generated by the Simulink for the sixth element and the excitation is applied on the midpoint of the horizontal element of portal frame structure without PID control. The graph shows that the amplitude is maximum at 0.1 sec time but as the time increases the amplitude is decreased due to damping effect.

4.9 Displacement Graph of Portal Frame of Carbon Fiber Reinforced Plastic with Midpoint Load and having PZT Patch and PID Controller

In this case collocated patches are serially placed on each element of the portal frame of carbon fiber reinforced plastic. The response are taken by giving excitation on the top side of the portal frame and the output is plotted by using sensors, at this stage actuators are active i.e. actuator is controlling vibration generated due to excitation. The graph shows that the displacement amplitude at that frequency which is generated due to excitation and displacement amplitude of their control.

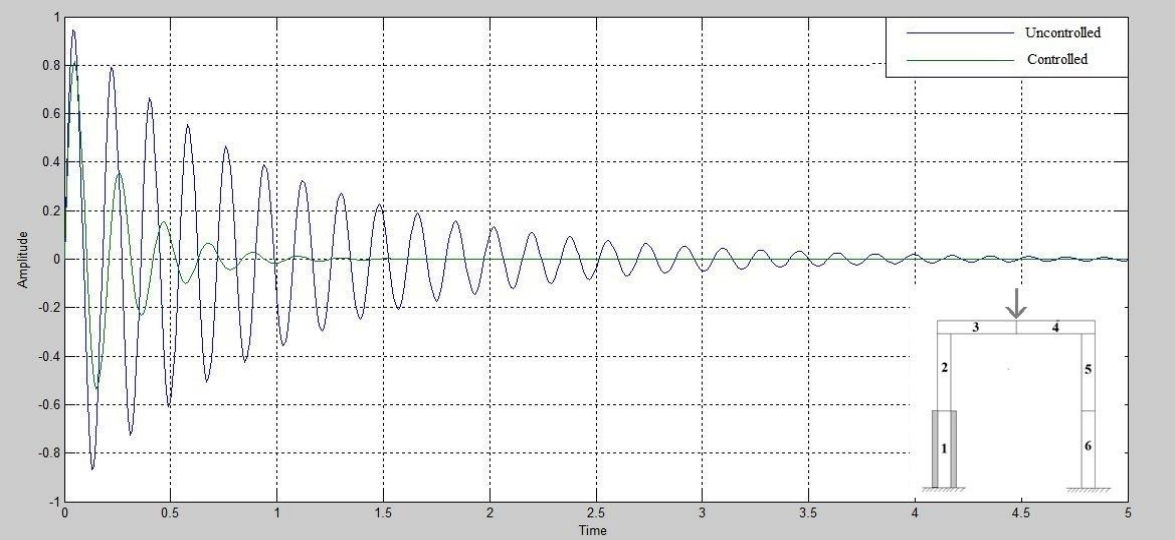

Fig.4.55 Displacement of Element-1 of Portal Frame (CFRP) having midpoint load

The displacement graph of portal frame of alloy steel is shown in fig.4.55.This graph is generated by the Simulink for the first element and the excitation is applied on the midpoint of the horizontal element of portal frame structure with PID control. The graph shows that the amplitude is maximum at 0.1 sec time but as the time increases the amplitude is decreased due to damping effect. The vibration generated in portal frame due to force of 1 KN applied on fourth element is controlled in 1.5 sec.

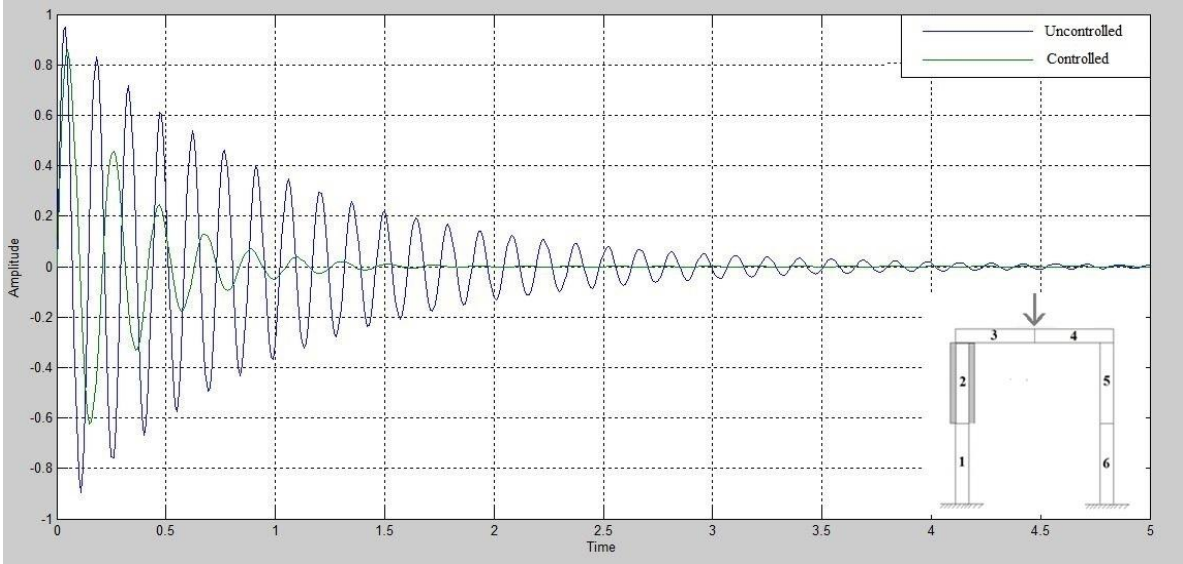

Fig.4.56 Displacement of Element-2 of Portal Frame (CFRP) having midpoint load

The displacement graph of portal frame of alloy steel is shown in fig.4.56. This graph is generated by the Simulink for the second element and the excitation is applied on the midpoint of the horizontal element of portal frame structure with PID control. The graph shows that the amplitude is maximum at 0.1 sec time but as the time increases the amplitude is decreased due to damping effect. The vibration generated in portal frame due to force of 1 KN applied on fourth element is controlled in 2 sec.

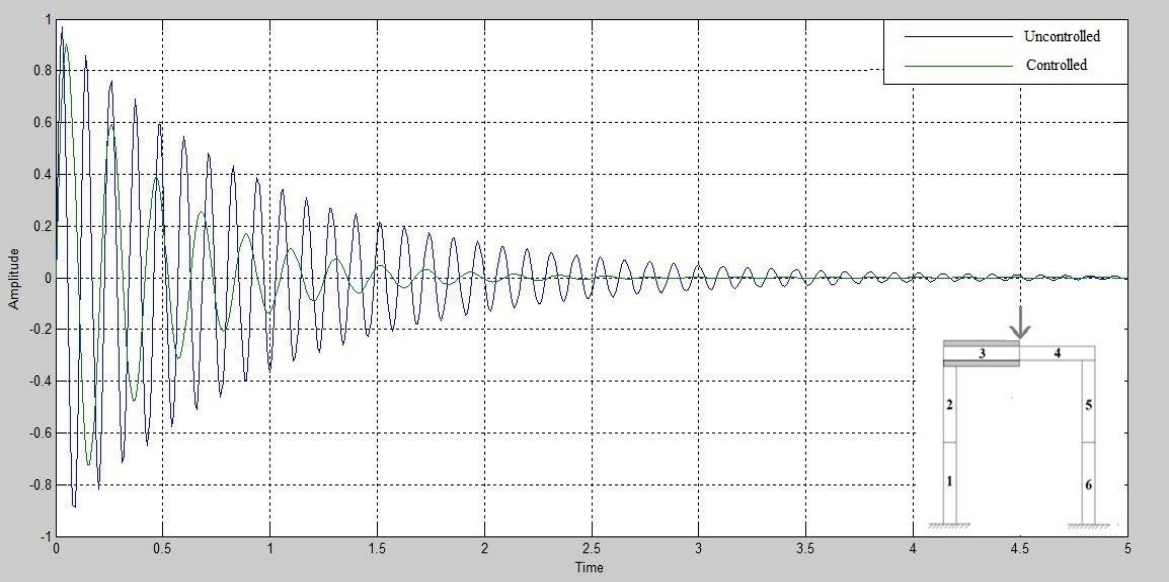

Fig.4.57 Displacement of Element-3 of Portal Frame (CFRP) having midpoint load

The displacement graph of portal frame of alloy steel is shown in fig.4.47. This graph is generated by the Simulink for the third element and the excitation is applied on the midpoint of the horizontal element of portal frame structure with PID control. The graph shows that the amplitude is maximum at 0.1 sec time but as the time increases the amplitude is decreased due to damping effect. The vibration generated in portal frame due to force of 1 KN applied on fourth element is controlled in 2.5 sec.

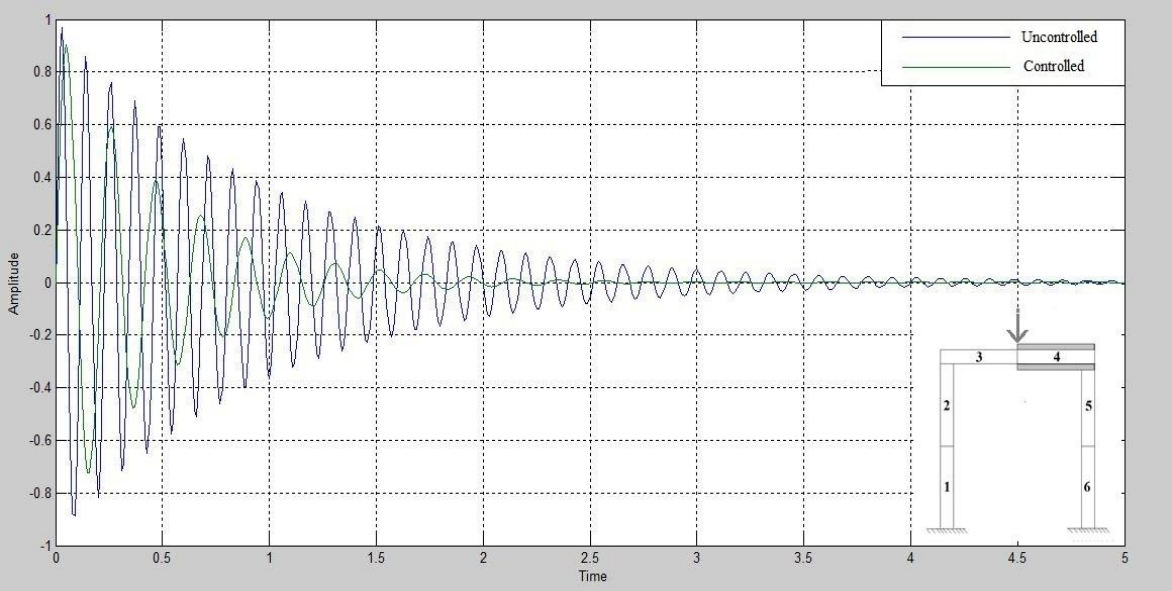

Fig.4.58 Displacement of Element-4 of Portal Frame (CFRP) having midpoint load

The displacement graph of portal frame of alloy steel is shown in fig.4.58. This graph is generated by the Simulink for the fourth element and the excitation is applied on the midpoint of the horizontal element of portal frame structure with PID control. The graph shows that the amplitude is maximum at 0.1 sec time but as the time increases the amplitude is decreased due to damping effect. The vibration generated in portal frame due to force of 1 KN applied on fourth element is controlled in 2.5 sec.

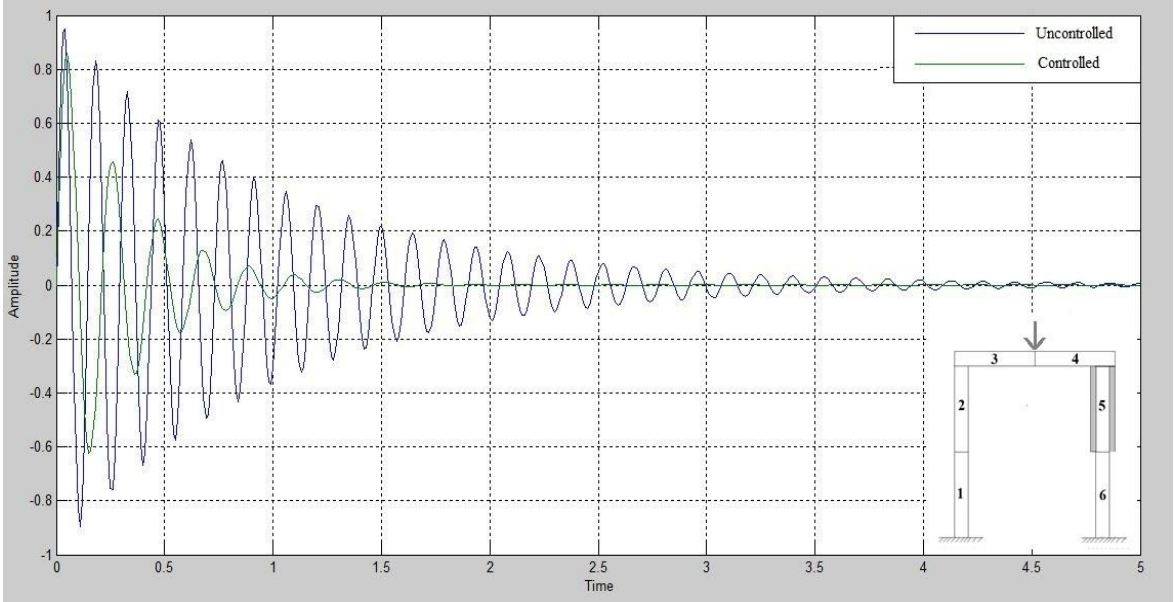

Fig.4.59 Displacement of Element-5 of Portal Frame (CFRP) having midpoint load

The displacement graph of portal frame of alloy steel is shown in fig.4.59. This graph is generated by the Simulink for the fifth element and the excitation is applied on the midpoint of the horizontal element of portal frame structure with PID control. The graph shows that the amplitude is maximum at 0.1 sec time but as the time increases the amplitude is decreased due to damping effect. The vibration generated in portal frame due to force of 1 KN applied on fourth element is controlled in 2 sec.

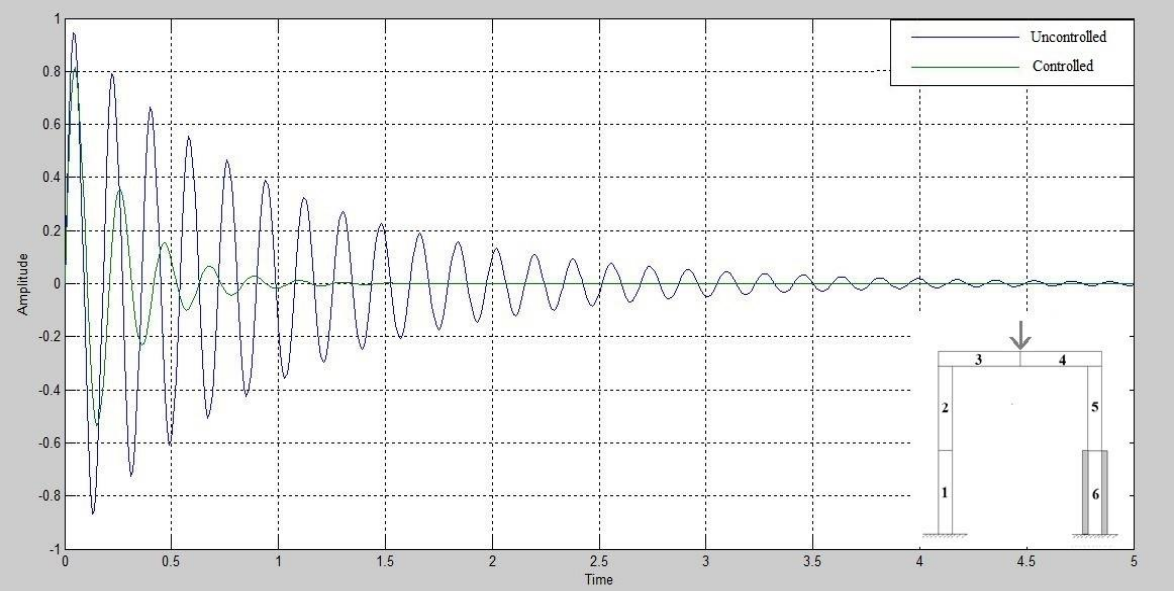

Fig.4.60Displacement of Element-6 of Portal Frame (CFRP) having midpoint load

The displacement graph of portal frame of alloy steel is shown in fig.4.60. This graph is generated by the Simulink for the sixth element and the excitation is applied on the midpoint of the horizontal element of portal frame structure with PID control. The graph shows that the amplitude is maximum at 0.1 sec time but as the time increases the amplitude is decreased due to damping effect. The vibration generated in portal frame due to force of 1 KN applied on fourth element is controlled in 1.5 sec.

4.10. Validation of results obtained by Ansys Software with Finite Element Analysis

The Analysis of frequency of the Alloy Steel And Carbon Reinforced Plastic for different modes are also worked out manually by Finite Element Analysis. The results obtained by using Ansys software are compared with Finite Element Analysis as under;

ω^2(rad/s)	ω(rad/s)	FEM	ANSYS
14.8548	3.854193	61341	61059
10.1291	3.182625	50652	50807
5.9068	2.430391	38680	38629
3.0042	1.733263	27585	27628
0.2931	0.541387	8616	8740
1.2325	1.11018	17669	17168

Table 4.1. compared result Finite Element Analysis & Ansys software of Alloy Steel

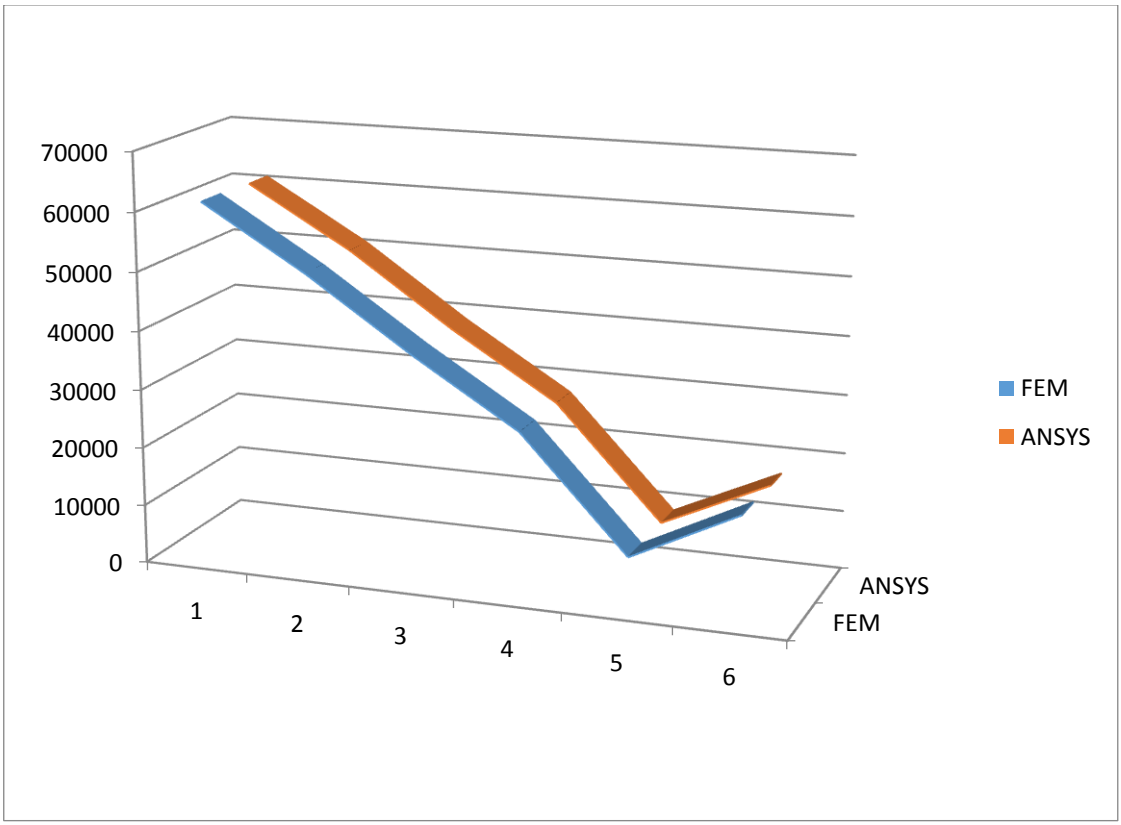

Fig 4.61 compared result shown by Finite Element Analysis & Ansys software of Alloy Steel

ω^2(rad/s)	ω(rad/s)	FEM	ANSYS
3038.739	55.12	8772.6	8783.2
450.897	21.23	3378.8	3379.5
7.393	2.71	431.3	430.4
131.358	11.46	1823.9	1820.5
1566.505	39.57	6297.7	6298.1
1808.434	42.52	6767.2	6768.3

Table 4.2. compared result Finite Element Analysis & Ansys software of CFRP

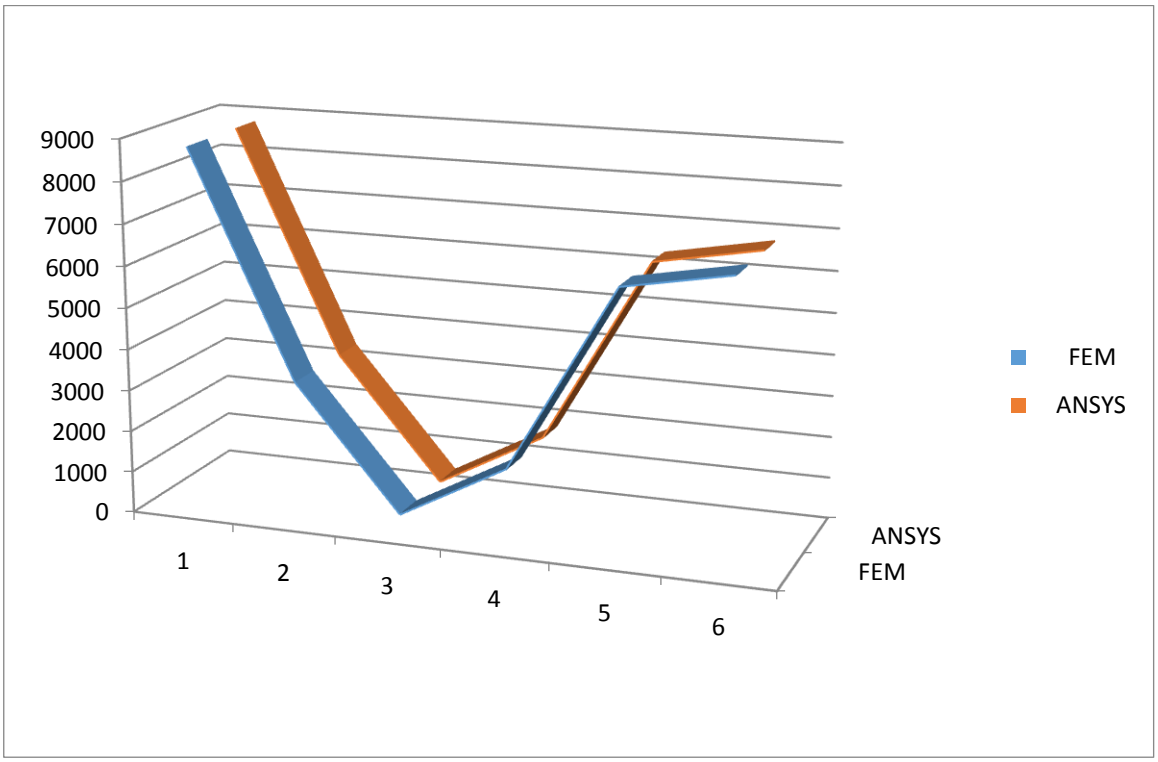

Fig 4.62 compared result Finite Element Analysis & Ansys software of CFRP

Alloy Steel	Carbon Fiber Reinforced Plastic
124.6	277.93
204.6	456.33
264.93	595.19
838.15	1871.1
873.5	1948.2
1194	2671.2

Table 4.3. Compared results between Alloy Steel & Carbon Fiber Reinforced Plastic

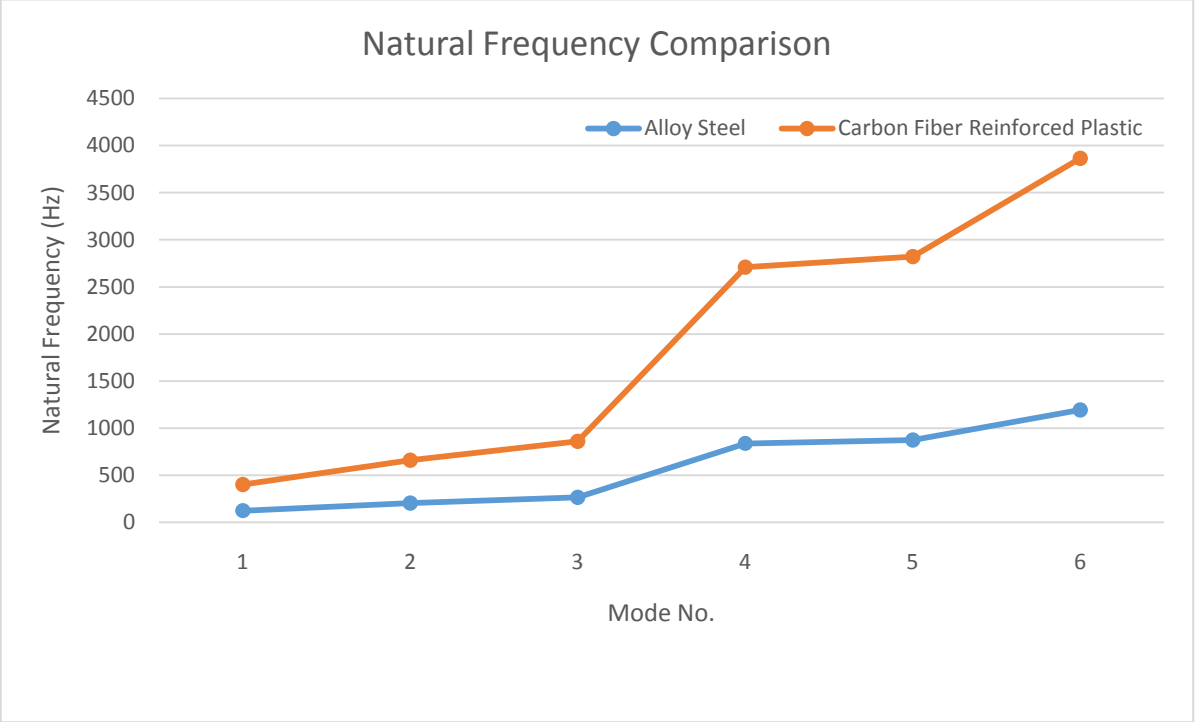

Fig.4.62.Compared results between Alloy Steel & Carbon Fiber Reinforced Plastic

CHAPTER – 5

SUMMARY AND CONCLUSION

This work focuses on active vibration control of a portal frame structure. For the analysis portal frame of two materials were considered in which one is alloy steel and the other is Carbon Fiber Reinforced Plastic under different boundary conditions. Modal analysis of these frames has been done through ANSYS WORKBENCH 14.0. Natural frequency and mode shape are obtained through modal analysis. After model analysis mathematical modelling of the portal frame is done using finite element method and solved for eigen values and eigen vectors. Now, for active vibration control the whole structure is divided into six elements and piezoelectric patches are bonded as sensor/actuator pair, one by one on each element. PID controller is implemented to obtain the control response on the Simulink toolbox of MATLAB Platform.

This technique has made possible by applying the counter force to the structure which is appropriately out of phase (eccentric) but equal in amplitude to the original force. As a result two opposite forces cancel each other and structure stop vibration. The piezoelectric patches were used to control such complex structures. The controller may be P, PI and PID. But the PID controller is best suitable among three because of its robustness. The piezo-electric patches are fixed on each element sequencely (one-by-one on each element) of the structure and PID controller is implemented to obtain the control response on the MATLAB platform of the Simulink toolbox. The results are obtained and optimum location is found for the effective control of the structure. The control response obtained for the frame structure is optimized which be used for controlling the vibration of mechanical equipment's. After applying PID controller on each element, it has been found that the best control has obtained at element one near the fixed end in case of eccentric point excitation as well as in case of midpoint excitation optimum control has obtained at element six near the fixed end.

The progression from conventional structures, where the intervention is carried out through human observation only to intelligent structures, where continuous measurement and control through feedback to alter structure behavior, requires increasing sophistication of information technology to read, reduce and manage data. On the other hand engineering judgment remains important.

Based on the analysis of present work, the following conclusions have been drawn

- From the present study it has been found that without control, response is paramount but after applying control force sufficient vibration suspension has been achieved. Responses are taken in account of placing the piezo-electric sensor/actuator pair are placed at the fixed end and the middle part (element) of the frame. It is concluded that the best result is obtained when the piezo-electric patches are bonded near the fixed end.
- In this research two materials are analyzed in which alloy steel has found suitable because it is efficiently optimized as compare to carbon fiber reinforced plastic.
- In this work, two boundary conditions are employed for both the materials and the result is found that for both the cases the best optimization is found near the fixed end of the portal frame.
- The natural frequencies for the both the materials are obtained through ANSYS and the results are verified through finite element method theoretically. The natural frequency of carbon fiber reinforced plastic is found higher than the alloy steel.

After the whole analysis the concluded result is that the best material for the application of active vibration control through piezo-electric patches is alloy steel.

SCOPE OF THE WORK

This work can be extended with advance technology, digital environment and robust control under the following area of research.

1. Active vibration control can be analysis through LQR Technique.(Linear Quadratic Regulator)
2. Active vibration control can be used for typical and complicated structures.
3. Work can be easily extended for Multi-Input Multi-Output (MIMO) systems to optimize complex structures.
4. Work can be carried out through Advanced control design methods which is based on state space equations.(numerical optimization tool).
5. Active vibration control can be implemented for service and damage detection of the structure.

BIBLIOGRAPHY

AlirezaKhaligh, Peng Zeng, and Cong Zheng, "Kinetic energy harvesting using piezoelectric and electromagnetic technologies—state of the art", IEEE transactions on industrial electronics, Vol. 57, No. 3, March 2010.

ArmenBagdasaryan. "Discrete dynamic simulation models and technique for comple control systems" Institution of the Russian Academy of Sciences, V.A. Trapeznikov Institute for Control Sciences of RAS, 65 Profsoyuznaya, 117997 Moscow, Russia, Simulation Modelling Practice and Theory 19 (2011) 1061–1087.

Ahmad 'AthifMohdFaudzi, Khairuddin bin Osman, M.F. Rahmat, Nu'man Din Mustafa, M. AsyrafAzman , Koichi Suzumori. "Controller Design for Simulation Control of Intelligent Pneumatic Actuators (IPA) System". Department of Mechatronics and Robotics Engineering, Faculty of Electrical Engineering, UniversitiTeknologi Malaysia, 81310 Skudai, Malaysia, Department of Industrial Electronics, Faculty of Electrical and Electronics, UniversitiTeknikal Malaysia Melaka, Hang Tuah Jaya, 76100 Durian Tunggal, Melaka**,** "Department of Control and Instrumentation Engineering", Faculty of Electrical Engineering, UniversitiTeknologi Malaysia, 81310 Skudai, Malaysia,Graduate School of Natural Science and Technology, Okayama University, Okayama, Japan. Procedia Engineering 41 (2012) 593 – 599.

A.V. Lopatin, E.V. Morozov, "Symmetrical vibration modes of composite sandwich plates", Journal of Sandwich Structures and Materials, Vol. 13(2), pp. 189–211, 2010.
A. Arikoglu, I. Ozkol, "Vibration Analysis of Composite Sandwich Plates by the Generalized Differential Quadrature Method", AIAA Journal, Vol. 50(3), pp. 620–630, 2012.

A.K. Agrawal, J.N. Yang, "Optimal placement of passive dampers on seismic and wind excited buildings using combinatorial optimization", Journal of Intelligent Material Systems and Structures, Vol. 10, pp. 997–1014, 2000.

A.Preumont, "Vibration Control of Active Structure", third edition, vol. 4 Issue.2.pp 169-179, 2011.

A. Townley, "Vibrational energy harvesting using mems piezoelectric generators", Electrical Engineering, University of Pennsylvania.

Abdel-Rohman M," Feasibility of active control of tall buildings against wind", Journal of Structural Engineering" Department Civil Engineering, American University of Sharjah, United Arab Emirates 1987;113:349–62.

Adam B, Smith I, "Tensegrity active control: multi-objective approach." Department of JComputCivi Engineering ''Enzo Ferrari'', University of Modena and Reggio Emilia, Via Vignolese 905/B, 41125 Modena, Italy, Composite Structures 128 (2007) 21, 33-10.

Arpita Mukherjee and Uma Datta, "Comparative study of piezoelectric materials properties for green energy harvesting from vibration", Electronics and Instrumentation Lab, Central Mechanical Engineering Research Institute (CSIR).

AndrezaTangerinoMineto, Meire Pereira de Souza Braun, HélioAparecido Navarro and Paulo SérgioVaroto, "Modeling of a cantilever beam for piezoelectric energy harvesting", DINCON'10, 9th Brazilian Conference on Dynamics Control and their Applications, June 07-11, 2010.

ArunP.Parameswaran, B.Ananthakrishnan,K.V.Gangadharan, "Design and development of a model free robust controller for active control of dominant flexural modes of vibrations in a smart system", SOLVE Lab, Centre for System Design (CSD), National Institute of Technology Karnataka, Surathkal, Mangalore 575025, India, Journal of Sound and Vibration 355(2015)1–18.

A.S. Das, J.K.Dutt, K.Ray, "Active control of coupled flexural-torsional vibration in a flexible rotor–bearing system using electromagnetic actuator", Department of Mechanical Engineering in IIT Delhi, Hauz-Khas, New-Delhi 110016, India, International Journal of Non-Linear Mechanics 46 (2011) 1093–1109.

Antonio Zippo, Giovanni Ferrari, Marco Amabili, Marco Barbieri, Francesco Pellicano, "Active vibration control of a composite sandwich plate", Department of Engineering ''Enzo Ferrari'', University of Modena and Reggio Emilia, Via Vignolese 905/B, 41125 Modena, Italy, Composite Structures 128 (2015) 100–114.

AchimBleicher, Mike Schlaich, YozoFujino, Thomas Schauer, "Model-based design and experimental validation of active vibration control for a stress ribbon bridge using pneumatic muscle actuators", Department of Civil and Structural Engineering, Berlin Institute of Technology, Berlin, Germany, Engineering Structures 33 (2011) 2237–2247.

Antonello De Luca, Aldo Giordano, Elena Mele, Alessandra Romano, "A simple formula for predicting the horizontal capacity of masonry portal frames", Department of Structural Analysis and Design, University of Naples, "Federico II" P.leTecchio 80, 80125 – Naples, Italy, Engineering Structures 29 (2007) 2109–2123.

BartłomiejDyniewicz, JacekM.Bajkowski, CzesławI.Bajer, "Semi-active control of a sandwich beam partially filled with magneto rheological elastomer", Institute of FundamentalTechnological Research(IPPT), Polish Academy of Sciences, Pawińskiego 5b,02-106 Warsaw, Poland, Mechanical SystemsandSignalProcessing60-61(2015)695–705.

B.L. CLARKSON, R.J. POPE, "Experimental determination of modal densities and loss factors of flat plates and cylinders", Journal of Sound and Vibration, Vol. 77(4), pp. 535–549, 1981.

Bin Zi, Zhen-cai Zhu, Jing-li Du, "Analysis and control of the cable-supporting system including actuator dynamics" School of Mechanical and Electrical Engineering, China University of Mining and Technology, Xuzhou, Jiangsu 221116, China,School of Electromechanical Engineering, Xidian University, Xi'an, Shaanxi 710071, China, Control Engineering Practice 19 (2011) 491–501.

Chi-Chang Lin, Lyan-Ywan Lu, Ging-Long Lin, Ting-Wei Yang. "Vibration control of seismic structures using semi-active friction multiple tuned mass dampers"

Department of Civil Engineering, National Chung Hsing University, 250 Kuo-Kuang Road, Taichung 40227, Taiwan, ROC, Department of Construction Engineering, National Kaohsiung First University of Science and Technology, 1 University Road, Yenchao, Kaohsiung 824, Taiwan, ROC, Engineering Structures 32 (2010) 3404 -3417.

C.A. Morales, "Portal frame inertia and stiffness matrices by substructure synthesis", Center for Intelligent Material Systems and Structures, 310 Durham Hall, Virginia Tech, Blacksburg, VA 24061, USA, Journal of Sound and Vibration 283 (2005) 1205–1215.

Chih-Liang Chu (a), "Active vibration control of a flexible beam mounted on an elastic base", Bing-SongWu (b), Yih-Hwang Lin, a) Department of Mechanical Engineering, Southern Taiwan University of Technology, Tainan 710, Taiwan, Republic of China b) Department of Mechanical and Mechatronic Engineering, National Taiwan Ocean University, Keelung 202, Taiwan, Republic of China (Finite Elements in Analysis and Design 43 (2006) 59 – 67.

C. Mei, "Hybrid wave/mode active control of bending vibrations in beams based on the advanced Timoshenko theory", Department of Mechanical Engineering, The University of Michigan-Dearborn, 4901 Evergreen Road, Dearborn, MI48128, USA (Journal of Sound and Vibration 322 (2009) 29–38.

C.D. Johnson, D.A. Kienholz, L.C. Rogers, "Finite element prediction of damping in beams with constrained viscoelastic layers", Shock and Vibration Bulletin, pp. 71–81, 1980.

Dan J. Gordon, KaanErkorkmaz, "Accurate control of ball screw drives using pole-placement vibration damping and a novel trajectory prefilter" Precision Controls Laboratory University of Waterloo, Department of Mechanical & Mechatronics Engineering 200 University Avenue West, Waterloo, ON, N2L 3G1, Canada, S0141-6359(12)00141-9, 2012.09.009.

Duoc T. Phan, James B.P. Lim, Tiku T. Tanyimboh, A.M. Wrzesien, Wei Sha, R.M. Lawson, "Optimal design of cold-formed steel portal frames for stressed-skin

action using genetic algorithm", School of Planning, Architecture and Civil Engineering, David Keir Building, Queen's University, Belfast BT9 5AG, UK, Engineering Structures 93 (2015) 36–49.

Duoc T. Phan, James B.P. Lim, Tiku T. Tanyimboh, R. Mark Lawson, YixiangXu, Steven Martin, Wei Sha, "Effect of serviceability limits on optimal design of steel portal frames", School of Planning, Architecture and Civil Engineering, Queen's University Belfast, David Keir Building, Belfast, BT9 5AG, UK, Journal of Constructional Steel Research 86 (2013) 74–84.

D.J. Mead, S. Markus, "The forced vibration of a three-layer damped sandwich beam with arbitrary boundary conditions", Journal of Sound and Vibration, Vol. 10, pp. 163–175, 1969.

D. Ross, E.E. Ungar, E.M. Kerwin, "Damping of plate flexural vibrations by means of viscoelastic laminae", Colloquium on Structural Damping, American Society of Mechanical Engineers (1959).

D. Cvijovic, J. Klinowski, "Taboo search: an approach to the multiple minima problem", Vol. 267, pp. 664–664, 1995.

E. Minazara, D. Vasic and F. Costa, "Piezoelectric generator harvesting bike vibrations energy to supply portable devices", 2010.

F.X. Xin , T.J. Lu, "Analytical modeling of wave propagation in orthogonally rib-stiffened sandwich structures Sound radiation", Computers and Structures, Vol. 89, pp. 507–516, 2011.

F. Alijani, M. Amabili, "Nonlinear vibrations of laminated and sandwich rectangular plates with free edges. Part 1: Theory and numerical simulations", Composite Structures, Vol. 105, pp.422–436, 2013.

F. Amini, H. Karagah, "Optimal placement of semi active dampers by pole assignment method", Iranian Journal of Science and Technology, Transaction B: Engineering. Vol. 30, pp.31–41, 2006.

F. Braghin, S. Cinquemani, F. Resta, "A model of magnetostrictive actuators for active vibration control", Politecnico di Milano, Dipartimento di Meccanica, Campus BovisaSud, via La Masa 1, 20156 Milano, Italy, Sensors and Actuators A 165 (2011) 342–350.

FerhanÖztürk, SelimPul, "Experimental and numerical study on a full scale apex connection of cold-formed steel portal frames", Karadeniz Technical University, Civil Engineering Department, 61080 Trabzon, Turkey, Thin-Walled Structures 94 (2015) 79–88.

Fabio Minghini, NerioTullini, FerdinandoLaudiero, "Elastic buckling analysis of pultruded FRP portal frames having semi-rigid connections", Department of Engineering, University of Ferrara, Ferrara, Italy, Engineering Structures 31 (2009) 292-299.

Antonio Zippo, Giovanni Ferrari and Marco Amabili. "Active vibration control of a sandwich plate by non-collocated positive position feedback", Department of Mechanical Engineering, McGill University, Macdonald Engineering Building, 817 Sherbrooke Street West, Montreal, Canada H3A 0C3, Journal of Sound and Vibration 342(2015)44–56.

G. Boschetti, D. Richiedei, A. Trevisani. "Delayed reference control for multi-degree-of-freedom elastic systems: Theory and experimentation" Dipartimento di Tecnica e GestionedeiSistemiIndustriali—DTG, Universit a degliStudi di Padova, Stradella S. Nicola 3, 36100 Vicenza, Italy, Control Engineering Practice 19 (2011) 1044–1055.

Guillaume Barrault, Dunant Halim, Colin Hansen, ArcanjoLenzi. "High frequency spatial vibration control for complex structures". Department of Mechanical Engineering, UFSC, Florianopolis, Brazil, School of Mechanical Engineering, The University of Adelaide, SA 5005, Australia. Applied Acoustics 69 (2008) 933–944.

HanifRamli, M.S. Meon, T.L.T. Mohamed, A.A.M. Isa, Z. Mohamed. "A Fuzzy-Active Force Control Architecture Based in Characterizing Nonlinear

Systems'Behavior". Faculty of Mechanical Engineering, UnivProcedia Engineering 41 (2012) 1389 – 1397 ersitiTeknologi MARA, Shah Alam, Malaysia.

Hyun-Su Kim, Joo-Won Kang, "Semi-active fuzzy control of a wind-excited tall building using multi-objective genetic algorithm" Division of Architecture, Sunmoon University, Asan-si, Republic of Korea School of Architecture, Yeungnam University, Gyeongsan-si, Republic of Korea, Engineering Structures 41 (2012) 242–257

Hui-Min Yen, Tzuu-Hseng S. Lia,, Yeong-Chan Chang, "Design of a robust neural network-based tracking controller for a class of electrically driven non holonomic mechanical systems, Department of Electrical Engineering, National Cheng Kung University, 1 University Road, Tainan 701, Taiwan, ROC, Department of Electrical Engineering, Kun-Shan University, 949 Da-Wan Road, Yung-Kang District, Tainan 71003, Taiwan, ROC, Information Sciences 936 (2012) 515–522.

HarijonoDjojodihardjo, Mohammad Jafari, SurjatinWiriadidjaja, KamarulArifin Ahmad, "Active Vibration Suppression of an elastic piezoelectric sensor and actuator fitted cantilevered beam configurations as a generic smart composite structure", University Putra Malaysia, 34400 UPM Serdang, Selangor DarulEhsan, Malaysia, Composite Structures 132 (2015) 848–863.

H.Y. Guo, L. Zhang, "Optimal placement of MR dampers for structural control using identification crossover genetic algorithm", Journal of Low Frequency Noise, Vibration and Active Control, Vol. 23, pp. 167–178, 2004.

H. Zheng, C. Cai, X.M. Tan, "Optimization of partial constrained layer damping treatment for vibrational energy minimization of vibrating beams", Computers & Structures, Vol. 82, pp. 2493–2507, 2004.

H. Movaffaghi, O. Friberg, "Optimal placement of dampers in structures using genetic algorithm", Engineering Computations, Vol. 23, pp. 597–606, 2006.

H. R. Hamidzadeh, "The effect of visco-elastic core thickness on modal loss factors of a thick three-layer cylinder, Proceedings of the Institution of Mechanical Engineers", Part K: Journal of Multi-body Dynamics, Vol. 223, pp. 1–8, 2009.

H.D. Chalak, A. Chakrabarti, M.A. Iqbal, A.H. Sheikh,"Vibration of laminated sandwich beams having soft core", Journal of Vibration and Control, Vol. 18(10), pp. 1422–1435, 2011.

Heung Soo Kim, Joo-Hyong Kim and Jaehwan Kim, "A review of piezoelectric energy harvesting based on vibration", International journal of precision engineering and manufacturing, Vol. 12, No. 6, pp. 1129-1141.

IoanDoré Landau, Marouane Alma, Tudor-BogdanAirimitoaie, "Adaptive feedforward compensation algorithms for active vibration control with mechanical coupling", Control System Department of GIPSA-Lab, BP 46 St Martin d'Héres, 38402, France, Automatica 47 (2011) 2185–2196.

Iván M. Díaz, Emiliano Pereira, Malcolm J. Hudson, Paul Reynolds, "Enhancing active vibration control of pedestrian structures using inertial actuators with local feedback control", Escuela de Arquitectura, Universidad de Castilla-La Mancha, Campus Tecnológico de la Fábrica de Armas, Av. Carlos III s/n, E-45041 Toledo, Spain, Engineering Structures 41 (2012) 157–166.

I.Takewaki, "Optimal damper placement for minimum transfer functions", Earthquake Engineering and Structural Dynamics, Vol. 26, pp. 1113–1124, 1997.

I.Takewaki, S. Yoshitomi, "Effects of support stiffnesses on optimal damper placement for a planar building frame", Structural Design of Tall and Special Buildings, Vol. 7, pp. 323–336,1998.

I.Takewaki, S. Yoshitomi, K. Uetani, M. Tsuji, "Non-monotonic optimal damper placement via steepest direction search", Earthquake Engineering and Structural Dynamics, Vol. 28, pp. 655–670, 1999.

I.Takewaki, "Optimal damper placement for critical excitation, Probabilistic Engineering Mechanics", Vol. 15, pp. 317–325, 2000.

I.Takewaki, "Optimal damper placement for planar building frames using transfer functions", Structural and Multi disciplinary Optimization, Vol. 20, pp. 280–287, 2000.

Ibrahim. R.A. "Recent advances in nonlinear passive vibration isolators", Department of Mechanical Engineering, Wayne State University, Detroit, MI 48098, USA. ournal of Sound and Vibration 314 (2008) 371–452.

Israel Lopez, NesrinSarigul-Klijn. "A review of uncertainty in flight vehicle structural damage monitoring, diagnosis and control: Challenges and opportunities", Mechanical and Aerospace Engineering, Space Engineering Research and Graduate Program, University of California at Davis, Davis, CA 95616-5294, USA, Progress in Aerospace Sciences 46 (2010) 247–273.

John H. Crews, Michael G. Mattson, Gregory D. Buckner, "Multi-objective control optimization for semi-active vehicle suspensions" Department of Mechanical and Aerospace Engineering, North Carolina State University, Raleigh, NC 27695-7910, USA, Journal of Sound and Vibration 330 (2011) 5502–5516.

Joono Cheong, Youngsu Cho, Seung-Ik Lee," Invariant slow manifold approach for exact dynamic inversion of singularly perturbed linear mechanical systems with admissible output constraints. Department of Control and Instrumentation Engineering, Korea University, 208 Seochang-ri, Jochiwon-eup, Chungnam 339-700, Republic of Korea IT Convergence Technology Research Lab., Electronics and Telecommunications Research Institute, Daejeon 305-700, Republic of Korea, Journal of Sound and Vibration 331 (2012) 3710–3720.

Jing Na ,XuemeiRen, Guido Herrmann, ZhiQiao. " Adaptive neural dynamic surface control for servo systems with unknown dead-zone". aculty of Mechanical and Electrical Engineering, Kunming University of Science and Technology, Kunming 650093, PR China School of Automation, Beijing Institute of Technology, Beijing,

100081, PR China Department of Mechanical Engineering, University of Bristol, Bristol, BS8 1TR, UK. Control Engineering Practice 19 (2011) 1328–1343.

JuhaOrivuori, IliasZazas, Steve Daley." Active control of frequency varying disturbances in a diesel engine" Aalto University School of Electrical Engineering, Department of Automation and Systems Technology, PO Box 15500, 00076 AALTO, Finland Institute of Sound and Vibration Research, The University of Southampton, Southampton, SO171BJ, UK, Control Engineering Practice 20 (2012) 1206–1219.

Josep M. MiratsTur, SergiHernàndez Juan. "Tensegrity frameworks: Dynamic analysis review and open problems" Institut de RobòticaiInformàtica Industrial (IRI), CSIC-UPC, Barcelona, Spain, Mechanism and Machine Theory 44 (2009) 1–18.

Justin D. Marshall, Finley A. Charney. "A hybrid passive control device for steel structures, II: Physical testing". Civil Engineering Department, Auburn University, Auburn, AL, USA, Department of Civil and Environmental Engineering, Virginia Polytechnic Institute and State University, Blacksburg, VA, USA, Journal of Constructional Steel Research 66 (2010) 12871294.

Jiˇrı´ Tu ma, Jiˇrı´ ˇSimek, Jaromı´r ˇSkuta, Jaroslav Los, "Active vibrations control of journal bearings with the use of piezoactuators", Faculty of Mechanical Engineering, VSB—Technical University of Ostrava, 17.listopadu 15, Z70833, Ostrava, Czech Republic, Mechanical Systems and Signal Processing 36 (2013) 618–629.

John E. Mottersheada, Yitshak M. Ram, "Inverse eigenvalue problems in vibration absorption: Passive modification and active control", Department of Engineering, Mechanical Engineering Division, University of Liverpool, Liverpool L69 3GH, UK, Mechanical Systems and Signal Processing 20 (2006) 5–44.

J.A. Bishop, A.G. Striz, "On using genetic algorithms for optimum damper placement in space trusses, Structural and Multidisciplinary Optimization", Vol. 28, pp. 136–145, 2004.

J. Ro, A. Baz, "Optimum placement and control of active constrained layer damping using modal strain energy approach", Journal of Vibration and Control, Vol. 8, pp. 861–76, 2002.

J.S. Grewal, R. Sedaghati, E. Esmailzadeh, "Vibration analysis and design optimization of sandwich beams with constrained viscoelastic core layer", Journal of Sandwich Structures and Materials, Vol. 15(2), pp. 203–228, 2013.

Jacques Lottin, Fabien Formosa, MihaiVirtosu, Laurent Brunetti ESIA, "About optimal location of sensors and actuators for the control of flexible structures", Université de Savoie (REM 2006 Research and Education in Mechatronics KTH, Stockholm, Sweden June 15-16, 2006)

JuntaoFei, "Active Vibration Control of Flexible Steel Cantilever Beam Using Piezoelectric Actuators", Department of Mechanical Engineering, University of Akron, Akron, OH 44325 USA

John Kymissis, Clyde Kendall, Joseph Paradiso and Neil Gershenfeld, "Parasitic power harvesting in shoes", Physics and Media Group MIT Media Laboratory, E15-410, Cambridge, MA. 02139, USA.

J. G. Rocha, L. M. Gonçalves, P. F. Rocha, M. P. Silva, and S. Lanceros-Méndez, "Energy harvesting from piezoelectric materials fully integrated in footwear", IEEE Transactions on Industrial Electronics, Vol. 57, No. 3, March 2010.

Jing-Quan Liu, Hua-Bin Fang, Zheng-Yi Xu, Xin-Hui Mao, Xiu-Cheng Shen,Di Chen, Hang Liao and Bing-Chu Cai, "A MEMS-based piezoelectric power generator array for vibration energy harvesting", Microelectronics Journal, 39 (2008), pp. 802–806.

KhairulAnam , Adel Ali Al-Jumaily. "Active Exoskeleton Control Systems: State of the Art", University of Jember, Jember 68121, Indonesia, University of Technology Sydney, Sydney 2007 Australia. Procedia Engineering 41 (2012) 988 – 994.

Kendra L.Van Buren, Thomas M.Hall, Lindsey M.Gonzales, François M.Hemez, Steven R.Anton, "A case study to quantify prediction bounds caused by model-form uncertainty of a portal frame", Los Alamos National Laboratory, NSEC, Mail Stop T001, Los Alamos, NM 87544, USA, Mechanical Systems and Signal Processing 50-51(2015) page 11–26.

K. Khorshidi, E. Rezaei, A.A. Ghadimi, M. Pagoli, "Active vibration control of circular plates coupled with piezoelectric layers excited by plane sound wave", Sound and Vibration Laboratory, Department of Mechanical Engineering, Faculty of Engineering, Arak University, Arak 38156-8-8849, Iran, Applied Mathematical Modelling 39 (2015) 1217–1228.

K. Misiurek, P. Sniady, "Vibrations of sandwich beam due to a moving force", Composite Structures, Vol. 104, pp. 85–93, 2013.

L. Wu, A. Agren, U. Sundback, "A study of the initial decay rate of two-dimensional vibrating structures in relation to estimates of loss factor", Journal of Sound and Vibration, Vol.206(5), pp. 663–684, 1997.

L.L. Sun, C.H.Hansen, C.Doolan, "Evaluation of the performance of a passive–active vibration isolation system", School of Mechanical Engineering, Shandong University, Jinan 250061, China, Mechanical SystemsandSignalProcessing50-51(2015)480–497.

Liang Wang, Huai-hai Chen, Xu-dong He, "Active HN control of the vibration of an axially moving cantilever beam by magnetic force", MOE Key Lab of Structure Mechanics and Control for Aircraft, Institute of Vibration Engineering Research, Nanjing University of Aeronautics and Astronautics, Nanjing 210016, China, Mechanical Systems and Signal Processing 25 (2011) 2863–2878.

Lin C-C, "Active control of irregular buildings considering soil-structure interaction Effects", Soil Dynamics Earthquake Eng, 2010;30:98–109.

LiliDong,Yao Zhang, ZhiqiangGao, "A robust decentralized load frequency controller for interconnected power systems" Department of Electrical and Computer Engineering, Cleveland State University, Cleveland, OH 44115, USA, ISA Transactions 51 (2012) 410–419.

Mats Jonassona, Fredrik Roos, "Design and evaluation of an active electromechanical wheel suspension system" Department of Chassis and Vehicle Dynamics, Volvo Car Corporation, SE-405 31 Go¨teborg, Sweden, KTH Vehicle Dynamics, SE-100 44 Stockholm, Sweden, KTH Mechatronics, SE-100 44 Stockholm, Sweden, Mechatronics 18 (2008) 218–230.

Malekzadeh P, Fiouz AR, Razi H. "Three-dimensional dynamic analysis of laminated composite plates subjected to moving load" Laboratoire de Tribologie et Dynamique des Systèmes, Équipe D2S, UMR CNRS 5513, ÉcoleCentrale de Lyon, 36, Avenue Guy de Collongue, 69134 ÉcullyCedex, France. Compos Struct 2009;90:105–14.

MurelitharanMuniandy, KanesanMuthusamy. "An Innovative Design to Improve Systematic Odometry Error in Nonholonomic Wheeled Mobile Robots" Faculty of Science and Technology, Open University Malaysia, JalanTun Ismail 50480 Kuala Lumpur, Malaysia, Institute of Quality, Research and Innovation (IQRI), Open University Malaysia, JalanTun Ismail 50480 Kuala Lumpur, Malaysia. Procedia Engineering 41 (2012) 436 – 442.

Mauro Manetti, Marco Morandini, Paolo Mantegazza. "High precision massive shape control of magnetically levitated adaptive mirrors", Politecnico di Milano, Dipartimento di IngegneriaAerospaziale, via La Masa 34, 20156 Milano, Italy, Control Engineering Practice 18 (2010) 1386–1398.

Morales.A.L, Rongong. J.A, Sims.N.D. "A finite element method for active vibration control of uncertain structures" A´rea de Ingenierı´aMeca´nica, E.T.S.I. Industriales, Universidad de Castilla – La Mancha, Avda. Camilo Jose´Cela s/n, 13071 Ciudad Real, Spain, Department of Mechanical Engineering, The University of Sheffield, Mappin Street, Sheffield S1 3JD, United Kingdom, Mechanical Systems and Signal Processing 32 (2012) 79–93.

Mohebpour S. R, Fiouz AR, Ahmadzadeh A.A. "Dynamic analysis of laminated composite plates subjected to a moving oscillator by FEM" Department of Mechanical Engineering, School of Engineering, Persian Gulf University, Bushehr 75168, Iran, Department of Civil Engineering, School of Engineering, Persian Gulf University, Bushehr 75168, Iran, Department of Mechanical Engineering, School of Engineering, Persian Gulf University, Bushehr 75168, Composite Structures 93 (2011) 1574–1583.

Martin Proetzsch, Tobias Luksch, KarstenBerns, "Development of complex robotic systems using the behavior-based control architecture iB2C. University of Kaiserslautern, Robotics Research Lab, Gottlieb-Daimler-Str., 67663 Kaiserslautern, German, Robotics and Autonomous Systems 58 (2010) 46-67.

M. Domaneschi, "Simulation of controlled hysteresis by the semi-active Bouc-Wen model" Department of Structural Engineering, Politecnico di Milano, Milan, Italy, Computers and Structures 106–107 (2012) 245–257.

MirosławGalicki, "Two-stage constrained control of mobile manipulators" Faculty of Mechanical Engineering, University of ZielonaGóra, ZielonaGóra, Podgorna 50, Poland Institute of Medical Stat. Comp. Science Documentation, Friedrich Schiller University, Jena, Germany, Mechanism and Machine Theory 54 (2012) 18–40.

Moon K.Kwak, Dong-HoYang, "Dynamic modelling and active vibration control of a submerged rectangular plate equipped with piezoelectric sensors and actuators", Department of Mechanical, Robotics and Energy Engineering, Dongguk University-Seoul, 30, Pildong-ro 1gil, Jung-gu, Seoul 100-715, Republic of Korea, Journal ofFluidsandStructures54(2015)848–867.

Mohammad Saranik, David Lenoir, Louis Jézéquel, "Shaking table test and numerical damage behaviour analysis of a steel portal frame with bolted connections", Laboratoire de Tribologie et Dynamique des Systèmes, Équipe D2S, UMR CNRS 5513, ÉcoleCentrale de Lyon, 36, Avenue Guy de Collongue, 69134 ÉcullyCedex, France, Computers and Structures 112–113 (2012) 327–341.

M.J. Lam, D.J. Inman, W.R. Saunders, "Vibration control through passive constrained layer damping and active control", Journal of Intelligent Material Systems and Structures, Vol. 8, pp.663–677, 1997.

M.P. Singh, L.M. Moreschi, "Optimal placement of dampers for passive response control", Earthquake Engineering and Structural Dynamics, Vol. 31, pp. 955–976, 2002.

M. Alvelid, "Optimal position and shape of applied damping material", Journal of Sound and Vibration, Vol. 310, pp. 947–965, 2008.

Marcelo A. Tindade, Carlos C. Pagani Jr., Leopoldo P.R. Oliveira. "Semi-modal active vibration control of plates using discrete piezoelectric modal filters", Department of Mechanical Engineering, São Carlos School of Engineering, University of São Paulo, 13566-590 São Carlos, Brazil, Journal of Sound and Vibration 351(2015)17–28.

M.H. Milman, C. Chu, "Optimization methods for passive damper placement and tuning, journal of guidance", Control, and Dynamics, Vol. 17, pp. 848–56, 1994.

M. Gurgoze, P.C. Muller, "Optimal positioning of dampers in multi-body systems", Journal of Sound and Vibration, Vol. 158, pp. 517–530, 1992.

M.R. Maheri, R.D. Adams, "Finite-element prediction of modal response of damped layered composite panels", Composites Science and Technology, Vol. 55, pp. 13–23, 1995.

M. N. Fakhzan and Asan G. A. Muthalif, "Vibration based energy harvesting using piezoelectric material", 4th International Conference on Mechatronics (ICOM), pp. 17-19, May 2011, Kuala Lumpur, Malaysia.

M. Ericka, D. Vasic, F. Costa, G. Poulin and S. Tliba, "Energy harvesting from vibration using a piezoelectric membrane", J. Phys. IV France 128 (2005), pp. 187–193, EDP Sciences, Les Ulis.

N.E. duToit, Brian L. Wardle, and Sang-Gook Kim, "Design considerations for mems-scale piezoelectric mechanical vibration energy harvesters", Integrated Ferroelectrics, 71: 121–160, 2005.

N.H. Diyana, Asan G.A. Muthalif, M.N. Fakhzan and A.N.Nordin, "Vibration energy harvesting using single and comb-shaped piezoelectric beam structures: Modeling and Simulation", Procedia Engineering 41 (2012), pp. 1228 – 1234, Published by Elsevier Ltd. International Symposium on Robotics and Intelligent Sensors 2012 (IRIS 2012).

N. Challamel, F. Bernard, C. Casandjian, "Out-of-plane behaviour of partially composite or sandwich beams by exact and finite element methods", Thin-Walled Structures, Vol. 48, pp. 561–580, 2010.

N.R. Fisco, H. Adeli, "Smart structures: Part I—Active and semi-active control" Department of Civil and Environmental Engineering and Geodetic Science, The Ohio State University, 470 Hitchcock Hall, 2070 Neil Avenue, Columbus,OH 43220, USA, ScientiaIranica A (2011) 18 (3), 275–284.

Nudehi .S , NerioTullini, FerdinandoLaudiero, "Active vibration control of a flexible beam using a buckling type end force", Journal Dynamic System Measure Control , Department of Engineering, University of Ferrara, Ferrara, Italy Engineering Structures 31, (2006), 292-299.

O Furuya, H Hamazaki, S Fujita, "Proper placement of energy absorbing devices for reduction of wind-induced vibration caused in high-rise buildings", Journal of Wind Engineering and Industrial Aerodynamics, 74-76, pp. 931–942, 1998.

Peng Lina, YingminJia, "Distributed rotating formation control of multi-agent systems", Institute of Astronautics and Aeronautics, University of Electronic Science and Technology of China, Chengdu 610054, PR China, Seventh Research Division, Beihang University (BUAA), Beijing 100191, PR China. Systems & Control Letters 59 (2010) 587–595.

Patrick S. Keogh. "Contact dynamic phenomena in rotating machines Active/passive considerations" Department of Mechanical Engineering, University of Bath, Bath BA2 7AY, UK, Mechanical Systems and Signal Processing 29 (2012) 19–33.

P.K.Sinha (Dept. of Aerospace Engineering, IIT Kharagpur) "Active Vibration Control of composite sandwich beams with distributed piezoelectric extension-bending and shear actuator", S Raja (Structures Divison, NAL Bangalore), G Prathap (C-MMACS, Bangalore), Sept. 2000.

Patrick S. Keogh, "Contact dynamic phenomena in rotating machines Active/passive considerations" Department of Mechanical Engineering, University of Bath, Bath BA2 7AY, UK, Mechanical Systems and Signal Processing 29 (2012) 19–33.

Paul D. Mitcheson, Eric M. Yeatman, G. Kondala Rao, Andrew S. Holmes, and Tim C. Green, "Energy harvesting from human and machine motion for wireless electronic devices", March 2010.

P. J. Torvika, B. Runyon, "Modifications to the method of modal strain energy for improved estimates of loss factors for damped structures", Shock and Vibration, Vol. 14, pp. 339–353, 2007.

Peng Lina, YingminJia, "Distributed rotating formation control of multi-agent systems", Institute of Astronautics and Aeronautics, University of Electronic Science and Technology of China, Chengdu 610054, PR China, Seventh Research Division, Beihang University (BUAA), Beijing 100191, PR China. Systems & Control Letters 59 (2010) 587–595.

Preumont A, "The damping of a truss structure with a piezoelectric transducer", Computer Structure 2008; 86:227–39.

Qinglei Hu Student, Guangfu Ma , "Spacecraft Vibration Suppression Using Variable Structure Output Feedback Control and Smart Materials", Distinguished Professor of Aerospace Engineering, Department of Control Science and Engineering, Harbin Institute of Technology, China.

R. Subasri, S.Suresh, A.M.Natarajan, "Discrete direct adaptive ELM controller for active vibration control of nonlinear base isolation buildings", School of Computer Engineering, Nanynag Technological University, Singapore, Neurocomputing129(2014) page 246–256.

Reza Ahmadian and P. RajuMantena. "Modal characteristics of structural portal frames made of mechanically joined pultruded flat hybrid composites", Department of Mechanical Engineering, University of Mississippi, Elsevier Science Limited, Composites: Part B 27B (1996) 319-328. University, MS 38677, USA.

R.A.S. Moreira, J.D. Rodrigues, "Partial constrained viscoelastic damping treatment of structures: A modal strain energy approach", International Journal of Structural Stability and Dynamics, Vol. 6, pp. 397–411, 2006.

R. SETOLA, "A SPLINE-BASED STATE RECONSTRUCTOR FOR ACTIVE VIBRATION CONTROL OF A FLEXIBLE BEAM", Facolta_ di Ingegneria\ Universita_ degliStudi del Sonnio\ Corso Garibaldi\ Palazzo Bosco\ 71099\ Benevento "BN#\ Italy

.

R.K. Kincaid, "Solving the damper placement problem via local search heuristics", OR Spektrum, Vol. 17, pp. 149–58, 1995.

S. Kodiyalam, J. Molnar, "Optimization of constrained viscoelastic damping treatments for passive vibration control", Structural Dynamics and Materials Conference, 1992.

SAID I. HILMY and JOHN F. ABEL. "MATERIAL AND GEOMETRIC NONLINEAR DYNAMIC ANALYSIS OF STEEL FRAMES USING COMPUTER GRAPHICS", Department of Structural Engineering and Program of Computer Graphics, Cornell University, Ithaca, NY 14853, U.S.A, Computers & Structures Vol. 21. No. 4. pp. 825-840. 1985.

SyDzung Nguyen, Quoc Hung Nguyen, Seung-Bok Choi, "A hybrid clustering based fuzzy structure for vibration control – Part 2:An application to semi-active vehicle seat-suspension system", Department of Mechanical Engineering, Smart Structures and Systems Laboratory, Inha University, Incheon 402-751, Republic of Korea, Mechanical SystemsandSignalProcessing56-57(2015)288–301.

S.C. Kattimani, M.C. Ray, "Control of geometrically nonlinear vibrations of functionally graded magneto-electro-elastic plates", Department of Mechanical Engineering, Indian Institute of Technology, Kharagpur 721302, India, International Journal of Mechanical Sciences 99(2015)154–167.

Samuel da Silva, "Non-linear model updating of a three-dimensional portal frame based on Wiener series", Western Parana´ State University, UNIOESTE, CentrodeEngenhariaseCiˆenciasExatas,Av.Tarquı´nio JoslindosSantos,1300,85870-900FozdoIguac- u, Parana´, Brazi, International Journal of Non-Linear Mechanics 46 (2011) 312–320.

Shun-Qi Zhang, Ya-Xi Li, Rudiger Schmidt, "Active shape and vibration control for piezoelectric bonded composite structures using various geometric nonlinearities", Institute of General Mechanics, RWTH Aachen University, Templergraben 64, D-52062 Aachen, Germany, Composite Structures 122 (2015) 239–249.

S.G. Won, S.H. Bae, J.R. Cho, S.R. Bae, W.B. Jeong, "Three-layered damped beam element for forced vibration analysis of symmetric sandwich structures with a viscoelastic core", Finite Elements in Analysis and Design, Vol. 68, pp. 39–51, 2013.

S.A. Hambric, A.W. Jarrett, G.F. Lee, J.J. Fedderly, "Inferring viscoelastic dynamic material properties from finite element and experimental studies of beams with constrained layer damping", Transactions of the ASME, Journal of Vibration and Acoustics, Vol. 129, pp. 158–68, 2007.

S.S. Joshi, "Damper placement for spaceborne interferometers using h-norm optimization", American Control Conference, Vol. 6, pp. 3855–3859, 2000.

S.W. Park, “Analytical modeling of viscoelastic dampers for structural and vibration control”, International Journal of Solids and Structures, Vol. 38, pp. 8065–8092, 2001.

Shad Roundy, Paul K. Wright and Jan Rabaey, “A study of low level vibrations as a power source for wireless sensor nodes”, Computer Communications, 26 (2003), pp. 1131–1144.

Salem Saadon and Othman Sidek, “Transient analysis of ambient vibration-based micro-electro-mechanical systems (MEMS) piezoelectric energy harvester using ANSYS approach”, 2011 International Conference on Computer Applications and Industrial Electronics (ICCAIE 2011).

S. P. Beeby, M. J. Tudor and N. M. White, “Energy harvesting vibration sources for microsystems applications”, Institute of Physics Publishing, Meas. Sci. Technol., 17 (2006), R175–R195.

Shea K, “Developing intelligent tensegrity structures with stochastic Search”, Advance Engineering Inform 2002, 16, 21–40, 2011.

Sheng Wang, Kwok Ho Lam, Cheng Liang Sun, Kin Wing Kwok, Helen Lai Wa Chan, Ming SenGuo and Xing-Zhong Zhao, “Energy harvesting with piezoelectric drum transducer”, Applied Physics Letters 90, 113506 2007.

Singiresu S. Rao, “Mechanical Vibrations”, fifth edition, 2011, page-13-17.

SinanKorkmaz, “Adaptive structures Intelligent structures, A review of active structural Control”, challenges for engineering informatics 2011.

TéoLenquist da Rocha, Samuel da Silva, Vicente Lopes Jr. Paulista, “ OPTIMAL LOCATION OF PIEZOELECTRIC SENSOR AND ACTUATOR FOR FLEXIBLE STRUCTURES”, State University - UNESP, Department of Mechanical Engineering, Brazil (11th International Congress on Sound & Vibration, 2004, St. Petersburg, Russia)

T. Roy, D. Chakraborty, "Genetic algorithm based optimal design for vibration control of composite shell structures using piezoelectric sensors and actuators", International Journal of Mechanics and Materials in Design, Vol. 5, pp. 45–60, 2009.

U. K. Singh and R. H. Middleton, "Piezoelectric Power Scavenging of Mechanical Vibration Energy", 2009.

V. SUDHAKAR, K. VIJAYARAJU, S. GOPALAKRISHNAN, "Development of a new finite element for the analysis of sandwich beams with soft core", Journal of Sandwich Structures and Materials, Vol. 12, pp. 649–683, 2010.

Wei Zhan, Yukang Cui, Zhiguang Feng, K.C.Cheung, James Lam, HuijunGao, "Joint optimization approach to building vibration control via multiple active tuned mass dampers", Research Institute of Intelligent Control and Systems, Harbin Institute of Technology, Harbin, Heilongjiang, China, Mechatronics 23 (2013) 355–368.

Wilkie.W.K, "Helicopter dynamic stall suppression using piezoelectric active fiber composite rotor blades" College of Mechanical and Electronic Engineering, Northwest A&F University, Yangling 712100, China. Presented at the AIAA/ASME/AHS structures, structural dynamics, and materials conference, Long Beach, CA, 1998.

X.Q. PENG, K.Y. LAM and G.R. LIU, "ACTIVE VIBRATION CONTROL OF COMPOSITE BEAMS WITH PIEZOELECTRICS: A FINITE ELEMENT MODEL WITH THIRD ORDER THEORY", Department of Mechanical and Production Engineering\ National University of Singapore\ 09 Kent Ridge Crescent\ Singapore 008159 (Journal of Sound and Vibration "0887# 198"3#\ 524_549).

Xingjian Jing," Frequency domain analysis and identification of block-oriented nonlinear systems" Department of Mechanical Engineering, Hong Kong Polytechnic University, Hung Hom, Kowloon, Hong Kong, Journal of Sound and Vibration 330 (2011) 5427–5442.

Y.F. Wang, D.H. Wang, T.Y. Chai, "Active control of friction self-excited vibration using neuro-fuzzy and data mining techniques", School of Mechanical Engineering and Automation, Northeastern University, Shenyang, Liaoning 11004, China, Expert Systems with Applications 40 (2013) 975–983.

YingWu, Kaiping Yu, Jian Jiao, Rui Zhao, "Dynamic modeling and robust nonlinear control of a six-DOF active micro-vibration isolation manipulator with parameter uncertainties", Department of Astronautic Science and Mechanics, Harbin Institute of Technology, 92 West Da-Zhi Street, Nangang District, Harbin, China, Mechanism and Machine Theory 92 (2015) 407–435.

YikR.Teo, Andrew J.Fleming, "Optimal integral force feedback for active vibration control", Precision Mechatronics Lab, School of Electrical Engineering and Computer Science, Faculty of Engineering and Built Environment, The University of Newcastle, Callaghan, New South Wales 2308, Australia, Journal of Sound and Vibration 355(2015)1–18.

Yuan Yun, Yangmin Li, "A general dynamics and control model of a class of multi-DOF manipulators for active vibration control", Department of Electromechanical Engineering, Faculty of Science and Technology, University of Macau, Av. Padre Tomás Pereira, Taipa, Macao SAR, PR China, Mechanism and Machine Theory 46 (2011) 1549–1574.

Yunlong Li, Xiaojun Wang, Ren Huang, ZhipingQiu. "Active vibration and noise control of vibro-acoustic system by using PID controller", Institute of Solid Mechanics, Beihang University, Beijing 100191, China, Journal of Sound and Vibration 348(2015)57–70.

Y. C. Shu and I. C. Lien, "Analysis of power output for piezoelectric energy harvesting systems", Institute Of Physics Publishing Smart Material and Structure, 15 (2006), pp. 1499–1512.

Yavuz Yaman1, Tarkan Çalışkan1, Volkan Nalbantoğlu2, Eswar Prasad3, David Waechter3, "ACTIVE VIBRATION CONTROL OF A SMART BEAM", (2001-01) 1.

Department of Aeronautical Engineering, Middle East Technical University, Ankara, Turkey 2. ASELSAN Electronics Industries, Ankara, Turkey 3. Sensor Technology Limited, Collingwood, Ontario, Canada.

YavuzYaman , "ACTIVE VIBRATION CONTROL OF A SMART PLATE", Department of Aerospace Engineering, Middle East Technical University, Ankara, Turkey, TarkanCaliskan Department of Aerospace Engineering, Middle East Technical University, Ankara, Turkey, VolkanNalbantoglu ASELSAN Electronics Industries, Akyurt, Ankara Turkey, Eswar Prasad Sensor Technology Limited, Collingwood, Ontario, Canada, David Waechter Sensor Technology Limited, Collingwood, Ontario, Canada (2002-08)

ZengkangGan, Andrew J.Hillis, Jocelyn Darling. "Adaptive control of an active seat for occupant vibration reduction", Centre for Power Transmission and Motion Control, Department of Mechanical Engineering, University of Bath, Claverton Down, Bath BA2 7AY, United Kingdom, Journal of Sound and Vibration 349(2015)39–55.

Zeki KIRAL, "Active Control of Residual Vibrations of a Cantilever Smart Beam", Levent MALGACA, Murat AKDA˘G DokuzEyl¨ul University, Faculty of Engineering, ˙Izmir-TURKEY, (Turkish J. Eng. Env. Sci.32 (2008) , 51 – 57.c_T¨UB˙ITAK).

Zhanfeng Song, Tingna Shi, Changliang Xia, Wei Chen, "A novel adaptive control scheme for dynamic performance improvement of DFIG-Based wind turbines" Department of Electrical Engineering & Automation, Tianjin University, Weijin Road 92, Tianjin 300072, China, Department of Electrical Engineering & Automation, Polytechnic University, Tianjin 300160, Chin, Energy 38 (2012) 104e117.

Ziegler F, "Computational aspects of structural shape control." Computer Structure Centre for Power Transmission and Motion Control, Department of Mechanical Engineering, University of Bath, Claverton Down, Bath BA2 7AY, United Kingdo, 2005, 83, 1191–204.